OCS Study
BOEM 2013-221

Collaborative Archaeological Investigations and Sound Source Verifications within the Massachusetts Wind Energy Area

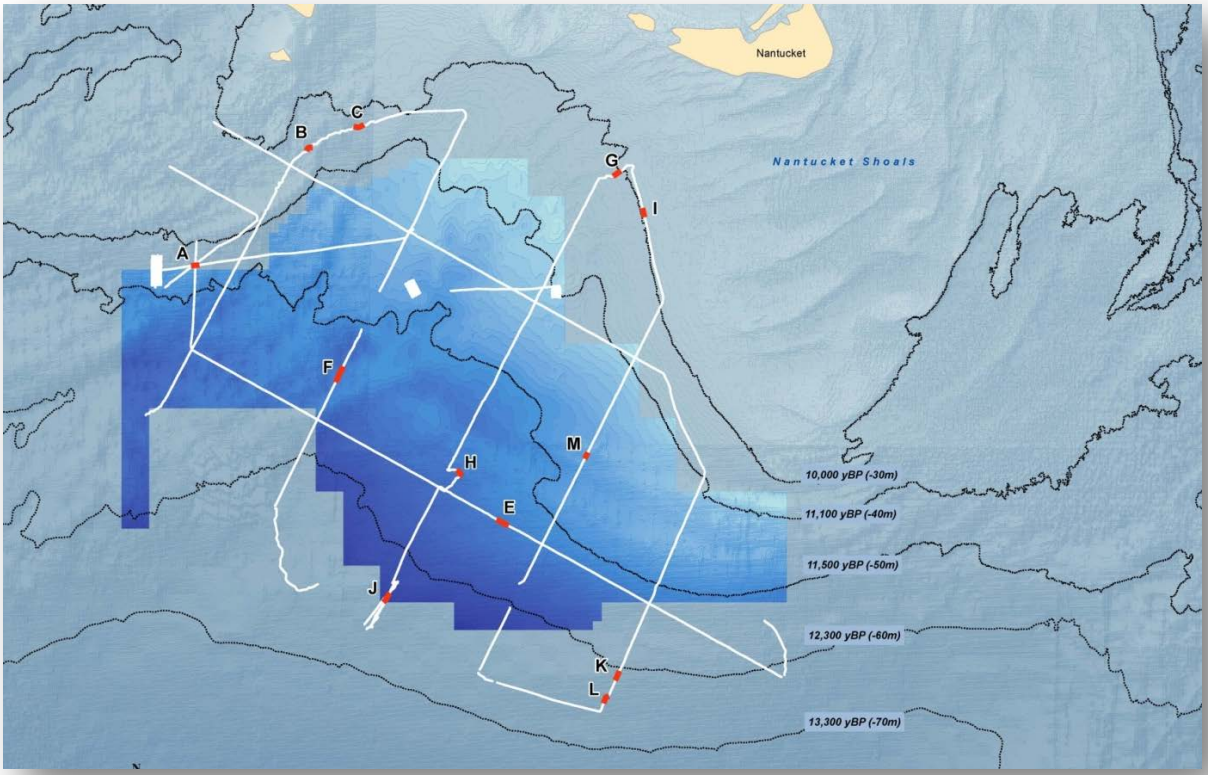

U.S. Department of the Interior
Bureau of Ocean Energy Management
Office of Renewable Energy Programs
www.boem.gov

BOEM
Bureau of Ocean Energy Management

OCS Study
BOEM 2013-221

Collaborative Archaeological Investigations and Sound Source Verifications within the Massachusetts Wind Energy Area

Authors

John Bright
Brandi Carrier
David Conlin
William Danforth
William Hoffman
John King
Brian Oakley
Jeff MacDonnell
David Robinson
William Schwab
Mikhail Zykov

Prepared by
Bureau of Ocean Energy Management, Office of Renewable Energy Programs; JASCO Applied Sciences; National Park Service, Submerged Resources Center; United States Geological Survey, Woods Hole Science Center; and University of Rhode Island, Graduate School or Oceanography.

Published by
U.S. Department of the Interior
Bureau of Ocean Energy Management **Herndon, VA**
Office of Renewable Energy Programs **December 2013**

DISCLAIMER

This report was prepared under various contracts between the Bureau of Ocean Energy Management (BOEM) and JASCO Applied Sciences; the National Park Service, Submerged Resources Center; the United States Geological Survey, Woods Hole Science Center; and the University of Rhode Island, Graduate School of Oceanography. This report has been technically reviewed by BOEM and has been approved for publication. Approval does not signify that the contents necessarily reflect the views and policies of BOEM, nor does mention of trade names or commercial products constitute endorsement or recommendations for use. It is, however, exempt from review and in compliance with BOEM editorial standards.

REPORT AVAILABILITY

The report may be downloaded from the boem.gov website through the Environmental Studies Program Information System (ESPIS). You will be able to obtain this report from BOEM or the National Technical Information Service by writing to the following addresses.

U.S. Department of the Interior
Bureau of Ocean Energy Management
Office of Renewable Energy Programs
381 Elden Street
HM 1328
Herndon, Virginia

U.S. Department of Commerce
National Technical Information Service
5285 Port Royal Road
Springfield, Virginia 22161
Phone: (703) 605-6040
Fax: (703) 605-6900
Email: bookstore@ntis.gov

CITATION

Bright, J., B. Carrier, D. Conlin, W. Danforth, W. Hoffman, J. King, B. Oakley, J. MacDonnell, D. Robinson, W. Schwab, and M. Zykov. 2013. Collaborative Archaeological Investigations and Sound Source Verifications within the Massachusetts Wind Energy Area. Final Report to the U.S. Department of the Interior, Bureau of Ocean Energy Management, Office of Renewable Energy Programs. OCS Study BOEM 2013-221. 266 pp.

ABOUT THE COVER

Cover image (Map of acoustic reflectors of interest) courtesy University of Rhode Island, Graduate School of Oceanography.

Acknowledgments

The authors and their respective agencies and institutions would like to thank Ms. Ramona Peters (Tribal Historic Preservation Officer, Mashpee Wampanoag Tribe) and Mr. Victor Mastone (Director, Massachusetts Board of Underwater Archaeological Resources) for their invaluable knowledge. Ms. Brandi Carrier (BOEM) served as the Contracting Officer's Representative (COR) for four of the contracts comprising the archaeological aspects of this project and managed administrative matters pertaining to this research. Mr. Tre Glenn (BOEM) served as the COR for the sound source characterization contract for this project. Ms. Constance Murphy assisted with editing the report. The authors would also like to acknowledge our appreciation of the technical contributions of Brian Jordan and James Moore (BOEM); Walter Barnhardt (USGS); Matthew Lawrence, Joseph Hoyt, and Sophie Van Parijs (NOAA); and countless others who contributed to this project.

Foreword

Victor T. Mastone
Massachusetts Board of Underwater Archaeological Resources

The recent headline reads "Fisherman Finds Mammoth Tooth in Load of Scallops." On February 19, 2013, a scallop fisherman recovered what is believed to be a mammoth tooth south of the Isles of Shoal, Gulf of Maine (Macalaster 2013). While recovering unexpected items in fishermen's nets are not rare events, this relatively near shore find is none-the-less quite unusual and, more importantly, speaks to the time when the now drowned continental shelf off the Northeast region of North America was dry land. Why is this so important? It illustrates the maritime landscape is a continuum – physically, temporally, and culturally.

The local, regional, and national importance of the maritime legacy of New England, and Massachusetts in particular, is readily evident. Massachusetts has long been a major center of maritime commerce and naval activity in North America. The ports of Massachusetts, such as Boston, Plymouth, Salem, Gloucester, Provincetown, New Bedford, Nantucket, and Newburyport, can be best described as the maritime gateway to the commerce of North America. These ports and numerous smaller ports provided the extensive maritime infrastructure for vital commercial and naval activities. More than 2,000 terrestrial maritime-related historical sites have been identified just around Massachusetts Bay alone (Cultural Resources Committee 1989). It has been reliably estimated that over 3,000 shipwrecks are located in the waters off Massachusetts (Mastone 2001). Well before European exploration and colonization, the ancient Native American peoples – and continuing through their subsequent generations – utilized this maritime landscape as a dwelling place, sustainable larder, and spiritual space.

This collaborative effort lead by the U.S. Department of the Interior, Bureau of Ocean Energy Management for the Massachusetts Wind Energy Area (MA WEA) expands upon the early pioneering desk top assessment undertaken by the U.S. Bureau of Land Management regional studies of the Continental Shelf (for results of those studies, see Barber 1979 and Bourque 1979). At the sub-regional/local level, the present study serves as an innovative approach when viewed from the perspective of its four accomplishments:

- assessing the "accuracy, effectiveness, and efficiency" of the data collection techniques and parameters found in survey guidelines and recommendation;
- collecting baseline data that can serve as a prototype for future data gathering efforts;
- utilizing a robust cross-government, multi-disciplinary approach in planning, execution, and analysis; and
- fully engaging indigenous peoples at the early stages of project design and throughout the project.

In order to accelerate responsible offshore development, it is essential to reassess tools and techniques to find the most effective and efficient method of data collection. We must also recognize their appropriateness may vary due to scale, research questions, anticipated resources (material culture), and local/regional conditions. Beyond technology, this baseline study is clearly innovative through its collaborative approach to sharing resources (personnel, equipment) and knowledge. In particular, the full engagement of the Wampanoag Tribe in all stages of the study recognizes there is

no disconnect between ancient and modern indigenous peoples regarding the exploitation and value of the marine environment. The oral traditions of the indigenous peoples inform us on subsistence lifestyle and settlement patterns, and the strong spiritual connection. This in turn guides us in the location and identification of submerged ancient Native American material culture. We must recognize that "achieving and maintaining healthy coastal and marine ecosystems requires a fundamental understanding of the relationships between people and the environment. Cultural heritage, which belongs to all people, emphasizes these connections, whether that heritage takes the material form of, for example, maritime resources (such as shipwrecks), natural resources (such as marine species and habitats), or sacred places. …cultural relationships among people and historic, natural, and place-based heritage resources are preserved and perpetuated in ways that recognize and share multiple cultural voices and knowledge systems for the benefit of all" (Marine Protected Areas Federal Advisory Committee 2011).

This study's paleoenvironmental context sets a broad scale understanding of the evolving surficial landscape for the areas south of Martha's Vineyard and Nantucket. This paleogeography reveals the entire MA WEA would have been exposed uplands between 26,500 to 12,300 years before present (yBP); inundation commences at that time with the MA WEA fullly submerged by 10,000 yBP. While resource exploitation continues today, the potentially inhabitable landscape was only available for a short time. There is an assumption that the general topographic structure that we see closely reflects the past. This broad scale topography (major landscape features and characterization) provides an excellent starting point for modeling potential archaeological sensitivity, but its value is limited by its inability to fully reveal the top of the post-glacial land surface without other data inputs.

The historical context spans the full range of human use and potential occupation of the MA WEA starting at approximately 13,500 yBP to the present. Bell (2009) provides an excellent cultural context summary of our knowledge for this region. Our archaeological knowledge of ancient Native American peoples prior to 7,500 yBP is quite limited. When ancient peoples exploited these locales, today's coastal sites were the uplands of their time. Merwin (2001; 2003) emphatically states "we know virtually nothing about coastal adaptation" prior to 6,000 yBP. Ancient peoples adapted to this changing environment. Insights into their responses may assist us today. Similarly, our knowledge of post-contact use of this vast area has limitation. If we look to reported wrecks and extrapolate vessel traffic, this area was not a major route. Much traffic went via Nantucket Sound to north or further offshore to avoid Nantucket Shoals. The same general characterization is seen with fisheries activities until the modern period. Of the reported wreck sites for this locale, the majority of fishing vessels (mainly trawlers) are likely transiting the area rather than fishing in it. Unlike the geo-referenced precision of terrestrial sites, nearly all published shipwreck inventories suffer from an imprecision and/or validation in location and resource description. Thus, they cannot replace investigatory surveys at this time.

The detection and identification of the material culture remains on and under submerged lands is dependent upon a variety of remote sensing technologies. This baseline study included analyses of the major technologies used to identify potential resources: sub-bottom profiling, magnetometry, side-scan sonar and interferonmetric sonar. There may be limitations to geophysical data (acoustic, magnetic) when collected without consideration of potential cultural properties. A valuable component of the historical context section is the informative discussion on detection of the material remains of past cultures. Similarly, the chapters on each technology inform us of their

appropriateness, value, and limitations. While the study's inability to detect buried preserved paleolandscape features (e.g., glacial water courses and wetlands) and verify listed archaeological sites (e.g., shipwrecks) was somewhat disappointing, this may be a result of possible limitations of each instrument type and the data collecting parameters (e.g., line spacing) and the lack of selective and/or systematic geotechnical sampling (e.g., vibracoring) to further characterize and validate interpretations. Unfortunately, there is no single instrument or technique that does it all. However, this study nonetheless provides a useful basis for the design of future data-gathering efforts.

In summary, this baseline study is informed by desktop archival research, geophysical interpretation and oral tradition of native peoples. It was not intended to replace site-specific studies to be undertaken by potential lessees, but to assist them in their future data gathering efforts. Understanding bottom conditions (i.e., currents, sediment transport, bottom type, seasonal variation) will enhance the detection and preservation potential of pre- and post-contact cultural resources (e.g., ancient Native American sites and shipwrecks). We must recognize that it is not simply viewing the submerged landscape, but rather the need to view the buried paleolandscape at a level which allows us to identify, with some reliability, areas of archaeological sensitivity. In conclusion, this baseline study, through its robust collaborative effort utilizing a variety of technologies, serves as a model for future studies by BOEM and as well as serving the needs of potential lessees for this area and other locations.

NB: The views expressed herein are those of the authors and do not necessarily reflect those of the Commonwealth of Massachusetts.

Preface

Brian Jordan
Bureau of Ocean Energy Management

Locating, identifying, and interpreting archaeological sites on land is difficult; the task becomes much more challenging when trying to detect sites that have been submerged and/or buried beneath the ocean. The marine remote-sensing surveys are expensive and time consuming, specialized equipment is needed, expert scientists are required to monitor and interpret the data collection, and the results must be written in a clear and concise fashion for the final reports that are increasingly needed to inform decision-makers and other stakeholders that may lack the required expertise. This project, Collaborative Archaeological Investigations and Sound Source Verifications with the Massachusetts Wind Energy Area, serves as an example of a successful joint effort between scientists and experts from Tribal, State, and Federal government agencies in cooperation with private industry to answer key questions about survey standards and the effects of these surveys on the environment.

The U.S. Department of the Interior's Bureau of Ocean Management (BOEM), who managed and partially funded this study, is dedicated to utilizing applied science and adaptive management to ensure that the best available scientifically-derived information is available to decision makers to achieve expeditious and orderly development of energy and mineral resources on the Outer Continental Shelf while minimizing impacts on the environment. The partners involved in the project included the best available government and industry scientists from the fields of geology, sedimentology, geophysics, oceanography, archaeology, historic preservation, and bioacoustics, as well as the unique and specialized expertise from the Mashpee Wampanoag Tribe, to develop a research design that asked and attempted to answer specific questions related to offshore marine remote-sensing survey requirements currently required by BOEM in advance of the construction of wind energy projects in the Atlantic, and the effects of these surveys on marine mammals and other organisms.

The project is limited in scope and geography, but it is hoped that the collaborative approach will be used as a template for conducting future cost-effective and interdisciplinary marine research efforts. The results also serve to illustrate the benefits of methodological testing and adaptive management to ensure that the best available science and practices are utilized when managing offshore energy and mineral resources.

Abstract

In August and September 2012, the Bureau of Ocean Energy Management (BOEM), Office of Renewable Energy Programs conducted an interdisciplinary, multi-agency study designed to inform the bureau's decision-making with respect to archaeological resources and geophysical surveys offshore the Commonwealth of Massachusetts. Focused in and around the Massachusetts Wind Energy Area, the study was designed to (1) collect empirical data on background and survey acoustics; (2) collect limited data on submerged relic landforms that may have the potential to contain archaeological resources; and (3) conduct a qualitative experiment designed to test the efficiency and effectiveness of interferometric sonar for identifying archaeological resources on the seafloor. In comparison with acoustic models, the observed received levels were below the model estimates with few exceptions. With respect to submerged relic landforms that may have the potential to contain archaeological resources, sub-bottom profiling revealed certain reflectors of interest for future study; the future collection of cores is a necessary component of any effort to conclusively identify paleolandforms. The 234 kHz interferometric sonar system performed as well as the 100 and 500 kHz side scan sonar, with respect to the specific tested equipment, ranges, water depths, and other operational parameters. Finally, additional background and discussion are provided on the physics of underwater sound, magnetic survey for the identification of archaeological resources, and recommendations for consideration with respect to BOEM's *Guidelines for Providing Geological and Geophysical, Hazards, and Archaeological Information Pursuant to 30 CFR Part 585.*

Contents

List of Figures

List of Tables

Abbreviations and Acronyms

AMAR	Autonomous Multichannel Acoustic Recorders
AWOIS	Automated Wreck and Obstruction Information System
BOEM	Bureau of Ocean Energy Management
BS	broadside
BUAR	(Massachusetts) Bureau of Underwater Archaeological Resources
γ	gamma
CG	Coast Guard
Cgs	centimeter-gram-seconds, a measurement of dipole moment
CPA	closest point of approach
CRM	NOAA/NGDC Coastal Relief Model
cSEL	cumulative sound exposure level
CTD	conductivity, temperature, depth
dB	decibel
dB re 1 µPa	decibels with a reference pressure of 1 microPascal
DGPS	differential global positioning system
EF	end fire
ESRI	makers of ArcGIS software
FM	frequency modulation
FSSB	Full Spectrum Sub-bottom
Guidelines	*Guidelines for Providing Geological and Geophysical, Hazards, and Archaeological Information Pursuant to 30 CFR Part 585*
GIS	geographic information system
GPS	global positioning system
GSO	(University of Rhode Island) Graduate School of Oceanography
HRG	high-resolution geophysical
Hz	hertz
JASCO	JASCO Applied Sciences
kHz	kilohertz
km	kilometers
lb	pound
LDEO	Lamont-Doherty Earth Observatory
LGM	Last Glacial Maximum
LIS	Laurentide Ice Sheet
m	meter
MA	Massachusetts
MA CZM	Massachusetts Office of Coastal Zone Management
MA WEA	Massachusetts Wind Energy Area
MLW	mean low water
MLLW	mean lower low water
MO	Master of Oceanography
MoD	maximum-over-depth
MRU	motion reference unit
µs, µsecs	microseconds
MS	Master of Science
ms	meters per second

MSL	mean sea level
µPa	microPascal
MWP-1B	Meltwater Pulse 1B
NAD83	North American Datum 1983 (published 1986), a geodetic reference system used in North America
NAV88	North American Datum of 1988
NEFSC	Northeast Fisheries Science Center
NHPA	National Historic Preservation Act
nm	nautical miles
NMFS	National Marine Fisheries Service
NOPP	National Ocean Partnership Program
NOS	National Ocean Service
NPS SRC	National Park Service Submerged Resources Center
NOAA	National Oceanic and Atmospheric Administration
NOAA/NGDC	NOAA National Geophysical Data Center
OCS	outer continental shelf
OREP	Office of Renewable Energy Programs
PEIS	Programmatic Environmental Impact Statement
PhD	Doctor of Philosophy
psu	practical salinity units
RICRMC	Rhode Island Coastal Resources Management Council
rms	root mean square
SEA	Systems Engineering and Assessment, equipment manufacturer
SEG-Y	Society of Exploration Geophysicists Y format for seismic data
SEL	sound exposure level
SIOSEIS	Scripts Institute of Oceanography (SIO) computer program for enhancing and manipulating marine seismic reflection and refraction data
SPL	sound pressure level
SP	shot point
SRC	Submerged Resources Center
SRVx	NOAA vessel *R/V Small Research Vessel experimental*
SSC	sound-source characterization
TIN	triangular-irregular network
USGS	United States Geologic Survey
URI-GSO	University of Rhode Island Graduate School of Oceanography
UTC	Coordinated Universal Time
UTM	Universal Transverse Mercator
WB	wide band
WEA	Wind Energy Area
WGS84	World Geodetic System of 1984
WHOI	Woods Hole Oceanographic Institution
yBP	years before present

CHAPTER 1

INTRODUCTION

This study gathered baseline geophysical and archaeological information within the Massachusetts Wind Energy Area (MA WEA) in addition to evaluating recommendations made by various parties to the Bureau of Ocean Energy Management (BOEM), Office of Renewable Energy Programs (OREP). It considers the application of additional methods and equipment for archaeological resource identification surveys conducted prior to developing an offshore area for wind energy and characterized sound emitted during these surveys for use in environmental analyses. This report is designed for use by BOEM and federal agencies; tribal, local, and state governments; wind energy developers; and stakeholders in order to facilitate environmentally sound development of our nation's wind energy resources.

1.1 BOEM'S INTEREST AND ROLE IN THE STUDY

BOEM manages the exploration and development of the nation's offshore energy and mineral resources over approximately 1.76 billion acres of the Outer Continental Shelf (OCS), as defined by the OCS Lands Act and the Energy Policy Act of 2005. Specifically, BOEM oversees energy and mineral development on the OCS from initial resource assessments and lease offerings through exploration, development, production, and decommissioning. To meet its management responsibilities, BOEM's strategic goals include:

- achieving expeditious and orderly development of energy and mineral resources;
- minimizing impacts on the environment; and
- developing and employing sound science and partnerships.

To assist in gathering the types of information needed to manage OCS development while minimizing impacts to the environment, BOEM seeks to leverage opportunities that allow partnerships with other federal agencies, state agencies, and tribal governments. These partnerships create efficiencies in BOEM's processes and reduce data-gathering expenditures for multiple agencies and the taxpayers they serve. They also build relationships that will extend these efficiencies and cost reductions into the future; benefit the partners who participate; and provide needed data to inform sound, environmentally-responsible decision-making in the present. As of August 2013, OREP has initiated and/or funded collaborative studies offshore Massachusetts (MA), Virginia, and North Carolina to support efficient and environmentally-responsible wind energy development. This report documents the first of OREP's collaborative research studies, which focused on areas offshore MA.

1.2 THE MASSACHUSETTS BASELINE SURVEY

In July 2012, BOEM invited a number of federal, state, and tribal partners to collaborate with BOEM and its contractor, JASCO Applied Sciences, on an interdisciplinary study offshore MA. These partners included:

- The National Park Service Submerged Resources Center (NPS);
- The United States Geological Survey Woods Hole Science Center (USGS);
- The National Oceanic and Atmospheric Administration Office of National Marine Sanctuaries (NOAA) Stellwagen Bank National Marine Sanctuary and Northeast and Great Lakes Region;
- NOAA National Marine Fisheries Service (NMFS) Northeast Fisheries Science Center Passive Acoustic Research group;
- The University of Rhode Island Graduate School or Oceanography (URI);
- The Massachusetts Board of Underwater Archaeological Resources; and
- The Mashpee Wampanoag Tribe.

These collaborative partners provided scientific and technical advice, shared resources, and assisted BOEM with conducting the survey and analyzing the resulting data. This research could not have been completed without their dedication, hard work and positive team spirit. Detailed synopses of agency and collaborative partners are provided as Appendix A and an index of scientific and advisory personnel is provided as Appendix B.

After agreeing to contribute their expertise to the project through interagency, cooperative, and other agreements and contracts, the research team committed to a two-week period during which to execute the experiment and survey work described in this report. Work in support of the collaborative baseline survey offshore Massachusetts was conducted offshore between August 25 and September 5, 2012.

1.2.1 Study Area: The Massachusetts Wind Energy Area

The survey was conducted offshore MA, in and near the MA Wind Energy Area (WEA). Part of the "Smart from the Start" Atlantic wind energy initiative, WEAs are offshore areas on the Atlantic OCS that appear most suitable for commercial wind energy activities. BOEM, in collaboration with its MA Intergovernmental Renewable Energy Task Force, identified the area depicted in Figure 1-1.

The northern boundary of the MA WEA begins approximately 22 kilometers (km; 12 nautical miles [nm]) south of Martha's Vineyard and 24 km (13 nm) southwest of Nantucket. From its northern boundary, the WEA extends roughly 61 km (33 nm) south. The WEA has an east/west extent of approximately 87 km (47 nm). The northern boundary of the WEA is at an approximately 30-meter (m; 98-foot [ft]) ocean depth and extends to approximately the 60-m (197-ft) bathymetric contour along the south-western boundary. The entire area extends over 300,000 hectares (877 square nm) of the OCS.

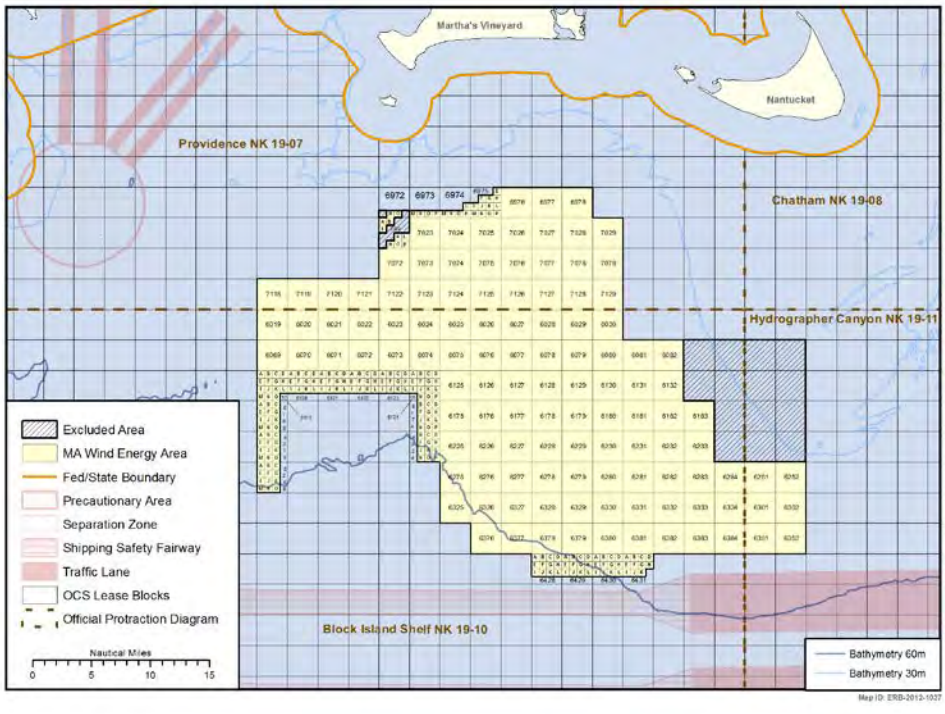

Figure 1-1. Massachusetts Wind Energy Area.

1.3 GOALS OF THE MASSACHUSETTS BASELINE SURVEY

BOEM and the task force members wanted to collect baseline data within the MA WEA to make sound decisions about how to minimize impacts and support BOEM's responsibilities under Sections 106 and 110 of the National Historic Preservation Act (NHPA). In considering these data needs, BOEM also identified a number of other goals that could be met during a single data-collection effort.

This collaborative baseline survey was neither designed, nor intended, to replace site-specific geophysical, hazards, archaeological and other surveys that potential developers may need to conduct prior to submitting a Site Assessment Plan or Construction and Operations Plan (see 30 CFR 585). However, the data collected during this survey may assist in identifying areas of archaeological interest that warrant further investigation as lessees prepare their plan documents. In addition, this study provides the framework for a historic context against which to understand any historic properties that might be identified by developers as projects commence.

Additionally, BOEM wanted to independently field test the feasibility of recommendations that the agency has received with regard to survey methods conducted in support of commercial development. BOEM's *Guidelines for Providing Geological and Geophysical, Hazards, and Archaeological Information Pursuant to 30 CFR Part 585* (*Guidelines*) are supported by decades of survey and research in the Gulf of Mexico and an extensive Environmental Studies Program; but one suggestion received by the National Ocean Partnership Program (NOPP) recommended that the agency also consider interferometric sonar systems as a survey tool. Additionally, consultations with

various parties, including Federally-recognized Tribes, had resulted in the recommendation that BOEM add paleolandscape reconstructions to its requirements for reporting archaeological resources. These consultations also led to recommendations that BOEM further consider the effects of these surveys on acoustically-sensitive marine mammals. BOEM concluded that considering these recommendations in further revisions of the *Guidelines* was warranted and possible within the same field effort and mobilization.

Based on the goals outlined above, the project was designed to achieve four major objectives:

- provide data to consider the effectiveness and efficiency of various recommendations made with respect to conducting surveys, including the use of interferometric sonar and paleolandscape reconstructions (Section 1.3.1);
- obtain limited baseline geophysical, archaeological, and acoustic sound source data within selected portions of the MA WEA and serve as a prototype for future data-gathering efforts, as time permitted (Section 1.3.2);
- leverage partnerships with federal, state, and tribal governments to share project-related resources such as scientific staff, survey equipment, and ship time (Section 1.3.3); and
- involve the Wampanoag people in the identification of submerged paleolandscapes that may retain evidence of prehistoric archaeological resources of interest to them (Section 1.3.4).

1.3.1 Consider and Test Recommendations Concerning Archaeological Resource Identification

The first of the project's main objectives was to provide data to consider the effectiveness and efficiency of various aspects of the NOPP's recommendations for conducting surveys, including paleolandscape reconstruction (Chapter 2), and the use of interferometric sonar (Chapter 6).

1.3.1.1 Evaluate Paleolandscape Reconstruction

The project's planning stage included the preparation of the initial phases of a preliminary paleolandscape reconstruction of the subject study area (Chapter 2). This initial modeling was based on known marine geophysical, geological, and paleoenvironmental data within the MA WEA that would be supplemented with sub-bottom profiler data and may be verified at a later time by the collection and analysis of vibracores. The resulting preliminary reconstruction would then be used to identify areas of potential for retaining evidence of the former subaerial landscape and, in turn, areas that may have the potential to contain submerged precontact archaeological sites. Decided with preference given to the Mashpee Wampanoag Tribe's expressed areas of interests within the WEA, several areas were selected for sub-bottom profiler survey. Sub-bottom profiling was conducted using the EdgeTech system at various settings as shown in Section 1.4.4. below, and described in Chapter 4. After the survey, the reconstruction was revised based on data analysis. Preparation of the preliminary paleolandscape reconstruction was informed by the methods used by Westley et al., 2011, which was previously utilized in a number of other submerged landscape investigations (e.g., Fedje and Josenhans 2000; Gafney et al., 2007).

After the survey was complete, the reconstruction continued by analyzing the sub-bottom profiler data to determine if elements of the past landscape are buried beneath modern seabed sediments. The

analysis identified buried geomorphic features of interest, such as in-filled channels, that would require further sampling to conclusively determine their nature.

The paleolandscape reconstruction is depicted in Chapter 2. A historic context is presented in Chapter 3. How these results may be incorporated into a future vibracoring program to sample areas of archaeological potential is discussed in Chapter 9.

1.3.1.2 Evaluate Interferometric Sonar

Survey activities involved a qualitative experiment to test the effectiveness and efficiency of SWATH*plus* interferometric sonar against the side scan sonar in two separate locations within the MA WEA. To be effective at identifying archaeological resources, the team determined that the interferometric sonar must be able to resolve objects of 0.5 to 1.0 m (1.6 to 3.3 ft) or greater. A subjective determination of quality of data also was made.

It was estimated that in 30 to 35-m (98 to 115-ft) water depth, the SWATH*plus* sonar would attain a maximum effective range of approximately 120 m (394 ft) on each of the transducers. In the deepest portion of the WEA (60 m [197 ft]), the range was estimated to be about 200 m (656 ft). The Klein side scan sonar specifications estimate a maximum effective range of approximately 50 m (164 ft) at 900 kHz and 150 m (492 ft) at 455 kHz. The team surveyed a grid in two areas with defined targets using a trackline spacing of 75 m (246 ft), which provided overlapping coverage between the survey lines for the 900 kHz data. The term "trackline" refers to the path followed while collecting geospatial data.

The length of the survey tracklines run was dependent on the size of the target utilized for testing. Perpendicular cross-ties were run using a survey trackline spacing of 150 m (492 ft), unless radically different backscatter was observed. In that case, cross-tie trackline spacing was reduced with additional lines.

This approach enabled the team to mosaic both the low and high frequencies from the Klein system and thereby assess the resolution and quality of the sonar image at both frequencies. The survey allowed for simultaneous collection of the SWATH*plus* at its maximum range, and then compiled several mosaics and grids using various combinations of the trackline data. This provided a dataset that allowed direct comparison of the backscatter from the 234 kHz SWATH*plus* system to the Klein higher frequency data, and also how the higher grazing angles of the SWATH*plus* (a system that is pole-mounted to the vessel at the surface) compares with the lower grazing angle data from the Klein (a system that is towed in the water column behind the vessel) when imaging known targets. The results are presented as Chapter 6. A background on the physics of underwater sound, a context in which to understand these results, is presented in Chapter 5.

1.3.2 COLLECT BASELINE DATA WITHIN THE MA WEA

The second of the project's main objectives was to obtain limited baseline geophysical, archaeological, acoustic and magnetic data within selected portions of the MA WEA and serve as a prototype for future data-gathering efforts, as time permitted. This included obtaining sub-bottom profiler data throughout the MA WEA to support the paleolandscape reconstruction (Chapter 2); conducting limited searches for a select few historic shipwreck listings with high locational

reliability (see Section 1.3.2.1, below); and performing sound source characterizations of the sonar equipment utilized during the survey to determine the noise impact to the surrounding environment (Chapter 7). Although evaluation of magnetometer survey techniques and execution was not originally a goal of this study, the baseline data collection effort offered an opportunity to gather limited magnetometer data within the MA WEA and prompted preliminary research and recommendations with respect to survey techniques (Chapter 8).

1.3.2.1 Ground Truth Shipwreck Listings with High Locational Reliability

According to BOEM's *Inventory and Analysis of Archaeological Site Occurrence on the Atlantic Outer Continental Shelf* (TRC 2012) and Atlantic OCS Shipwreck Database, within the current boundaries of the WEA, there are 25 reported shipwrecks, obstructions, or objects of unknown character; an additional four listings are located within 2 km (1 nm) of the boundaries of the WEA (Chapter 3). The researchers sought to ground-truth the entries in the database with the highest locational reliability and, for as many as possible, confirm or deny their presence at the listed locations. Eight listed wrecks in four different locations were selected for the search, including several that had been listed at multiple locations (Numbers 7623 and 9031 and Numbers 7624 and 9032 (Table 1-1). These reported locations were surveyed in an effort to ground-truth their entries in the database.

Table 1-1.
Previously identified wreck-, obstruction-, and object-entries with high locational reliability.

Name	Number	Depth (m)	Locational Reliability	Type	Lost
Viking	9277	-39	1	F/V[1]	Unk[2]
Unk	9282	-47	1	F/V	Unk
Unk	7625	-45.5	2	Hang; 1979; Loran C	Unk
Adventure II	7623	-46	2	Trawler of 119 gross tonnage	1943
L. & W.B. Co. 11	7624	-46	2	Barge of 862 gross tonnage	1945
PT 200	10009	-46	2	Patrol boat of 33 gross tonnage	1944
Adventure II	9031	-46	3	Trawler of 119 gross tonnage	1945
L. & W.B. Co. II	9032	-46	3	Barge of 862 gross tonnage	1943

[1] F/V= fishing vessel. [2] Unk = Unknown.

A survey grid was established over each of these potential site locations and a survey was conducted. To maximize the likelihood of using one of the listed wrecks for the side scan and interferometric comparisons, the SWATH*plus* interferometric sonar also was operated at the same time as the side scan sonar and the magnetometer, each instrument being mounted or towed in a configuration to reduce possible interference. For detailed discussions of technical methods employed for each of these instruments during the survey, see Chapters 6-8.

Despite thorough searches performed at 30-m (98-ft) line spacing over an area of a quarter mile surrounding the listed wreck locations, none of the eight were identified within that quarter-mile buffer. This is likely due to the source material used to compile the database – that is, many of these listings were made by informants using unreliable navigational equipment (i.e. Loran) in the 1960s

and 1970s and many represent net hangs, which are subject both to boat length and net drag position inaccuracies. Another possible explanation is that objects may have been buried or moved from their original locations by storm events or trawling activities, the latter of which were observed during the survey and are known to occur throughout the MA WEA.

These results are consistent with a 2003 study conducted by BOEM's (formerly MMS) Gulf of Mexico region that attempted to ground truth listings in their similarly-constructed 2001 database. The survey of 20 target locations revealed that only nine target areas contained bottom features indicative of submerged cultural resources and of those nine only one represented a shipwreck (Pearson et al., 2003). As noted in their work and also applicable to BOEM's Atlantic OCS Shipwreck Database, these are extremely small sample sizes and cannot be extrapolated to reflect the entirety either of the Gulf of Mexico or the Atlantic OCS. On the contrary, they underscore the fact that appropriate site-specific survey is necessary to confirm the presence or absence of historic properties.

Because no cultural resources were identified during the search, alternate locations for the testing of the interferometric sonar were selected in nearshore environments at locations of previously identified sites. These testing results are discussed in Chapter 6.

1.3.2.2 Characterize Sound Sources for Noise Impact Analysis

High-resolution geophysical survey equipment used to identify archaeological resources on and under the seafloor operates by sending sound through the water column. While laboratory-measured acoustics analyses have been conducted, few direct measurements of commonly-used equipment have been collected in the ocean during active surveys. Because whales and other sound-sensitive species frequent these waters and use sound to communicate, surveying for archaeological resources may have impacts on them. This study provided a unique opportunity to monitor potential noise impacts of the acoustic survey equipment, providing direct measurements that can be compared with the modeled estimates frequently used in National Environmental Policy Act review documents.

Sound Source Characterization (SSC) of the acoustic survey equipment, the vessel, and background acoustics was performed by JASCO Applied Sciences. Acoustic measurements of the interferometric sonar and the sub-bottom profiler were performed to determine the noise impact to the surrounding environment. The final sound level results for each source and discussion are presented as Chapter 7.

1.3.3 Leverage Partnerships and Share Resources

The third of the project's main objectives was to leverage existing resources, such as survey equipment, vessel time, and scientific expertise, from the pool created by interagency, extra-agency, and tribal government-to-government relationships. Limited additional funding was available from BOEM's Environment Branch for Renewable Energy's funding for reviews under the National Environmental Policy Act to support this survey effort. Data collected is applicable to a number of interests and mission objectives across the spectrum of federal, tribal, state, and local governments. NOAA's Stellwagen Bank and Monitor National Marine Sanctuaries facilitated BOEM's access to the research vessel SRVx from which the survey was conducted (Figure 1-2; Section 1.4.1) and partner agencies provided equipment (Sections 1.4.2- 1.4.7) and skilled technicians and scientists to operate it.

Figure 1-2. Geophysicist William Schwab (far left of frame; starboard side of vessel) from the United States Geological Survey oversees equipment loading on the stern of NOAA's vessel SRVx.

1.3.4 PROVIDE OPPORTUNITIES FOR WAMPANOAG TRIBAL INVOLVEMENT

The final project objective was to involve members of the Mashpee Wampanoag Tribe in the identification of submerged paleolandscapes that may retain evidence of prehistoric archaeological resources of interest to them. During the planning process, however, two additional elements became increasingly clear to the researchers.

First, it was immediately evident how important the sound source characterizations would be. Instead of just another additional data collection effort of the survey, this element – confirming the actual sound release and quantifying the impacts of our survey activities – was of great interest to the Wampanoag tribal members and leadership because of the cosmological, subsistence, and ideological relationship the Wampanoag people historically have – and continue to have – with marine mammals. Wampanoag cosmology discusses Moshup the Giant and his activities that established the Wampanoag people's continuing relationship with the whales. Furthermore, whaling was a precontact subsistence activity that Mashpee and other Wampanoags' ancestors taught to European colonists. The Mashpee continue to view the whales as their relatives and expressed appreciation and interest in the results of this aspect of the survey as a way in which to protect acoustically-sensitive marine mammals.

Secondly, the project and the researchers involved benefitted from having the involvement of Mashpee Wampanoag tribal cultural resources monitors aboard the survey vessel. During their time aboard, Marcus Hendricks and David Weeden discussed Wampanoag traditional subsistence practices and lifeways and suggested why nearshore sites might be more difficult to identify than inland sites because their ancestors tended to live in transitory nearshore camps rather than semi-permanent or permanent inland village sites (Wampanoag oral histories). These tribal members also provided their perspective as Mashpee Wampanoag cultural resource monitors on the project's ongoing activities and decisions. Their continued involvement, and the guidance of Ms. Ramona Peters, Tribal Historic Preservation Officer for the Mashpee Wampanoag Tribe, was a beneficial and important aspect of the project. In the reconstruction of potential paleolandforms on which Wampanoag ancestors may have lived (Chapter 2) and our understanding of this historic context (Chapter 3), the project has greatly benefited from the Mashpee Wampanoag Tribe's involvement.

1.4 SURVEY EQUIPMENT

Cooperation in this project extended to the use of equipment provided and operated by the survey partners, described below.

1.4.1 *R/V SMALL RESEARCH VESSEL EXPERIMENTAL*

NOAA's Stellwagen Bank and Monitor National Marine Sanctuaries facilitated BOEM acquiring access from the Northeast and Great Lakes Region to use the research vessel from which the survey was conducted. The SRVx, *Small Research Vessel Experimental*, (see Figure 1-3 and Appendix C) was the newest research vessel in the East Coast fleet of the National Oceanic and Atmospheric Administration's Office of National Marine Sanctuaries. Equipped with berthing space for eight scientists plus crew living onboard for a seven- to 10-day mission, this vessel provided the archaeologists, acousticians, and tribal participants of the survey the ability to stay on the water for extended time periods, thus allowing them to conduct their research in a more efficient and timely manner. The SRVx has over 200 square feet of dry lab space, a boom crane on the stern with an 1800-kilogram (kg; 4,000-pound [lb]) capacity, and a variety of scientific equipment on board.

The 26-m (85-ft) long fiberglass sandwich core hulled vessel was one of a dozen originally built as Navy gun boats. After extensive modifications, it was given to NOAA for research missions. Because it was originally intended as a patrol boat, the vessel's top speed is 35 knots, with a 2.1-m (7-ft) draft. Especially helpful for remote areas or where rough seas occur throughout the year, the SRVx is capable of filling the gap between missions that use other types of small vessels suitable for day trips, and those that require larger NOAA ocean-going research vessels. The versatility encourages collaborations within NOAA as well as the public and private sectors, particularly appropriate for BOEM's collaborative baseline survey on the OCS.

Through interagency agreements with BOEM, the USGS and NPS provided not only skilled expertise and personnel but also equipment to collect survey data. The following sections discuss equipment utilized during the study and general methods for processing the data. Additional discussion of methods for various aspects of the project is included in the appropriate chapter. Manufacturers' specification sheets are provided as Appendix C.

Figure 1-3. NOAA's geotechnical survey vessel, *R/V Small Research Vessel Experimental* (SRVx).

1.4.2 KLEIN 3000H SIDE SCAN SONAR

Sonar data acquisition was conducted with the NPS's Klein 3000 dual frequency (445 kHz & 900 kHz) side scan sonar. The manufacturer's specifications for this instrument are provided as Table 1-2.

Table 1-2.
Manufacturer-supplied specifications for the Klein 3000H Side Scan Sonar.

Component	Specification
Frequencies	445 kHz; 900 kHz
Transmission Pulse	Tone burst, operator selectable from 25 to 400 μsecs. Independent pulse controls for each frequency
Beams	Horizontal - 0.21° @ 445 kHz, 0.21° @ 900 kHz
	Vertical - 40°
Beam Tilt	5, 10, 15, 20, 25° down, adjustable
Range scales	15 settings — 25 to 1,000 meters

All acoustic data were acquired in Sonar Wiz 5.0, and was processed in either Sonar Wiz 5.0 or Sonar Pro 13.0 software packages. Processed acoustic data were imported and reviewed in ArcGIS to identify and tag anomalies and to correlate, where possible, with magnetic anomalies.

1.4.3 SEA SWATHPLUS INTERFEROMETRIC SONAR

The manufacturer specifications for the sonar are:

- operational frequency: 234 kHz;
- horizontal beamwidth: 0.55°;
- transmit pulse length: 8 to 500 µs; and
- declination angle: 30°.

Co-located bathymetry and acoustic backscatter were acquired using USGS's Systems Engineering & Assessment, Ltd. (SEA) SWATH*plus* interferometric sonar operating at a frequency of 235 kHz. The SWATH*plus* transducer heads measure approximately 45 x 15 x 45 centimeters (cm; 18 x 6 x 8 inches [in]) and the instrument weighs approximately 16 kg (35 lb). The SWATH*plus* was deployed and recovered on-site using a stable side mount.

Vessel motion (heave, pitch, roll, and yaw) was recorded continuously using a Coda Octopus F180 motion reference unit (MRU). Bathymetric data were processed using SWATH*plus* Swath Processor and CARIS-Hydrographic Image Processing Software. Navigation was inspected and outliers edited; MRU and sound velocity data were used to reduce the effects of vessel motion and refraction artifacts. The Generic Mapping Tools processes "blockmedian" and "surface" were used to filter the processed soundings further and create an interpolated bathymetric grid.

The transducer of the side scan sonar consisted of two elements facing opposite directions. The main beam axis is perpendicular to the tow axis pointing 30° below the horizontal. The transducer elements for the sonar are davit-mounted on the port side of the vessel at about mid-ship. The depth of the transducers was fixed at 1.5 m (4.9 ft) below the waterline. The deepest point of the vessel hull was below the transducers by about 0.3 m (1 ft). The hull blocked the beam in a vertical sector from 90° above the horizontal to 5° below.

1.4.4 EDGETECH GEOSTAR FSSB SUB-BOTTOM PROFILING SYSTEM AND SB-0512I TOWFISH

The EdgeTech 3200 SB-0512i sub-bottom profiler operates at frequencies from 500 Hz to 12 kHz. The system transmits a frequency-modulated pulse (called a chirp) that is swept over a frequency range over the duration of the pulse (e.g., 2 to 12 kHz over a pulse length of 20 ms). The amplitude of the signal changes with time and, therefore, with frequency. The system can transmit two types of pulses: frequency-modulated (FM) and wide-band (WB).

Two transducers, KT–504 and KT–216A2, are installed on the profiler towfish along the tow axis (EdgeTech 2009). These transducers have different diameters 34.3 to 16.5 cm (13.5 to 6.5 in) and, therefore, different resonance frequencies. The 3200 SB-0512i has a source level of 210 dB re 1 µPa @ 1 m. The beamwidth is 53° at 5 kHz and 19.6° at 12 kHz (Rob Morris, EdgeTech Marine Customer Service Manager, personal communication). The main beam axis of the transducer points downward. In this configuration, the beam pattern in the horizontal plane is expected to be approximately uniform. The towfish (Figure 1-4) was towed about 30 m (98 ft) behind the vessel, approximately 3 m (9.8 ft) below the water surface.

Figure 1-4. The towfish of the EdgeTech 3200 SB-0512i sub-bottom profiler aboard the R/V SRVx.

Chirp seismic-reflection data were collected using USGS's EdgeTech GeoStar FSSB sub-bottom profiling system and an SB-0512i towfish (frequency modulation [FM] frequency of 0.5 to 12 kHz). The dimensions of the towfish are 104 x 66 x 38 cm (41 x 26 x 15 in) and the towfish weighs approximately 80 kg (178 lb). Data were recorded at appropriate shot rate, pulse length, and frequency sweep to optimize data resolution as a function of water depth and logged in the Society of Exploration Geophysicists-Y (SEG-Y) Rev. 1 format.

1.4.5 AUTONOMOUS MULTICHANNEL ACOUSTIC RECORDERS

Underwater sound was recorded with two Autonomous Multichannel Acoustic Recorders (AMARs, JASCO Applied Sciences). Each recorder was fitted with a TC4014 omnidirectional hydrophone by the Danish company RESON. Acoustic data were stored in 60-min files on internal solid-state flash memory. Data were recorded continuously with the following settings:

- 16-bits per sample;
- 687,500 samples per second;
- 16 to 338,250 Hz useable frequency range; and
- −186 ± 3 dB re 1 V/µPa hydrophone sensitivity

The two AMARs were deployed to the seabed with dual acoustic releases and anchor weights. AMAR 1 (A-1) was deployed directly on Test Track, and AMAR 2 (A-2) was deployed 100 m (328 ft) from Test Track. Test Tracks were sailed for each combination of sources that were operated simultaneously during normal survey operations and at various operating frequencies.

1.4.6 GEOMETRICS G-882 MARINE MAGNETOMETER

Magnetic remote sensing was conducted with NPS's Geometrics G-882 cesium-vapor magnetometer. The Geometrics 882 Magnetometer is equipped with a Tritec PA 500-6 acoustic altimeter for precise height over bottom control. The unit has a downward-looking 500 kilohertz (kHz) acoustic transceiver with a 6 degree beam spread. The 18 kg (40 lb) sensor has a maximum operating depth of 2700 m (9,000 ft). At 30-m line spacing, with the tow fish no greater than 3 m (10 ft) above the seafloor, there is a 92% detection rate for a 45 kg (100 lb) ferrous object that is 5 m (16 ft) from the sensor. Ferrous objects that are smaller and/or further from the sensor will have a smaller probability of detection.

Magnetic data were acquired via Hypack 2012 software, then post-processed using a combination of purpose-built NPSSRC software, AutoCAD, Quicksurf contouring software and ARC GIS. Final data were displayed as ArcGIS datalayers with contours in gammas (nanoteslas) appropriate to the research design.

Data were mathematically corrected with regard to sensor height over bottom as part of the post-processing methodology. Significant magnetic anomalies were noted and correlated (if possible) with acoustic anomalies noted as a separate datalayer in ArcGIS. ArcGIS spatial analyst was used to determine datapoint saturation in the survey areas with concurrent detectability thresholds for different sized ferrous objects based on magnetic contour interval, instrument noise and datapoint saturation.

1.4.7 OTHER EQUIPMENT

Other equipment used during the survey include: a SV Plus^{v2} Sound Velocimeter, and a Hemisphere Power Max Differential Global Positioning System (DGPS) Receiver.

Sound velocity profiles were collected using USGS's ODIM MVP30 moving vessel profiler (a time-of-flight sound velocimeter). Soundings were collected approximately every 2 or more hours when required.

All remote sensing data were positioned with DGPS data supplied by USGS's Hemisphere Power Max DGPS receiver with sub-meter accuracy. Datum North American Datum 1983 (NAD83) was used throughout all data collection, and post-processed for Universal Transverse Mercator (UTM) Zone 19, which covers all of the MA WEA. Following post-processing, all data were integrated for final products in ArcGIS.

1.5 SUMMARY OF CHAPTERS

The results of the Collaborative Archaeological Investigations and Sound-Source Verifications within the MA WEA were prepared by multiple agencies and authors, as described in Table 1-3. The paleogeography of the project area is presented as Chapter 2, followed by a historic context of human settlement and activity as Chapter 3. Chapter 4 presents the results of the sub-bottom profiling conducted during the survey. Chapters 5 and 6 together provide a background on the physics of underwater sound and an evaluation of the operational efficiency and effectiveness of interferometric sonar at identifying archaeological resources. Chapter 7 describes the sound source

characterizations of equipment used during the survey and compares these empirical data against extant models. Chapter 8 discusses marine magnetic sensing for archaeological materials. Finally, Chapter 9 details the agency partners' recommendations for BOEM's *Guidelines* to improve identification of archaeological resources.

Table 1-3.
Authors of each chapter, with affiliations.

Chapter and Title		Author	Affiliation
1	Introduction	Brandi Carrier	Bureau of Ocean Energy Management.
2	Paleogeography and Archaeological Sensitivity Assessment within the Massachusetts Wind Energy Area	Brian Oakley	University of Rhode Island, Department of Geosciences, College of the Environment and Life Sciences
		John King and David Robinson	University of Rhode Island, Graduate School of Oceanography
3	Historic Context of the Massachusetts Wind Energy Area	John Bright and David Conlin	National Park Service Submerged Resources Center
		Brandi Carrier and William Hoffman	Bureau of Ocean Energy Management
4	Results of Sub-Bottom Profiling within the Massachusetts wind Energy Area	David Robinson and John King	University of Rhode Island Graduate School of Oceanography
		William Danforth	United States Geological Survey, Coastal and Marine Geology Program, Woods Hole Science Center
5	Physics of Underwater Sound	John Bright and David Conlin	National Park Service Submerged Resources Center
		William Danforth and William Schwab	United States Geological Survey, Coastal and Marine Geology Program, Woods Hole Science Center
6	Acoustic Imaging for Archaeological Resources: Operational Evaluation of Interferometric Sonar Efficiency and Effectiveness	John Bright and David Conlin	National Park Service Submerged Resources Center
		William Danforth and William Schwab	United States Geological Survey, Coastal and Marine Geology Program, Woods Hole Science Center
7	Sound Source Characterizations for the Collaborative Baseline Survey Offshore Massachusetts	Mikhail Zykov and Jeff MacDonnell	JASCO Applied Sciences, Dartmouth, Nova Scotia, Canada
8	Magnetic Sensing for Archaeological Resources	John Bright and David Conlin	National Park Service Submerged Resources Center
9	Recommendations	David Robinson	University of Rhode Island, Graduate School of Oceanography
		John Bright and David Conlin	National Park Service Submerged Resources Center
		Mikhail Zykov and Jeff MacDonnell	JASCO Applied Sciences, Dartmouth, Nova Scotia, Canada

CHAPTER 2

PALEOGEOGRAPHY AND ARCHAEOLOGICAL SENSITIVITY ASSESSMENT OF THE MASSACHUSETTS WIND ENERGY AREA

The following paleoshoreline reconstruction was prepared by Brian Oakley of the Department of Geosciences, College of the Environment and Life Sciences, at the University of Rhode Island. The presurvey archaeological sensitivity assessment model was prepared by John King and David Robinson of the University of Rhode Island Graduate School of Oceanography.

2.1 PALEOSHORELINE RECONSTRUCTION

This reconstruction depicts the predicted configuration of the paleogeography around the MA WEA south of Martha's Vineyard and Nantucket, MA.

2.1.1 METHODS

2.1.1.1 Bathymetric Data

The paleogeographic reconstructions in this report are based on the topographic/bathymetric digital elevation model produced by the National Oceanic and Atmospheric Administration National Geophysical Data Center (NOAA/NGDC). The NOAA/NGDC Coastal Relief Model (CRM) of the northeast Atlantic basin is a raster grid with a horizontal resolution of 3 arc seconds (approximately 82 m [269 ft]) and a vertical resolution of 1 m (3 ft), compiled from a variety of hydrographic surveys by the National Ocean Service, USGS, and other academic partners (NGDC 1999). A higher resolution model exists around Nantucket (cell size 1/3 arc second [approximately 10 m; 33 ft]), but does not cover the entire MA WEA, and was not used. The higher resolution does not improve the accuracy of the reconstructions at the scale of this project.

2.1.1.2 Vertical and Horizontal Datums of the Coastal Relief Model

The vertical datum of the CRM can be assumed to be the North American Vertical Datum of 1988 (NAVD88) even though the hydrographic data used to generate the grids are tied to mean low water (MLW) or mean lower low water (MLLW) and the topographic data was relative to NAVD88 (NGDC 1999). No attempt was made to correct for the offset between the hydrographic and topographic datum (NGDC 1999). The difference between NAVD88 and MLLW at nearby tide gauges (Newport, Rhode Island (RI; 0.624 m [2 ft]); Woods Hole, MA (0.41 m [1.35 ft])) are within the vertical resolution (+/- 1 m [3 ft]) of the raster grid. The difference between NAVD88 and mean sea level (MSL) is considerably less than the resolution of the data (Newport, (0.1 m [0.03]) and Woods Hole (0.11 m [0.36 ft]), so for the rest of this section, the elevations are referred to as relative to MSL. The CRM was originally projected on the Latitude/Longitude-based World Geodetic System of 1984 (WGS84), but was the reprojected to the Universal Transverse Mercator projection, relative to the North American Datum of 1983 (meters), zone 19N for compatibility with existing isobase and other GIS surfaces.

2.1.1.3 Geographic Information System (GIS) Methods

The NOAA relief model for the northeast Atlantic basin was clipped to an extent well beyond the proposed MA WEA (Figure 2-1). The portion of the CRM deeper than 200 m (656 ft) below MSL (beyond the continental shelf – slope break) was 'set null' using the ESRI ArcMap 10 'Raster Calculator'. This reduces the amount of stretching of the color ramp, and allows for a more consistent color scheme across the reconstructions. The raster CRM surface was contoured at 10 m (33 ft) using ESRI ArcMap 10 Spatial Analyst extension, and the contour lines at -30 m, -40 m, -50 m, -60 m and -70 m (-98 ft, -131 ft, -164 ft, -197 ft, and -230 ft) below present sea level were extracted and exported as individual ESRI shapefiles. The contour line generated by Spatial Analyst was smoothed using a moving window at 250 m (820 ft). This removed dangling nodes and some of the 'jagged' edge effects of contouring the CRM surface, without sacrificing accuracy. The smoothed contour polylines were converted to closed polygons in MapInfo v. 8 GIS software. The CRM raster grid was split into two grids using the 'raster clip' tool in ESRI ArcMap 10, producing two grids for each paleogeographic reconstruction. One grid represents the area above sea level for a given paleoshoreline, one below sea level. This changed the minimum and maximum elevations of the grids for each reconstruction and caused the slight differences in the color ramps on Figures 2-5 to 2-9.

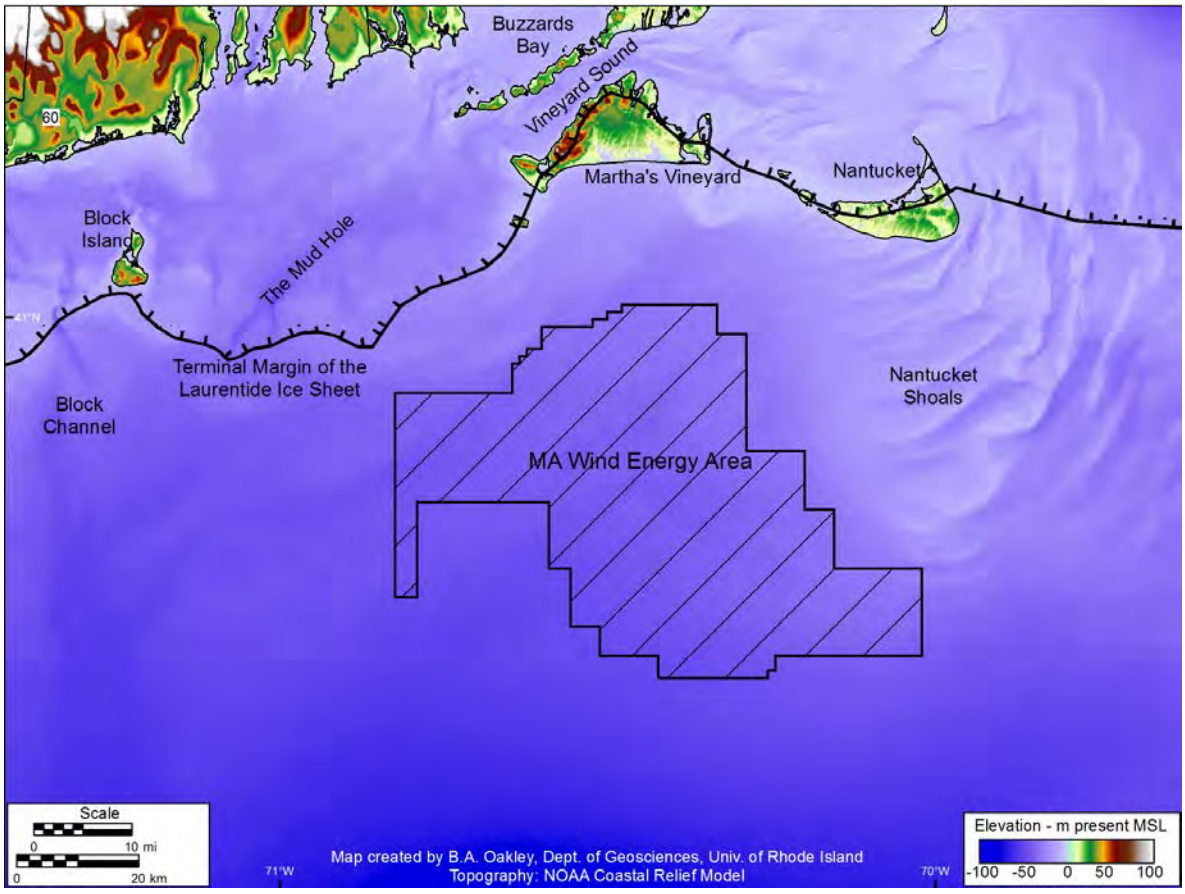

Figure 2-1. Digital elevation model of the study area, showing the location of Massachusetts Wind Energy Area and pertinent geographic locations discussed in the text and the maximum extent of the Laurentide Ice Sheet modified from Schafer and Hartshorn.

2.1.1.4 Eustatic and Relative Sea Level

The paleogeographic reconstructions are based on the eustatic sea level curve of Peltier and Fairbanks (2006). Relative sea level is based on the curve presented in Oakley and Boothroyd (2012), which was developed for the terminal margin of the Laurentide Ice Sheet (LIS) at Block Island, Rhode Island (75 km [135 nm] west of the MA WEA), but is thought to be applicable to the area around Martha's Vineyard and Nantucket. The difference in age of any given sea level for the MA WEA is generally less than 200 years (Table 2-1; Figure 2-2). Relative sea level curves were generated using the algebraic difference between isostatic adjustment and eustatic sea level. For additional details on the sea level curve, see Oakley and Boothroyd (2012). The isostatic rebound curve has a half-life of 1,000 years, and is flat prior to 16,000 yBP with the assumption that isostatic rebound did not begin prior to this (Ridge 2004).

Table 2-1.
Summary of the relative and eustatic sea levels used herein.

Sea level (meters below present)	Relative Sea Level (Oakley and Boothroyd 2012) (years before present)	Eustatic Sea Level (Peltier and Fairbanks 2006) (years before present)
-30	10,000	10,000
-40	11,100	11,100
-50	11,500	11,500
-60	12,400	12,300
-70	13,500	13,300

2.1.1.5 Pre-rebound Surfaces

Isostatic adjustment from the loading and unloading of the LIS was accounted for by creating isobase surfaces reflecting the total isostatic depression (Figure 2-3A). Using the linear plane of rebound measured in coastal New England of 0.85 m · km-1 uplifted northwest (336º) towards the presumed center of the LIS in Hudson Bay Canada (Koteff and Larsen 1989; Koteff et al., 1993), raster surfaces were created in a geographic information system. A 1-km (0.5-nm) grid of points matching the extent of the study area was created using the 'Hawth's Tools' extension for ESRI ArcMapTM 9.3, and the 'Near' command calculated the distance from each of the generated points to the baseline 50 km (27 nm) south of the terminal margin. This distance was multiplied by the assumed uplift profile, interpolated into a Triangular-irregular network (TIN), and converted into a raster grid surface (pixel size 82 m [269 ft]) (Figure 2-3). The isobase surfaces were subtracted from the coastal relief model in ESRI ArcMap 10 'Raster Calculator' to produce the pre-rebound isostatic elevation models in a manner similar to that presented in Leverington et al. (2002).

2.1.2 RESULTS AND DISCUSSION

2.1.2.1 Assumptions

A major assumption in this work is that there has not been significant erosion or deposition on the continental shelf after the LIS retreated from southern New England. The topography below present sea level is based on modern bathymetric data and was not corrected to reflect post-glacial deposition. No attempt was made to account for sediment lost to erosion since deglaciation and it is

assumed that the post-glacial deposition is in the same order of magnitude of post-glacial erosion. During marine transgression, the same processes act on the modern shoreface (e.g., wave and tidal currents, storms). The identification of 'paleoshorelines' in this report approximates the position of the shoreline based on the present understanding of regional sea level rise during latest Pleistocene to Holocene time. This does not identify coastal features (i.e. barriers, lagoons [Coleman 2008]) which have been completely modified during transgression and submergence. While the topography has been modified, the general structure remains; for example, the area known as Nantucket Shoals would have remained a promontory, and closed depressions like 'The Mud Hole' would have been potential lakes and estuaries during sea level rise.

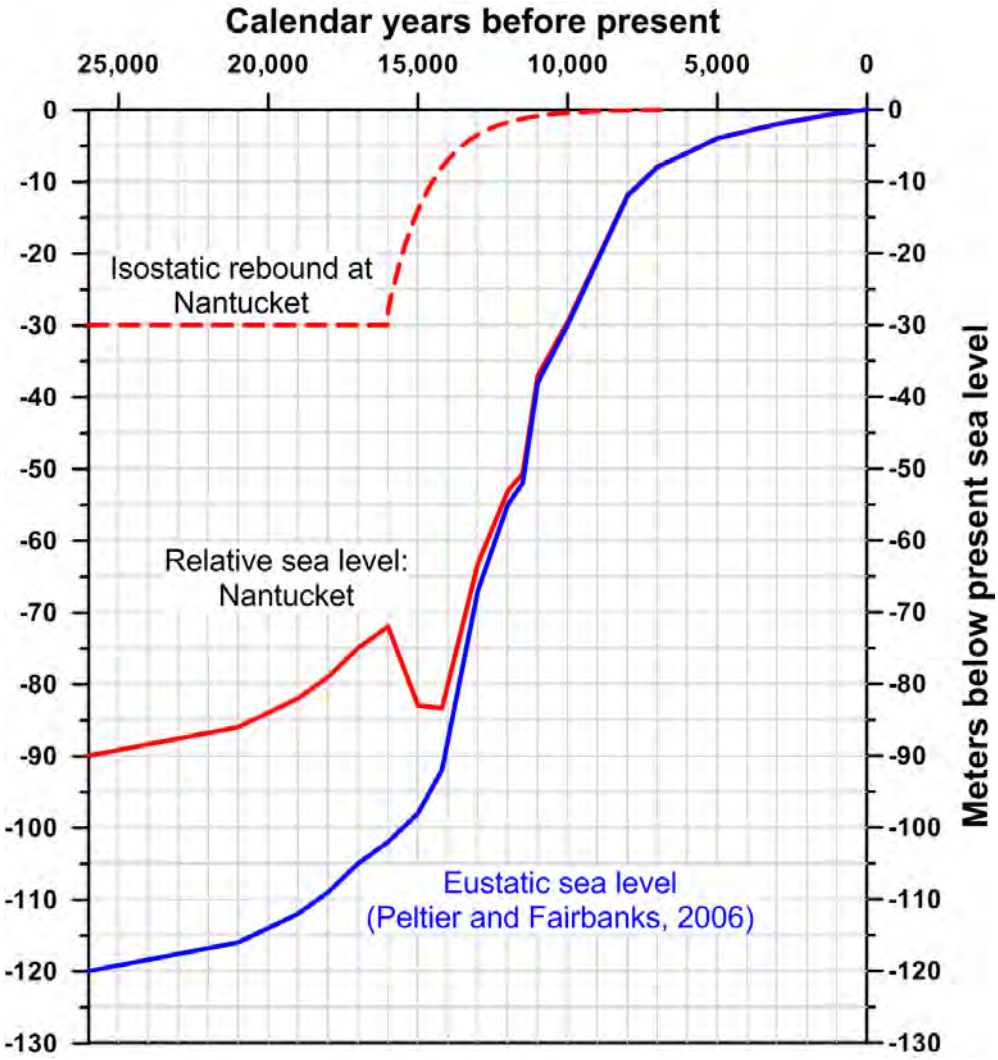

Figure 2-2. Relative sea level and isostatic rebound curve for the Late Wisconsinan terminal margin at Nantucket, Massachusetts. Total isostatic depression is assumed to be 30 m and delayed until 16 ka (Ages in calendar years before present). Eustatic sea level curve is a best-fit line drawn through the points presented in previously published sea level curves (Donnelly and Bertness, 2001; Oldale and O'Hara, 1980; Peltier and Fairbanks, 2006; van de Plassche et al., 1998). The Late Pleistocene and Early Holocene time portion of the curve closely mirrors the curve of Peltier and Fairbanks (2006) while the Late Holocene portion of the curve indicates sea level in southern New England is slightly older than the original Peltier and Fairbanks (2006) model. Relative sea level curve is the algebraic difference between the eustatic and isostatic curves.

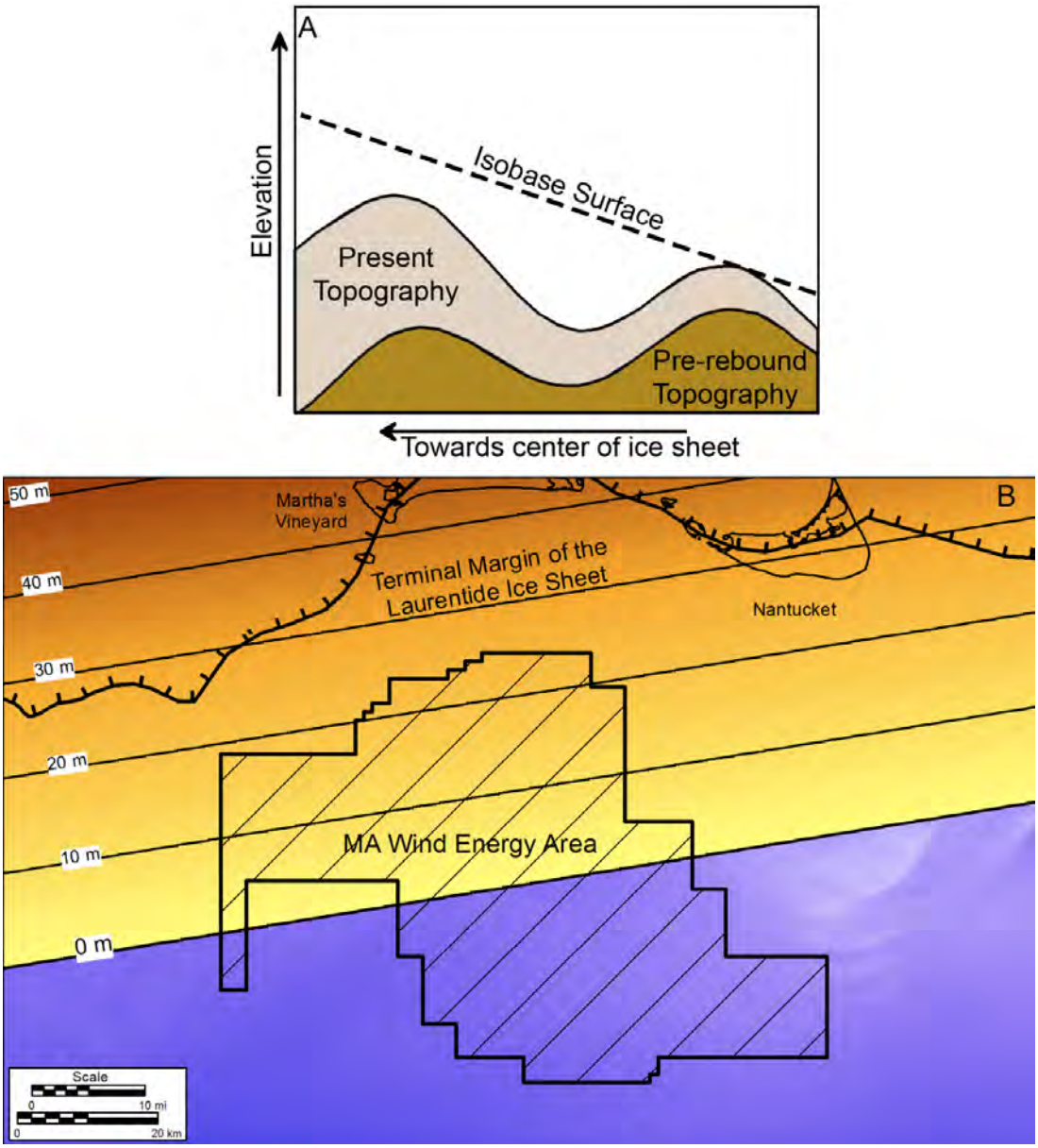

Figure 2-3. A) Schematic cross-section of modern topography, an isobase surface and the pre-isostatic rebound topography (Modified from Leverington et al., 2002 and Oakley and Boothroyd, 2012). B) Isobase surface reflecting 30 m of depression at the terminal moraine.

The isostatic uplift profile used in this work assumes that the profile of isostatic rebound (0.85 m · km-1) was consistent beyond the terminal margin of the LIS. This uplift profile of isostatic rebound may decrease with increasing distance south of the terminal margin, and the isobase surfaces used here may overestimate depression in the area around the MA WEA. The presence of a peripheral forebulge beyond the terminal margin of the ice sheet remains debated. This study assumes that if there was a peripheral forebulge, it was a collapsing, non-migrating forebulge (amplitude 20 to 40 m [66 to 131 ft] (Barnhardt et al., 1995; Dyke and Peltier 2000; Stanford 2010) at a distance greater than 150 km [81 nm] beyond the terminal margin). A forebulge greater than 150 km [81 nm] south of the terminal margin of the LIS would have been located beyond the edge of the continental shelf, and would not have had a major impact on relative sea level in southern New England.

2.1.2.2 Paleogeographic Reconstructions

The assumed lack of rebound beyond the 0 m isobase produces no change in the topography in the southern portion of the MA WEA (Figure 2-3). Prior to the onset of isostatic rebound around 16,000 yBP, relative sea level at the terminal margin (i.e. Nantucket) would have been -72 m (236 ft) below present sea level *if* the land to the south was depressed enough to allow inundation (Figure 2-4). The topography of the outer shelf around the MA WEA area, specifically the lack of an incised channel (i.e. Block Channel south of Montauk, NY and Block Island, RI) (Figure 2-1), suggests that there was no significant inundation of the inner shelf south of Martha's Vineyard and Nantucket. Consequently, there were no paleoshorelines in the MA WEA prior to the onset of isostatic rebound. As eustatic sea level rose from its last glacial maximum lowstand at greater than 120 m (394 ft) below present 26,000 yBP, the shoreline would have transgressed across the outer continental shelf during the late Pleistocene, and would not have undergone a more complicated transgression/regression history similar to the Gulf of Maine (Barnhardt et al., 1995; Belknap et al., 1987).

By 13,300 yBP (relative sea level 70 m [230 ft] below present) the paleoshoreline would have been approximately 10 km (5 nm) south of the MA WEA (Figure 2-5). Marine water began to inundate the southern end of the MA WEA by 12,300 yBP (sea level 60 m [197 ft] below present) (Figure 2-6). A narrow embayment may have been flooded just west of the MA WEA at this time. Transgression through the MA WEA continued, and approximately half of the site was inundated by 11,500 yBP (sea level 50 m [164 ft] below present) (Figure 2-7). Sea level rise across the northern half of the MA WEA would have been relatively rapid between 11,500 and 11,000 yBP rising from 55 to 35 m (180 to 115 ft) below present sea level during that time (see Figure 2-2). This coincides with meltwater pulse 1B, although the timing and magnitude of MWP-1B is still debated (Bard et al., 2010). While these are described as roughly coincident with the onset and culmination of MWP-1B, the duration of the pulse may have been less than 300 years (Liu and Milliman 2004).

The reconstruction presented for sea level 40 m (131 ft) below present (Figure 2-8) shows a large embayment just west of the MA WEA that represents the 'paleo-Vineyard Sound.' The entire MA WEA was inundated by 10,000 yBP (sea level 30 m [98 ft] below present) (Figure 2-9). The topographic high east of the MA WEA known as 'Nantucket Shoals' would have been a promontory, although the absolute elevation of this landform cannot be determined. The bedforms (sand ridges and sand waves) on the seafloor of Nantucket Shoals are a modern (Holocene) construct, formed and modified by wave-generated and tidal currents.

2.1.3 CONCLUSIONS

Based on the current understanding of relative sea level and isostatic rebound in southern New England, paleogeographic maps were generated for the proposed Massachusetts wind energy area south of Martha's Vineyard and Nantucket, Massachusetts. There was no inundation of the MA WEA area prior to approximately 13,000 yBP. Shoreline transgression and sea level rise through the southern half of the MA WEA would have been relatively consistent (approximately 1 m (3 ft)/1,000 years) based on the eustatic curve of Peltier and Fairbanks (2006). Sea level rise through the northern half of the MA WEA would have been rapid, coinciding with meltwater pulse 1B.

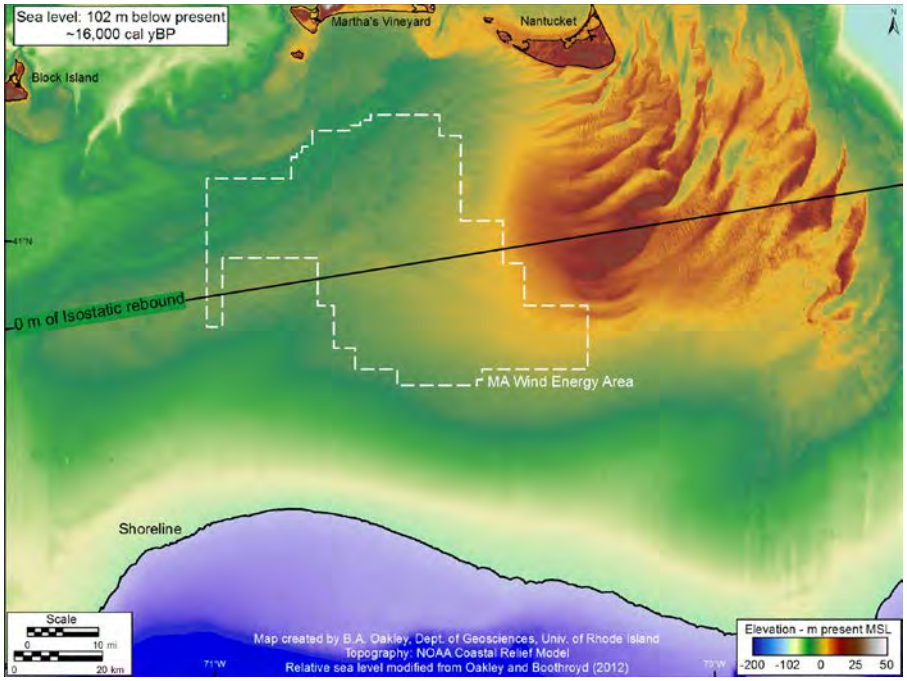

Figure 2-4. Paleogeography of the inner shelf south of Martha's Vineyard and Nantucket at 16,000 yBP; eustatic sea level 102 m (335 ft) below present. The landscape north of the baseline (0 m isobase) has been corrected for isostatic rebound. Reconstructions are all done using modern bathymetry, and do not include an assumption of the topography prior to marine transgression or any removal of sediment deposited since.

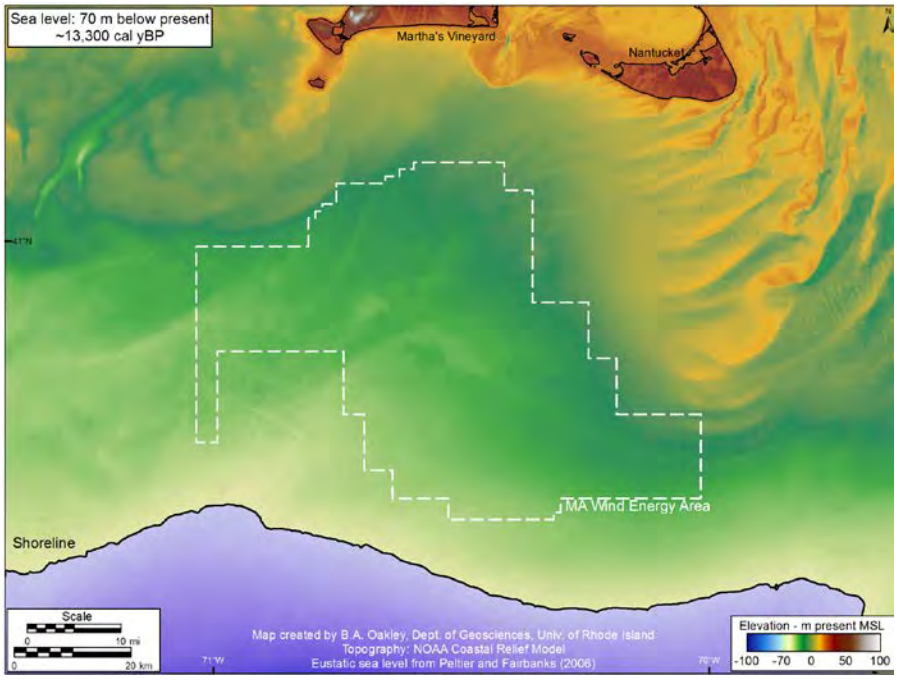

Figure 2-5. Paleogeography of the inner shelf south of Martha's Vineyard and Nantucket at 13,300 yBP; relative sea level 70 m (230 ft) below present. This is approximately coincident with the end of meltwater pulse 1A (Fairbanks 1989). Based on the relative sea level curve of Oakley and Boothroyd (2012), this would date to 13,500 yBP.

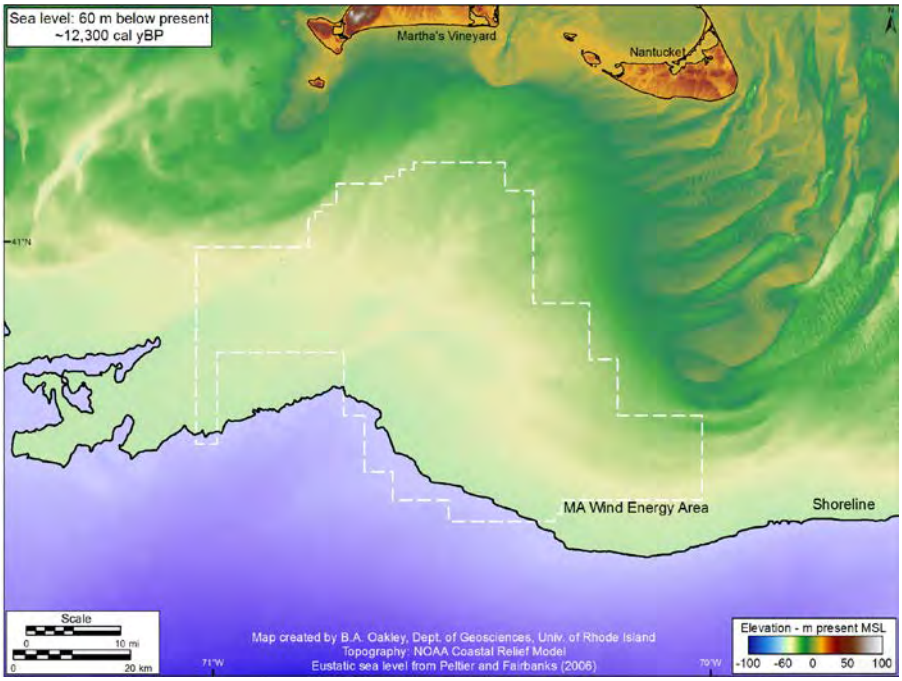

Figure 2-6. Paleogeography of the inner shelf south of Martha's Vineyard and Nantucket at 12,300 yBP (based on the eustatic curve of Peltier and Fairbanks (2006); relative sea level 60 m (197 ft) below present.

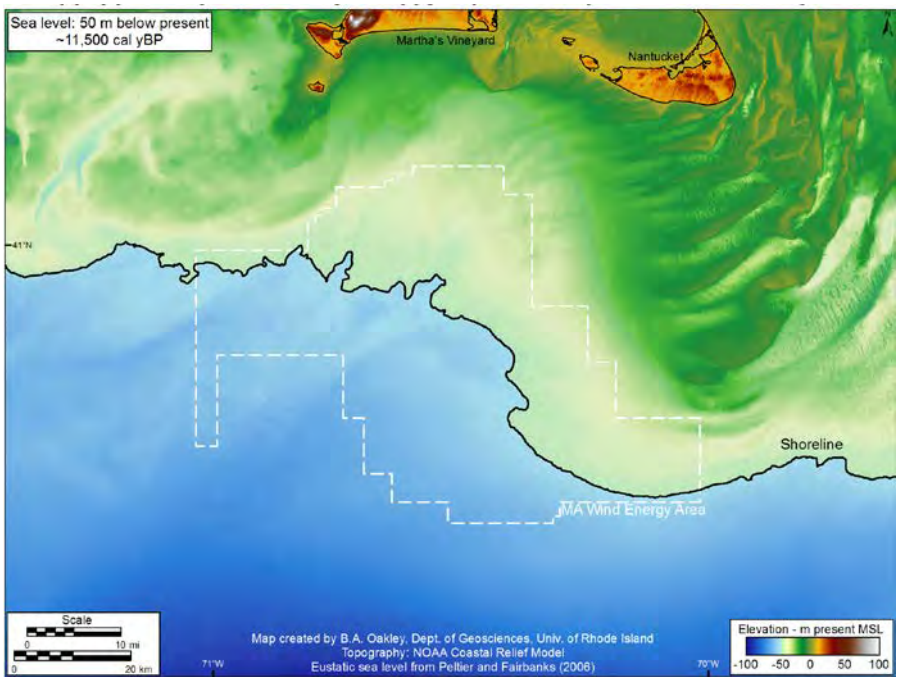

Figure 2-7. Paleogeography of the inner shelf south of Martha's Vineyard and Nantucket at 11,500 yBP; relative sea level 50 m (164 ft) below present. This is approximately coincident with the onset of meltwater pulse 1B (Fairbanks 1989), although the origin and magnitude of MWP 1B remains debated (Bard et al., 2010). By this time relative sea level is essentially in sync with eustatic sea level.

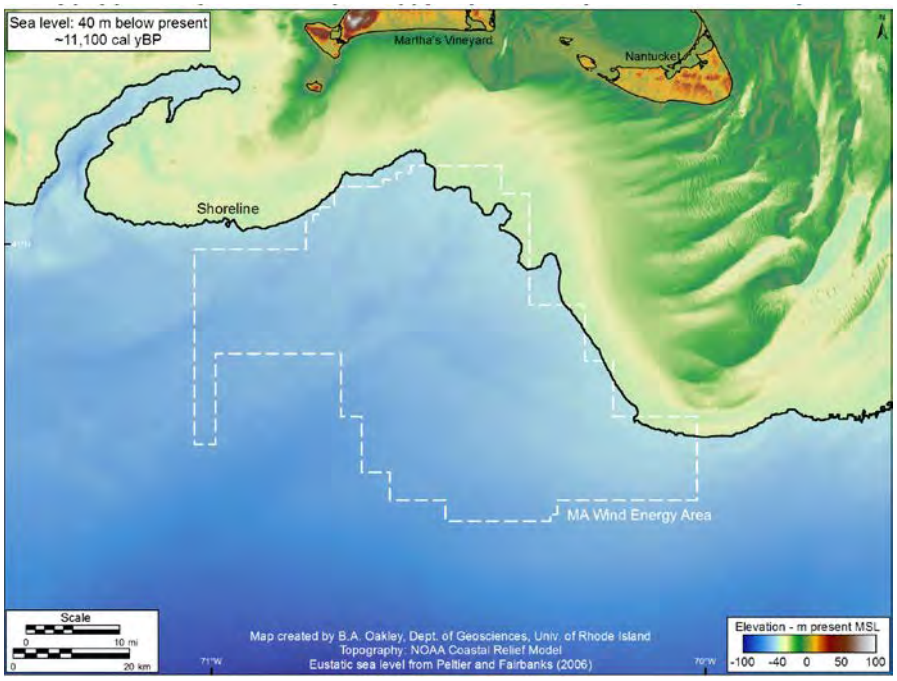

Figure 2-8. Paleogeography of the inner shelf south of Martha's Vineyard and Nantucket at 11,100 yBP; relative sea level 40 m (131 ft) below present. This is approximately coincident with the termination of meltwater pulse 1B (Fairbanks 1989), although the origin and magnitude of MWP 1B remains debated (Bard et al., 2010).

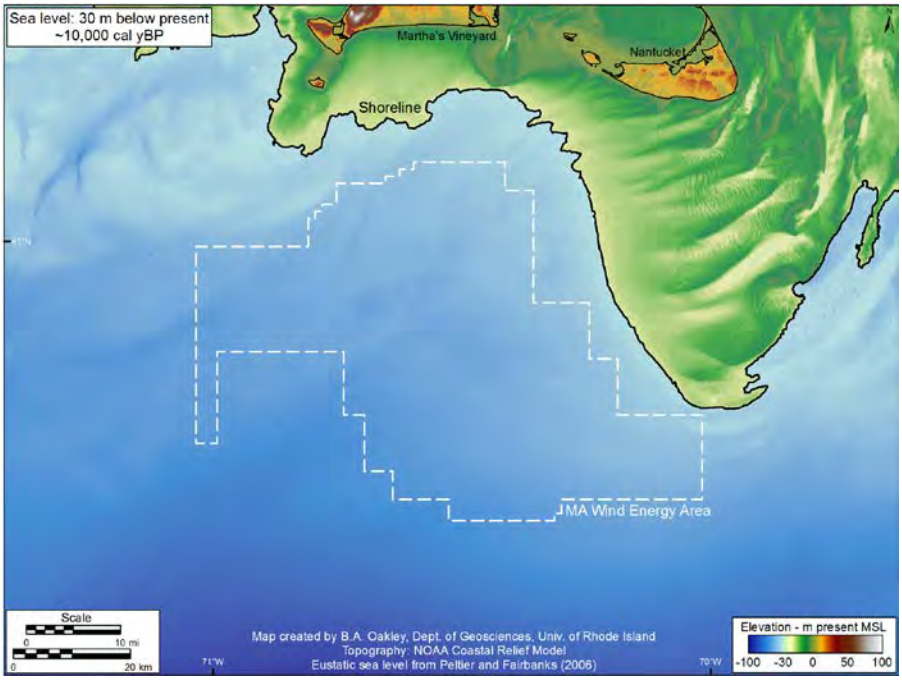

Figure 2-9. Paleogeography of the inner shelf south of Martha's Vineyard and Nantucket at 10,000 yBP; relative sea level 30 m (98 ft) below present.

2.2 PRESURVEY PRELIMINARY ARCHAEOLOGICAL SENSITIVITY ASSESSMENT MODEL

2.2.1 INTRODUCTION

A preliminary, pre-survey archaeological sensitivity assessment model was developed to assist in designing the field survey strategy. The assessment analyzed the paleoshoreline reconstruction (discussed in Section 2.1) and existing geophysical data from an archaeological perspective, taking into consideration the timing of the exposure of this portion of the continental shelf, as it relates to the known human occupation of the region, and drawing from analogies of where archaeological sites are known to be located on land. The archaeological sensitivity assessment provided recommendations on the most effective way to conduct broad-scale geophysical field survey, particularly sub-bottom profiling, within the MA WEA. The survey recommendations were designed to provide a general sampling of the formerly exposed land available for human occupation with the goal of identifying landforms or other features that may have the potential to contain precontact period ancient Native American archaeological deposits and that may warrant further investigation.

As a result of this research, a series of maps with recommended survey transects were created in ArcGIS and submitted to BOEM's field team for use in the planning of the 2012 field survey operations within the MA WEA. This section was prepared to accompany those drawings and briefly summarizes the methodological and theoretical contextual framework from which they were developed.

2.2.2 METHODS

Development of this preliminary pre-survey sensitivity assessment model for the MA WEA generally followed a proven modeling approach utilized throughout southern New England by Robinson (see Robinson et al., 2004), and by Westley et al., (2011) off the coasts of Ireland and Newfoundland during investigations of drowned landscapes of the Late Pleistocene to Early Holocene period.

The preliminary archaeological assessment is based on sea level rise data and the reconstructed paleoshorelines presented in Section 2.1 and on existing geophysical data that was obtained from URI-GSO's examination of several different online sources.

2.2.2.1 Preliminary Sea Level Rise and Paleogeographic Reconstruction

The paleoshoreline reconstructions developed for the MA WEA are presented in Section 2.1, above (see also Figures 2-4 through 2-9). Some important considerations need to be noted relevant to the application of these reconstructions to the discussion of archaeological potential within the MA WEA. A major assumption incorporated into the paleogeographic reconstruction is that there has not been significant erosion or deposition on the continental shelf after the LIS retreated from southern New England. That is, the topography below present sea level is based on modern bathymetric data and was not corrected to reflect post-glacial deposition. No attempt was made to account for sediment lost to erosion since deglaciation, as Oakley (above) assumes that the post-glacial deposition would have been on the same order of magnitude as was post-glacial erosion. During the marine transgression of the MA WEA, the same processes acting on the modern

shoreface (wave and tidal currents, storms, etc.) may have been working on the faces of the paleoshorelines, though they are not necessarily identical given that the rates of sea level rise changed as the WEA was inundated.

The identification of "paleoshorelines" in this model must be seen for what they are – preliminary approximations of former shoreline positions based on the present understanding of regional sea level rise during latest Pleistocene to Holocene time and the limited geophysical data available for the MA WEA. Absent more detailed, MA WEA-specific sub-bottom profiling and geotechnical (e.g., vibracores or borings) sampling data, this model does not identify specific coastal features (i.e. barriers, lagoons, etc., as was attempted for the waters south of Block Island by Coleman and McBride [2008]), nor does it take into account the transformative effects of transgression and submergence. It is assumed that while the formerly subaerial topography of the MA WEA has been modified, its general structure remains similar to what it was in the past. For example, the area known as "Nantucket Shoals" northeast of the MA WEA may have been a promontory, and closed depressions, like "The Mud Hole," west of the MA WEA, may have been lakes and estuaries or a glacial drainage system subsequently filled prior to sea level rise and their transgression. Without sub-bottom profiler data and cores, any estimation of formation processes is preliminary.

2.2.2.2 Existing Geophysical Data

A preliminary review of online geophysical databases and URI GSO's survey data archives was completed in support of this modeling effort to determine the availability of extant geophysical data recorded previously within the MA WEA study area and whether or not any of it provided information that would help identify areas of interest where the 2012 field survey efforts could be focused.

Online databases reviewed as part of this review included NOAA's National Geophysical Data Center (http:// www. ngdc.noaa.gov/ngdc. html); USGS Coastal and Marine Geoscience Data System (http://cmgds.marine.usgs.gov); and Lamont-Doherty Earth Observatory's (LDEO) Marine Geoscience Data System (http://www.marine-geo.org/portals/seismic/). NOAA, USGS, and LDEO each maintain extensive databases of publically-available oceanographic data, including sediment and biological samples, bathymetry, sidescan sonar and sub-bottom profiler data. These databases are accessible through online mapping software, which enables the user to highlight the geographic area of interest and view the data available in that area. In addition, the databases also provided links to cruise reports, scientific papers, and, in some instances, GIS data layers. While each of these databases is updated frequently to include recently acquired data, they also include select older analog data that have been scanned and uploaded. Bathymetry data from NOAA's National Geophysical Data Center were used to prepare Figure 2-10 for the purposes of pre-cruise survey planning. No other data available in the researched databases were relevant to this study.

In addition to online public databases, URI-GSO maintains an archive of research data acquired from research cruises conducted from URI-GSO vessels. Of particular interest are several surveys conducted in the 1960s aboard the *R/V Trident*, which bisected the MA WEA. The results of one of these studies, an unpublished 1967 Ph.D. thesis by L. Garrison entitled *Cretaceous-Cenozoic Development of the Continental Shelf South of New England*, contains a number of interpreted sub-bottom profiles in or near the WEA. Three additional sub-bottom profiles were published by Knott and Hoskins in 1968, though navigational accuracy is of concern with profiles of this age.

2.1.3 CONCLUSIONS

The paleogeographic reconstruction of relative sea level and the approximate locations of paleoshorelines within the MA WEA are based on the eustatic sea level curve of Peltier and Fairbanks (2006) and Oakley and Boothroyd's (2012) relative sea level rise curve developed for coastal RI. These reconstructions indicate that at the time of the Last Glacial Maximum (LGM), about 26,500 and 19,000 years before present (yBP), the southern terminus of the Wisconsin Ice Sheet extended southward to within between 16 to 32 km (9 to 17 nm) of the northern limits of the MA WEA, sea level was between 120 and 135 m (399 to 443 ft) lower than it is today, and the entire MA WEA was exposed land available for human habitation (see Figures 2-4 to 2-6).

Based on Oakley's paleogeographic reconstructions (see section 2.1), the entire MA WEA would have been exposed and available for human habitation between about 26,500 and 12,300 yBP (a period of approximately 14,200 years; see Figures 2-5 through 2-9). Beginning at 12,300 yBP, an increasingly smaller portion of the MA WEA would have been part of the exposed and inhabitable landscape, with the southern half of the MA WEA inundated within 800 years and the remainder (i.e., the northern half) of the MA WEA submerged within another 1,500 years after that. Because the entire MA WEA was submerged by 10,000 yBP, the only known cultures of native tribal people that could be represented in the MA WEA's archaeological record would be those of the pre-Clovis (pre-12,500 yBP), Paleoindian (12,500 to 10,000 yBP), and Late Paleoindian (10,500 to 9,500 yBP)/Early Archaic (10,000 to 7,500 yBP) periods (Garrison et al., 2011).

Assuming that the region's ancient tribal people would likely have been drawn towards the more resource-rich coasts of the ocean, rivers, and lakes for the purposes of resource procurement and settlement, as well as access to more easily travelled transportation routes via the shoreline and the coastal waters (Fischer 1997; Garrison et al., 2011), examination of the existing geophysical survey data resulted in the identification of areas hypothesized to have higher potential for retaining evidence of submerged precontact archaeological sites, based on the reconstructed/modeled locations of paleoshorelines and the existing bathymetry's suggested locations of buried paleochannels, lakes, ponds and embayments. Robinson and King's (Robinson et al., 2004) previous experience identifying archaeologically sensitive buried paleosols in a high-energy offshore environment indicates that the interior flanks of topographic lows, such as those revealed in the available bathymetric contours, are optimal locations for conducting field survey to acquire data that will further inform the post-survey sensitivity assessment model, particularly sub-bottom profiling, because of their higher potential for preservation of paleosols.

The arrangement of proposed survey transects focuses on intersecting as many of these features as possible, while at the same time providing a more generalized dataset from survey transects distributed broadly across the entire MA WEA (Figure 2-10). The transects consist of four broadly spaced and strategically located high priority primary survey transects following the strike of the reconstructed paleoshorelines, and five associated tie-lines, which follow the dip of the seafloor. Areas within the overall distribution of survey tracklines were also identified as being optimal locations for conducting more detailed survey within the MA WEA, time permitting. In light of the minimal amount of existing data presently available for the MA WEA, any new geophysical survey data that is acquired represent a significant contribution to our present knowledge of the MA WEA's geomorphology and archaeological sensitivity for containing precontact archaeological deposits.

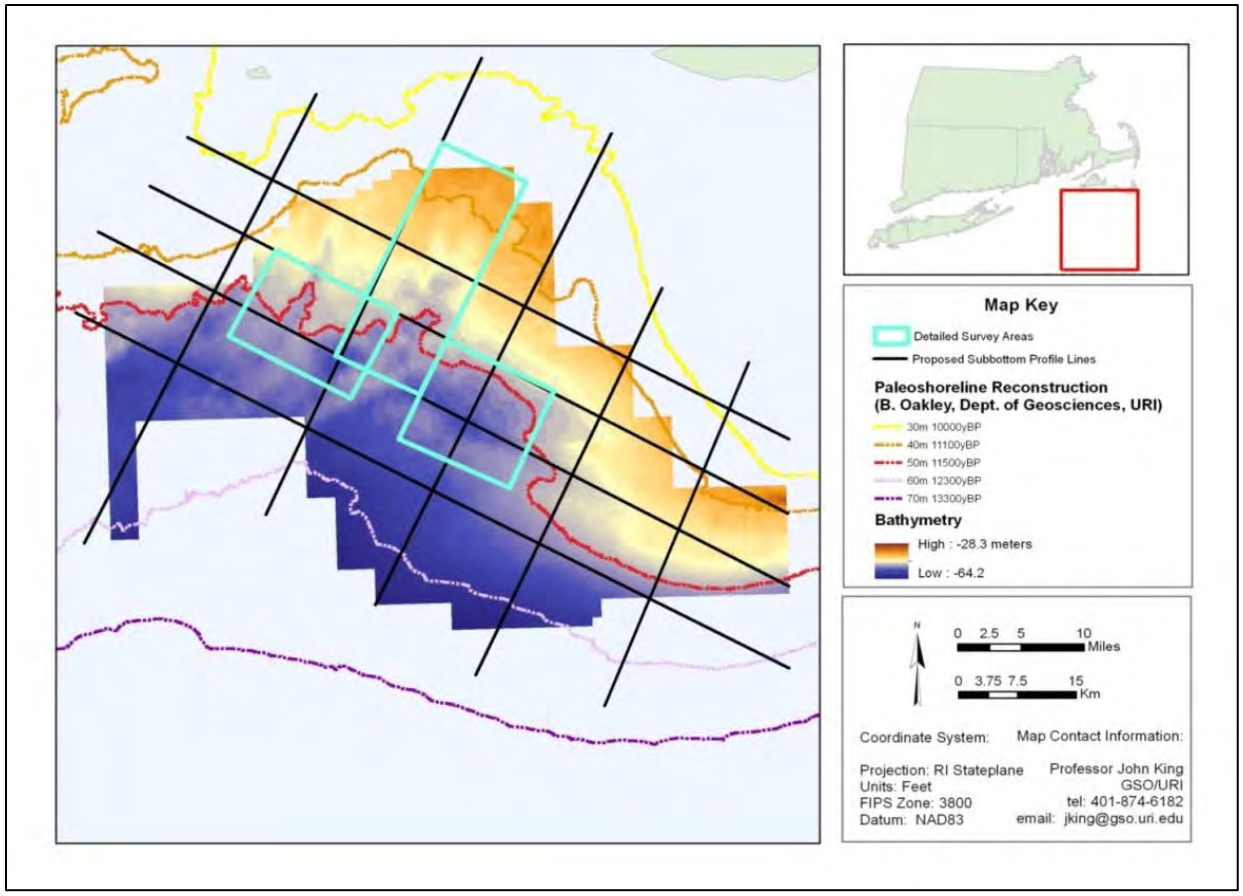

Figure 2-10. Reconstructed paleoshorelines, proposed survey transects and areas of detailed survey within the MA WEA.

CHAPTER 3

HISTORIC CONTEXT OF THE MASSACHUSETTS WIND ENERGY AREA

The following historic context was prepared by multiple authors working in collaboration. The discussion of the area's material culture was prepared by John Bright and David Conlin of the National Park Service Submerged Resources Center and Brandi Carrier of the Bureau of Ocean Energy Management. The estimations of potential for the presence of submerged precontact and historic cultural resources and the number of previously listed wrecks and obstructions were prepared by Brandi Carrier and William Hoffman of the Bureau of Ocean Energy Management.

As part of the Cooperative Baseline Survey Offshore Massachusetts, a historic context was prepared to inform researchers about the patterns of human cultural behavior that occurred in the vicinity of the Massachusetts WEA. According to the *Secretary of the Interior's Standards and Guidelines for Archaeology and Historic Preservation*, contexts serve as the foundation for decisions about the identification, evaluation, listing on the National Register of Historic Places, and treatment of historic properties. As such, contexts are an important tool in the stewardship of historic properties. This context is not intended to be exhaustive, but rather to provide preliminary background information for any historic properties that may be identified through the activities of developers in the future, and a basis for understanding these properties as part of the broad patterns of Cape Cod's maritime history. The context comprises the available evidence of human habitation in the southern Cape Cod area, including Martha's Vineyard and Nantucket and demonstrates that, from the precontact through historic periods, this area served as an important source of maritime resources.

Known information about the MA WEA is relatively sparse; no systematic archaeological surveys have been conducted either immediately within – or in the vicinity of – the MA WEA and no bathymetric surveys have been conducted since the 1960s. Thus, the majority of the researchers' knowledge about the potential for historic properties to be present within the MA WEA comes from BOEM's *Inventory and Analysis of Archaeological Site Occurrence on the Atlantic Outer Continental Shelf* and BOEM's Atlantic OCS Shipwreck Database (TRC 2012). For the historic period, these were compiled from primary and secondary sources from multiple repositories, institutions, and agencies with an interest in maritime history and are comprised largely of commercial and government databases (TRC 2012). For the precontact through protohistoric periods, these sources primarily were compiled from late Pleistocene/early Holocene site and settlement pattern information from terrestrial sites, used as analogs for nearby coastal areas submerged during the Holocene transgression, coupled with the work of the University of Rhode Island (see Chapter 2 and Figure 3-1). Contributions to this chapter were also based on the oral histories of the Wampanoag people shared by Mashpee Wampanoag tribal members and cultural resources monitors Marcus Hendricks and David Weeden during the survey. Of particular relevance is Elizabeth A. Little's 1987 *Bibliography for Historic and Prehistoric Nantucket Indian Studies.* Ms. Little granted permission to the Wampanoag Confederation for use of the bibliography and Ms. Ramona Peters, Tribal Historic Preservation Officer for the Mashpee Wampanoag tribe, provided the bibliography to the research team to support this effort.

3.1 PRECONTACT PERIOD

3.1.1 ARCHAEOLOGICAL EVIDENCE

The southern New England coastal plain "was perhaps one of the last places [in North America] to be colonized" (Speiss, et al. 1998), but, regardless of the mechanism, by 13,000 yBP, Paleoindian populations were resident there (Bell 2008; Doug Harris, pers. communication). Though now submerged, the MA WEA was, at this time, a terrestrial, late Pleistocene/early Holocene landscape resplendent with diverse resources available to support human occupation. Positioned south of Cape Cod and what are now the islands of Nantucket and Martha's Vineyard, the MA WEA was a continuation of the same coastal plain marine landscape. At the horizon in which archaeological remains appear in the Cape Cod area, sea level was rising and inundating large portions of the previously exposed MA WEA, an area which was dry land for the sixteen thousand years prior. Over the course of a five thousand year period following the last glacial maximum, sea level transgressed and, by the Early Archaic transition of 10,000 yBP, inundated the entirety of the MA WEA (see the paleoshoreline reconstruction in Chapter 2, Figures 2-1 through 2-6 and Figure 3-1).

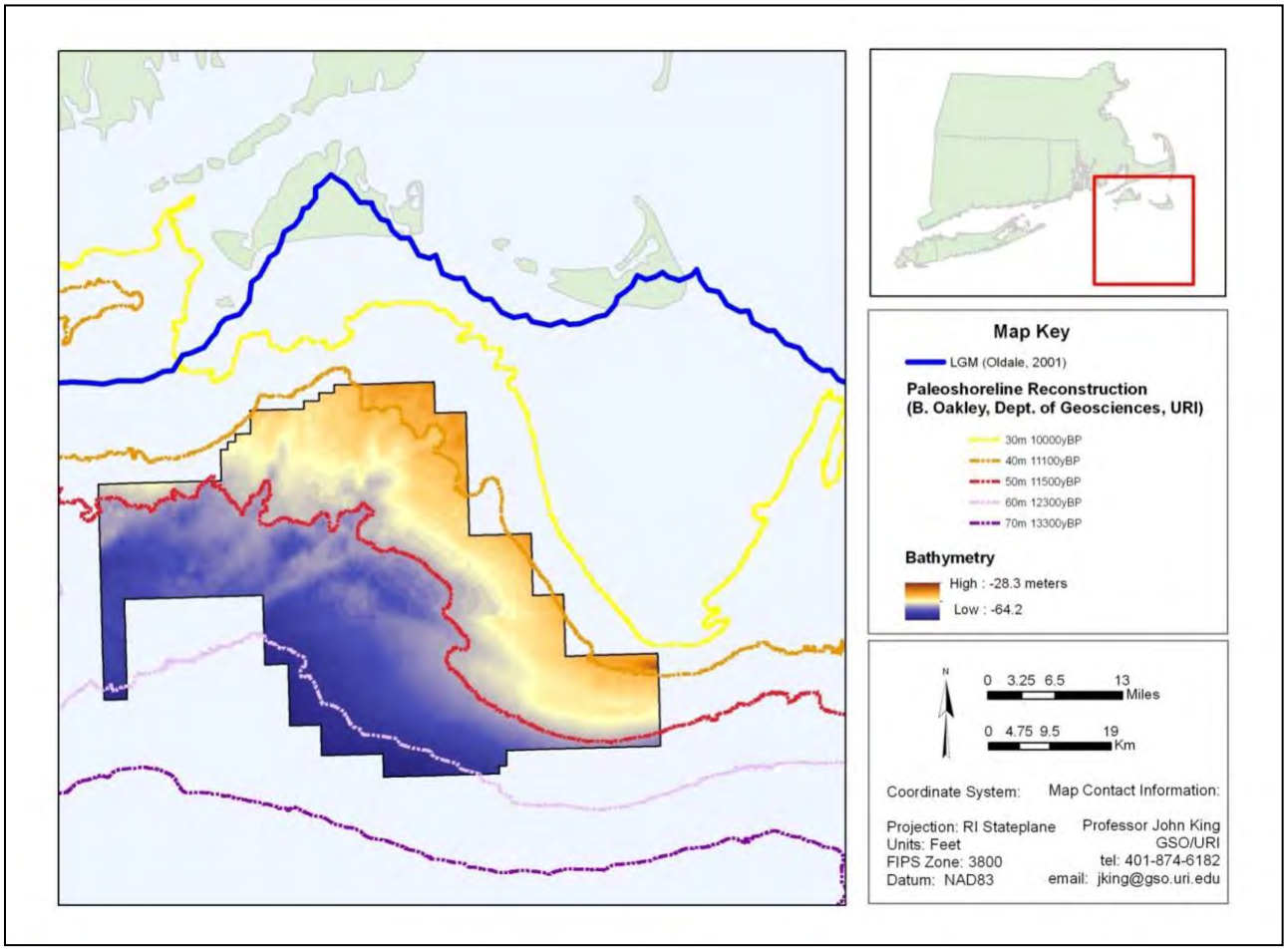

Figure 3-1. Reconstructed circa 13,300 yBP to 10,000 yBP paleoshoreline locations within and in the vicinity of the MA WEA (see Chapter 2).

The submergence of the WEA around 10,000 yBP sealed the area from introduction of Native American habitation sites generated by later cultural traditions. Based on relative sea level mapping, the only possible Native American remains deposited in the area would be from either Paleoindian (12,500 yBP to 10,000 yBP) or Early Archaic (from 10,000 yBP to 7,500 yBP) cultural traditions, and perhaps only small amounts of the latter. Materials dating to subsequent cultural periods may only have been transported to this area through episodes of secondary deposition.

During the course of this transgression, it is likely that precontact people occupied the areas along these shifting shorelines. Assuming continuity with known subsistence patterns of the Wampanoag Tribe, these Paleoindian and Early Archaic inhabitants would have seasonally utilized marine resources and thus moved in concert with the rising shoreline (Marcus Hendrix, pers communication). According to Wampanoag oral histories, seasonal subsistence patterns would have brought the Wampanoag ancestors toward the shoreline for the establishment of warm-weather housing; during cooler seasons Wampanoag ancestors retreated inland for access to a wider variety of resources and the shelter of the families' homes or *wetuash*. Archaeological remains of these practices in the WEA could have been buried following inundation (see Stright 1986; Merwin et al., 2003; Faught 2002, 2004; Merwin 2010). Some geological processes accompanying inundation (see McMaster 1984; Peck and McMaster 1991), and subsequent superstorms, however, could also inhibit the preservation of archaeological resources. Nevertheless, the presence of submerged archaeological materials in the inshore areas of the Gulf of Mexico and New England suggests the possibility of similar preservation in the WEA.

Oral histories of the Wampanoag and Narragansett tribes document that, throughout precontact times, Native American ancestors maintained a highly-flexible scheme of adaptation to the environment that included seasonal camp sites near the marine coast with more permanent camps inland, utilization of all available resources throughout the area of occupation, and rotation of habitation spaces to afford time for resources to revitalize and repopulate (Marcus Hendrix, pers. communication). The known archaeological record for the Paleoindian and Early Archaic periods in this part of New England empirically manifest this oral history; documented site types from mainland Massachusetts include a few large "marshalling" camps occupied by considerable numbers of people as well as smaller camps utilized by small, highly-mobile groups (Bell 2008). Furthermore, preference for littoral, estuarine, and riverine landscapes with access to rich fresh-water resources and transportation pathways is substantiated by study of the body of early precontact sites throughout New England (Bell 2008). Precontact people traversed the easternmost areas of Massachusetts using regional river drainages – the Ipswich, Merrimack, Mystic, Charles, Neponset, and Taunton Rivers (Bell 2008) – and relocated to other resource procurement areas as needed. According to the oral histories, Wampanoag and Narragansett people had long-range formal and informal trade associations that spread throughout the localities operating under the Wampanoag national identity, as well as outside of it (Doug Harris and Ramona Peters, pers. communication).

Known, stratified sites with reliable temporal contexts dating from the Paleoindian and Early Archaic periods remain rare along the New England Coastal Plain. One possible explanation for this lack of evidence suggests that current terrestrial archaeological survey paradigms for locating sites from these periods in New England are lacking, at best. In other words, just because archaeologists have not identified these sites, does not necessarily mean that they do not exist. Additionally, the rapidly changing environment characterizing the late Pleistocene to early Holocene time period that affected the MA WEA also affected both the site types utilized by the prehistoric inhabitants of New

England as well as the geography of the landscape itself. The need for flexibility of both social and economic behavior with respect to changing environmental conditions would have produced an archaeological record that reflects limited temporal occupation and varying functionality, such as small interior camps and coastal extraction sites. Along with these, larger habitation sites situated near interior water bodies (such as large wetlands) and associated with water and food resources may have been inundated by rapidly changing environmental conditions. Like their counterparts on the outer continental shelf, large Early Archaic period archaeological sites situated near large lakes, rivers, and extensive wetlands and their secondary, perennial drainage systems may have been common on the Coastal Plain of New England, but were submerged by rising sea level (TRC 2012).

3.1.1.1 Paleoindian Period

Throughout North America, the Paleoindian cultural tradition is characterized by small bands of nomadic hunters that utilized stone and bone tools. Paleoindian sites are identified through diagnostic lithic artifact types, including fluted or lanceolate projectile points; imported, exotic lithic materials; and non-diagnostic artifact assemblages, which often include gravers, scrapers, and channel flakes (PAL 2011).

The corpus of known and archaeologically-recorded Paleoindian sites in New England is small, diverse, and located well inland (Bell 2008). Until very recently, no *in situ* evidence of Paleoindian occupation had been documented on Martha's Vineyard. Several isolated finds of diagnostic projectile points have been located in personal artifact collections (Bouck et al., 1983) and from disturbed contexts (from plowed soils at the Lucy Vincent Beach Site; Chilton and Doucette 2002). A July 2012 report by Fathom Research mentions that the Carnegie Museum of Natural History has discovered evidence of possible Paleoindian occupations on Martha's Vineyard (Robinson 2012), though nothing has yet been published. The same is true for Nantucket: fluted points have been inventoried in artifact collections but no known *in situ* site locations have been identified and excavated (PAL 2011). Nevertheless, as these islands are part of the continuing landscape and continuous occupation is the oral tradition of the Wampanoag and Narragansett tribes, the lack of evidence more likely reflects poor site preservation and survey bias toward more visible, coastal shell-midden features which date to much later temporal and cultural periods (Robinson, Cozzi, and Wright 2012).

Poor site preservation, an advancing shoreline due to sea level rise, and the population's necessary cultural adaptations to the resulting ecosystem evolution all contribute to this apparent lack of evidence. First, known Paleoindian sites in New England are even further inland today than during their occupation due to rising sea levels: distance to shore and its abundant maritime resources must be understood with reference to the shoreline at that time period. The Paleoindian MA shoreline is in some places 80 km (43 nm) east of the present MA coast. Because of the submergence of many of the earliest of sites, and of an entire site-type – marine coastal sites – our cultural understanding of Paleoindians is already limited. Second, rising sea levels and changing ecosystems resulted in faunal and floral displacement or extinction while other species moved in, requiring often temporally dramatic cultural adaptations by the Paleoindians resident at these margins. Lack of preservation of botantical and faunal remains complicates the picture, as material evidence of Paleoindian presence in New England is very rare. Finally, New England Paleoindians were a diverse group with respect to regional adaptations; this variability makes it more difficult to identify Paleoindian sites by unifying cultural attributes, especially when coupled with rapid adaptations necessary within the

same geographic space resulting from dramatic ecosystem evolution (Bell 2008). Examination of submerged Paleoindian sites will undoubtedly append and at times, possible amend, our understanding considerably (Bell 2008).

3.1.1.2 Early Archaic Period

Population and environmental changes across North America at approximately 10,000 yBP fostered the emergence of a new cultural tradition with a distinct material culture: the Archaic. Climactic warming at the end of the most recent Ice Age, in addition to widespread hunting, placed pressure on big game populations across North America. The result was a gradual dwindling of mega-fauna, the primary food source for most Paleoindians in North America. Simultaneously, Paleoindian populations were growing as they learned to exploit a wider variety of resources. Hunter-gatherer groups adapted by becoming more locally specialized in small game, marine, and plant resources. As specialization in resources developed, so too did a specialization in tools. During this time, Archaic people developed more sophisticated stone tools, stone-vessels, and the atlatl or spear thrower (Wetmore 1975:3-11; Phelps 1983:17-22; Perdue 1985:1-7; West and Morris 2004:128-130). Archaic assemblages also may include ground-stone tools, drills, anvil stones, choppers, and scrapers (PAL 2008, 2011; Snow 1980).

In New England, Early Archaic tool forms have been discovered in a variety of environmental settings suggesting a more broad-based subsistence pattern operating within established territories that were smaller than those exploited by Paleoindian groups (PAL 2008, 2011). Social groups moved within established territories, practicing an increasingly generalized subsistence strategy based on river and lake systems and other freshwater sources (Robinson, Cozzi, and Wright 2012). This pattern is linked to the changing climate of the Early Archaic transition in New England. The regional climate became warmer and drier and gradually the postglacial boreal forest evolved into a mixed deciduous/coniferous forest (Robinson, Cozzi, and Wright 2012) with pine as the dominant species and birch and oak secondary (PAL 2008, Dunwiddie 1990).

Early Archaic sites are rare and social and technological adaptations in New England at this time are not well understood (Robinson, Cozzi and Wight 2012). On Martha's Vineyard, Early Archaic settlements may be inferred by the presence of diagnostic bifurcate base projectile points both in stratified contexts as well as in local collections. Examples in local collections exist from the Norton Site and Oak Bluffs, though according to Robinson, Cozzi and Wright (2012) "there are no known intact Early Archaic cultural components associated with these finds." Other Early Archaic components were recorded at Major's Cove (19-DK-81) and Felix Neck 4 (19-DK-98) sites in Edgartown/Oak Bluffs, and Tiasquim River (19-DK-6) site and West Tisbury. In Aquinnah, an isolated point fragment was collected from the Saxifrax Knoll (19-DK-192) site, an interior upland location and a single bifurcate base point was identified at the East Pasture site near Menemsha Pond (Robinson, Cozzi, and Wright 2012). The evidence on Nantucket includes several isolated bifurcate base projectile points but their provenience is uncertain. A small concentration was collected from the area of Squam Swamp and Sesachacha Pond, and another lanceolate "Dalton-like" point interpreted to be Early Archaic was found near Foulger Creek (PAL 2011), further reinforcing the relationship of these sites to fresh water sources.

3.1.2 Potential for the Presence of Submerged Precontact to Protohistoric Resources

The MA WEA is considered to have a high potential for the presence of submerged precontact cultural resources (TRC 2012) although the potential for the preservation of these sites is complex and localized (Merwin and Bernstein 2003; Merwin, Lynch, and Robinson 2003; Stanford and Bradley 2012). Around 18,000 BP, glaciation began receding and around approximately 16,500 BP portions of the southern New England area were exposed as dry land (Boothroyd and August 2008; Coleman and McBride 2008; Peck and McMaster 1991; RICRMC 2010). Relative sea level and isostatic rebound in southern New England indicate that the WEA would have been subaerial prior to approximately 13,000 yBP (see Chapter 2). By 12,300 yBP (sea level 60 m [197 ft]below present), marine water began to inundate the southern end of the WEA. Shoreline transgression and sea level rise through the southern half of the WEA would have been relatively consistent (approximately 1 m [3 ft]/1,000 years) based on the eustatic curve of Peltier and Fairbanks (2006), and approximately half of the MA WEA was inundated by 11,500 yBP (sea level 50 m [164 ft] below present) (see Chapter 2). Sea level rise across the northern half of the MA WEA would have been relatively rapid between 11,500 and 11,000 yBP (sea level 50 to 40 m [164 to 131 ft] below present) (Bard et al., 2010). The entire MA WEA was inundated by 10,000 yBP (sea level 30 m [98 ft] below present) (see Chapter 2; Oakley and Boothroyd 2012).

When it was exposed, the inner continental shelf would have had aspects like modern coastal zones of southern New England and Long Island, comprising estuaries, lagoons, and protected embayment environments, all creating the potential for human settlement and exploitation, consistent with terrestrial sites in the region from the same temporal periods (Robinson et al., 2004; TRC 2012; PAL 2008 and 2011; Robinson, Cozzi, and Wright 2012). Therefore, the potential exists for submerged precontact archaeological sites within the WEA to range from the pre-Clovis times (earlier than 13,000 BP) and Clovis Paleoindian times (between 13,000 and 11,500 BP), to Early Archaic times (between 11,500 BP to 9,000 BP) (RICRMC 2010, Robinson et al., 2004; TRC 2012). Archaeological sites that could be present include a variety of Paleoindian and Early Archaic site types both with and without terrestrial correlates, such as coastal base camps, special-purpose activity areas, fishing and processing sites, and semi-permanent habitations along formerly exposed, inundated relic river margins and terraces (TRC 2012). Oldale and O'Hara (1980) and Oakley (Chapter 2) estimate submergence of the WEA was completed by 10,000 BP during the Early Archaic. Because the entire MA WEA was submerged by 10,000 yBP, the only known cultures that could be represented in the MA WEA's archaeological record would be those of the pre-Clovis (pre-12,500 yBP), Paleoindian (12,500 to 10,000 yBP), and Late Paleoindian (10,500 to 9,500 yBP)/Early Archaic (10,000 to 7,500 yBP) periods (Garrison, et al. 2011).

If the potential for the preservation of these sites is complex, so too is the process of identifying them. Both Paleoindian and Early Archaic material culture consists of small stone and bone tools, as well as human and faunal remains. Ceramics, larger than most small tools and slightly magnetized, post-date complete inundation of the WEA and would not be located therein unless carried into the area via secondary deposition such as drainage from a river. The implications for marine remote sensing are that the potential types of Native American artifacts in the WEA would be extremely difficult, if not impossible, to locate with conventional acoustic and magnetic remote sensing equipment. They are likely buried, which will prevent detection with a

high-resolution acoustic system, and lacking any significant form of magnetism, cannot be detected with a magnetometer (see also Chapter 7).

3.2 POST-CONTACT PERIOD

3.2.1 ARCHAEOLOGICAL EVIDENCE

Beginning with its earliest settlers, and throughout the colonial period, MA was an entrepôt of the European-Atlantic world and a wellspring for maritime resources such as whales, fish and shellfish. During this time, the waters off Cape Cod were a maritime hub for ships moving between Europe, Africa, the Pacific, and the vast colonies of the New World. As a result, Massachusetts itself became an economic, industrial, political, and cultural center of the New World. Following the establishment of the United States, MA sustained its central maritime role. The remains of this activity, which persist into the present day, litter the seafloor off Cape Cod, Martha's Vineyard, and Nantucket in the form of dozens, if not more, shipwrecks (see Morison 1961; Ferris 1994). The following information, discussed in BOEM's *Inventory and Analysis of Archaeological Site Occurrence on the Atlantic Outer Continental Shelf* (TRC 2012) pertains to historic shipping and shipwrecks on the Atlantic Seaboard.

Though early European exploration of the North American coast began approximately 1000 A.D., it is unlikely to have extended to the area of southern New England and no evidence either in North American or in Europe substantiates any other interpretation. Spanish seafaring constituted the majority of exploration and colonial and trading activities were focused in southern North America until approximately 1600 when early English efforts began in earnest. Refugee Protestant groups from England were arriving in New England to settle: first in Plymouth in 1620, and subsequently at Salem (1626), Massachusetts Bay (1628), Providence (1630), and Hartford (1635). Regular provisions of livestock and manufactured goods were needed to support the colonies, leading to an increase in maritime activity and a greater number of sailing ships. Locally-built small coastal and fishing vessels were added to the English-provided sailing ships and in time, American-made sailing ships replaced the English-built ones on New England coasts (TRC 2012).

Small craft were later provisioned as privateers, and in some cases merchant vessels were used in various military conflicts by outfitting them with guns. King George's War (1744-1748), the French and Indian War (1755-1763), and the American Revolutionary War (1776-1799) heavily utilized these small craft in New England waters. By the rise of the United States as a maritime power in 1794, New England shipbuilding and maritime activity were culminated in the establishment by Congress of the United States Navy. Transatlantic trade continued the growth of maritime activity off the east coast in the form of packet ships. Large, square-rigged ships of 350 tons or more, packet ships operated as common carriers, moving mail, perishable goods, and passengers between New England and Europe. Despite New England's political opposition to slavery, the region benefitted from the ongoing slave trade. Rhode Island was a major provisioner both of ships and of rum, the industries of which were both heavily involved in the slave trade, as substantiated in historic records from the early 1800s (TRC 2012).

The advent of steam engines and ironclads revolutionized the shipbuilding industries. The Civil War in particular had a significant effect on American shipping given that over 100,000 tons of shipping capacity had been lost to Confederate commerce raiders and another 800,000 tons had been removed

from the registries. The forests of the eastern seaboard were depleted of needed lumber and shipyards all over New England had ceased building wooden ships by 1870. Late 19th century steamships were replaced with American-built oil tankers. With World Wars I and II, military shipbuilding and military activities became the focus of the maritime industry in New England (TRC 2012).

The presence of historical artifacts bearing out these activities in the waters south of Cape Cod is unambiguous. Various agencies maintain shipwreck/obstruction/archaeological site databases which list numerous shipwrecks and other material in the vicinity of the WEA. In some instances, these locations are known, such as the numerous shipwreck sites visited by sport divers off Martha's Vineyard and Nantucket (Ferris 1994). These include ships of various sizes and configurations, ranging from small barges, to steam ships, to large steel freighters. Given the magnitude and duration of maritime activity off Cape Cod, especially to the south, a wide range of post-contact period maritime material culture almost certainly rests within the WEA.

Of present interest are the types of historical archaeological materials that could be found in the WEA, especially as pertains to their detectability via acoustic and magnetic imaging systems. Specifically, a delineation between non-magnetic (wood, aluminum, brass, copper, lead, ceramics, and glass) and ferromagnetic (iron and steel artifacts) generally defines the former and latter, respectively. Table 3-1 provides a list of various types of historical vessels, ranging from 18th to the 20th century, including their sizes and, for wooden vessels, an estimated amount of iron content. These range in size from a small French fishing ship (102 ft long, 400 tons) to a World War II aircraft carrier, USS *Enterprise* (824 ft long, 19,875 tons). These vessels span wooden ships, iron-hulled steamers, armed warships, coastal vessels, and large ocean liners—all vessel types know to ply the water in the vicinity of the WEA (Figures 3-2 and 3-3). Though these are not actual shipwrecks in the WEA, they serve as a representative sample from which to model the detection capabilities of specific acoustic and magnetic systems, discussed in subsequent sections.

Aside from shipwrecks, other elements of maritime material culture may also be located within the WEA. These items, however, would be considerably smaller than the mass of an entire shipwreck, such as a partial shipwreck. For instance, a wooden-hulled steamer that wrecked and decayed to the point where only boilers and machinery remained would have a much different acoustic and magnetic signature. Table 3-2 lists various items with their sizes; included are several types of marine engines, anchors, historical ordnance, machinery, and rigging gear (Figures 3-4 through 3-7). Individually, these items are still quite large; aggregated, they would constitute a large site comparable to that of a shipwreck. All of these artifacts, furthermore, are made from iron and steel and so the masses depicted are largely masses of ferromagnetic materials. Large historical artifacts made from other materials, such as lead ballast, brass ordnance, and organic material (e.g., wood, hemp, canvas) could also constitute large archaeological sites. Acoustically, they would produce a similar signature as a metallic object of similar shape and size. Magnetically, however, they would be undetectable.

Other small artifacts may also be present within the MA WEA. These items would be things such as personal effects, fishing tackle, tools, and the sundry other forms of small material culture representative of the colonial, post-colonial, industrial, and modern eras of the United States, and might be associated with larger materials, such as a shipwreck or aircraft wreck. The sheer diversity of these types of material culture, and the low likelihood that any of these objects individually could

be detected with conventional acoustic and magnetic equipment, precludes a more descriptive inclusion. Later discussion on remote sensing capabilities uses hypothetical sizes and masses of objects (such as 50 kilograms [kg; 110 pounds] and 1 m [3 ft] long) as a representation of most small material culture.

Table 3-1.
Descriptions and sizes for various historical vessels.
A representative collection of vessel types which may be found within the MA WEA.

Type	Capacity (tons)	Capacity (Kg)
18th Century French Fishing Ship	400 tons; 50 tons of Iron	45,359 kg
Frigate Boston	514 tons; 64 tons of Iron	58,059 kg
HMS Victory	2162 tons; 250 tons of Iron	226,796 kg
WWII Type VIIC U-Boat	860 tons (submerged)	780,179 kg
USS Monitor	987 tons	895,391 kg
City of Glasgow	1609 tons	1,459,660 kg
WWII Fletcher Class Destroyer	2,500 tons	2,267,962 kg
HMS Warrior	9,137 tons	8,288,947 kg
HMS Dreadnought	10,886 tons	9,875,613 kg
USS Enterprise	19,875 tons	18,030,297 kg
SS America	33,532 tons	29,937,096 kg

Table 3-2.
Listing of assorted maritime material culture items associated with shipwrecks.
(Source: Hughes 1917; Aerodata International 1987; Caruana 1994, 1997;
Bowers 1999; Curryer 1999; CFM International 2010).

Object	Mass (lbs)	Mass (kg)
Compound Steam Engine	590	267
Wright R-1820-40 Cyclone Radial Engine (WWII Fighter Plane)	1,183	537
18th cent. Iron 4 pounder	1,263	572
Small 3x Expansion Engine	2,100	952
Wright R-3350 Duplex Cylone Radial Engine (B-29 Bomber)	2,672	1,212
Small (4th bower) 17th Cent. Anchor	2,800	1,270
CFM56-3B-2 Jet Engine (Boeing 737)	4,299	1,950
18th cent. Iron 24 Pounder	4,800	2,177
18th cent. Iron 42 Pounder	5,537	2,511
Large 17th Century Anchor	6,160	2,794
Large Admiralty Bower	9,072	4,115
Large Water Tube Boiler	9,670	4,386
Early Stockless Anchor	21,280	9,652
Large 3x Expansion Engine	32,150	14,582
600 ft. Anchor Chain	36,512	16,561
Modern Stockless Anchor	40,000	18,143
Single-End Scotch Boiler	80,000	36,287

Larger artifacts are conspicuous objects which should not escape detection from a properly designed remote sensing survey. The threshold of detection, however, for smaller types of artifacts, such as a cannon or small anchor, depends entirely upon the parameters of the survey. Both magnetic and acoustic systems have physical limitations resulting from inherent operation of the equipment, as well as from environmental factors. Data collected during this study facilitates the quantification of both types of limitations in order that future surveys in the WEA be adequately designed to assure detection of the desired types of material culture.

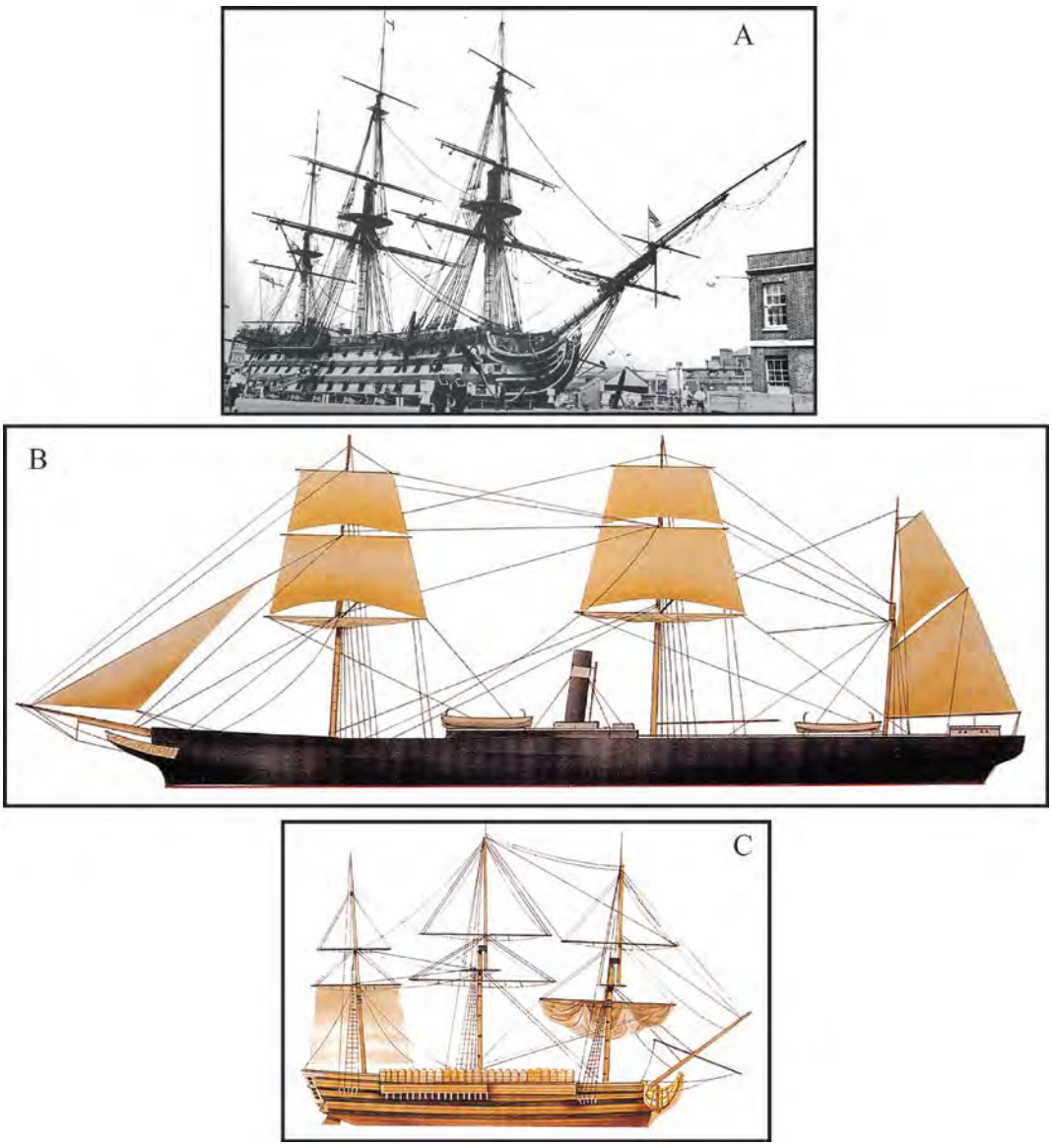

Figure 3-2. From the Top: A) HMS Victory, a 100-Gun British Warship (Source McKay 1987:21); B) Iron-Hulled, Steam-Powered Passenger Liner City of Glasgow (Source: Gibbons 2001:100); C) Late 18th Century French Fishing Vessel, Which Frequently Fished Grand Banks (Source: Gibbons 2001:67).

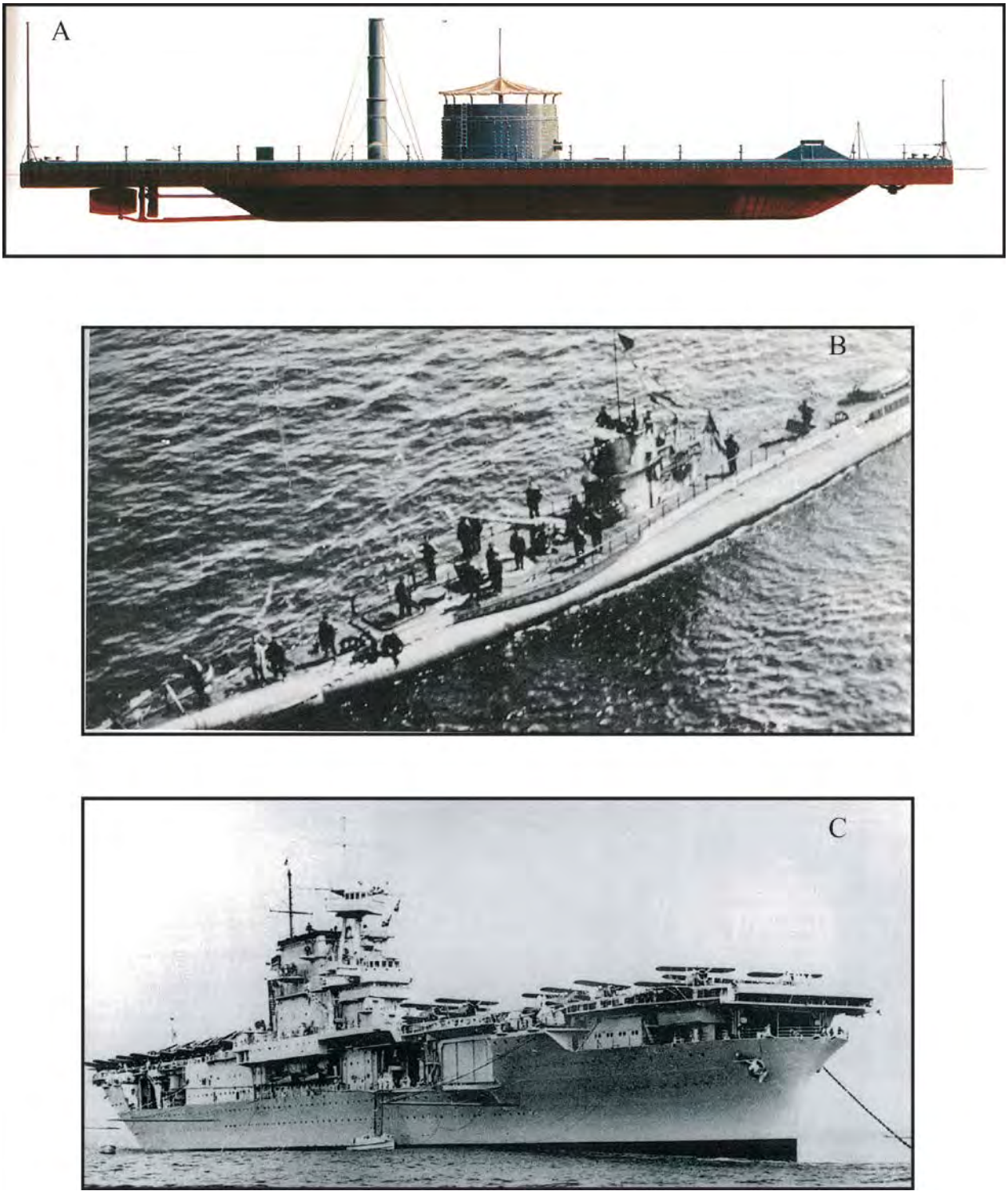

Figure 3-3. From the Top: A) Civil War Ironclad USS Monitor (Source: Miller 1978:31); B) A WWII German Type VIIC U-Boat (Source Tarrant: 1989:51); C) WWII Aircraft Carrier USS Enterprise (Source: Gibbons 2001:373).

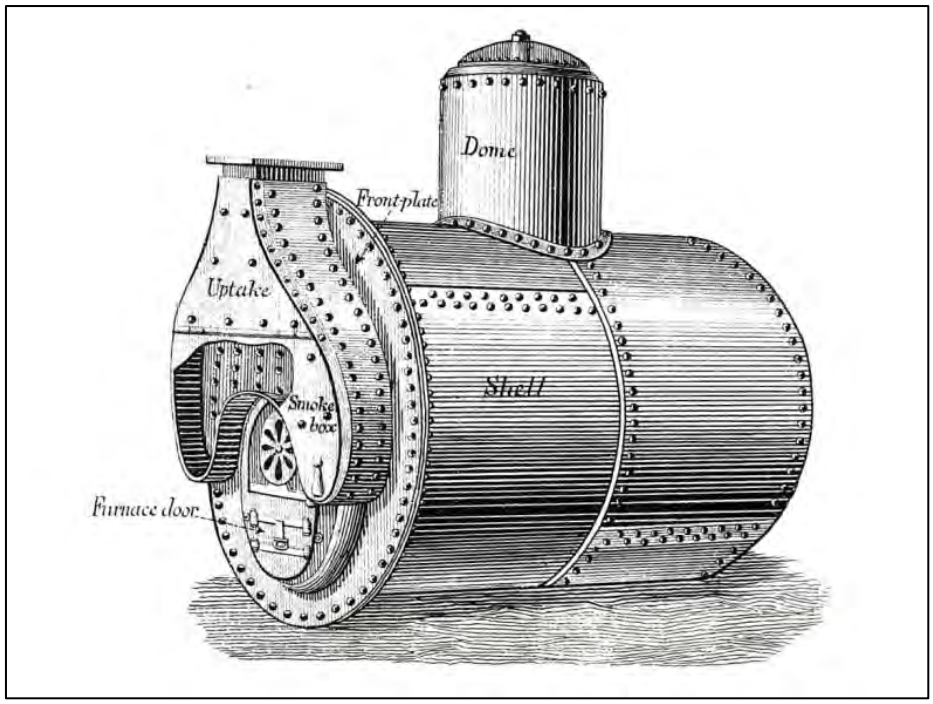

Figure 3-4. Historic Iron Boiler (Source Paasch 1885: Plate 41).

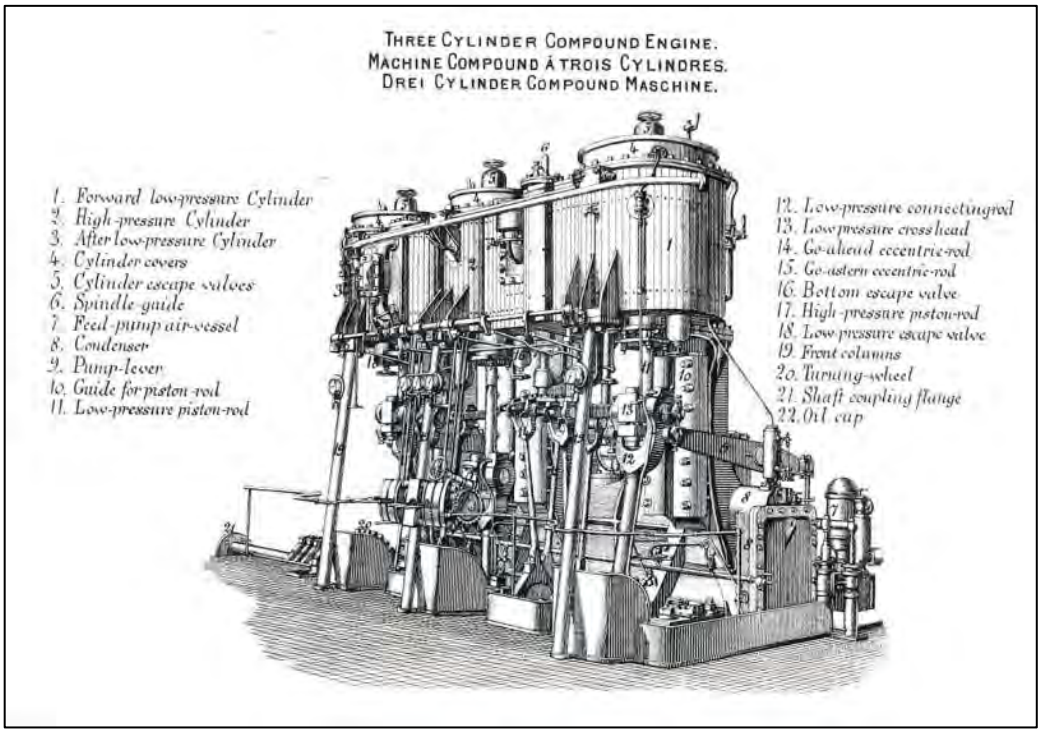

Figure 3-5. Typical Compound Steam Engine (Source Paasch 1885: Plate 49).

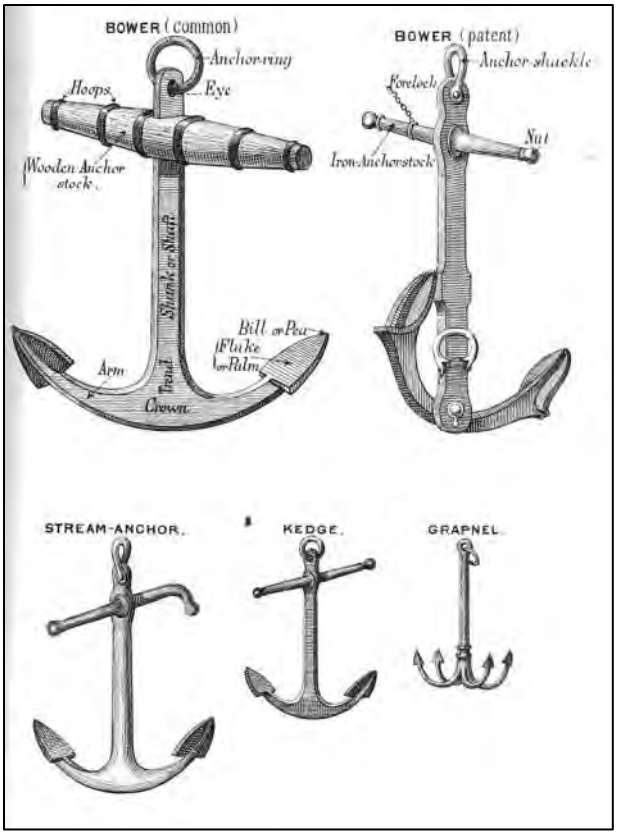

Figure 3-6. Various Types and Sizes of Historical Anchors (Source Paasch 1885: Plate 64).

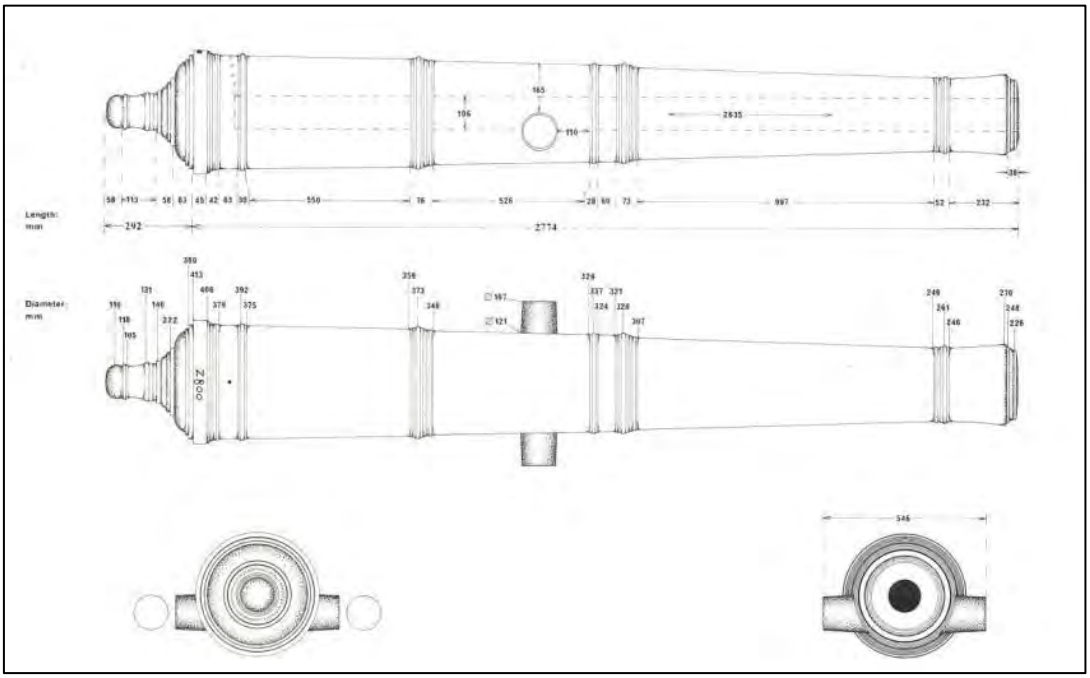

Figure 3-7. 2,800 lb Iron Canon (Source Caruana 1994:43).

3.2.2 Potential for the Presence of Post-Contact Period Shipwrecks

Shipwrecks from the 17th to 20th centuries—particularly ocean-going and coastal sailing vessels and steamers, fishing vessels, and small vernacular craft—could be located in the WEA (Albion et al. 1972; Bauer 1988; Massachusetts Executive Office of Energy and Environmental Affairs 2009; Mather and Jensen 2010; McLoughlin 1978; Massachusetts Ocean Resource Information System n.d. from the Massachusetts Office of Coastal Zone Management Online Mapping Tool]; Massachusetts Office of Coastal Zone Management (MA CZM) n.d.; RICRM 2010; Automated Wreck and Obstruction Information System NOAA Office of Coast Survey n.d.; Robinson et al. 2003; Rhode Island Shipwreck Database n.d.; TRC 2012).

The potential for finding shipwrecks increases in areas of historic shipping routes, harbor approaches, fishing grounds, and narrow straits, reefs, and shoals. Positioned between larger ports in Boston and New York, the WEA is situated in an area that has experienced extensive regional and national maritime activity from the 17th century to the present. Archaeological material discovered on the outer reaches of Cape Cod suggests that European settlers were trading goods with native inhabitants from the early-17th century up to 1620 (Massachusetts Historical Commission (MHC) 1987). As coastal development increased, maritime shipping and packet routes were established between the mainland and the islands south of Cape Cod. The waters south and west of the islands contain one of the primary shipping channels for southbound vessel traffic going into New Bedford and New York that was used from the mid-18th century up to the present (MHC 1987). During the 19th century, several maritime industries thrived in the region, including passenger and cargo transportation, whaling, fishing (fin and shell fish), tourism, and shipbuilding (commercial and naval). This extensive maritime history increases the potential for the presence of shipwrecks within the WEA (Mather and Jensen 2010; Bauer 1988). Accordingly, BOEM's Atlantic OCS Shipwreck Database identifies the WEA as located in a region of high probability for shipwreck presence (TRC 2012).

3.2.3 Previously Listed Wrecks and Obstructions within the MA WEA

BOEM's Atlantic OCS Shipwreck Database (TRC 2012) currently lists 762 known or reported wrecks offshore MA. Within the current boundaries of the WEA, there are 25 listed shipwrecks, obstructions, or objects of unknown character; an additional four listings are located within 2 km (1 nm) of the boundaries of the WEA. All 29 listings are included in Table 3-3, organized first by locational reliability and then by increasing depth.

An item of locational reliability '1' is a wreck location confirmed through physical verification and has been accurately positioned (e.g., with GPS or on an accurate modern map) or is identified on the basis of accurately positioned remote-sensing survey. The location is considered to be very reliable such that a wreck would be easy to relocate using standard DGPS equipment. An item of reliability '2' represents a specific location that is provided for a wreck or a vessel loss by an informant, reported in the literature or on a map. Included in this category are wrecks or losses whose position is given to at least the nearest actual minute of latitude and longitude, to a specific offshore lease block, and those that have been discovered and positioned using LORAN. The location reliability of these wrecks or losses is considered to be moderate to good. It is anticipated that these wrecks could be discovered, but discovery would require a moderate amount of field survey with remote sensing

equipment, plus it may require additional historical research. A location reliability of '3' indicates that the location is given generally rather than specifically by an informant, in the literature, or on a map. Those locations that are unreliable or vague – such as "off the coast of North Carolina" or "at sea" – are ranked '4.'

Additional source and comment information for previously identified wrecks, obstructions, and objects listed in Table 3-3 are provided in Appendix D.

Table 3-3.
Previously identified wrecks, obstructions, and objects within 1 nautical mile of the MA WEA.

Name	Number	Depth (m)	Locational Reliability	Type	Year Lost
Viking	9277	-39	1	F/V[1]	Unknown
Unknown	9282	-47	1	F/V	Unknown
Princess	7609	-37	2	F/V; Hang; 1969; Loran A	Unknown
Olive M. Williams (outside WEA)	7748	-38	2	F/V; 1969: Loran A	Unknown
Unknown (outside WEA)	8919	-38	2	Unknown	Unknown
Captain Bill II (outside of WEA)	7610	-39	2	Hang; 1979; Loran C	Unknown
JoAnne	7750	-39.5	2	F/V	1980
Alert	10345	-40	2	Oil Screw F/V of 25 gross tonnage built 1925; wooden hulled.	1942
Unknown Object (outside WEA)	7637	-40	2	Possible drill mine	Unknown
Pat & Judy3	7629	-41	2	Hang; 1979; Loran C	Unknown
Skipper	7747	-44	2	F/V; 1969 Loran A	Unknown
Unknown	7617	-44	2	Hang; 1979; Loran C	Unknown
David C. Winslow	7761	-44	2	Tug	Unknown
Unknown	7625	-45.5	2	Hang; 1979; Loran C	Unknown
Adventure II	7623	-46	2	Trawler of 119 gross tonnage	1943
L. & W.B. Co. 11	7624	-46	2	Barge of 862 gross tonnage	1945
PT 200	10009	-46	2	Patrol boat of 33 gross tonnage	1944
St. John	7621	-48	2	Unknown hang; 1979; Loran C	Unk
Pat & Judy3	10019	-51	2	F/V; 1969; Loran A	Unknown
Unknown	8911	-51	2	Tug	Unknown

Table 3-3. (continued)
Previously identified wrecks, obstructions, and objects within 1 nautical mile of the MA WEA.

Name	Number	Depth (m)	Locational Reliability	Type	Year Lost
Star of the Sea	7616	-52.5	2	F/V; 1979; Loran A	Unknown
Unknown	9215	-53	2	Unknown	Unknown
Object Airplane	7613	-53	2	Hang; 1979; Loran C	Unknown
Doreen Lee	10168	-53.5	2	Oil Screw F/V of 85 feet	1905
Unknown	7615	-55	2	Unknown hang; 1979; Loran C	Unknown
Object UXO[2]	7766	-55	2	Possible torpedo	Unknown
Peter Rickmers	7602	-63	2	Unknown	Unknown
Adventure II	9031	-46	3	Trawler of 119 gross tonnage	1945
L. & W.B. Co. II	9032	-46	3	Barge of 862 gross tonnage	1943

[1]FV= fishing vessel [2]UXO=unexploded ordinance [3] The vessel Pat and Judy appears twice in this table because different sources give different locations for this shipwreck.

CHAPTER 4

RESULTS OF SUB-BOTTOM PROFILING WITHIN THE MASSACHUSETTS WIND ENERGY AREA

The following chapter was prepared by multiple authors working in collaboration. The sub-bottom data was acquired and processed by William Danforth of the United States Geological Survey, Coastal and Marine Geology Program, Woods Hole Science Center. The geophysical and geotechnical data review was conducted by David Robinson and John King of the University of Rhode Island, Graduate School of Oceanography.

The paleolandscape/paleoshoreline reconstructions described in Chapters 2 and 3 were used to enable the identification of areas of potential for retaining evidence of submerged precontact archaeological deposits within the Massachusetts WEA. This chapter presents the results of the University of Rhode Island, Graduate School of Oceanography's (URI-GSO) review of the 2012 chirp sub-bottom profiling field survey data, acquired by the USGS, and is based on the archaeological sensitivity assessment modeling effort presented in Chapter 2.

4.1 SUB-BOTTOM DATA ACQUISITION AND PROCESSING

4.1.1 DATA COLLECTION

Approximately 810 km (437 nm) of high-resolution chirp seismic-reflection sub-bottom profiles were collected by the USGS during the 2012 MA WEA survey by using an EdgeTech 3200 Full Spectrum Sub-bottom (FSSB) topside system and a SB-512i towfish (0.5-12 kHz) (EdgeTech, 2012). Data were acquired using a 0.5- to 8- kHz frequency sweep, a 5-millisecond pulse length, a 0.25-second shot rate, and a 150-millisecond record length using a 46 micro-second sampling interval. During the survey, SonarWiz acquisition software (Chesapeake Technology Inc., 2012) was used to control the Edgetech 3200 topside unit and digitally log trace data in SEG-Y revision 1 standard format (Society of Exploration Geophysicists, 2012). The SB-512i towfish was towed astern of the vessel at approximately 5 m (16 ft) water depth. Navigation coordinates in arc-seconds were obtained from a Coda Octopus F185R motion reference unit DGPS antenna and logged to the SEG-Y trace headers. Manufacturers' specifications for the instruments and equipment used in this survey are presented in Appendix C.

4.1.2 POST-SURVEY PROCESSING

Post-survey processing of the raw SEG-Y traces in each data file was performed by the USGS using SIOSEIS (Henkart 2011) seismic processing software. Software scripts were created to shift traces vertically to remove the effects of sea surface heave and fish depth, mute water column portions of the traces, and apply time varying gain and automatic gain control. Navigation data also were inspected and edited, and a layback was applied to the navigation data to properly transfer the DGPS antenna location to that of the towfish. Final trace data, plotted as PNG images, and geolocated trackline files were created and imported into ESRI's ArcGIS.

4.2 DATA REVIEW

Review of sub-bottom profiling data for archaeological assessment purposes included examinations of the project field survey log, the PNG images of final trace data/individual profile plots, and the geolocated trackline plots and related data files output in ESRI's ArcGIS. Acoustic "reflectors of interest" were identified by URI and their positions plotted relative to the MA WEA, the survey tracklines, and the map of pre-survey reconstructed paleoshoreline locations from Chapter 2 for interpretation purposes (Figure 4-1).

4.2.1 GEOPHYSICAL DATA

To further inform the archaeological assessment of the acquired sub-bottom data, the project's post-processed side-scan sonar data and the results of previous geophysical surveys (Garrison 1967; Knott and Hoskins 1968; and Seigel et al., 2012) and geotechnical sampling studies (Bothner et al., 1981; Reid et al., 2005; and Wigley and McIntyre 1964) that were completed within and in proximity to the MA WEA also were reviewed. The locations of these previous investigations' geophysical survey tracklines and geotechnical sampling and their results also were plotted (Figures 4-2, 4-3, and 4-4). One caveat must be noted, however. Although acceptable to the reconnaissance nature of this study, the positional accuracy of these older data is somewhat suspect by virtue of the limitations of the technology available at the time of survey. Review of these data, however, provided information on the basic structure of the substrate geomorphology within the MA WEA.

Garrison (1967) conducted some of the earliest seismic survey in the area, and three of his survey tracklines (i.e., "P," "X2," and "X3") cross through the MA WEA (see Figure 4-2). Although state-of-the-art in the early days of continental shelf exploration, Garrison's work was based on widely-spaced reconnaissance and produced sub-bottom profiles whose positional accuracy was limited by the technology available during the time of his work.

Garrison describes the shelf as being strongly reflective of a geologically recent exposure to subaerial conditions, with large portions of it displaying evidence of lower sea levels in the form of erosional terraces, major and minor channels, and deltaic fans with an overall relief that is generally low, ranging from between about -150 m (-492 ft) to -2 to -3 m (-7 to -10 ft). Garrison notes that sediments of the inner continental shelf in the vicinity of the project area "form a distribution so unique that it was possible for ship's captains to gain a fair idea where they were from sounding the bottom and examining sediments" with seamen identifying the area's sandy silt as "Block Island Soundings" (Garrison 1967).

Garrison further describes the "Pleistocene Unconformity," a nearly universally present reflector/group of reflectors on the shelf that lies generally about 30 m (98 ft) below sea floor surface and is extremely rough and irregular. This unconformity is channeled to depths of more than 80 m (263 ft) on the inner part of the shelf, and it is interpreted to be at the base of the Pleistocene deposit (Garrison 1967). This Pleistocene unconformity was caused by the removal, through erosion, of an unknown thickness of older coastal plain deposits during one or more stages of lowered sea level, which accompanied Pleistocene glaciation. The sediment unit overlying this unconformity, whose upper boundary forms the present shelf surface, consists of material reworked from older beds below, as well as clastic debris transported by stream action across the expanded coastal plain.

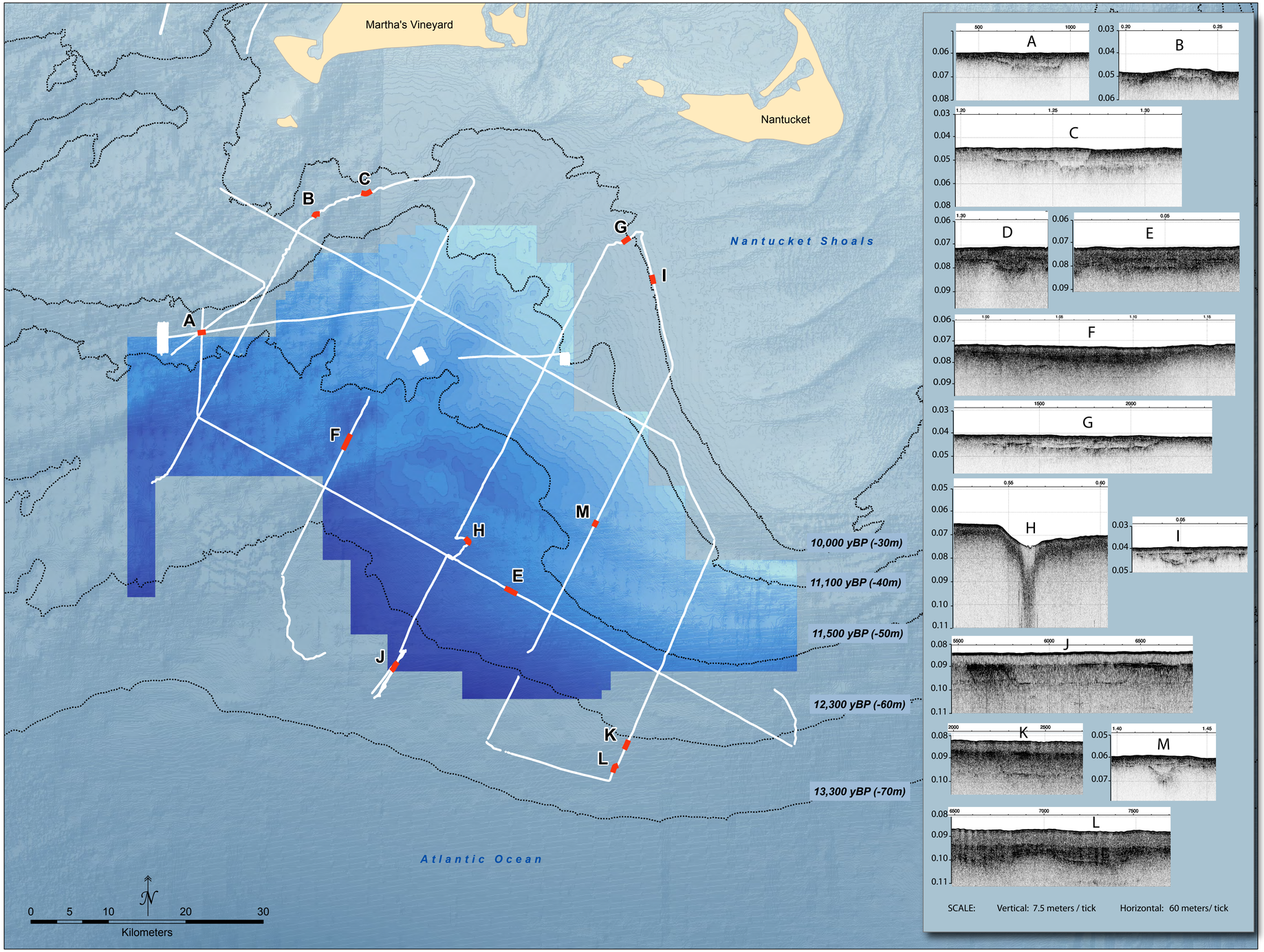

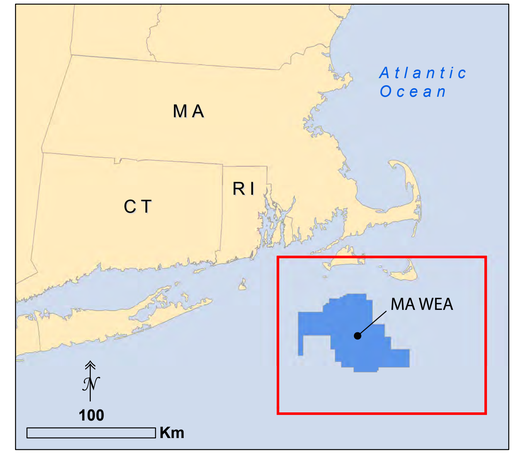

Map Key

- Survey Tracklines
- Reflectors of Interest
- Paleoshoreline Reconstruction

Bathymetry

MA WEA (meters): High : 91 / Low : - 200

Surrounding Area (meters): High : 91 / Low : - 200

Data Sources

Bathymetry: NOAA National Geophysical Data Center, U.S. Coastal Relief Model, http://www.ngdc.gov/mgg/coastal/crm.html

Paleoshoreline Reconstructions: Oakley, B.A., 2012

Tracklines and Subbottom Profiles: U.S. Geological Survey, 2012. Sea Floor Mapping Group, Survey number 2012-020-FA.

Coordinate System:

WGS 1984_UTM Zone 19N
Projection: Transverse Mercator
Linear Unit: Meter

GCS WGS 1984
Datum: D WGS 1984

Map Contact Info:

John King/David Robinson
Grad. School of Oceanography
University of Rhode Island
South Ferry Road
Narragansett, RI 02882
401-874-6182

Figure 4.1 Map of acoustic “reflectors of interest” and their positions and relative to the MA WEA, the 2012 survey tracklines, and the pre-survey reconstructed paleoshoreline locations. (Source: URI-GSO, C. Gibson, cartographer.)

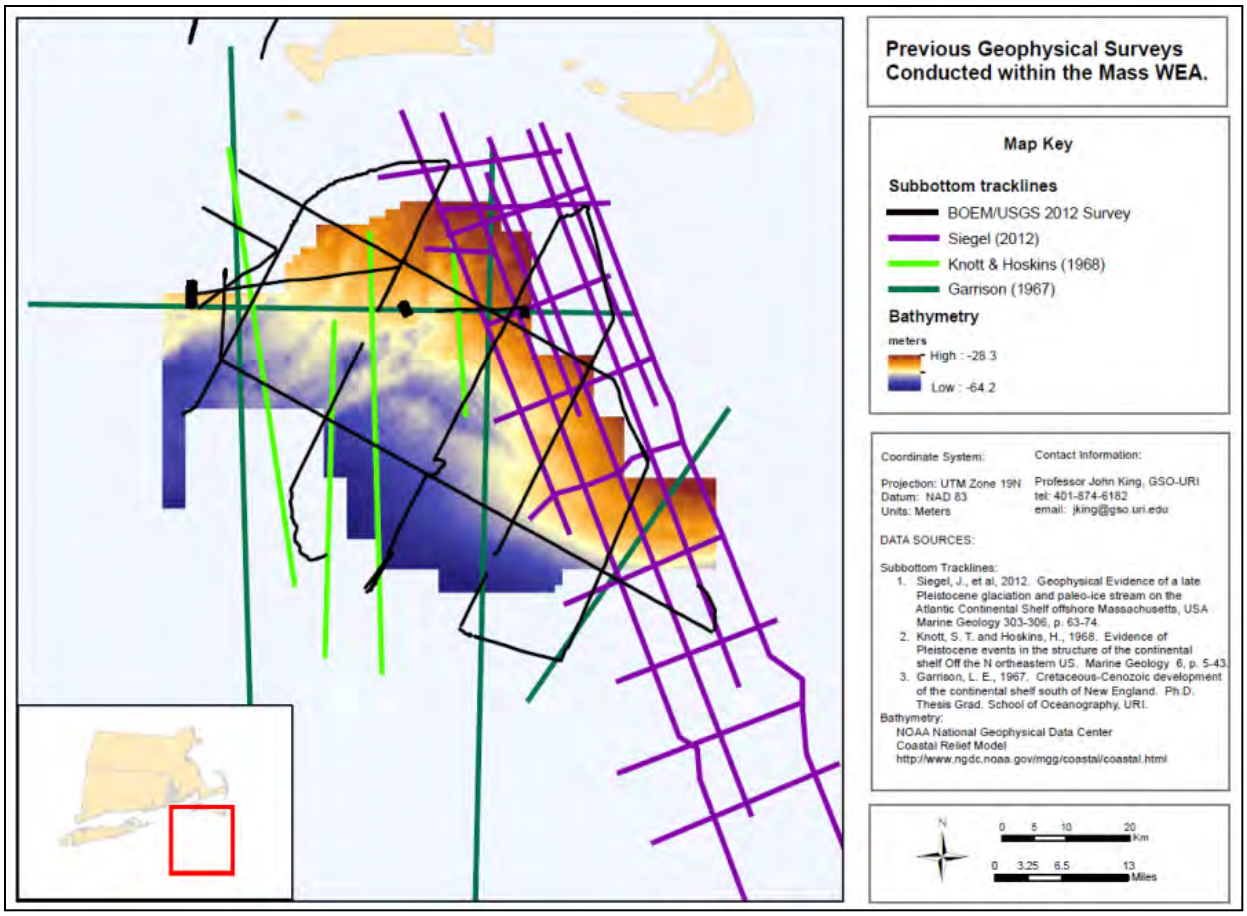

Figure 4-2. Survey trackline plot of previously acquired geophysical (i.e., sub-bottom profiler) survey data from within the MA WEA (source: C. Gibson, cartographer, URI-GSO).

Four major stages of continental shelf glaciation are known, and each caused a major lowering of eustatic sea level. Garrison states that the coast probably stood at the very edge of the continental shelf more than once, and that the entire width of the coastal plain was exposed to subaerial erosion at elevations of more than a 100 m (328 ft) above sea level. He also notes that erosion of the older, seaward dipping sediment beds during the subaerial exposures of the shelf during the Pleistocene was "enormous" and probably removed all of the Miocene and Pliocene shelf deposits, leaving only the truncated Oligocene, Paleocene-Eocene and Upper Cretaceous deposits under the overlying Pleistocene and Holocene deposits, forming the current substrate of the sea floor (Garrison 1967). Garrison's line drawing tracings of his surveyed continuous reflection profiles "P," "X2," and "X3" crossing the MA WEA reveal prominent acoustic reflectors that comprise a Holocene, Pleistocene, Tertiary and Upper Cretaceous sediment stratigraphic sequence.

Knott and Hoskins (1968) of the Woods Hole Oceanographic Institution (WHOI) describe the results of seismic reflection surveys they conducted in three areas (the outer shelf off New Jersey and Long Island, the shelf south of Martha's Vineyard within and in the vicinity to the MA WEA, and along Georges Bank) in 1958 and 1959. Knott and Hoskins's surveys utilized the first arrays of underwater spark sources and broad-band high resolution techniques, which enabled them to delineate reflectors as little as 4 to 6 m (13 to 20 ft) apart to depths of 100 to 300 m (328 to 984 ft) beneath the sea floor.

It is noteworthy that Knott and Hoskins observed that it will be "necessary to make more common place the simultaneous use of both high resolution and deeper penetrating techniques" in order to acquire complete profiles of the seafloor substrate on the shelf south of Martha's Vineyard. Unfortunately, their use of Loran-A positioning during data acquisition produced positioning accuracies of 0.8 to 3.2 km (0.4 to 1.7 nm).

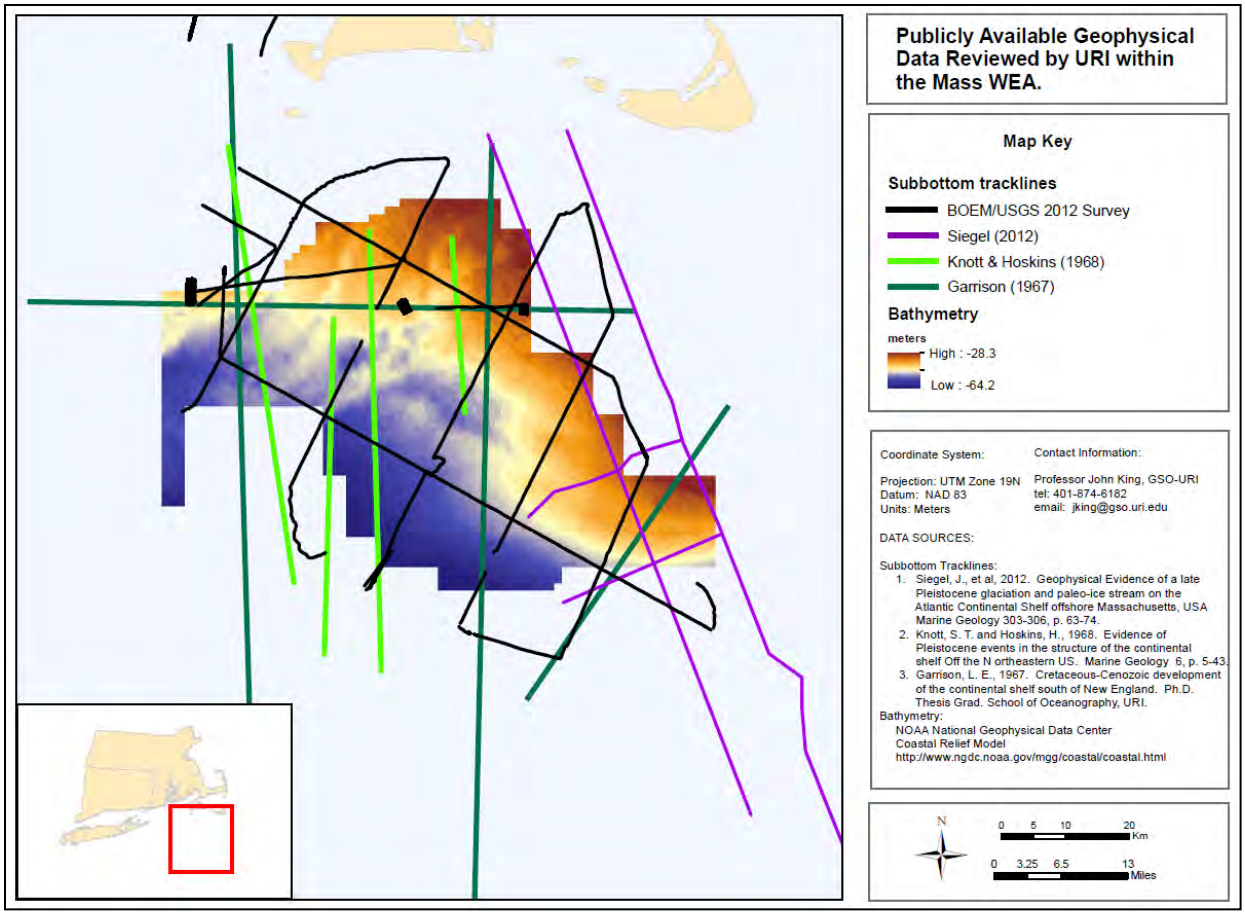

Figure 4-3. Publically available previously acquired geophysical (i.e., sub-bottom profiler) survey data from within the MA WEA (source: C. Gibson, cartographer, URI-GSO).

Four of Knott and Hoskins's survey lines cross through the MA WEA (from west to east: transects "38-39", "40-41," "43-42" and "44-45"). Based on their survey work, Knott and Hoskins described the "shallow layered" sediments south of Martha's Vineyard as being overlain by a "smooth veneer of sediments" 10 to 20 m (33 to 66 ft) thick and appearing to have been folded and generally disturbed by ice pressure (Knott and Hoskins 1968). The disturbed beds south of Martha's Vineyard are further described as lying along a lobate front running from northeast to southwest, hypothesized by Knott and Hoskins to represent the southern limit of glaciation and the edge of a glacial outwash fan (Knott and Hoskins 1968). Knott and Hoskins asserted that the shallow structure off the shelf south of Martha's Vineyard has, in general, a prograded form, whose development has been modified by the local environment with rates of deposition and erosion from wave action and also from a fluvial origin that varied considerably from one locality to another.

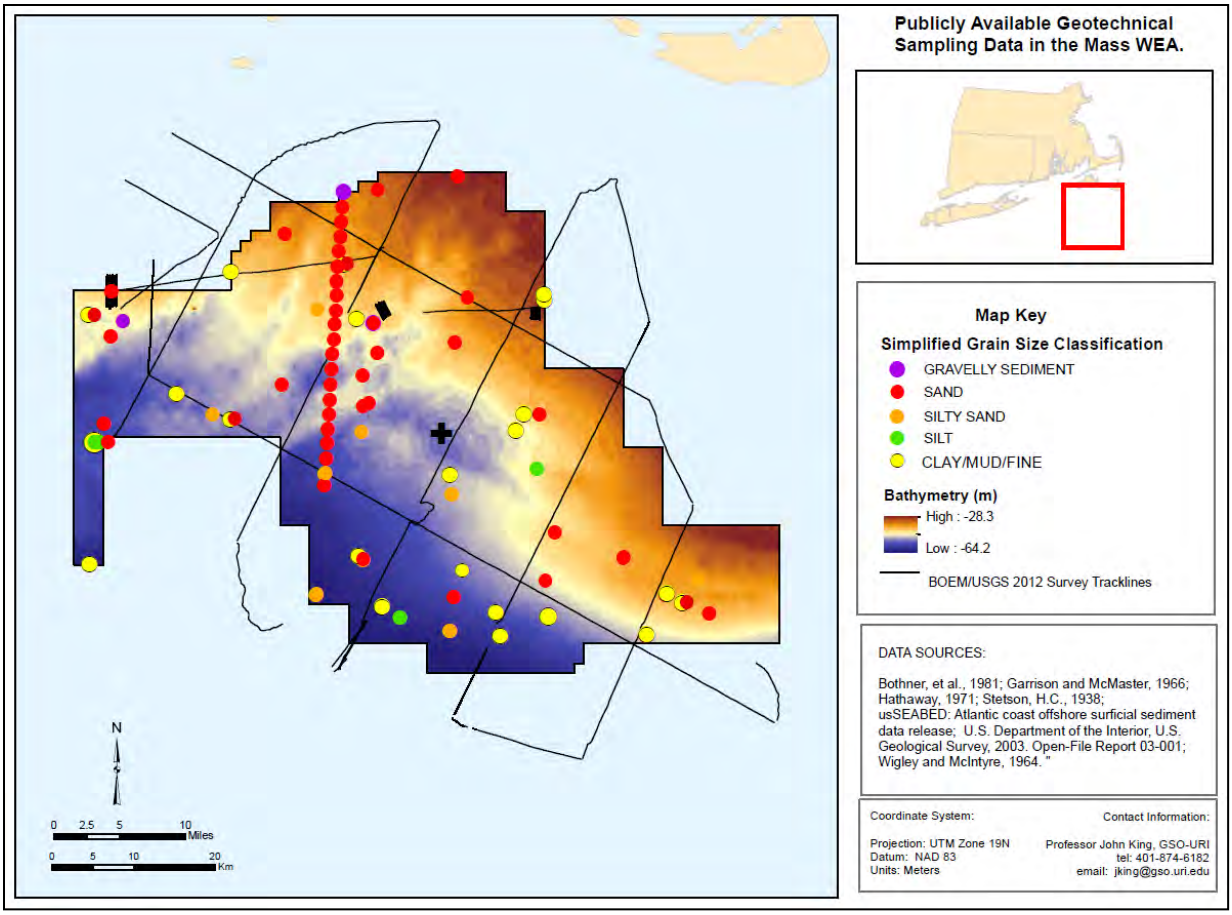

Figure 4-4. Publically available previously acquired geotechnical sampling data from within the MA WEA showing surficial sediment characteristics (source: C. Gibson, cartographer, URI-GSO).

High-resolution, multi-channel seismic survey data acquired in 2009 and reported in 2012 by Seigel et al., records, in detail, six stratigraphic sediment units in the 750-m (2,461-ft) deep sub-bottom profiles recorded within and in the vicinity of the MA WEA (Figure 4-5). These units include (from the sea floor surface downward):

- "Unit A" – a comparatively thin, 40-m (131-ft) thick, stratified Holocene-Pleistocene unit dating from the present to a late-Pleistocene (30,000 to 40,000 yBP) regional uniformity ("U2");
- "Unit B" (sub-divided into "B1" and "B2") – a thicker 30 to 50 m (98 to 492 ft) Pleistocene unit (40,000 to 2.6 million yBP) at the base of which is a second, older regional unconformity ("U1");
- "Unit C" – interpreted to be a Miocene (5.3-23 million yBP)/Oligocene (23-34 million yBP) unit;
- "Unit D" – interpreted to be a Eocene (34-56 million yBP)/Paleocene (56-66 million yBP) unit;
- "Unit E" – interpreted to be a Cretaceous (66-145 million yBP) unit; and
- "Unit F" – interpreted to be a Jurassic unit (145-201 million yBP).

For the purposes of archaeological assessment, the sea floor substrate's uppermost Holocene/Pleistocene stratigraphic unit ("Unit A") is of the greatest interest because it is the unit that could contain intact, archaeologically sensitive elements of the former subaerial late Pleistocene-early Holocene paleolandscape. Data were acquired along 16 track lines surveyed by Seigel, et al. within and in the vicinity of the MA WEA (see Figure 4-2). Of these 16 lines, images of four of them are included in Seigel, et al. (2012) (see Figure 4-3). The sub-bottom profiles recorded by Seigel, et al. (2012) are noteworthy, if for no other reason, because they demonstrate the ability to record deep, high-resolution profiles with the appropriately-powered acoustic source/seismic profiling system. Unfortunately, however, resolution was inadequate to resolve the Holocene marine transgressive surface, which is critical to this study.

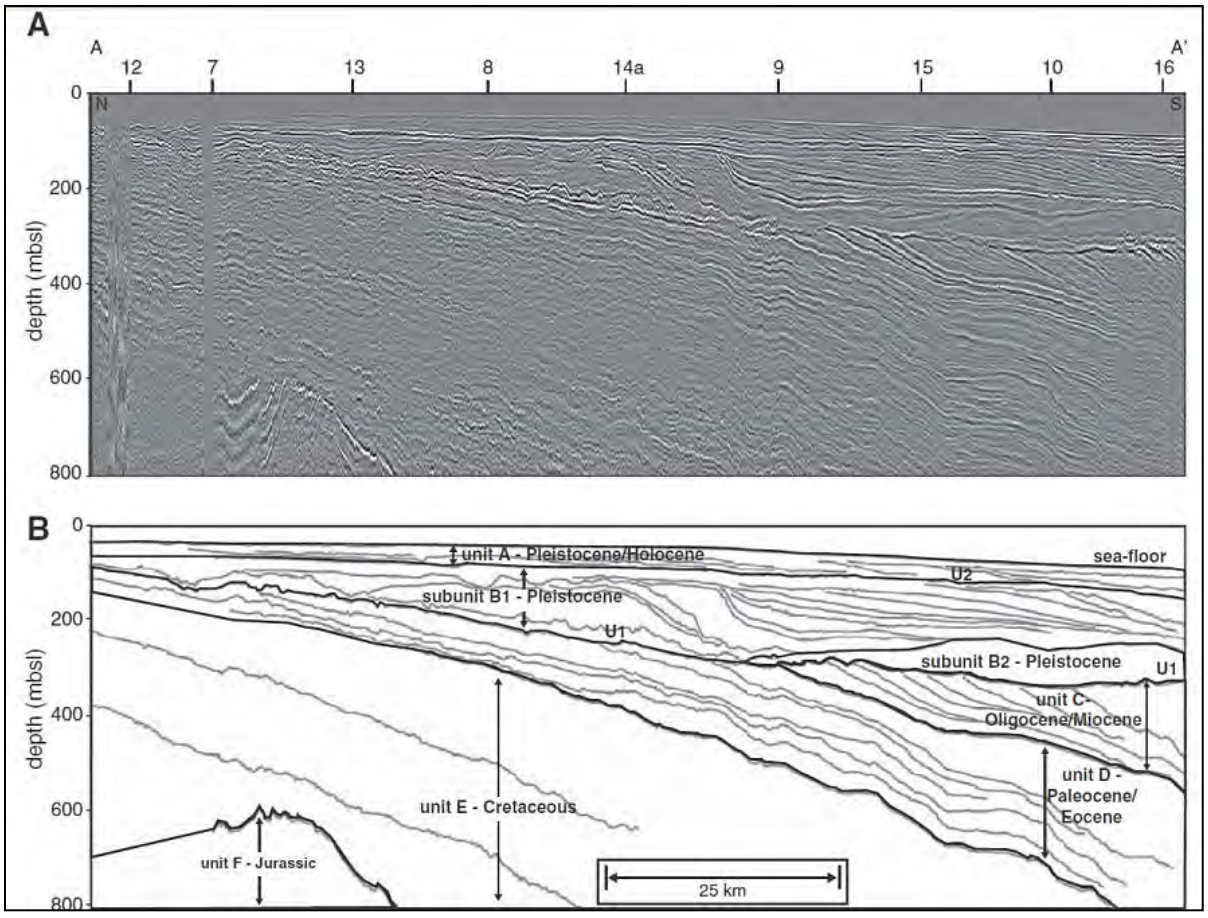

Figure 4-5. High-resolution, multi-channel seismic survey data acquired in 2009 and reported in Seigel, et al. (2012) showing full-penetration of sea floor substrate, and a detailed interpretive record of six stratigraphic sediment units ("A"-"F") in the -750 m (-2,461 ft) deep sub-bottom profiles recorded within and in vicinity of the MA WEA (source: Seigel, et al. 2012).

4.2.2 GEOTECHNICAL DATA

Review of existing geotechnical sampling data (i.e., surficial sediment type information obtained from a collection of grabs, snapper and core samples) found in publically available literature (i.e., Bothner et al., 1981; Reid et al., 2005; and Wigley and McIntyre 1964) indicates that the 78 samples taken within the MA WEA consisted primarily of sand (n=45) and clay/mud/fine (n=21) sediments,

with small amounts of silty sand (n=7), silt (n=3), and gravelly sediment (n=2) present, as well (see Figure 4-4).

Bothner et al. (1981), describe the only publically available core sample (Core 4527D – located in the middle of the MA WEA) (see the black 'X' in Figure 4-4). The core recovered sediments to a depth of just 35 cm (17 in) below surface consisting predominantly of sand and silt with a small percentage of clay and trace percentage of gravel. Radiocarbon dating of multiple samples from within and in the vicinity of the MA WEA area indicate that the surficial deposits of fine-grained material have been accumulating since the last transgression of the sea. Bothner, et al., attribute the source of the surficial sediment in the area as likely being from Georges Bank and Nantucket Shoals, where fine-grained sediments are winnowed during storms. Net current drift on the Middle and Outer Continental Shelf in the vicinity of Georges Bank is to the southwest, hence Bothner et al.'s assertion that the sources of the fine-grained sediments are Georges Bank and Nantucket Shoals – areas consisting of reworked glacial till and outwash that originally contained a large fraction of silt and clay, but which, at present, consist primarily of sand and coarser material.

They also describe a "Mud Patch" south of Martha's Vineyard – an area of fine-grained sediments possibly corresponding to the "Block Island Soundings" sediments mentioned by Garrison (1967), and described in the literature as early as 1872 as an aid to navigators on their approach to Nantucket or New Bedford in foggy weather. Bothner et al. (1981), consider the Mud Patch to be a modern feature and the area as a sink for fine-grained sediments. They argue that deposition in the Mud Patch is favorable because there is relatively lower energy in bottom waters compared to shoal areas to the northeast. This is a result of lower tidal current velocities and the greater water depths, which reduce turbulence from surface waves. Since the last transgression of the sea, continued winnowing of fine sediments from the glacial outwash and till by tidal- and wave-generated currents probably left a protective lag deposit of sand and gravel on Georges Bank and Nantucket Shoals. The result is that relatively little fine-grained material is being re-suspended and deposited in the Mud Patch.

4.3 RESULTS OF SUB-BOTTOM PROFILING

The 2012 sub-bottom profiling survey data were reviewed with the following questions in mind:

- are any elements of the paleolandscape visible in the data buried beneath more recently deposited marine/Holocene sediments;
- can any buried geomorphic features of the paleolandscape be identified in the data (e.g., lacustrine basins, lagoons, shoreline terraces, in-filled paleochannels, etc.); and
- are there any buried paleolandscape layers for which geotechnical sampling to conclusively identify their nature is recommended?

Examination for archaeological purposes of the sub-bottom profiling data recorded during the survey of the MA WEA revealed that while data *quality* was acceptable, the application of a higher-frequency chirp sub-bottom profiler to the survey of the MA WEA proved largely incapable of penetrating the reflective surface sediments of the sea floor. Consequently, the survey produced data of limited interpretative value that was insufficient for interpolating between lines and reconstructing paleo-land-surfaces, as planned. From the examination of the sub-bottom profiler data in Seigel, et al. (2012) (described in detail above), we know that there is complex and fully resolvable stratigraphic sequence present within the MA WEA that was not resolved by the CHIRP

sub-bottom profiler during the present survey. Instead, data revealed 13 "reflectors of interest" labeled A through L (Table 4-1; see corresponding locations and sub-bottom reflectors plotted and presented in Figure 4-1) were identified.

Table 4-1.
Reflectors of interest identified during sub-bottom profiler survey.

I.D.	Reflector Type	Maximum Depth Below Sea Floor		Maximum Length/Width	
		meters	feet	meters	feet
A	Infilled stratified channel (bend/cut-bank)	5	16	330	1,083
B	Outcrop of older, denser sediments	n/a	n/a	330	1,083
C	Infilled channel	7.5	25	660	2,165
D	Narrow infilled channel and unconformity/ ravinement surface with surrounding interfluvial channels	8	26	240	787
E	Broad infilled channel with unconformity/ravinement surface	7.5	25	480	1,575
F	Unconformity/ravinement surface with possible onlapping (shoreline)	5	16	1020	3,346
G	Stratified broad infilled channel or lacustrine feature	4	13	600	1,969
H	Depression with gaseous sediments	n/a	n/a	150	492
I	Unconformity/ravinement surface/infilled irregular channel	6	20	420	1,378
J	Unconformity/ravinement/basin-like structure	9.5	31	540	1,772
K	Unconformity/ravinement	12	39	300	984
L	Stratified infilled channel	10	33	660	2,165
M	Small infilled channel	8	26	165	541

These identified reflectors of interest were suggestive of buried elements of the former subaerially exposed paleolandscape. These geomorphic features of the paleolandscape included what appear to be infilled channels, unconformities/ravinement surfaces, an outcrop of denser sediments, stratified lacustrine features, and possibly, an area of onlapping. The features range in size from 150 to 1,020 m (492 to 3,346 ft) long and have maximum burial depths of between 4 and 12 m (13 and 39 ft) below the surface of the sea floor. All of the reflectors of interest would need to be geotechnically sampled with either vibracoring or boring programs to conclusively determine their nature and age and whether or not they contain archaeologically sensitive stratified paleosols. No element of any of these reflectors of interest were observed in the 2012 side scan sonar data that was acquired simultaneously with the sub-bottom profiler data in the MA WEA survey area; however, this absence may be the result of an possible malfunction in the side scan sonar system that seemed to affect the quality of some of the acquired side scan sonar data. Of the 13 reflectors of interest that were identified by URI-GSO, just five (E, F, H, J, and M) were located within the actual limits of the MA WEA. The distribution of these reflectors of interest was fairly uniform throughout the survey area, with no discernible cross-track line patterning or correlative features observed.

4.4 SUB-BOTTOM PROFILING AND GEOPHYSICAL/GEOTECHNICAL CONCLUSIONS

One of the principal goals of the review of the sub-bottom profiling data was to integrate what was observed and learned from the 2012 survey data with the pre-survey paleolandscape reconstruction

presented in Chapter 2. This integration would produce a post-survey paleoenvironmental landscape/shoreline reconstruction that would enable the identification of areas of high potential for retaining evidence of submerged precontact archaeological deposits within the MA WEA. Post-survey data analysis revealed what may be preserved elements of the formerly subaerial paleolandscape within the MA WEA, and background research identified previously-acquired survey data with a deeply-stratified sub-bottom record suggesting many more relict elements of the paleolandscape are buried under Holocene marine sediments within the MA WEA. However, due to the inability of the CHIRP sub-bottom profiler system used during the 2012 survey of the MA WEA to penetrate nearly all of the sea floor's surface below the Holocene within the study area, the density of adequately-resolved and usable sub-bottom profiles proved insufficient for meaningful correlations with the pre-survey paleoenvironmental reconstruction presented in Chapter 2 and the development of a detailed paleoenvironmental reconstruction of the formerly subaerial topography with clearly delineated areas of archaeological sensitivity.

Instead, the 2012 survey and the review of its data, informed by background research on previous investigations in the area, provide only a preliminary indication of the comparatively richer information potential that the use of a stronger, lower-frequency seismic sub-bottom profiler, combined with data obtained through sub-surface geotechnical sampling (i.e., vibratory cores or borings), would provide and would be necessary for reconstructing the paleoenvironmental topography within the MA WEA. Chapter 9 details these recommendations for future work in this and other areas of similar geomorphic composition.

CHAPTER 5

PHYSICS OF UNDERWATER SOUND

The following background on the physics of underwater sound was prepared by multiple authors working in collaboration, including John Bright and David Conlin of the National Park Service Submerged Resources Center and William Danforth and William Schwab of the United States Geological Survey, Coastal and Marine Geology Program, Woods Hole Science Center.

This chapter presents information on the behavior of sound (and thus sonar) in the ocean as a theoretical background to the comparison of sonar technologies presented in Chapter 6.

5.1 INTRODUCTION

In its most basic form, underwater acoustic imaging works by transmitting sound waves towards the bottom of a body of water and then interpreting, based on time and intensity, the return of those sound waves to create an image of the bottom.

Most acoustic systems are quite versatile and will produce useful data in a variety of environments and applications. The optimal system for a given survey application, however, requires incorporation of technologies to cope with a number of physical limitations: absorption, spreading, and scattering of the sound waves. These phenomena not only affect the emanation of sound into water, but also the manner in which sound waves are returned, sensed, and interpreted.

Sonar systems are, therefore, designed in various ways to cope with these limitations. Understanding the technical specifications in addition to the principles underpinning the operation of each system is necessary to make informed assessments about the functionality of any sonar seafloor mapping system.

5.2 SOUND WAVE CHARACTERISTICS

Underwater acoustic imaging works by transmitting sound waves towards the bottom of a body of water and then interpreting, based on time and intensity, the return of those sound waves to create an image of the bottom. Before comparing acoustic systems for seafloor mapping, a review of the physics governing sound in the ocean is required.

Acoustic energy broadcast into the water is described in terms of several distinct parameters that characterize the shape and intensity of the sound wave. These parameters are often adjustable in remote sensing platforms and are manipulated to optimize data collection for individual survey operations. Understanding these characteristics forms the basis for predicting the behavior of sound waves as they travel through the medium of water. This allows the appropriate selection of settings during the survey. The settings and their definitions are:

- frequency: the period of a sound wave, how many cycles are produced during a given time span. Frequencies are measured in Hertz (Hz) or kHz;
- pulse length: the duration of an individual release of sound waves; and

- beam angle: the shape into which the pulse forms as it emanates from the sensor.

Collectively, the interaction of these parameters with water determines the range and resolution of acoustic data.

Swath sonar systems operate through a range of frequencies, typically between 100 and 1,000 kHz. Low frequency waves have fewer cycles and are characterized by longer wavelengths; higher frequency waves with shorter wavelengths. Frequency plays a major role in the range and resolution of an acoustic system. Higher-frequency waves result in more detailed detection of objects, yet these waves are more quickly absorbed and scattered (attenuated) in water resulting in reduced range. Low frequency waves, on the other hand, are more stable over longer distance yet provide less detailed data (Figure 5-1).

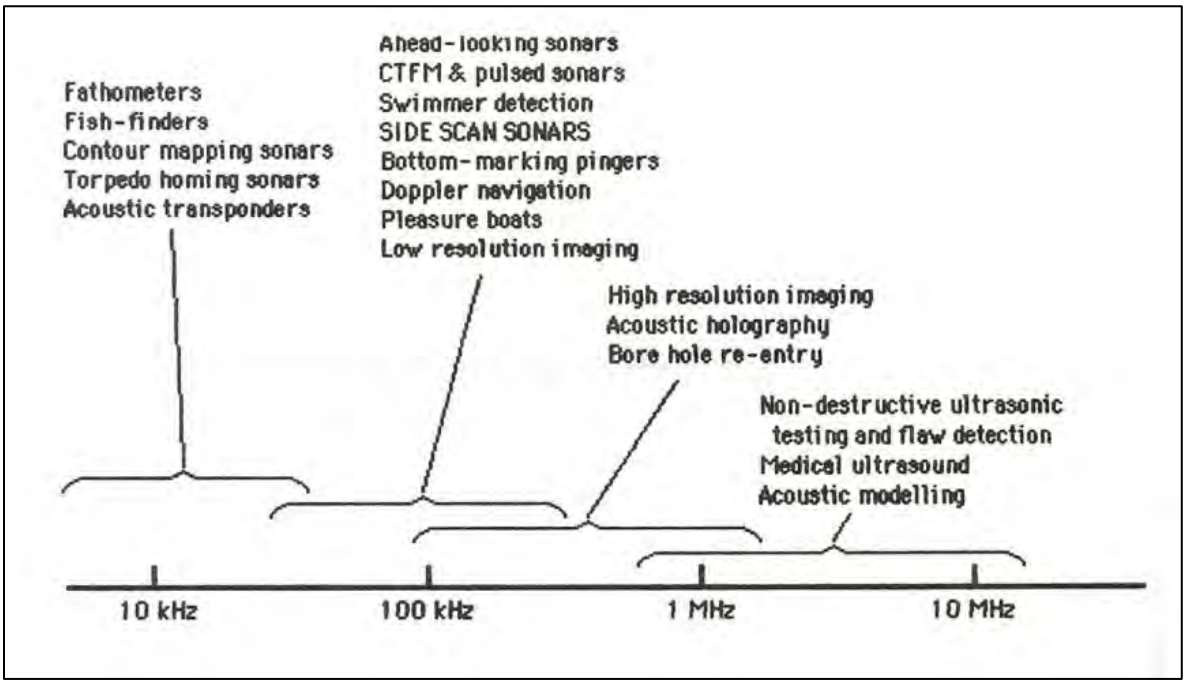

Figure 5-1. Sonar frequency selection for various applications. (Source Mazel 1985:2-10).

The duration of a given release of sound waves by a transducer is referred to as pulse length (Figure 5-2). Release of sound occurs on the scale of microseconds, ranging between 25 and 400 microseconds (μsecs). The duration of a transmission pulse is also adjustable within the same frequency range. As pulse width narrows, transmission times shorten and a narrower band of sound is produced. Since swath sonar systems extrapolate features based upon the time lapse between sound emission and return, a narrower beam emitting consecutive pulses will strike nearby objects at separate times, sending separate returns, and allowing the system to differentiate separate objects. A wider band of sound with a longer pulse rate will strike both objects simultaneously which will send a single return, effectively telling the system it struck a single object, a relationship shown in Figure 5-3.

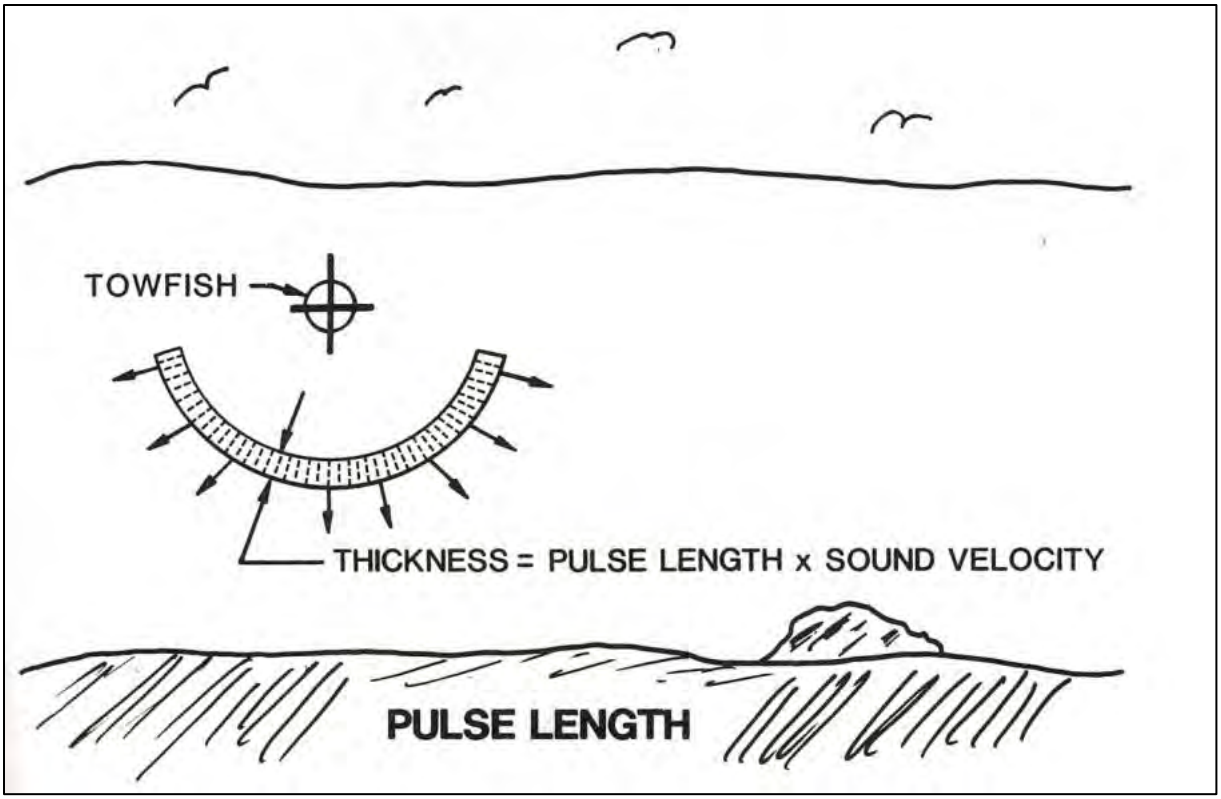

Figure 5-2. Cross section depiction of pulse length. (Source Mazel 1985:2-3).

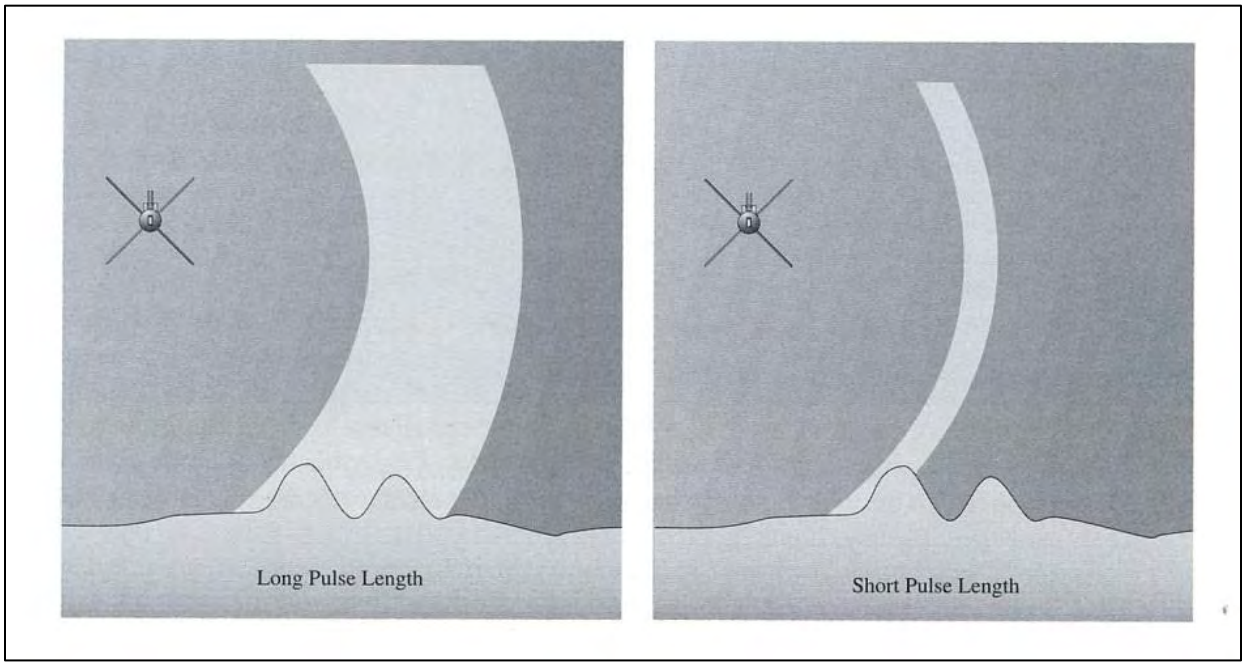

Figure 5-3. Relationship between pulse length and range resolution. (Source Fish and Carr 1990:35).

Thus, for higher resolution, a higher frequency and shorter pulse length is required. The trade-off, however, is these waves are incapable of propagating over long distances through the water. Lower frequencies and longer pulse lengths are capable of reaching longer ranges, but at the cost of resolution. The third parameter characterizing acoustic waves in water is beam angle. Up until this point, resolution was discussed as a general term, yet a differentiation is necessary. Two types of resolution are distinguishable: range and transverse. Range resolution is the degree to which a system can differentiate objects perpendicular to the path of the sensor. Pulse length, as described above and shown in Figure 5-3, is the determining factor of range resolution. Transverse resolution is the degree to which a system can differentiate objects parallel to the path of the sensor and is determined mainly by beam angle (Mazel 1985, Fish and Carr 1990).

Beam angle specifically describes the horizontal shape of the sound wave in the water; in vertical profile the pulse stretches across the entire water column, reaching both the bottom and the surface. As beam angle narrows, differentiation of objects parallel to the path of the fish increases. Figures 5-4 and 5-5 represent this relationship: as the narrow beam passes an object, the sound wave is returned to the sensor before the beam strikes the next object, allowing the system to differentiate the returns, and displaying two discrete objects. As beam angle increases, or as it spreads moving farther from the source, proximate objects are ensonified simultaneously, yielding a single return, and are displayed as a single object. Beam angle is not adjustable within a survey system, as it is controlled by the manufacturer's configuration of the transducers generating the sound waves.

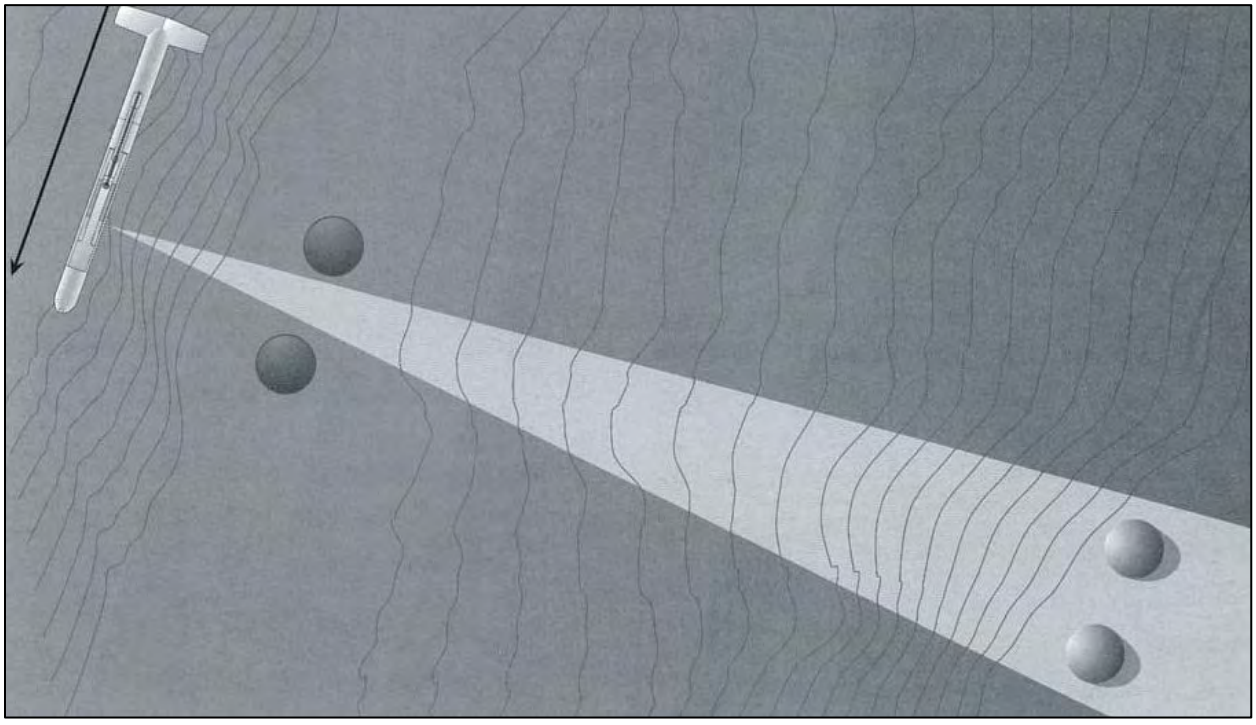

Figure 5-4. Relationship between beam angle and transverse resolution. (Source Fish and Carr 1990:34).

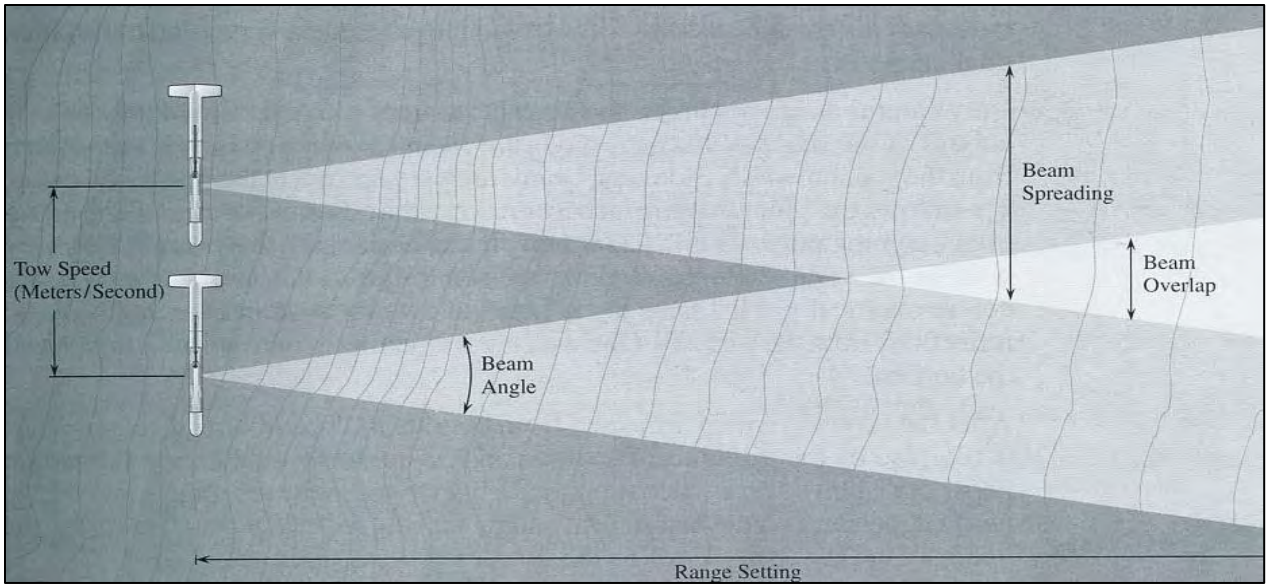

Figure 5-5. Illustration of beam angle as sensor moves down track line (Source Fish and Carr 1990:21).

5.3 FACTORS LIMITING THE PROPAGATION OF UNDERWATER SOUND

Every acoustic imaging system must accommodate the behavior of sound waves once released into the water. No hardware, mathematical formula, software package, or visualization method can influence sound once it has left the transducer into the water. Ultimately, the behavior of acoustic waves travelling through the water explains why sonar has limited range and resolution. Unlike aerial photography, which passively gathers light to create imagery, sonar is an active emission of energy in a highly viscous medium; water slows the speed of travel, and the incidence with heterogeneous surfaces reverberated by sound send the waves in sometimes unpredictable directions, with little actually returning to a sensor. These behaviors, therefore, explain the observed changes in data collection given various pulse lengths, frequencies, ranges, and collection (i.e. tow) speeds.

The density of the medium or, more accurately, the density profile of the water column, affects the specific movement of acoustic waves. The speed of sound through water determines how the return waves are interpreted by the imaging system, thus sound velocity characterization is crucial for proper data collection. Density differences between salt and fresh water drastically affect the velocity of sound. Temperature, which directly relates to fluid density, also affects the velocity of sound, with denser, colder water allowing waves to propagate faster. Within a body of salt water, therefore, variations in temperature and salinity, such as those at a river delta, along a glacial interface, or at the convergence of ocean currents, can create a complex profile though which sound will not travel uniformly. Operating proximate to the bottom, side scan sonar is usually within a density layer uniform with the bottom. A boat-mounted or surface-towed system, however, must broadcast sound through the entire water column and is therefore required to collect sound velocity data (temperature, salinity, and pressure) to mathematically correct for the variations in sound velocity these might cause.

Also an inherent property of the water is its molecular composition, the makeup of substances, including water itself, which are agitated as the force generated by the pressure of sound waves moves through them. According to the laws of thermodynamics, this exertion ultimately results in a diminishing of the intensity of the sound wave as some of its energy is dissipated in the transfer. Thus, the further a sound wave moves from the source, the weaker it becomes. Similarly, just as waves diminish in intensity as they move away from their source, they continue to diminish after reflecting off of surfaces. This principle is described as absorption. Due to the composition of salt water, mainly the large amount of dissolved salt, the magnitude of absorption is much greater, as shown in Figure 5-6.

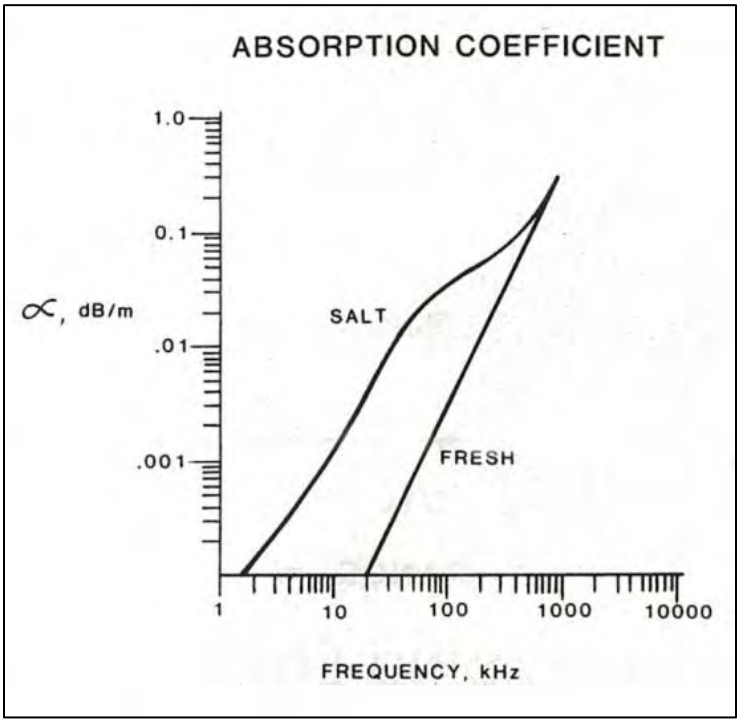

Figure 5-6. Frequency-based absorption levels in salt versus fresh water. Y-axis represents logarithmic absorption of sound in decibels per M (Source Mazel 1985:3-8).

As mentioned above, effective range is inversely proportional to selected frequency:

> As the sonar pulse travels through the water some of the energy is simply absorbed by the medium and therefore becomes unavailable for useful purposes….The absorption is due to frictional effects and molecular relaxation and is significantly greater in saltwater than in fresh water at the frequencies of interest in sonar (Mazel 1985:3-8).

Therefore, higher frequencies equate to shorter wavelengths. When moving through a dense medium, especially saltwater, shorter wavelengths are quickly absorbed, and effective range is greatly reduced. Thus, absorption plays a main role in the practical limitation of sonar range (see Figure 5-7).

The other factors limiting the movement of sound waves in water are not characteristics of the water itself, but rather characteristics of the sound waves: beam spread and scattering. Sound waves

produced from a discrete point emanate three dimensionally at an angle determined by the transducer producing them. This behavior is described by Mazel (1985):

> The sonar puts a fixed amount of energy into the water in the form of the sound pulse. As the pulse travels away from the transducer it occupies a larger and larger volume. The process is called spherical spreading. The further from the sonar, the lower the intensity of the pulse will be in a given area. The intensity falls off as the square of the distance.

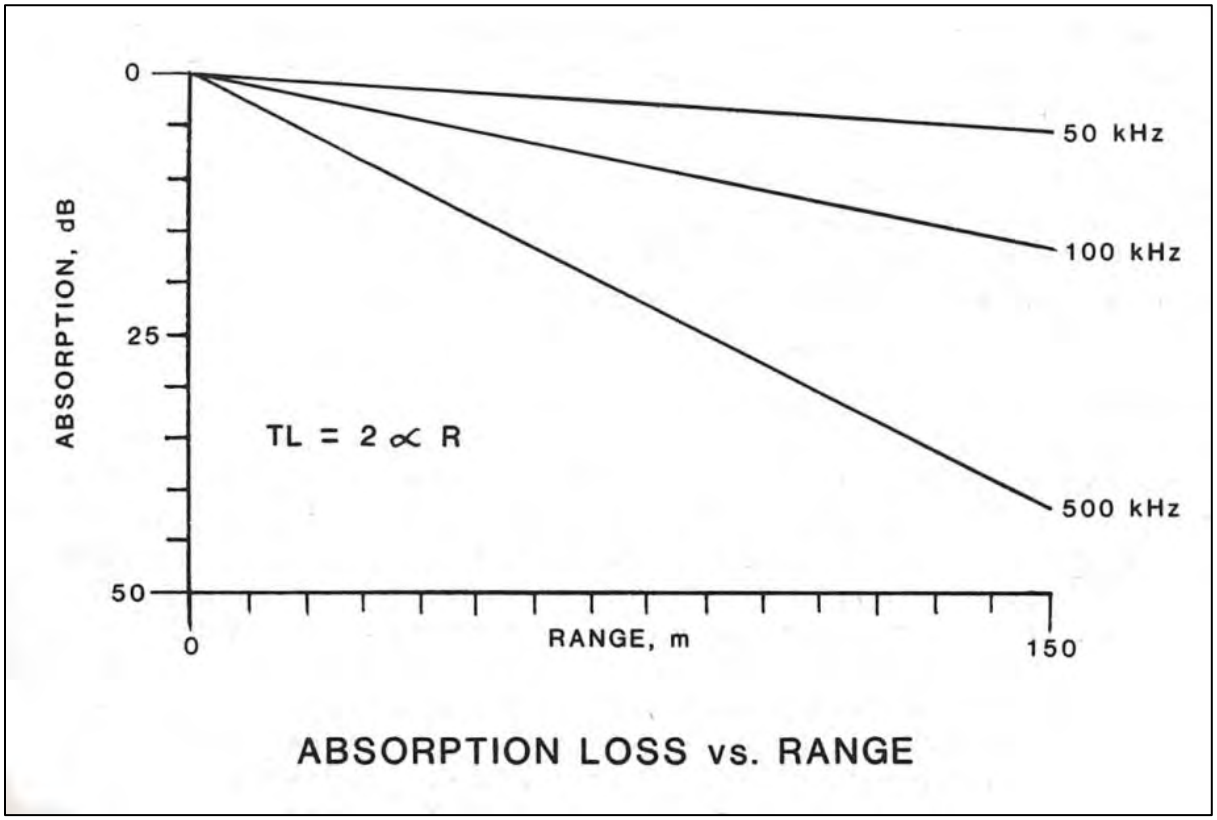

Figure 5-7. Absorption rate as a function of range and frequency for two-way travel from transducer to object and back again (Source Mazel 1985:3-9).

Not only does spreading limit range, it also limits resolution. In the previous section, Figure 5-4 illustrated the manner in which spreading reduced transverse resolution as a function of distance. Interestingly however, it also increases range resolution as a function of distance. Figure 5-8 illustrates this behavior, demonstrating how the acoustic footprint narrows as the distance increases, an effect similar to manipulating the pulse length. Unlike absorption, however, beam spreading is independent of frequency or pulse length; waves will spread and dissipate regardless of their wavelength or duration of the pulse. This relationship is graphed in Figure 5-9 and is the predominate factor limiting the effective range of sonar.

When the sound wave contacts objects, depending on the angle of incidence, they are broadcast in different directions. The result is described by Mazel (1985):

> The scattering of sound will have two primary effects. For one, it will decrease the amount of acoustic energy which is reaching the bottom, its intended destination. This is an additional factor which acts to decrease the

strength of signals with increasing range. The combined effects of scattering and absorption are called attenuation.

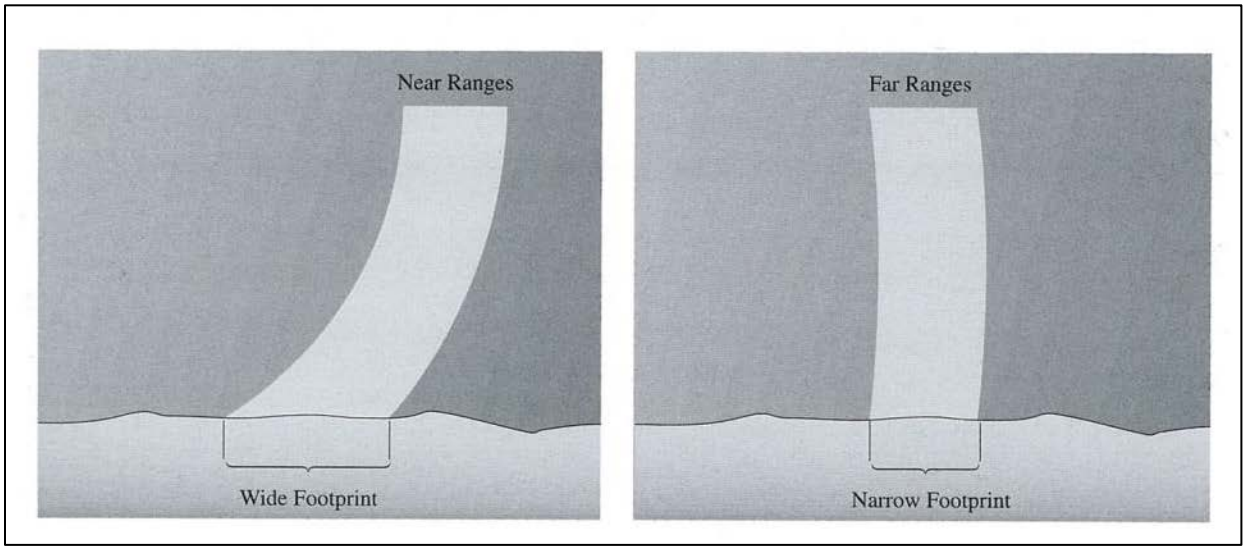

Figure 5-8. Illustration of the increase in range resolution produced by beam spreading as a pulse emanates from its source. (Source Fish and Carr 1990:35).

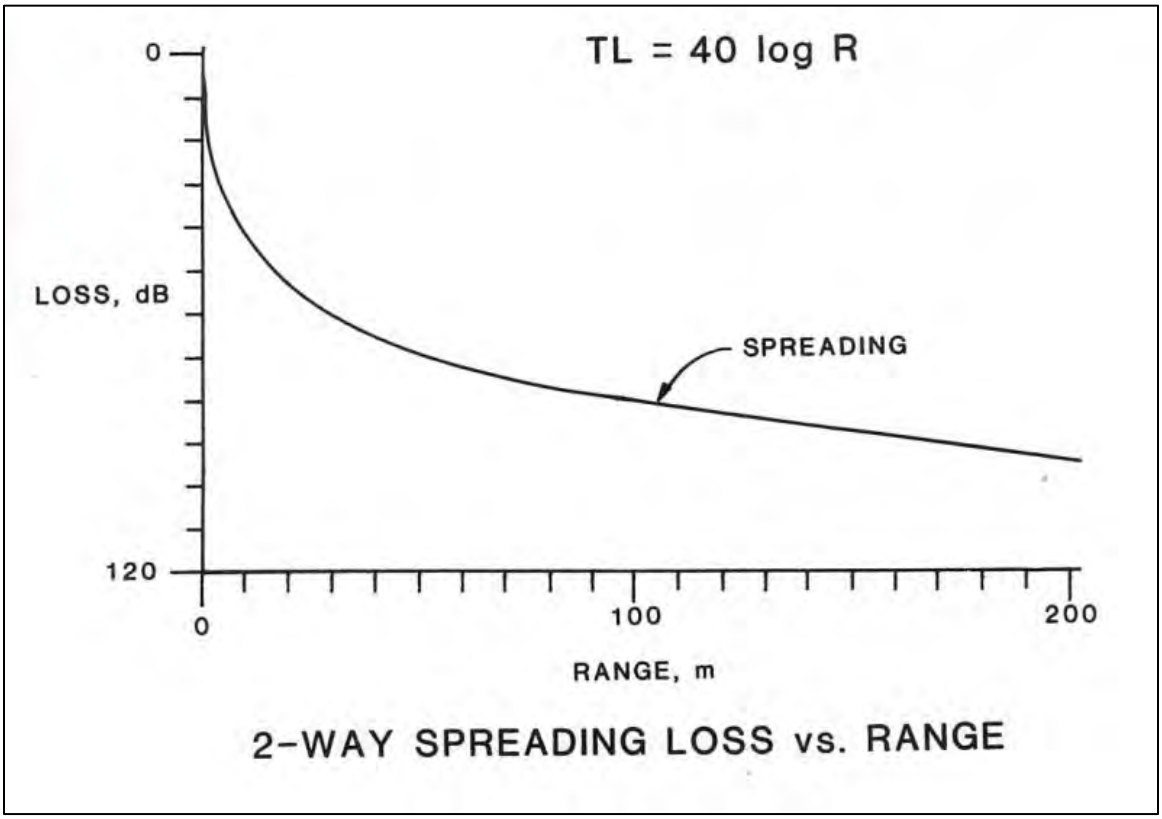

Figure 5-9. Relationship of signal loss over distance as a result of spherical spreading. (Source Mazel 1985:3-7).

Reflection and scattering, the last limiting factors, result from contact between sound waves and hard surfaces. This includes objects within the water column and sound waves contacting the bottom. Mazel (1985) continues, "the second effect is that there will be a relatively persistent, low level of acoustic energy reaching the sonar during each sweep." As sound waves contact bottom surfaces, only a portion of the pulse is reflected back in the direction of the transducer, further weakening the strength of returning signals—as absorption, spreading, and scattering continue to affect the wave on its return journey. In some ways, however, reflection is also an important diagnostic tool. The intensity of the reflection is a function of the amount of reverberation induced in the material being ensonified. Higher reverberation yields higher intensity returns, generally indicating harder, denser materials.

Absorption, spreading, reflection, and scattering will affect side scan sonar and interferometric systems alike, as these are unchangeable interactions between sound waves and water. Within each type of system, multiple filters and algorithms are employed to mitigate these effects and optimize data collection, many of them proprietary in nature. In both cases, however, sound wave energy is inevitably lost to these forces, imposing limitations on range and resolution. By collecting data close to the bottom, side scan sonar utilizes proximity to mitigate, to varying extents, these effects.

CHAPTER 6

ACOUSTIC IMAGING FOR ARCHAEOLOGICAL RESOURCES: OPERATIONAL EVALUATION OF INTERFEROMETRIC SONAR EFFICIENCY AND EFFECTIVENESS

The following operational evaluation of interferometric sonar for the identification of archaeological resources was prepared by multiple authors working in collaboration, including John Bright and David Conlin of the National Park Service Submerged Resources Center and William Danforth and William Schwab of the United States Geological Survey, Coastal and Marine Geology Program, Woods Hole Science Center.

This chapter describes tests used to evaluate and compare the effectiveness of acoustic imaging via interferometric sonar in detecting archaeological resources off the coast of Massachusetts.

Acoustic imaging of the seafloor provides archeologists with an efficient and detailed record from which to identify cultural material. Most survey archaeologists, however, do not have a wide array of acoustic imaging systems at their disposal. Interagency collaboration, such as that facilitated during this study offered the opportunity to bring together and test a variety of survey platforms under the same or similar conditions. In this case, side scan sonar and interferometric sonar systems were tested in the MA WEA. (Sub-bottom profiling was used in this survey for paleo-landform identification. Since sub-bottom profiling is a fundamentally different form of acoustic data collection than is side scan and interferometric sonar, it is addressed separately in Chapter 4).

Comparison between the side scan sonar and interferometric sonar systems provided a valuable opportunity to elevate relative assessment of these platforms beyond theoretical comparisons. Experimentation provided *in situ* observation of the operational capabilities of these systems, information that in the future will help guide regulatory decisions regarding archaeological surveys in federally-managed areas.

6.1 SWATH ACOUSTIC SONAR OPERATION

Swath acoustic systems transmit sound pulses that are narrow along the system's direction of travel, and broad perpendicular to it, thus covering a wide area or "swath" of the seafloor during a survey.

6.1.1 SWATH ACOUSTIC SONAR TYPES

Sonar system types are differentiated based upon the manner in which sound waves are propagated into the water, as well as the manner in which returning waves are interpreted and visualized. Currently there are three swath system types used to map and visualize the surficial characteristics of the seafloor:

- multibeam echo sounders;
- interferometric bathymetric sonars (also referred to as phase differencing bathymetric sonars); and
- side scan sonar systems.

6.1.2 BACKSCATTER AND REFLECTIVITY

Swath sonar systems operate at varying transmit frequencies, depending on the manufacturer and model, and yield results in the form of acoustic reflectivity or "backscatter" when the transmitted sound pulse returns to the system following reflection off the seafloor. These forms of acoustic data are utilized to produce images of the seafloor depicting the relative reflectivity of the seabed. They also provide information as to the general distribution and characteristics of the surficial sediment, outcropping strata, and man-made materials resting on the seabed. Additionally, multibeam echo sounders and interferometric sonars provide water depth across the swath of the seabed that is co-registered with the acoustic backscatter, providing dense bathymetric soundings of the survey area.

6.1.3 USE OF HIGH AND LOW FREQUENCIES

Swath acoustic systems are versatile equipment platforms offering a range of imaging capabilities. High-frequency swath sonar systems allow detailed mapping of targeted areas, while low-frequency systems allow for "regional" mapping in general survey areas. Used in tandem, a dual (or multi-) frequency survey can cover large areas of the seafloor while allowing archeologists to recover detailed imagery of specific targets.

6.1.4 FACTORS IN SELECTING SONAR SYSTEMS AND SURVEY TRACKLINE SPACING

Selecting an appropriate system for a subsea survey, therefore, is largely dependent upon the specific survey project objectives:

- location;
- desired resolution;
- physical dimensions of the objects that the survey expects to find,
- area that needs to be mapped (regional vs. site specific vs. target study which may include optical systems);
- cost; and
- time.

Collecting high-resolution imagery requires a considerably greater commitment of boat time per unit of survey area than performing a lower-resolution general survey. A more detailed survey, furthermore, utilizes narrow swath widths, while general surveys cover more area in less time by scanning with much wider swaths.

Often, surveyors will employ a dualistic approach. A relatively rapid, low resolution general area survey is used to create a list of targets or areas of interest which are re-visited with high resolution survey for more detailed imagery. The optimal survey platform is dependent entirely upon the situation.

6.2 SIDE-SCAN SONAR OPERATION

Side scan sonar operates by generating a discrete acoustic pulse which propagates vertically into the water column, a portion of which returns to the sensor after reflecting off the bottom. Upon

contacting the sensor, the same transducer that generated the sound is activated by the return pulses and in turn provides an image of the bottom. Thus, as Mazel (1985:1-2) describes:

> Sonar systems do not actually measure depth or distance. What sonars are really measuring and displaying is the time it takes for the transmitted sonar pulse to travel from the transducer to the target and return. The accuracy of the sonar depends on the ability to measure this time precisely.

6.2.1 OPERATIONAL CONSIDERATIONS AND CORRECTIONS

Several technical processes are required to overcome absorption, scattering, and spreading of the waves to ensure as high a degree of precision as possible (see Chapter 5). Fish and Carr (1990) describe the processes of speed correction and slant range correction. These are background functions that most remote sensing systems run automatically, when necessary.

Another corrective function executed by the system is time varied gain. This function compensates for the weakness of the returning sound signal as distance from the sensor increases. Even in an area where the seafloor is uniform, the signal reaching the sensor from the distant portion of the swath would be weaker than the initial returns, despite contacting the same material. Uncorrected, this would result in the bottom image intensities falling in amplitude, despite the surface being uniform. Since the rate of absorption, scattering, and spread are consistent, these effects are essentially cancelled out by applying an artificial enhancement to the weaker signals traveling from far away, in essence boosting a weaker signal from more distant objects to compensate for the loss of signal strength (Mazel 1985). Time varied gain is an automatic function in most systems; overall gain is user-adjustable and can be increased or decreased during data acquisition and processing for display purposes.

6.2.2 USER-CONTROLLED SETTINGS

The range of the signal produced by the side scan sonar is a user-controlled feature. As was previously discussed, selecting a given frequency allows the operator to select the appropriate range and resolution for a given survey area. Some systems, such as the Klein 3000H used in this study, are dual frequency, meaning they are capable of simultaneously operating at low and high frequency.

Another adjustable signal characteristic is pulse length. The thickness of the sound beam is a factor of the pulse length and the speed of sound in water (see Figure 5-2). Assuming a speed of 1,500 M/sec (Mazel 1985), pulse thicknesses for different pulse durations are calculated in Table 6-1. Theoretically, pulse thickness should equate to range resolution given that the appropriate frequency and range are used (see Figure 5-3). Operational testing, however, reveals that pulse thickness as a direct measurement of range resolution is not entirely accurate, and is discussed at length in Section 6.4 below.

Table 6-1.
Pulse thicknesses for various pulse durations, a proxy for range resolution.

Transmission Pulse Duration (µs)	Pulse Thickness (m)
25	0.0375
50	0.075
100	0.15
200	0.30
400	0.60

6.2.2 SOME LIMITATIONS OF SIDE SCAN SONAR

The processes and settings of side scan sonar systems adjust the shape of the sound signal broadcast into the water, then filter and amplify the returns based on known constants to account for absorption, spreading, and scattering. Nevertheless, beyond a certain threshold, time-varied gain and range correction no longer work; once the signal is reduced beyond a certain amount, no corrective solution is possible. In various environments and at various configurations, these thresholds will change. The point of the comparison experiment, therefore, is to quantify these limitations in the area south of Cape Cod; results are limited to the systems used in the survey, in that there are many similar systems on the market with regard to operational frequencies.

A final operational consideration regarding the use of side scan sonar deals with position fixing and geo-location of acquired data. In most surveys, the side scan sensor is towed behind the survey vessel by means of a 'smart' cable, a cable that is threaded through a digital counter and sends the amount of cable deployed to the acquisition program. The exact position of the sonar fish, therefore, is estimated by factoring the offset of the sonar sensor from the GPS receiver via the length of cable deployed and the altitude of the sensor off the seafloor. Errors made in estimating the exact position of the sensor result in erroneous geo-rectification of data as acoustic returns are processed by the survey system; as the sonar fish is moved further from the GPS receiver (i.e. in deeper surveys where longer cable lengths are needed) navigation errors can compound. Additionally, processing schemes for towed side scan sonar systems generally do not utilize attitude information, in particular heading and pitch from the towfish, as this information can be very erratic in areas of high current and/or heavy seas. Thus, surveys in deeper water utilizing side scan sonar may experience difficulty georectifying acoustic data, which can in turn lead to difficulty re-locating features present in a given acoustic dataset. When compared to a boat-mounted system (such a multi-beam or interferometric system) where a GPS receiver and a motion reference unit (MRU) can be placed in the exact position of the acoustic sensor, side scan systems lack a high degree of navigational accuracy.

6.3 INTERFEROMETRIC SONAR OPERATION

Interferometric sonar systems operate in the same manner as a side scan sonar system with regard to recording a swath time series of amplitudes (backscatter) returning from the seafloor. However, these systems offer the added benefit of recording the depths over the swath, similar to a multibeam echo sounder. Unlike multibeam systems, interferometric sonars are not beam-forming systems, but accurately measure depths at precise locations on the seafloor via the use of exactly spaced phase differencing transducer elements, which measure the phase offsets of acoustic returns. The phase offset is used to calculate the angle from which the return was received. The angle, in combination

with range based on two-way travel time, is used to calculate the position of the seafloor and objects upon it relative to the instrument (Gostnell 2004). Unlike a side scan system, where the same transducer that generates the sound waves also receives their return, an interferometric system utilizes a single transducer to produce sound waves and an array of precisely spaced receiving transducers to receive and interpret the return (see Figure 6-1).

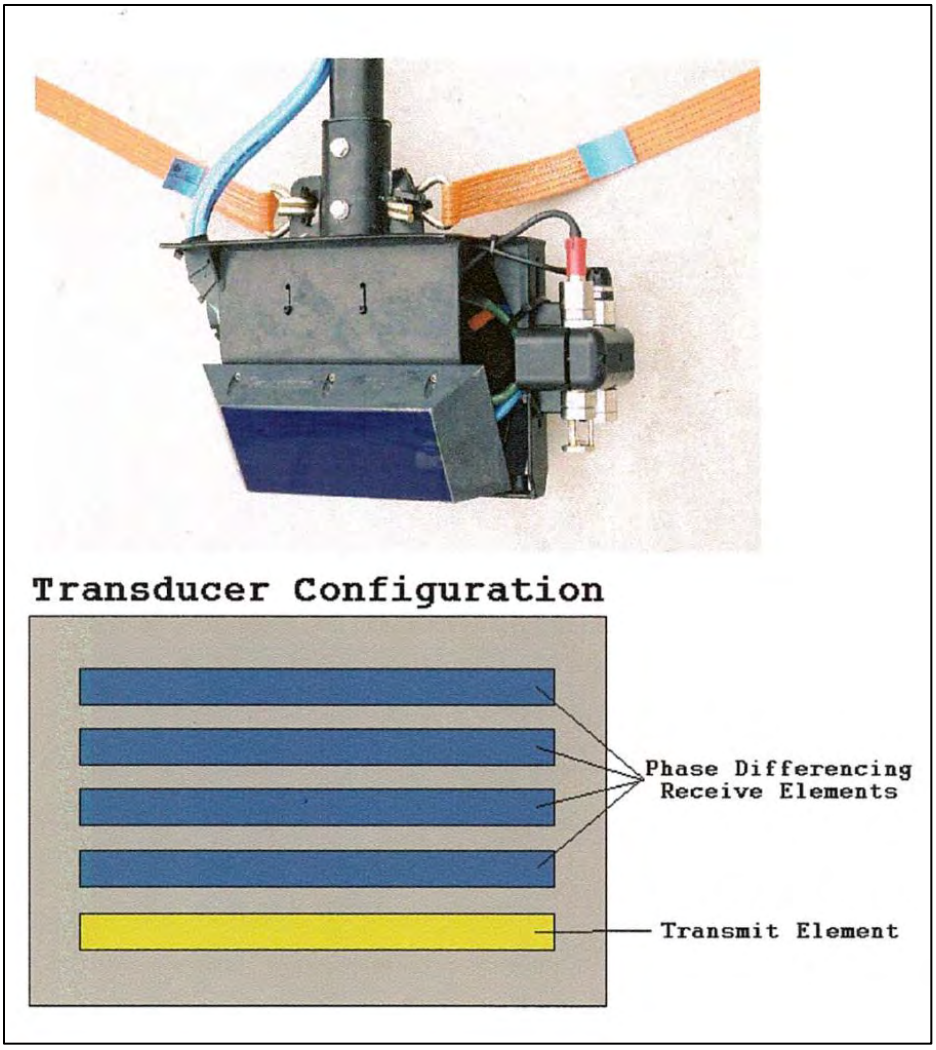

Figure 6-1. General configuration of phase differencing bathymetric sonar system. (Source: Gostnell 2004:4).

Interferometric systems record a relatively wide swath width, nearly 10 times the altitude of the instrument above the seabed, as compared to a swath width from side scan sonar that is 3 to 5 times the altitude of a multibeam system (Gostnell 2004; Gostnell et al. 2006). At some level, however, a depth threshold will impose limitations on the system; the sound waves cannot be broadcast and coherently interpreted through unlimited distance (depth) due to absorption, spreading, and scattering, which will eventually consume the energy of the wave. Interferometric systems are typically mounted on a pole attached to "side-mount" on the ship, or mounted directly onto the ship's hull. Interferometric sonars are coupled to a MRU that measures heave, pitch, heading, and roll of the MRU, and which has a built-in inertial navigation system that is linked to a DGPS system.

The MRU is located within the frame that holds the transducers; thus the navigation output, coupled with the attitude information from the MRU, gives the exact position of the transducers and subsequently the exact location of the ensonified swath. This is in contrast to towed side scan sonar systems in which the distance from the ship's navigation antenna to the towfish is estimated via layback methods.

Commercially available interferometric systems offer varying operational frequencies between 125 and 500 kHz. Though these frequencies are considerably less than commercially available high-frequency side scan sonars (greater than 500 kHz) the ability to collect medium frequency data across a large swath width is the greatest utility offered by these systems. Additionally, interferometric sonars simultaneously collect side scan sonar data, as shown in Figure 6-2; thus, these systems produce a precisely navigated, detailed bathymetric surface overlain with the acoustic backscatter data, useful in application as a general area archaeological survey platform.

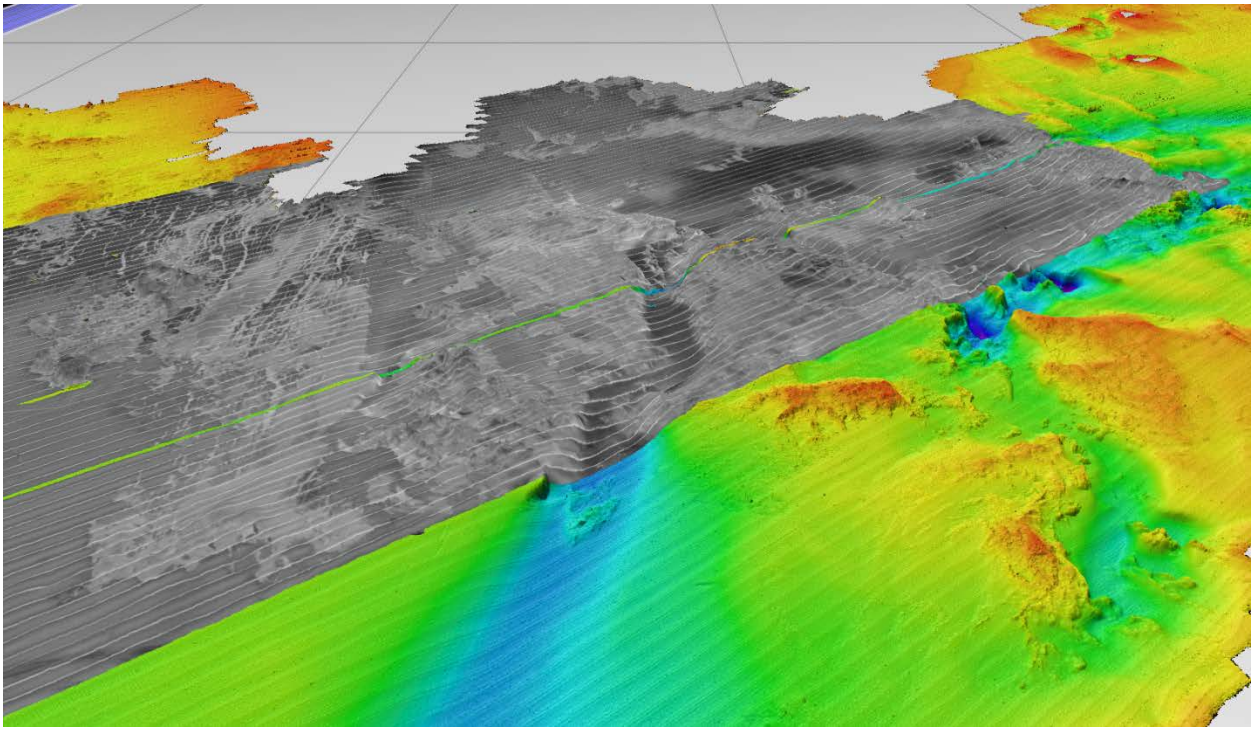

Figure 6-2. Bathymetric image produced from interferometric data co-located with a side scan sonar mosaic in Buzzards Bay, MA. (Source: Ackerman et al. 2013).

6.4 RESULTS OF OPERATIONAL TESTING

Having discussed the suite of physical laws governing the movement of sound waves through water in Chapter 5 and the technological strategies used by sonar systems to overcome them in this chapter, the question remains: to what degree do these factors limit the effective range and resolution of sonar systems, and, as a result, how is the optimal acoustic system selected for general and targeted survey?

In the case of the WEA, the optimal acoustic system was tested simultaneously by surveying the same targets with high- and low-frequency side scan sonar and with an interferometric system and

comparing their results. The USGS interferometric system operates at a frequency of 234 kHz. There were two different side scan sonar units used in this survey: a Klein 3000H and a Klein 3000. The Klein 3000H operated at 445 kHz (low frequency) and 900 kHz (high frequency) and the Klein 3000 sonar operated at 100 kHz (low frequency) and 500 kHz (high frequency). The Klein 3000 was substituted when it was discovered the low-frequency transducers in the NPS SRC's Klein 3000H were damaged and, therefore, incapable of collecting reliable data.

The first parameter considered was the effective range for each system and with each frequency. Since range refers to the area covered to only one side of the side scan sonar, twice the range is the actual swath width achievable by that system. Sensor altitude must also be a consideration, since elevation of the sensor will govern the range of the seafloor that is ensonified. As a general rule and for optimal results, the side scan sonar should be flown at an altitude that is 10 percent of the desired range for a particular survey. For example, a range of 100 m (328 ft), which produces a 200 m (656 ft) swath, would require that the sensor be towed at an altitude of 10 m (33 ft) from the seafloor. With an interferometric system, the water depth determines the effective range of the system. In general, interferometric systems can ensonify a swath of the seafloor that is approximately 7 to 10 times the water depth below the sensor, depending on the seafloor substrate. Lower ranges are achieved in low backscatter environments, whereas higher ranges are achieved in areas of high backscatter. For example, in 30 m (98 ft) of water, the interferometric sonar can theoretically ensonify the seafloor with a 210 to 300 m (689 to 984 ft) swath width.

Based on the known behavior of sound waves in water, higher frequencies were expected to yield less range than lower frequencies, and this was the case during comparative testing (Table 6-2). It is important to note that the 445 kHz transducer on the Klein 3000H was damaged, therefore these observations were not indicative of the capabilities of a functional unit. As expected, the lower frequencies were capable of a greater range, up to as much as 600 m (1,968 ft) for the 100 kHz channel. Unfortunately, line spacing was not planned sufficiently wide enough to test the range limits of each frequency, especially the 100 kHz, thus the only conclusion that could be reached was that the 500, 445, 234, and 100 kHz systems were functional out to 75 to 100 m (246 to 328 ft) ranges, typical spacing for archaeological survey. Additional testing is needed to quantify these ranges more precisely in the WEA, though each system demonstrated the capability to cover the ranges typically planned for archaeological survey. The high frequency side scan system, 900 kHz, demonstrated a lower effective range, as expected based on the attenuation of higher frequency sound pulses into the water column. When flown at an altitude of approximately 10 m (33 ft) from the bottom, the 900 kHz system resolved objects out to 25 m (82 ft).

Table 6-2.
Observed range versus reported range from five side scan sonar frequencies.

Frequency (kHz)	Manufacturer Spec. Range (m)	Observed Range (m)	Figure
900	50	25	Figure 6-3
500	150	greater than 75	Figure 6-4
445	150	greater than 75	Figure 6-5
100	600	greater than 75	Figure 6-6
234	7 to 10x water depth	greater than 75	Figure 6-7

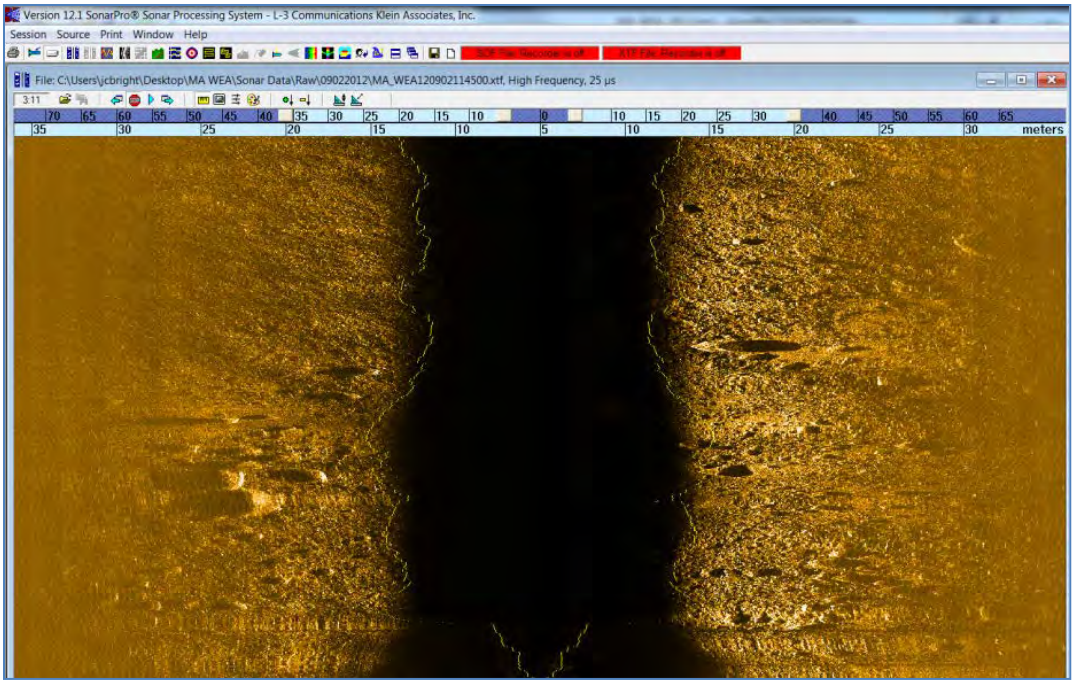

Figure 6-3. Observed range of 900 kHz side scan sonar. Range scale is indicated in the light blue band on top of the image.

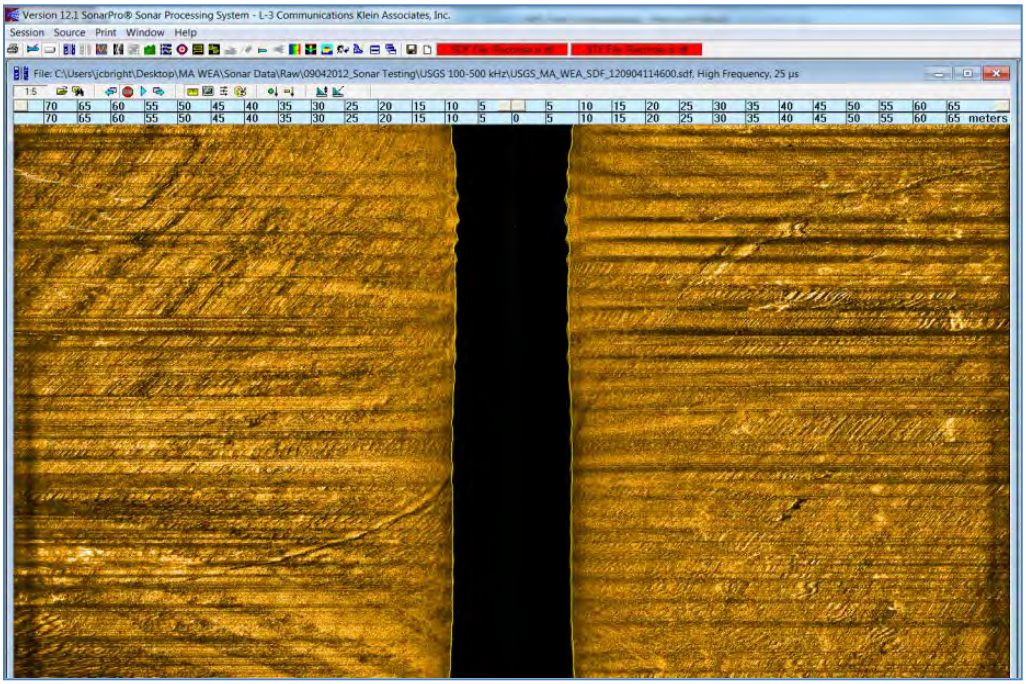

Figure 6-4. Observed range of 500 kHz side scan sonar. Range scale is indicated in the light blue band on top of the image.

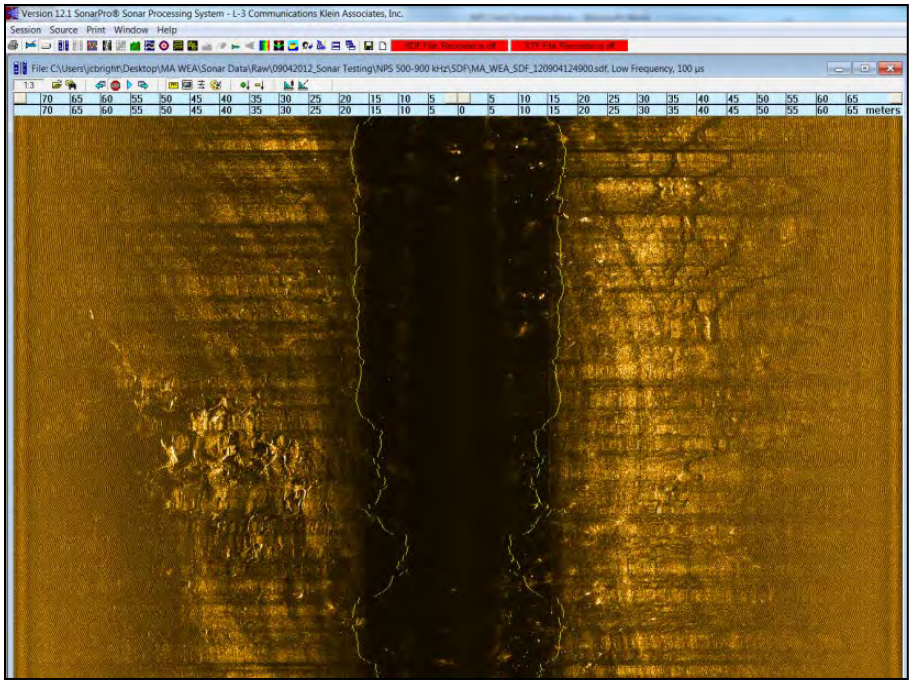

Figure 6-5. Observed range of 445 kHz side scan sonar data, though the transducer in the apparatus was damaged. Range scale is indicated in the light blue band on top of the image.

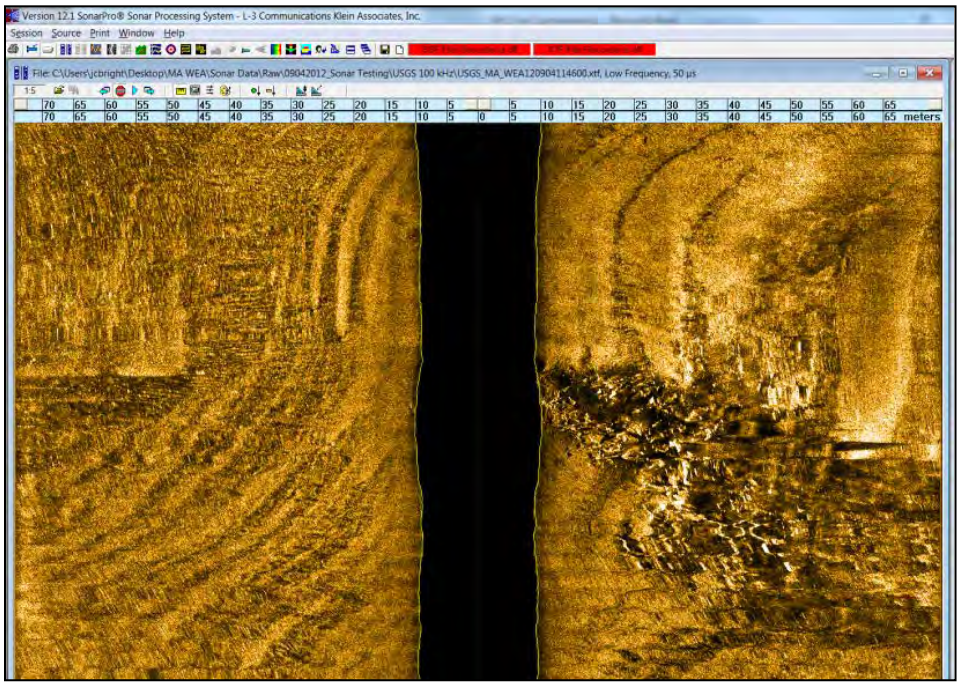

Figure 5-6. Observed range of 100 kHz side scan sonar. Range scale is indicated in the light blue band on top of the image.

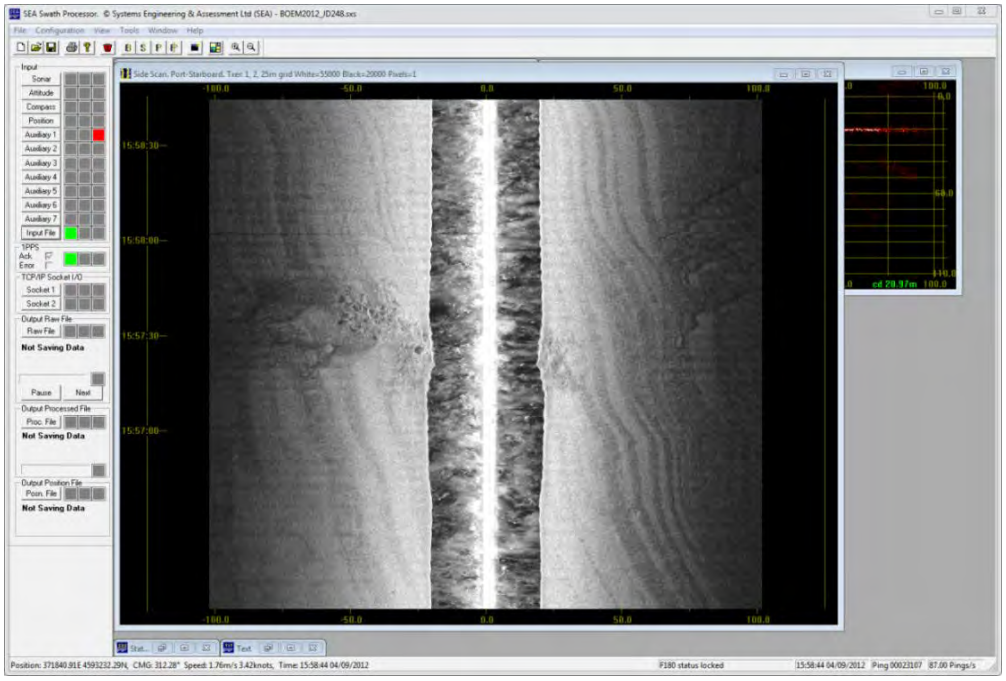

Figure 5-7. Observed range of the 234 kHz interferometric sonar. Range scale is indicated in the sonar window.

The next measured parameter was resolution, both transverse and range, for each frequency. Transverse resolution values are reported in Table 6-3, and range resolutions reported in Table 6-4. A combined resolution is shown in Table 6-5. Each frequency resolution was calculated by measuring the distances between objects parallel to the path of the sensor (transverse or along track) and arranged perpendicular to the sensor's path of travel (range or across track). To reduce errors in measure, most of the data were displayed as high resolution mosaics (15 cm [5.9 in] pixel size) in ArcGIS, or in full resolution mode in Sonar Wiz 5, allowing use of the measuring tool in each case to determine distances. These measurements were left on the screen images shown in each of the figures referenced in the tables below. Areas in the Vineyard Sound and Buzzards Bay data sets were chosen for measurement due to the presence of small and highly variable bottom type, geological substrates, and conspicuous sand waves.

Table 6-3.
Observed transverse resolution values for side scan sonar frequencies.

Frequency (kHz)	Beam Angle	Transverse Res. (m)	Figures
100	.70º	1.2	Figure 6-8
234	.55	.8	Figure 6-17
445	.21º	No data	n/a
500	.21º	.9	Figures 6-9, 6-10, and 6-16
900	.21º	.8	Figures 6-11 and 6-12

Table 6-4.
Observed range resolution values for side scan sonar frequencies.

Frequency (kHz)	Transmission Pulse (µsecs)	Pulse Thickness (m)	Range Res. (m)	Figures
100	50	.075	.9	Figure 6-13,
234	Variable (8.5 and up)	.013	.5	Figure 6-17
445	n/a	n/a	n/a	n/a
500	25	.0375	.57	Figures 6-14 and 6-16
900	25	.0375	.28	Figure 6-15

Table 6-5.
Minimum detectable size for each frequency.

Frequency (kHz)	Minimum Object Size (m)
100	1.2 x .9
234	.8 x .50
445	unknown
500	.9 x .57
900	.8 x .28

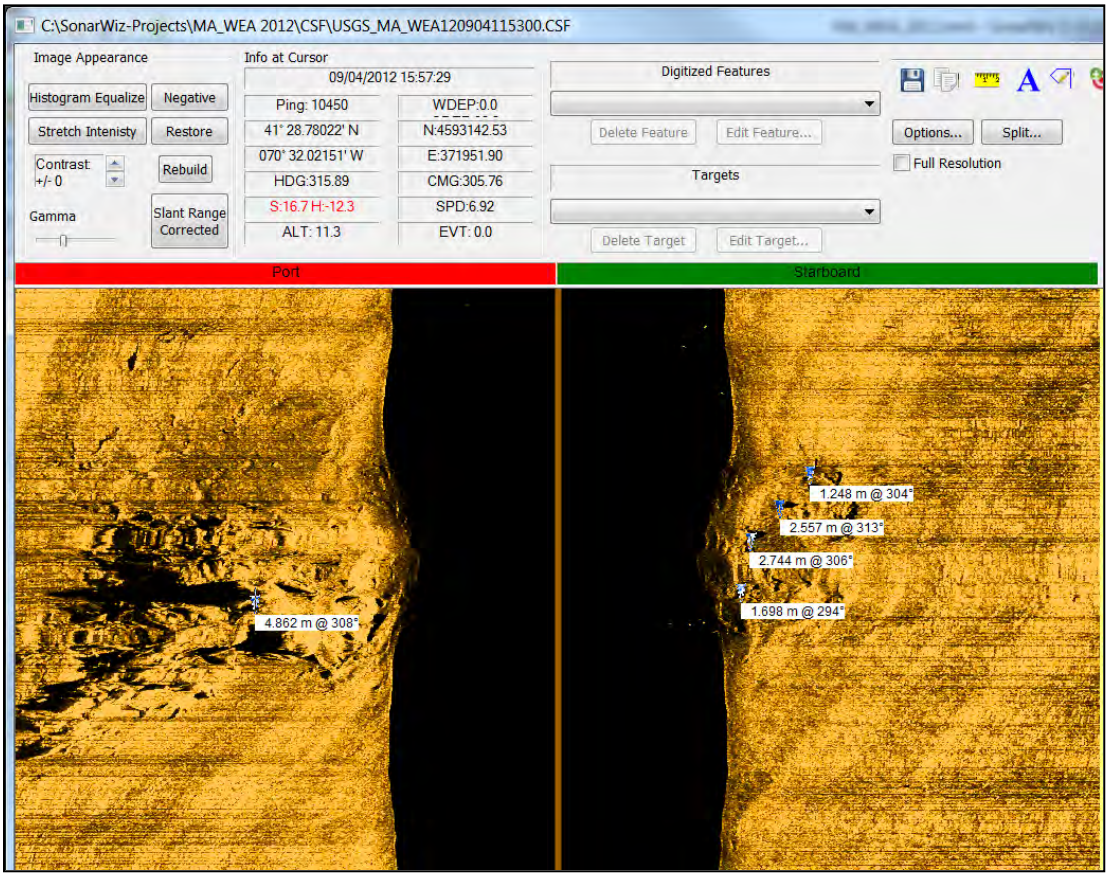

Figure 6-8. Observed transverse resolution of 100 kHz data. Bearings in degrees indicate direction of measurement

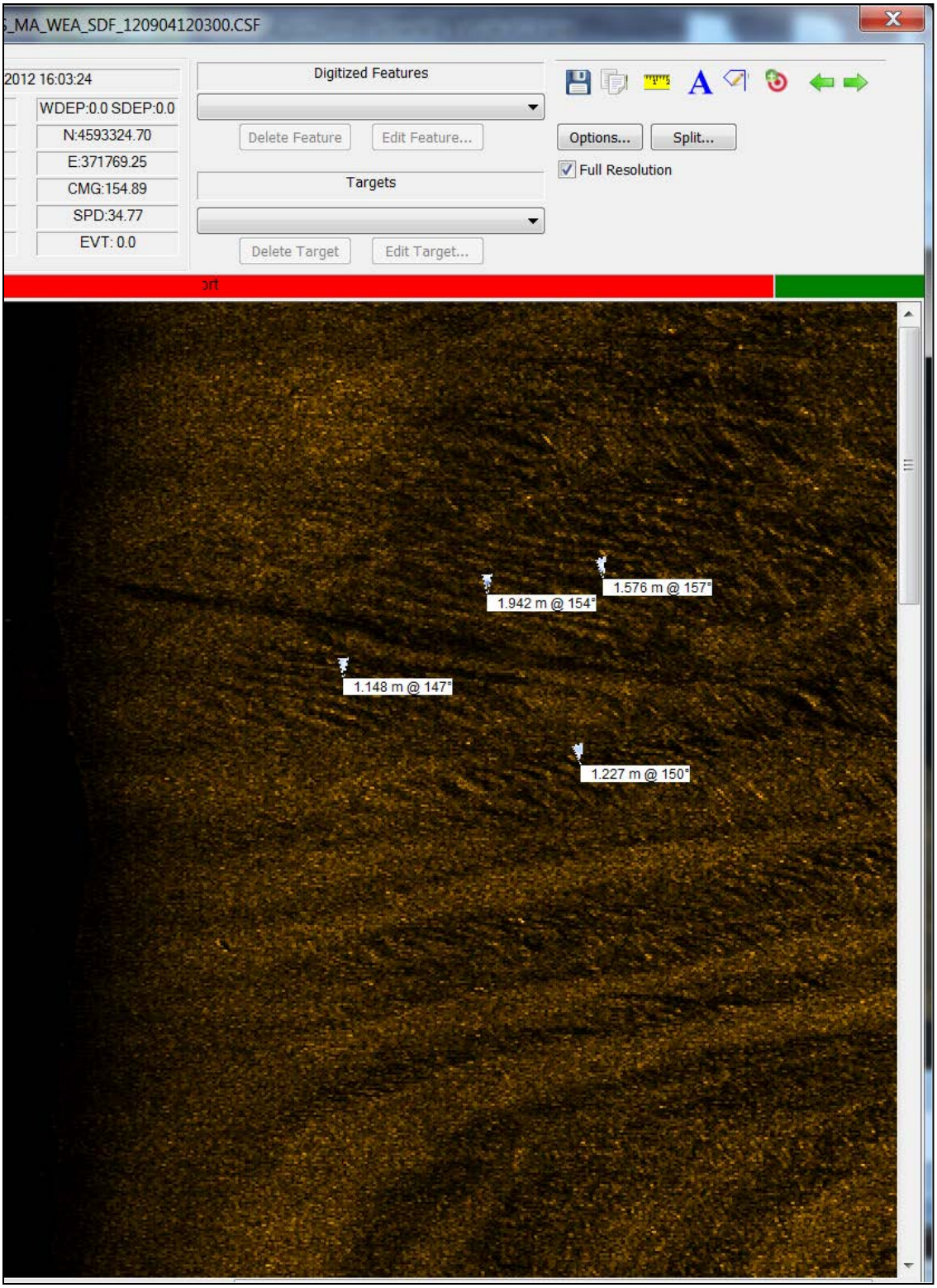

Figure 6-9. Transverse resolution of 500 kHz with small sand waves. Bearings in degrees indicate direction of measurement.

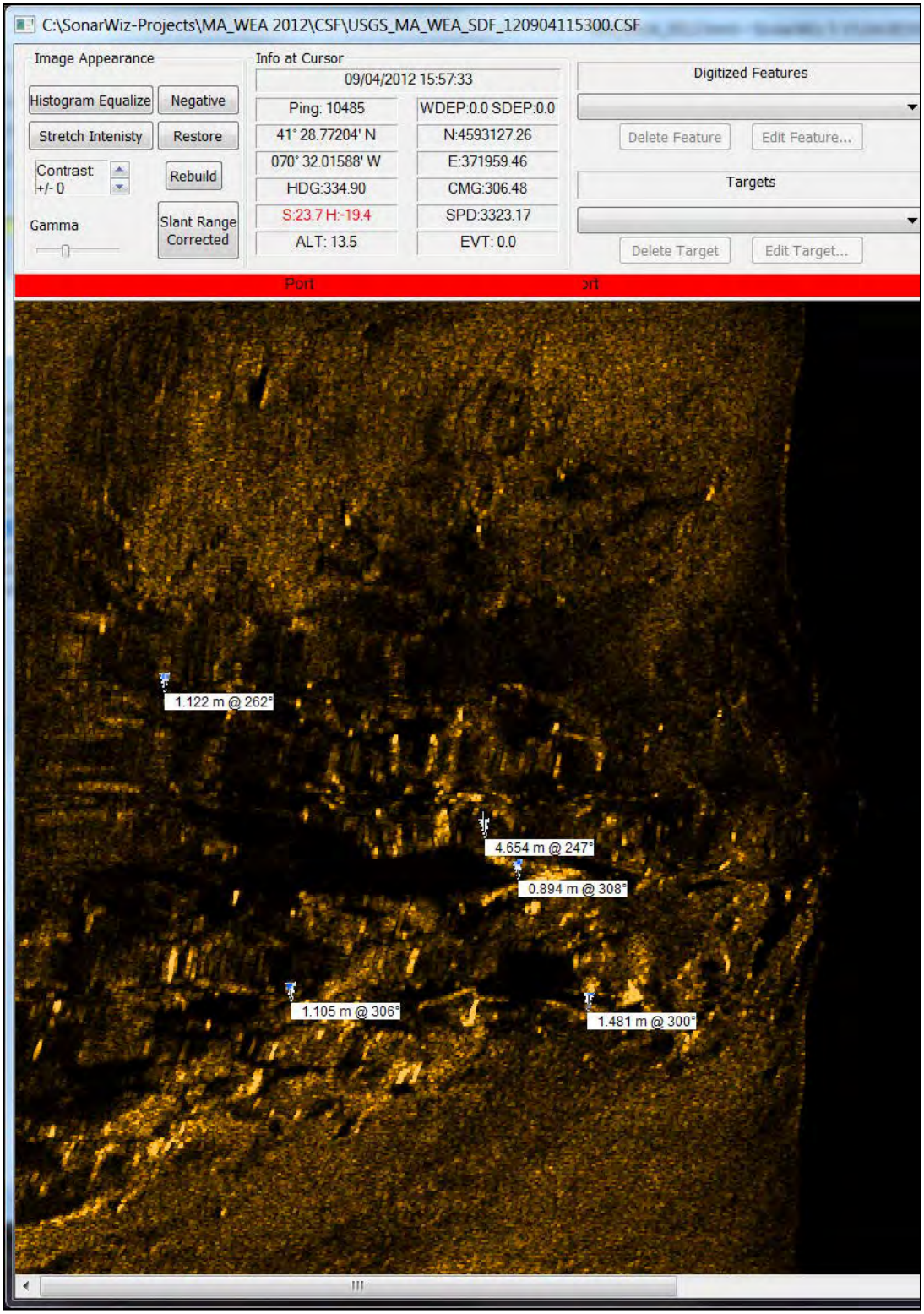

Figure 6-10. Transverse resolution of 500 kHz data with discrete features. Bearings in degrees indicate direction of measurement.

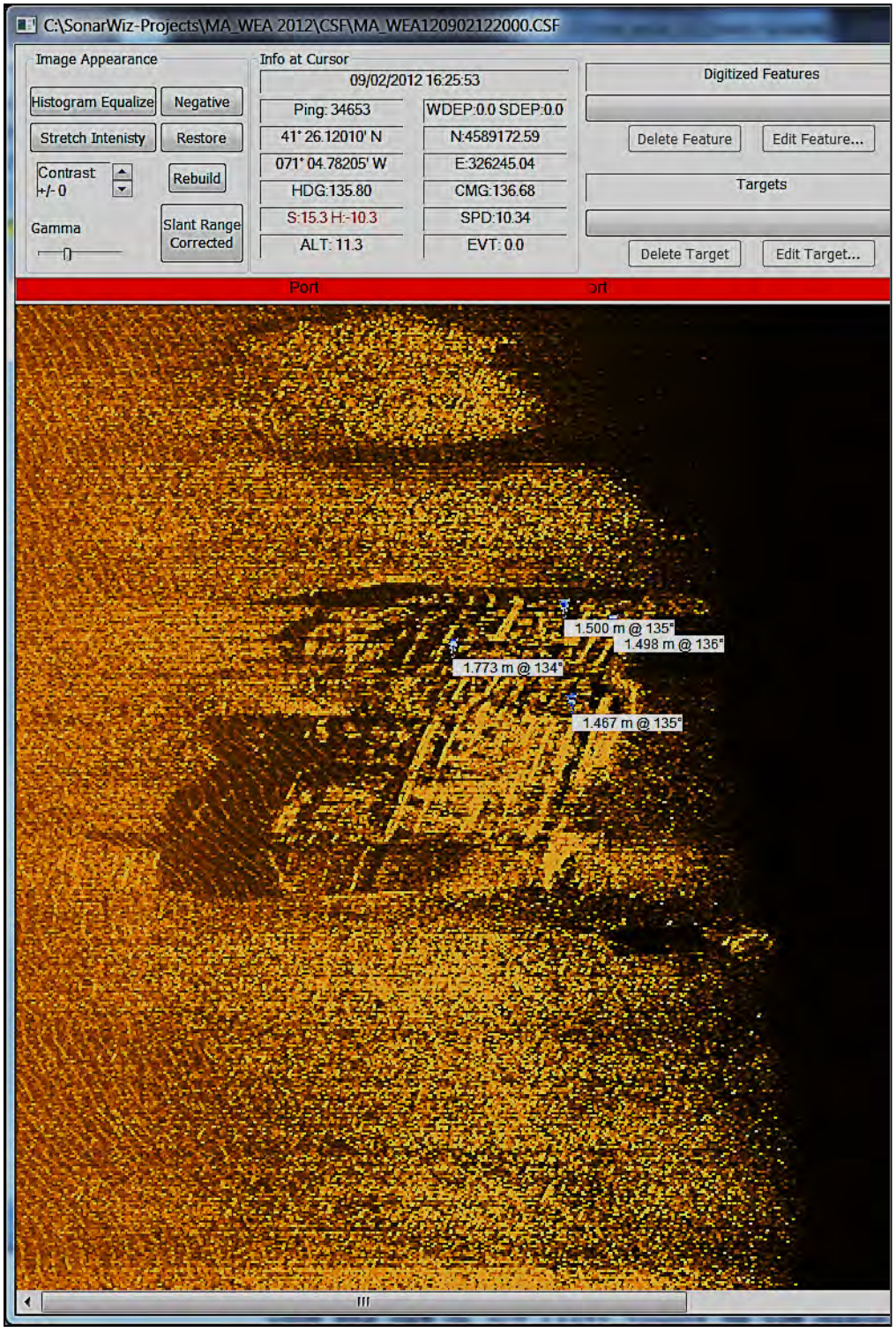

Figure 6-11. Transverse resolution of 900 kHz data on parallel features of shipwreck. Bearings in degrees indicate direction of measurement.

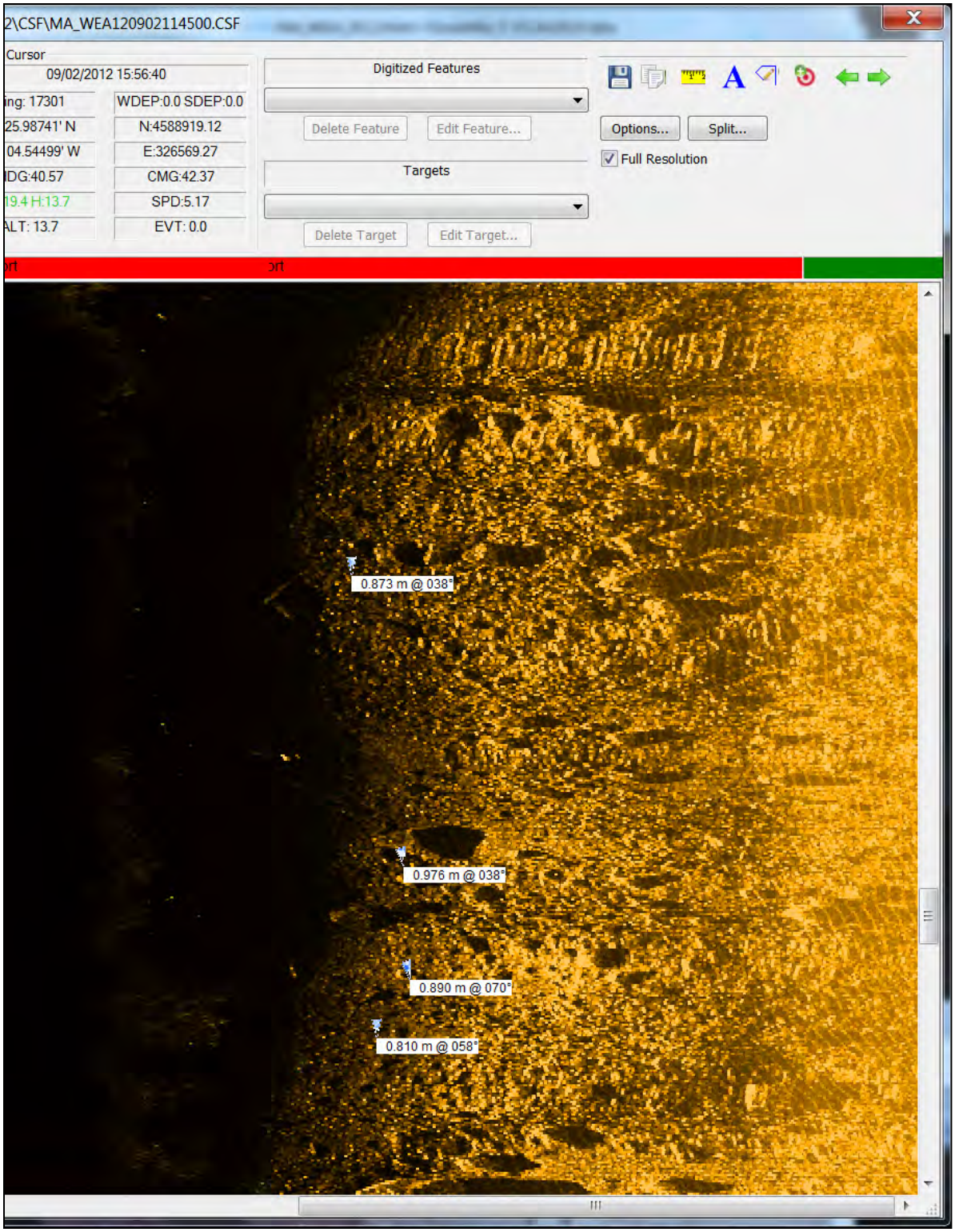

Figure 6-12. Transverse resolution of 900 kHz data based on discrete features. Bearings in degrees indicate direction of measurement.

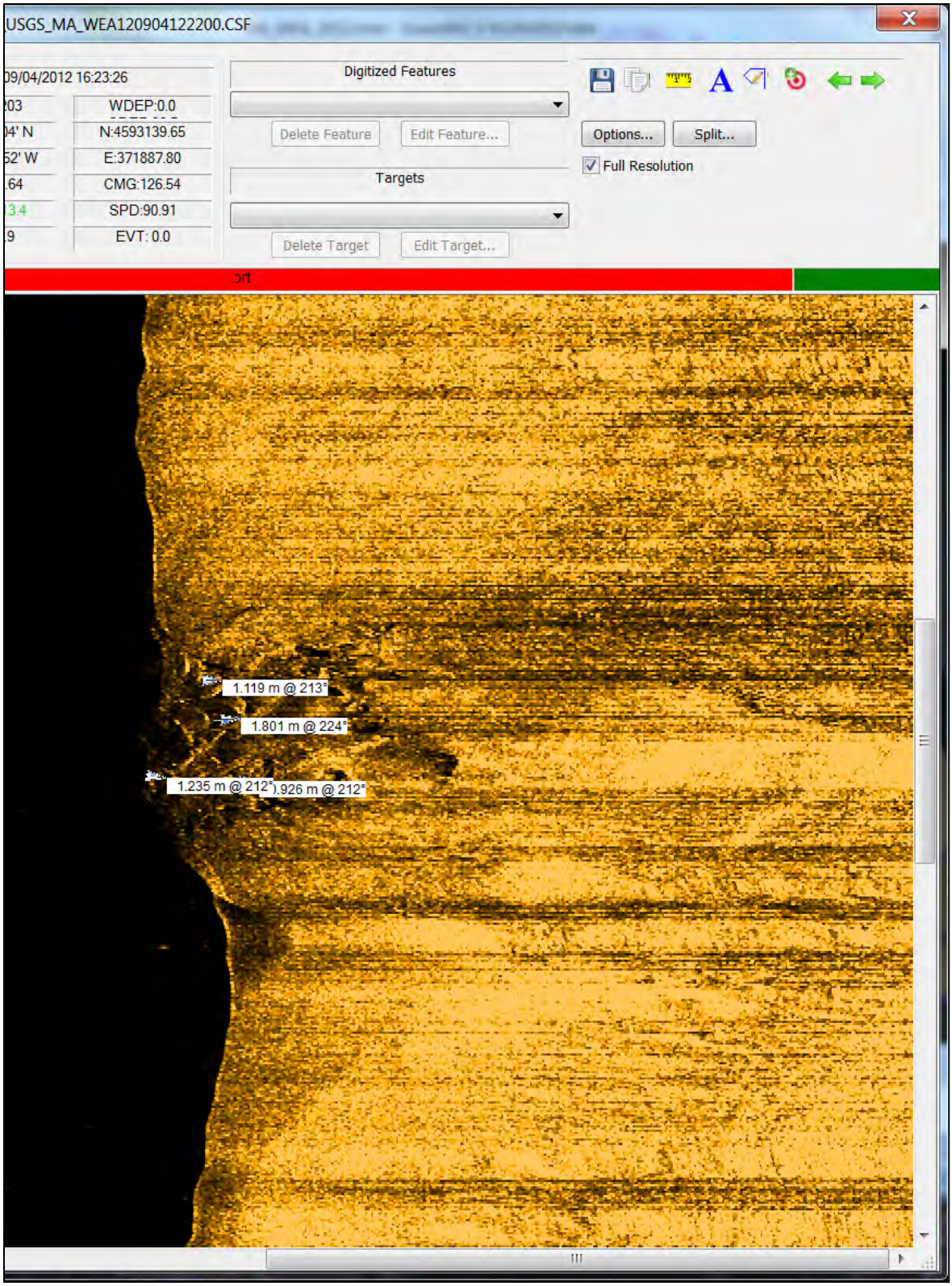

Figure 6-13. Observed range resolution for 100 kHz data. Bearings in degrees indicate direction of measurement.

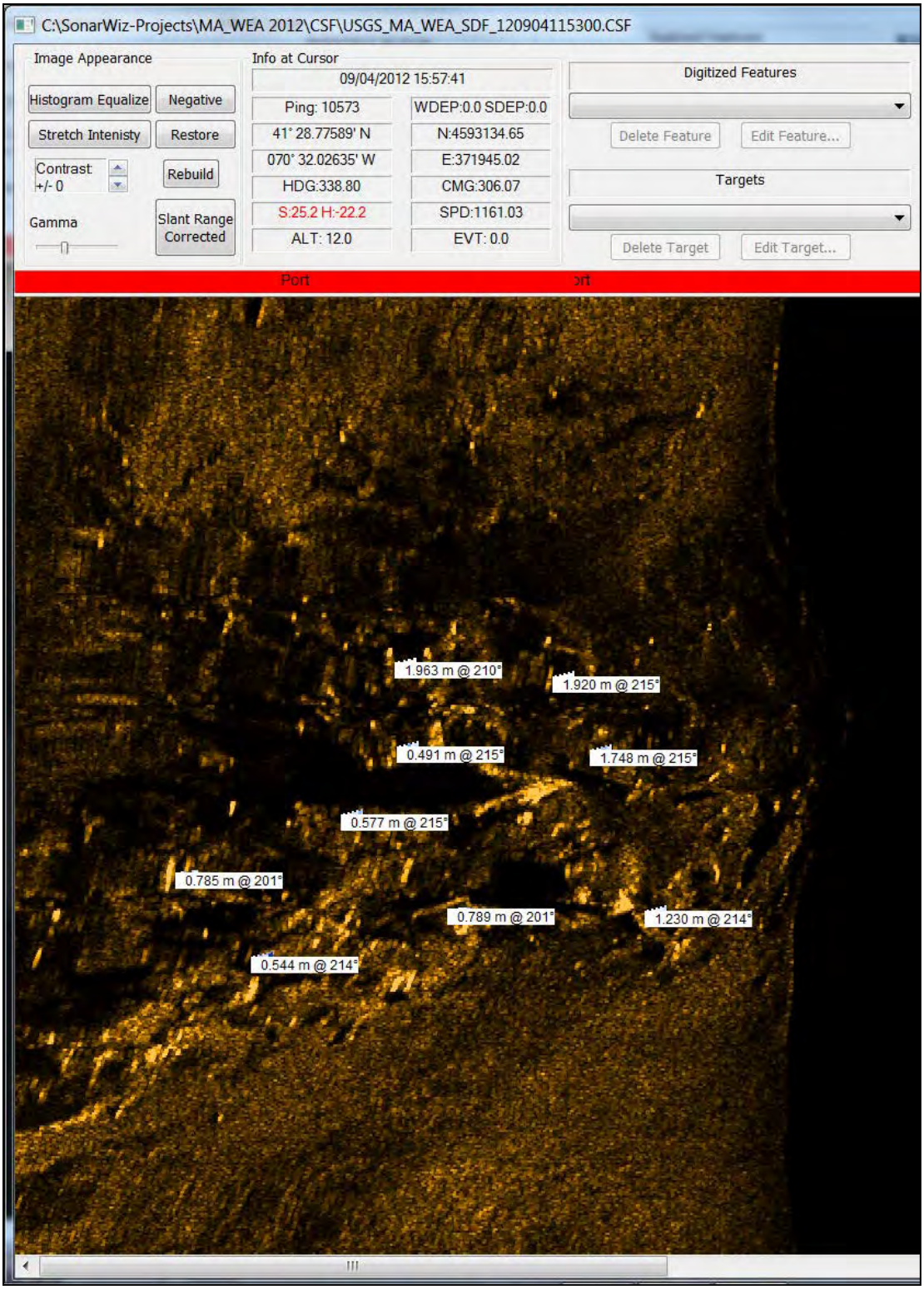

Figure 6-14. Observed range resolution of the 500 kHz data. Bearings in degrees indicate direction of measurement.

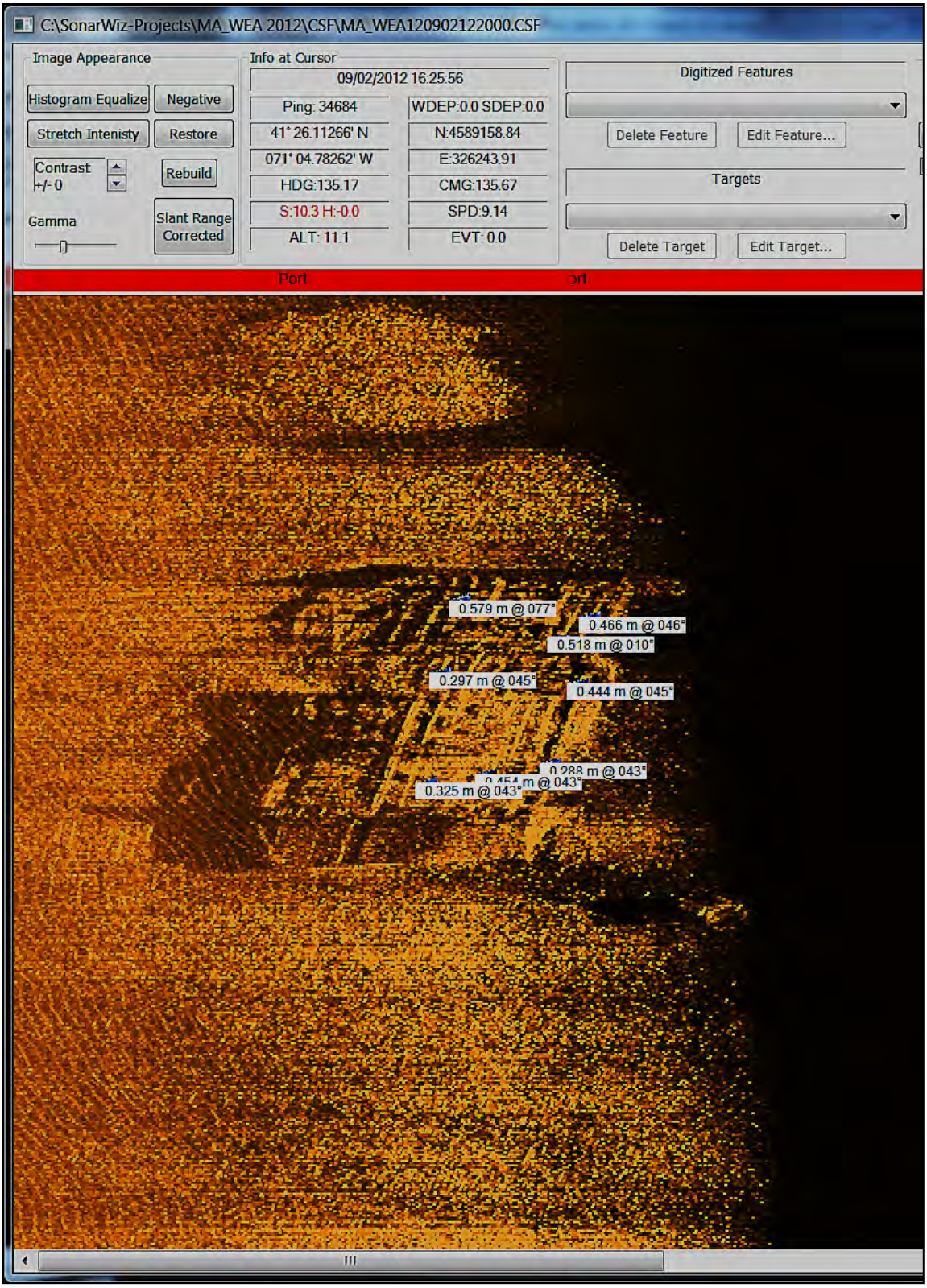

Figure 6-15. Observed range resolution for 900 kHz data on shipwreck site. Bearings in degrees indicate direction of measurement.

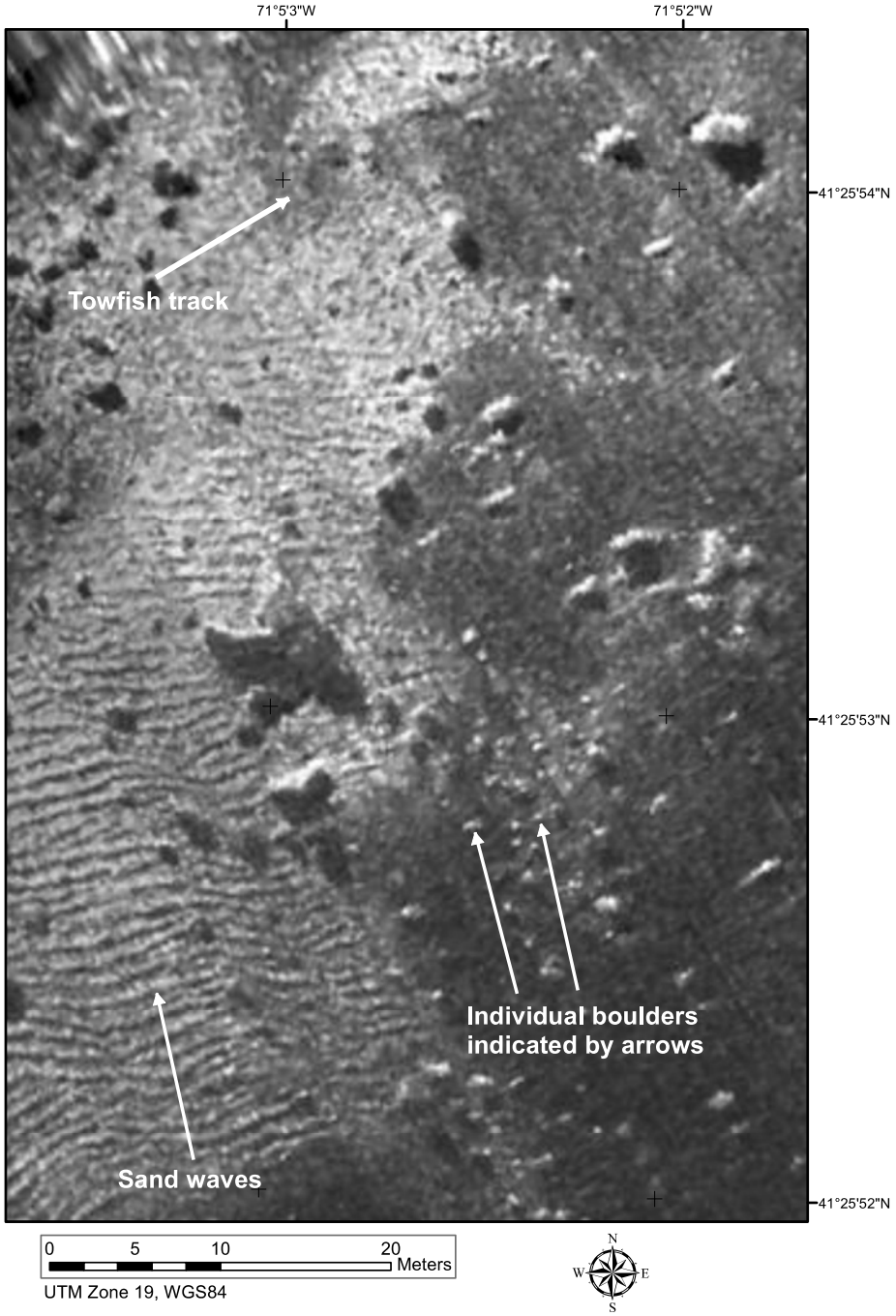

Figure 6-16. Boulder field and sand waves in Buzzards Bay ensonified by the 500 kHz side scan sonar. Individual boulders were measured with an along track (transverse) resolution average of 0.5 m (1.6 ft), and an across track (range) resolution average of 0.4 m (1.3 ft). Individual sand waves show an average trough to crest distance of 0.75 m (2.5 ft) across track.

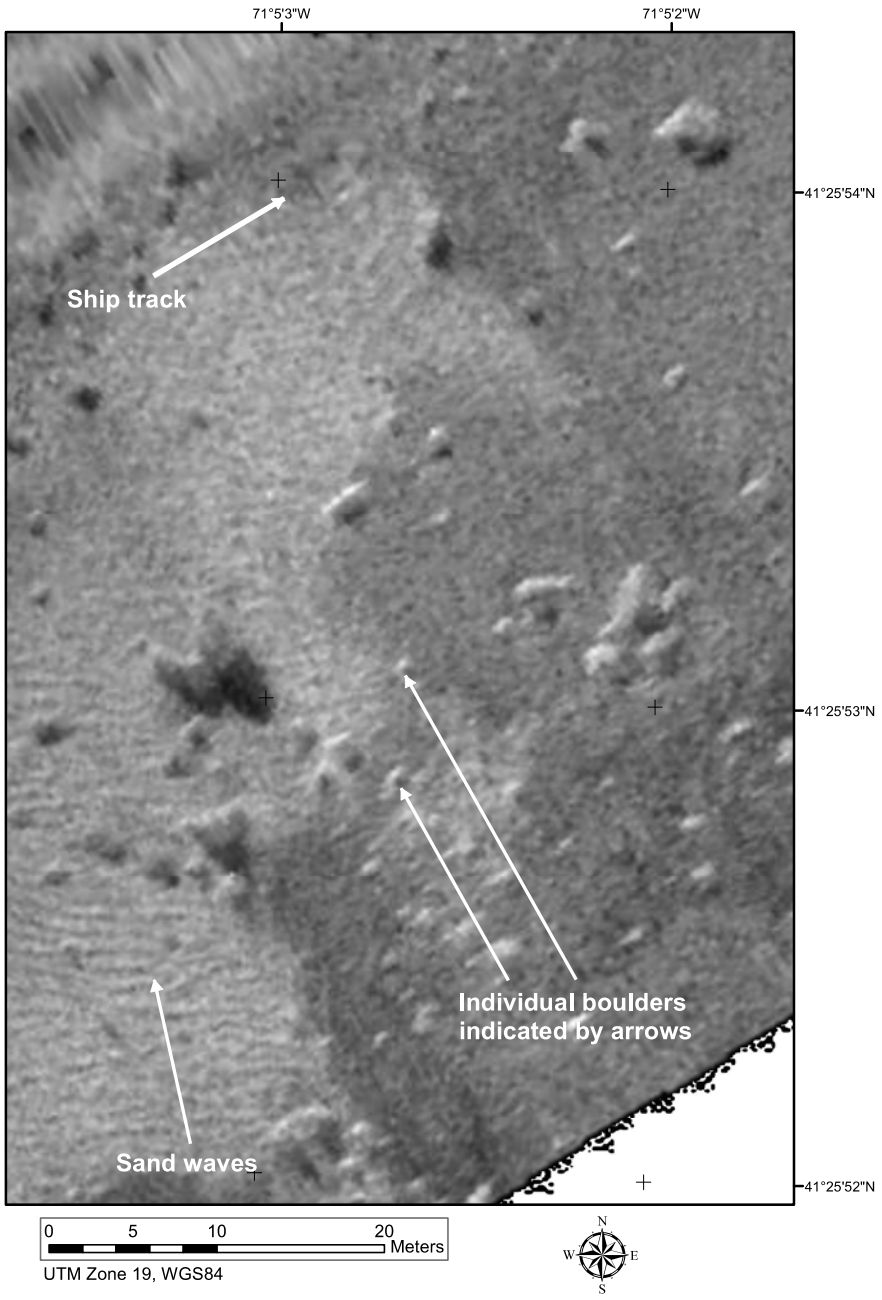

Figure 6-17. Boulder field and sand waves in Buzzards Bay ensonified by the 234 kHz interferometric sonar. Individual boulders were measured with an along track (transverse) resolution average of 0.8 m (2.6 ft), and an across track (range) resolution average of 0.5 m (1.6 ft). Individual sand waves show an average trough to crest distance of 0.75 m (2.5 ft) across track.

As expected, the higher frequencies had greater resolution. All systems, however, were able to resolve objects approximately greater than 0.5 m (1.6 ft) in size (across track) with the 500 and 900 kHz systems getting much finer resolution than that. Despite the failure of the 445 kHz system's transducers, a safe assumption is that it performs similar to the 500 kHz system. In terms of actual objects, on a uniform seafloor, each system could resolve the large and medium material culture items discussed in Chapter 3: shipwrecks, engines, anchors, cannon, and so on. The sonar mosaics shown in Figures 6-18 through 6-20 show the wreck imaged in Buzzards Bay with the 900 kHz and 500 kHz Klein systems, as well as the 234 kHz Interferometric SWATH*plus* system. Similarly, large geological features will be visible across all ranges of frequencies. Figures 6-21 and 6-22 show data collected from Vineyard Sound with the Klein 3000. Both show varied geological features, though the 500 kHz imaging is more detailed. Figure 6-23 shows the same features as imaged by the 234 kHz interferometric SWATH*plus* system. The image illustrates as much detail as the towed side scan system mosaics, however the contrast is not as pronounced due to the difference in the grazing angles of the incident and backscattered sound waves (a surface deployed interferometric sonar ensonifies the seafloor at higher grazing angles as opposed to the towed side scan sonar system). The lower grazing angles of the transmitted sound pulse from a towed system produce more pronounced shadows from discrete objects on the seafloor, giving the resulting image a more distinct contrast.

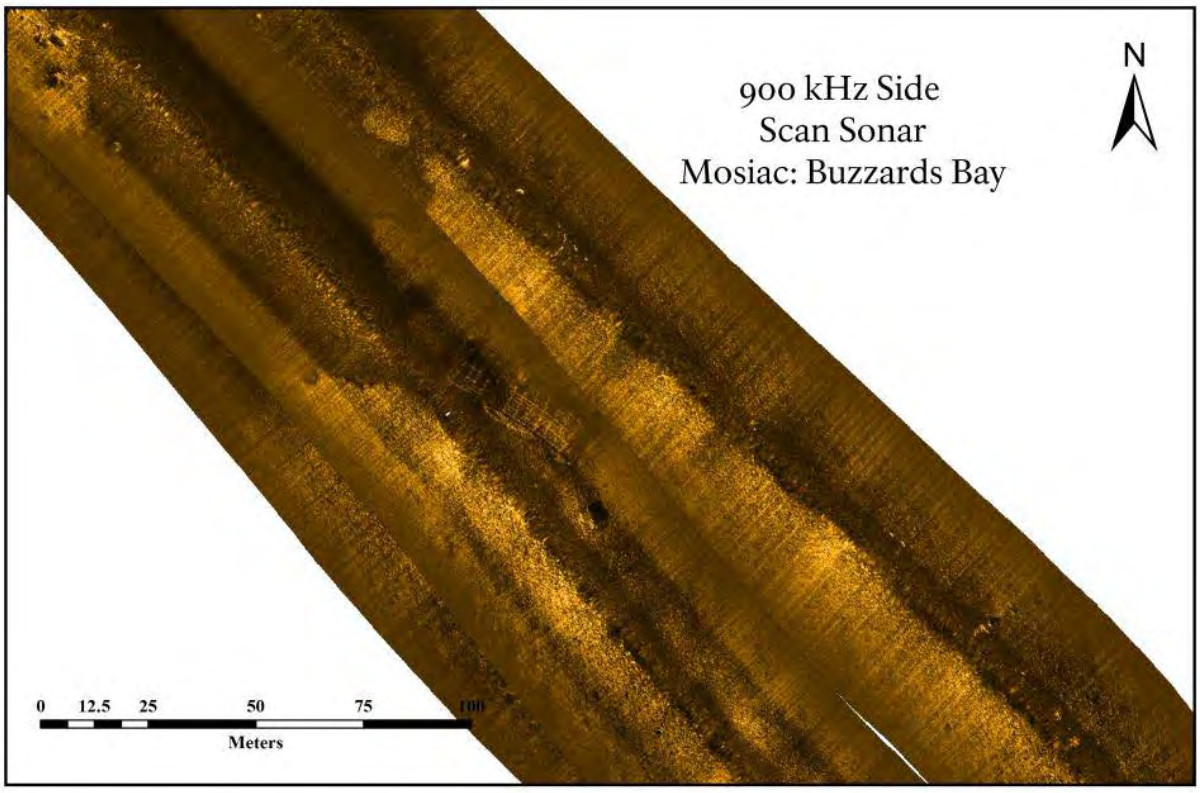

Figure 6-18. Mosaic of shipwreck in Buzzards Bay with 900 kHz system (source: J. Bright, NPS-SRC).

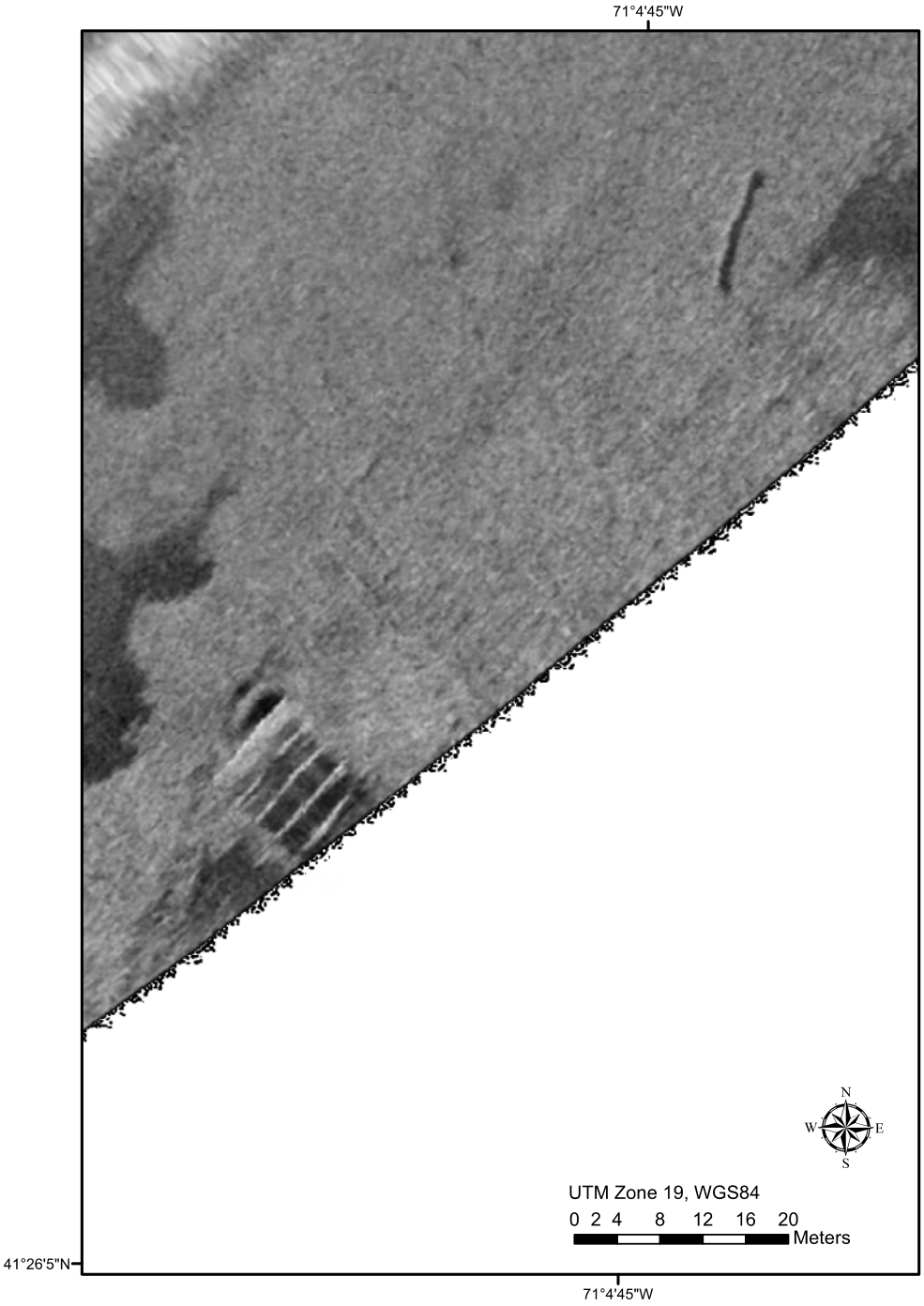

Figure 6-19. Buzzards Bay shipwreck ensonified with the SWATH*plus* 234 kHz interferometric sonar. Individual "ribs" or decking can be seen which are on the order of 20 to 50 cm (8 to 20 in) wide (across track) at a range of 60 m (197 ft). In the upper right is another anthropomorphic artifact that is approx. 50 cm (20 in) wide.

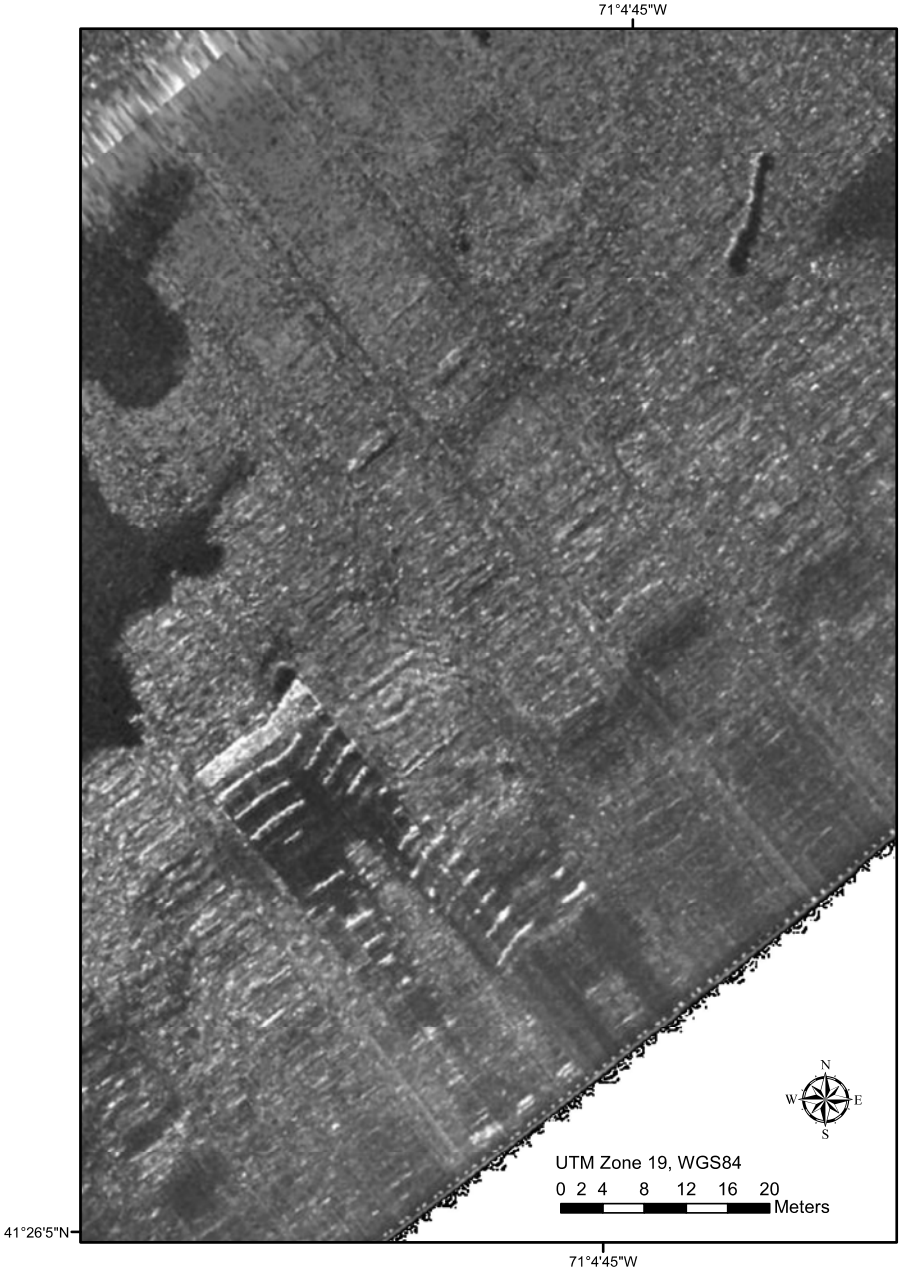

Figure 6-20. Buzzards Bay shipwreck ensonified with the Klein 500 kHz side scan sonar. Individual "ribs" or decking can be seen which are on the order of 20 to 50 cm (8 to 20 in) wide (across track) at a range of 60 m (197 ft) In the upper right is another anthropomorphic artifact that is approx. 50 cm (20 in) wide.

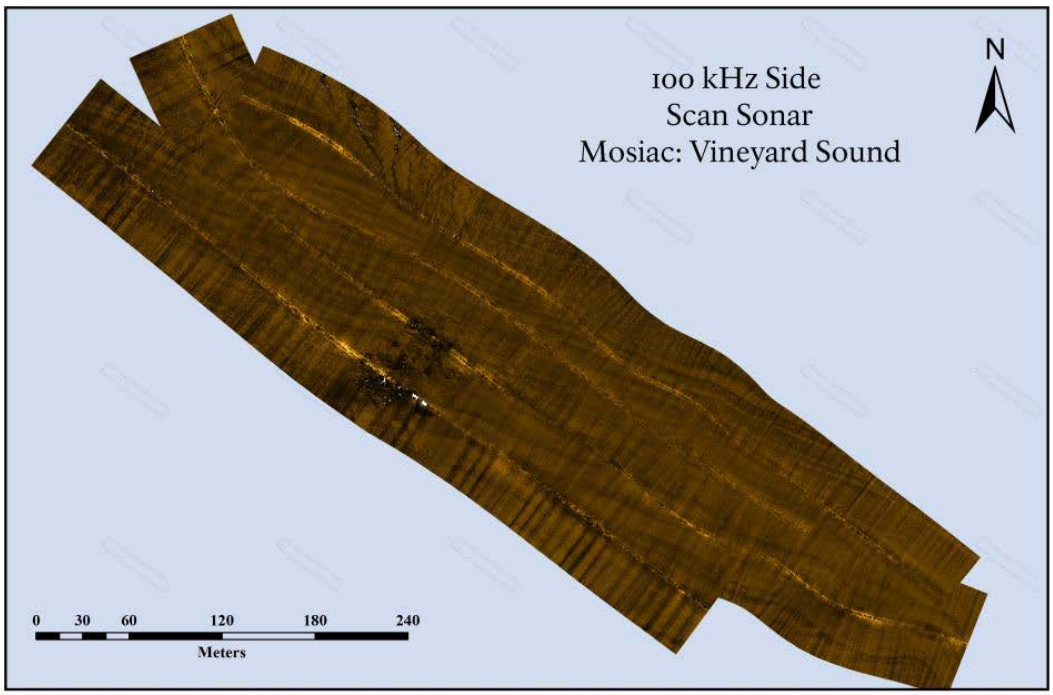

Figure 6-21. Low resolution mosaic of geological features in Vineyard Sound using 100 kHz side scan sonar.

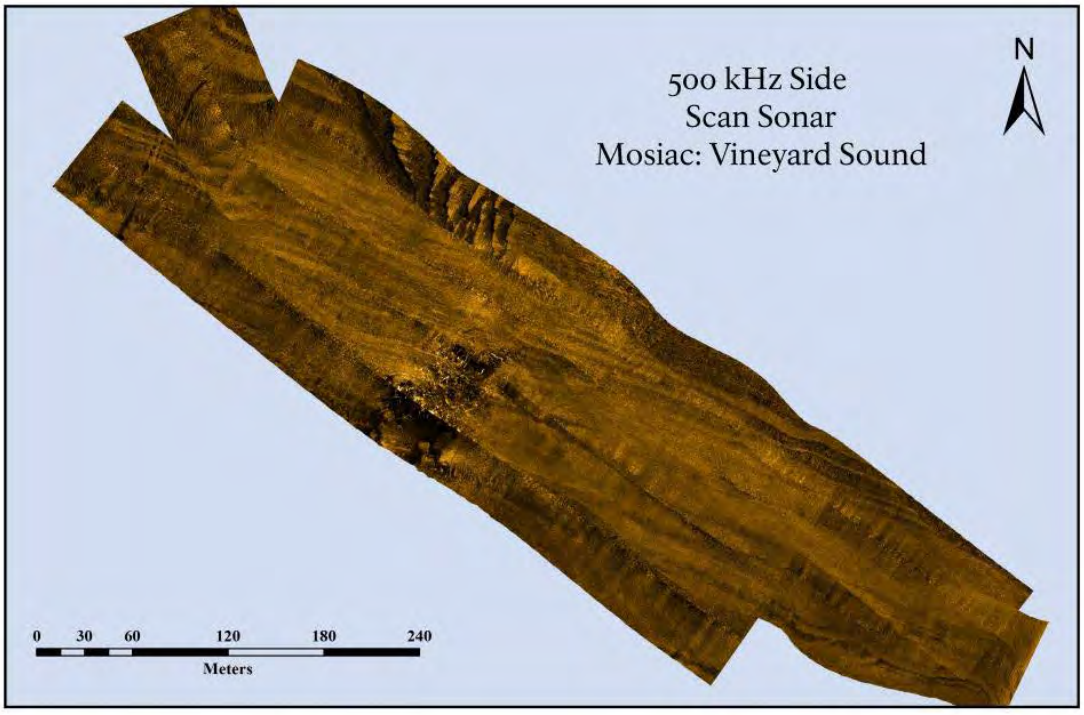

Figure 6-22. Medium resolution mosaic of geological features in Vineyard Sound using 500 kHz side scan sonar.

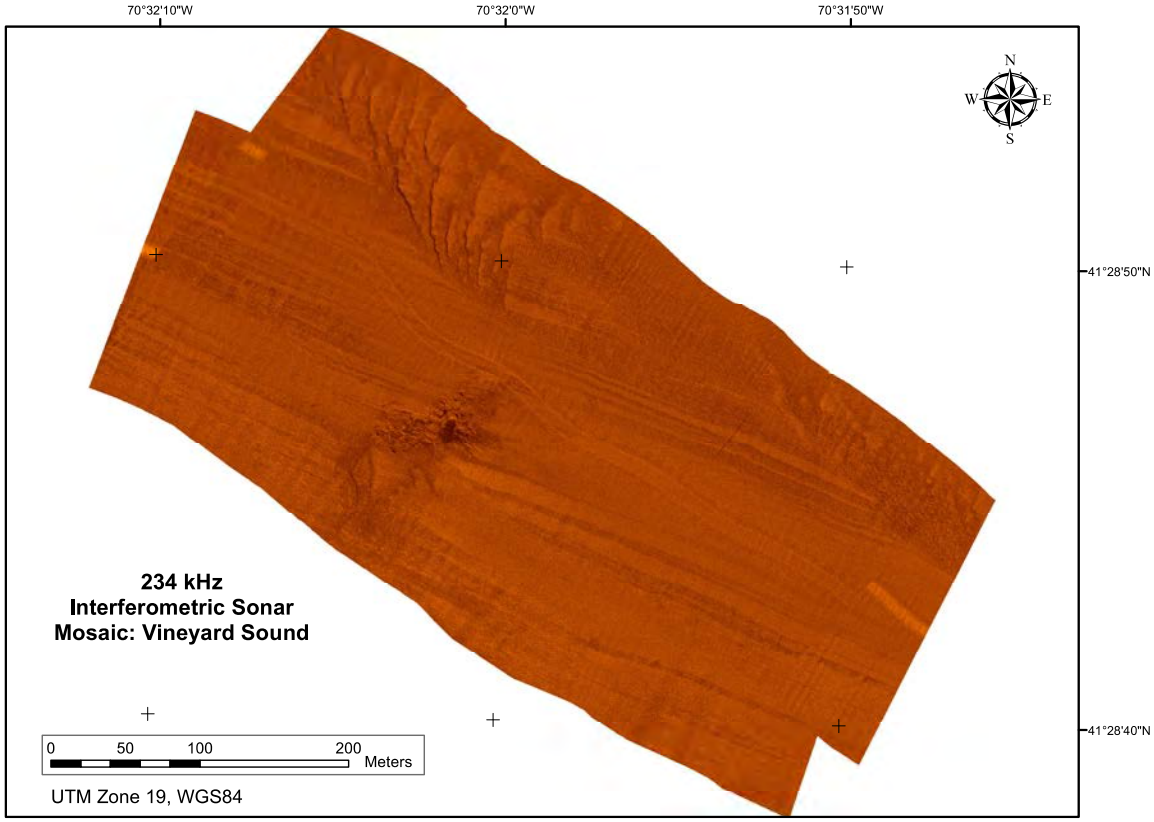

Figure 6-23. Medium resolution mosaic of geological features in Vineyard Sound using 234 kHz Interferometric Sonar.

Based upon the data from this study, each of the lower frequency systems would be able to resolve most historical artifacts within a range of 75 m (246 ft); additional testing will likely show that the 234, 445 and 500 kHz systems will resolve these objects out to 100 to125 m (328 to 410 ft), and the 100 kHz system out to 200 m (656 ft). Within short ranges, the 900 kHz will produce very detailed images of individual objects, though it is an inefficient sensor to use when conducting a general survey. In terms of smaller artifacts, such as Native American material culture, it is unlikely that any of these side scan sonar systems will be able to resolve such artifacts. In areas with any degree of geological relief, such as the areas around Vineyard Sound and Buzzards Bay, these small objects might be theoretically detectable, but in images produced by all of these instruments, they will be indistinguishable from the surrounding geology. Instead, direct sampling is necessary to detect the presence of prehistoric Native American sites.

The results of this testing demonstrate that the middle and lower frequency side scan sonar systems are more than adequate to detect objects 0.5 to 1 m (1.6 to 2.2 ft) and larger when run at 75 to100 m (246 to 328 ft) ranges. Additional testing is needed, however to determine the resolution of these systems at longer ranges. Manufacturer specifications describe a maximum range for the 445 and 500 kHz systems at 150 m (492 ft); it should be expected that their operational range is somewhat

less. The 100 kHz system, on the other hand, has an advertised range of 600 m (1,968 ft). If this is the case, the resolution at these longer ranges needs to be determined. Currently, BOEM archaeological survey standards call for survey trackline spacing no greater than 30 m (98 ft) when using magnetic sensing equipment, driving the collection of acoustic data at the same time. In any case, the acoustic system must have the ability to resolve discrete objects sized 0.5 to 1 m (1.6 to 3.3 ft) (BOEM 2012). Having not tested the 100, 445, and 500 kHz systems at all ranges using line this spacing, it is inconclusive if they are capable of resolving objects of this size. Based upon current testing, however, it seems likely that 150 m (492 ft) range is the threshold of detection for objects of this size.

The 234 kHz interferometric sonar system used in this test performed just as well as the 100 and 500 kHz side scan sonar systems with respect to resolving features greater than 0.5 m (1.6 ft) on the seafloor in water depths less than 30 m (98 ft) out to a range of 75 to 100 m (246 to 328 ft) range. As mentioned earlier, since the interferometric sonar was pole-mounted just below the ship's keel, the "grazing" angles (the angle at which the sound source intersects the seafloor) is much greater than that of a towed side scan sonar. The resulting difference in the final images from the towed side scan shows more pronounced "shadows" behind objects, making it somewhat easier to discern smaller, discrete objects on the seafloor, especially with increasing water depths.

Unfortunately the Klein 3000H side scan sonar was not working properly during the study where researchers ensonified the seafloor at depths of up to 80 m (262 ft), thus no comparative analysis was able to be conducted at these water depths between the towed side scan and the surface deployed interferometric sonar. Mainly due to time limitations and weather conditions, researchers deployed the replacement Klein 3000 (100 to 500 kHz) in shallower waters to run the comparative tests. In this respect, additional testing is needed to better understand the benefits and detriments of using an interferometric system versus a towed side scan sonar system in water depths greater than 30 m (98 ft) to discern discrete objects on the seafloor greater than 0.5 m (1.6 ft) in size.

6.5 SUMMARY OF SONAR FINDINGS

A summary of operational parameters considered in this portion of the study is presented in Table 6-6. Findings from this portion of the study also include:

- the SWATH*plus* interferometric sonar system performed as well at 234kHz as the Klein 3000 side scan sonar performed at 100 and 500 Khz with respect to these specific equipment, ranges, water depths, and other operational parameters;
- in the output from side scan sonar, it is easier to see small details on the sea floor because of the pronounced "shadows" behind objects detected via this method;
- the output from the pole-mounted interferometric sonar survey has greater geo-locational reliability than that from a towed side scan system; and
- it is unlikely that any of these systems will be able to detect artifacts smaller than 0.5 to 1 m (1.6 to 3.3 ft) on the sea floor, such as those from Native American material culture, or to distinguish them from the surrounding geology;

Table 6-6.
Summary of side scan and interferometric sonar survey data.

Sonar type	Frequencies Used (kHz)		Min. Effective Range (m)[1]	Min. Detectable Size (m^2)	Relevant Figures
	Low	High			
Klein 3000H Side Scan Sonar	445		Spec. Range 150, Est.75-100 (Figure 6-5)	unknown	6-5
Klein 3000H Side Scan Sonar		900	Spec. Range 50, Observed 25 (Figure 6-3)	0.8 x 0.28	6-11, 6-12, 6-15, 6-18
Klein 3000 Side Scan Sonar	100		Spec. Range 600, Observed greater than 75 (Figure 6-6)	1.2 x 0.9	6-8, 6-13, 6-21
Klein 3000 Side Scan Sonar		500	Spec. Range 150, Observed greater than 75 (Figure 6-4)	0.9 x .57	6-9, 6-10, 6-14, 6-16, 6-20, 6-22
Interferometric Sonar	234		75-100 (Figure 6-7)	0.8 x .50	6-17, 6-19, 6-23

[1] Observed range data from Table 6-2. [2] Data from Table 6-5.

CHAPTER 7

SOUND SOURCE CHARACTERIZATIONS FOR THE COLLABORATIVE BASELINE SURVEY OFFSHORE MASSACHUSETTS

The following chapter characterizing sound sources was prepared by Mikhail Zykov and Jeff MacDonnell of JASCO Applied Sciences, Dartmouth, Nova Scotia, Canada.

This chapter presents the final sound level results for three instruments utilized during the study.

7.1 INTRODUCTION

JASCO Applied Sciences (JASCO) performed sound source characterization (SSC) monitoring in Rhode Island Sound, 29 and 30 August 2012, on behalf of BOEM. The goal of this portion of the study was to determine the ensonification of the underwater environment during a geophysical survey with high-frequency sources. Acoustic measurements of three sources were performed during the two-day study (Table 7-1). This report presents final sound level results for each source, as well as those for the background ambient noise.

Table 7-1.
Sound sources monitored in Rhode Island Sound (29-30 August 2012).

Source	Details	Frequency (kHz)	Source Type
Research vessel	*R/V SRVx*	Broadband	Continuous
Interferometric sonar	SEA SWATH*plus*-M	234	Impulsive
Sub-bottom Profiler	EdgeTech 3200 SB-0512i	0.5-12	Impulsive

The continuous sound from the research vessel was quantified using the root-mean-square (rms) sound pressure level (SPL). Each pulse of the interferometric sonar and sub-bottom profiler was quantified using the 90% rms SPL, sound exposure level (SEL), and zero-to-peak SPL.

The objectives of the study were to:

- determine the acoustic signature of the research vessel at the survey speeds;
- determine the acoustic signature of the interferometric sonar at various power output settings;
- characterize the vertical and horizontal directivity of the interferometric sonar;
- determine the acoustic signature of the sub-bottom profiler at various operational settings (frequency bandwidth, pulse length, and pulse type);
- characterize the horizontal directivity of the sub-bottom profiler;
- characterize the variation in ensonification between water depths of 30 and 60 m;
- determine the background sound levels in the area; and
- compare the measurements with the predictive model results for similar sources.

Data were collected at two sites: a Shallow Site (30 m [98 ft] depth) and a Deep Site (60 m [197 ft] depth). Sixteen SSC scenarios were performed, 10 at the Shallow Site and 6 at the Deep Site, with various operational settings of the interferometric sonar.

7.2 METHODS

7.2.1 SOUND SOURCES MEASURED

Three sound sources were monitored: the *R/V Small Research Vessel experimental*, a SWATH*plus*-M interferometric sonar, and an EdgeTech 3200 SB-0512i sub-bottom profiler. The Klein 3000 and 3000H side scan sonars utilized during this study operate outside of the acoustic range of most marine mammals and acoustically-sensitive species and also outside of the range of the hydrophones used during the study. Thus, they were not measured.

7.2.1.1 R/V Small Research Vessel experimental

The *R/V SRVx* is a fiberglass sandwich-core vessel powered by two 2735 hp engines (Figure 7-1). The vessel is 26 m (85 ft) long and 7 m (23 ft) wide with a draft of 1.8 m (6 ft). Standard equipment aboard the *SRVx* includes a generator and depth sounder. The depth sounder was inactive during the SSC scenarios.

Figure 7-1. The geotechnical survey vessel, R/V Small Research Vessel experimental (NOAA).

7.2.1.2 SWATHplus-M Interferometric Sonar

The SWATH*plus*-M interferometric sonar (Systems Engineering & Assessment Ltd., Figure 7-2) was monitored at various power output settings: 30 to 50% and 100% at the Shallow Site and 30% and 100% at the Deep Site. A pulse length of 8217.6 µs was used with a pulse rate of 6.6 Hz (one pulse every 151 ms). The sonar operated at 234 kHz. The manufacturer specifications for the sonar are:

- operational frequency: 234 kHz;
- horizontal beamwidth: 0.55°;
- transmit pulse length: 8 to 500 µs; and
- declination angle: 30°.

The transducer of the interferometric sonar consisted of two elements facing opposite directions. The main beam axis is perpendicular to the tow axis pointing 30° below the horizontal. The transducer elements for the sonar are davit-mounted on the port side of the vessel at about mid-ship. The depth of the transducers was fixed at 1.5 m (5 ft) below the waterline. The deepest point of the vessel hull was below the transducers by about 0.3 m (1.0 ft). The hull blocked the beam in a vertical sector from 90° above the horizontal to 5° below.

Figure 7-2. The SEA SWATH*plus*-M interferometric sonar (Systems Engineering & Assessment Ltd.) before deployment from the R/V SRVx in Rhode Island Sound.

7.2.1.3 3200 SB-0512i Sub-Bottom Profiler

The EdgeTech 3200 SB-0512i sub-bottom profiler operates at frequencies from 500 Hz to 12 kHz. The system transmits a frequency-modulated pulse (called a chirp) that is swept over a frequency range over the duration of the pulse (e.g., 2 to 12 kHz over a pulse length of 20 ms). The amplitude of the signal changes with time and, therefore, with frequency. The system can transmit two types of pulses: frequency-modulated (FM) and wide-band (WB).

Two transducers are installed on the profiler towfish along the tow axis, KT–504 and KT–216A2 (EdgeTech 2009), which have different diameters (13.5 and 6.5 inches, respectively) and, therefore, different resonance frequencies. The towfish (Figure 7-3) was located about 30 m (98 ft) behind the vessel, approximately 3 m (10 ft) below the water surface.

Figure 7-3. The towfish of the EdgeTech 3200 SB-0512i sub-bottom profiler aboard the R/V SRVx.

The 3200 SB-0512i has a source level of 210 dB re 1 µPa @ 1 m (3 ft). The beamwidth is 53° at 5 kHz and 19.6° at 12 kHz (Rob Morris, EdgeTech Marine Customer Service Manager, personal communication). The main beam axis of the transducer points downward. In this configuration, the beam pattern in the horizontal plane is expected to be approximately uniform.

Sound levels from the sub-bottom profiler were measured for eight combinations of frequency band, pulse length, and pulse type, three of which are non-standard. Table 7-2 lists the remaining, unmeasured, standard operational combinations for comparison (EdgeTech 2009). The pulse repetition rate was 4 Hz (one pulse every 250 ms). For each frequency band, the central frequency and the expected beamwidth for that central frequency are provided. The beamwidth was estimated from known beamwidth values at specific frequencies with the transducer equation $\theta_{\text{bw}}(f) = 91440/(D \times f)$, where D is the transducer diameter in meters, f is the operational frequency in Hz, and θ_{bw} is the beamwidth in degrees (Kinsler 1950, ITC 1993). The beamwidth is defined as the total angular range within which the SPL of the main beam is within 3 dB of the on-axis peak level (Massa 1999).

7.2.2 DATA ACQUISITION

Underwater sound was recorded with two Autonomous Multichannel Acoustic Recorders (AMARs, JASCO Applied Sciences). Data were stored in 2.5 minute files on internal solid-state flash memory. Acoustic data were recorded continuously at 16 bits per sample and 687,500 samples per second. Each recorder was fitted with an M8E omnidirectional hydrophone (GeoSpectrum Technologies Inc., -163 ± 1 dB re 1 V/µPa in the range of 10 Hz to 20 kHz) providing a peak measurement level of 171 dB re 1 µPa. The operating frequency of the SWATH*plus*-M interferometric sonar is outside the flat-frequency response range of the M8 (10 Hz to 140 kHz); therefore, JASCO commissioned

GeoSpectrum to calibrate the response and directivity of the hydrophone from 40 to 250 kHz. The sensitivity of the M8 is -175 ± 3 dB re 1 V/µPa in the range of 210 to 250 kHz. The hydrophones maintain their omni-directionality in this frequency range. Further details of the calibrations are provided as Appendix E.

Table 7-2.
Pulse bandwidths and lengths for the EdgeTech 3200 SB-0512i sub-bottom profiler (Source: EdgeTech 2009).

Scenario	Standard combination ?	Frequency band (kHz)	Central frequency (kHz)	Beamwidth at central frequency	Pulse length (ms)	Pulse type
Measured configurations						
S9	Yes	0.5 to 2.7	1.6	166°	40	WB
D4	No	0.5 to 2.7*(4.5)	1.6 (2.5)	166° (106°)	40	WB
S5	No	0.5 to 2.7	1.6	166°	100	FM
S10	Yes	0.5 to 6.0	3.25	82°	20	WB
S6	Yes	0.5 to 7.2	3.85	69°	30	FM
S4, D3	Yes	0.5 to 8.0	4.25	62°	5	FM
S7, D6	No	1.0 to 6.0	3.5	76°	40	FM
S8, D5	Yes	2.0 to 12	7	38°	20	FM
Standard combinations not measured						
–	Yes	0.5 to 4.5	2.5	106°	50	FM
–	Yes	0.5 to 6.0	3.25	82°	9	FM
–	Yes	0.5 to 6.0	3.25	82°	18	FM
–	Yes	0.7 to 12	6.35	42°	20	FM

* Analysis showed the upper limit of the pulse bandwidth was likely 4.5 kHz (see Section 3.3).

SSC measurements were performed at two sites, a Shallow Site (30 m [98 ft] water depth) and a Deep Site (60 m [197 ft] depth), on 29 and 30 August 2012, respectively (Figure 7-4). AMARs were deployed at two locations at each site, identified as A1 and A2 at the Shallow Site and B1 and B2 at the Deep Site. Each AMAR was anchored to the seabed with primary and secondary anchor weights separated by approximately 100 m (328 ft) of sinking line (Figure 7-5). A surface float was attached to the secondary anchor weight for retrieval. The AMARs floated above the primary anchor, placing the hydrophone 5.5 m (18 ft) above the bottom. The AMARs were deployed along a roughly east-west line, with a nominal separation of 100 m (328 ft). Owing to weather conditions, the actual separation between the recorders was 165 m (541 ft) at the Shallow Site and 85 m (279 ft) at the Deep Site (Table 7-3).

Test Tracks A and B were oriented roughly north-south, passing directly over or as close as possible to A1 and B2, with 5 km (3 nm) of approach from the south and 2 km (1 nm) from the north (Figure 7-6). The survey vessel transited back and forth several times across the test tracks to capture each sound source with various operational settings. Owing to weather conditions, the actual sailed tracks deviated slightly from the planned course: during Scenario D1, the vessel passed closer to B1 rather than B2.

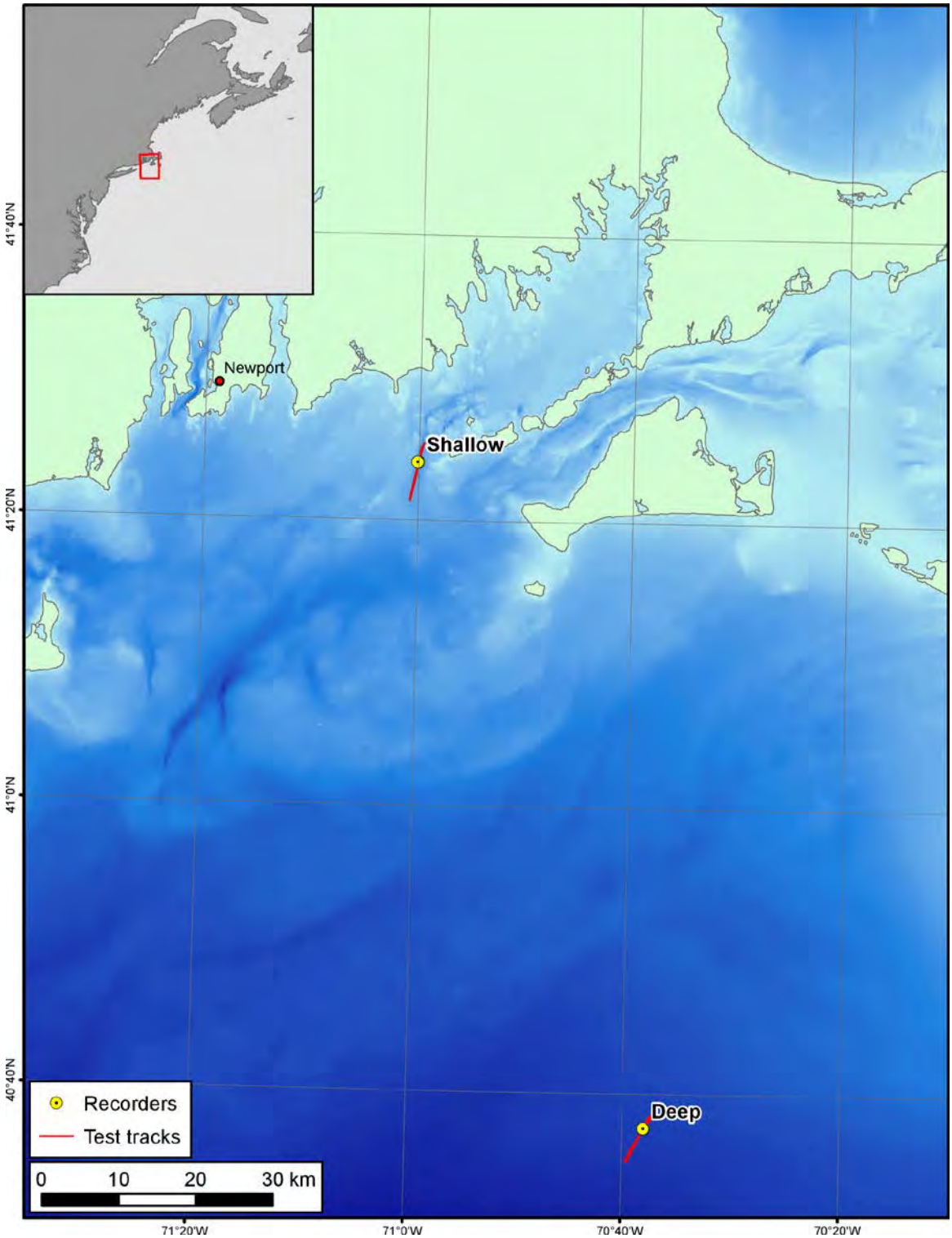

Figure 7-4. Test tracks for the sound source characterizations (SSC) in Rhode Island Sound, 29 to 30 August 2012.

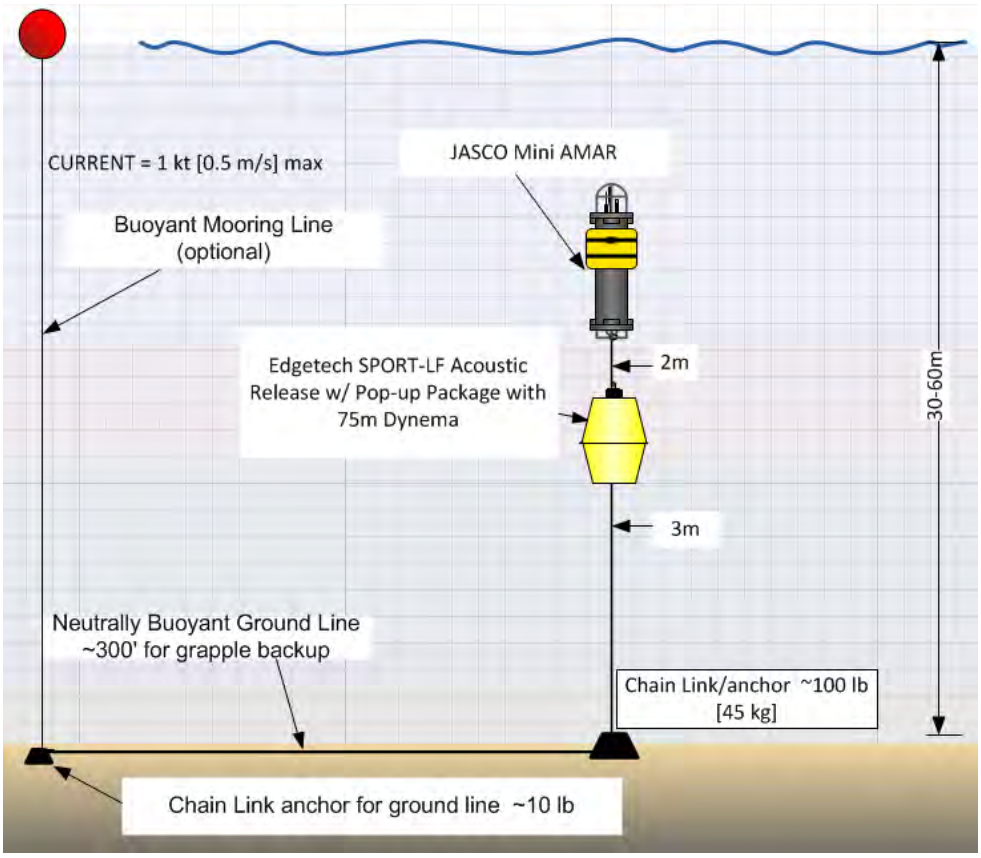

Figure 7-5. The mooring for the Autonomous Multichannel Acoustic Recorder (AMAR) with a surface float for retrieval.

Table 7-3.
Details of the Autonomous Multichannel Acoustic Recorder (AMAR) deployments and retrievals in Rhode Island Sound for the sound source characterizations (SSC), August 2012. Times are in UTC.

Location	AMAR	Deployed	Retrieved	Latitude	Longitude	Water depth (m)	Horizontal separation (m)
Shallow Site, 29 Aug							
A1	059	13:05	23:18	41°24.086′ N	71°00.042′ W	30	165
A2	071	13:16	23:04	41°24.096′ N	71°00.231′ W	27	
Deep Site, 30 Aug							
B1	059	11:26	19:20	40°37.615′ N	70°38.045′ W	60	85
B2	071	11:14	19:00	40°37.594′ N	70°37.991′ W	60	

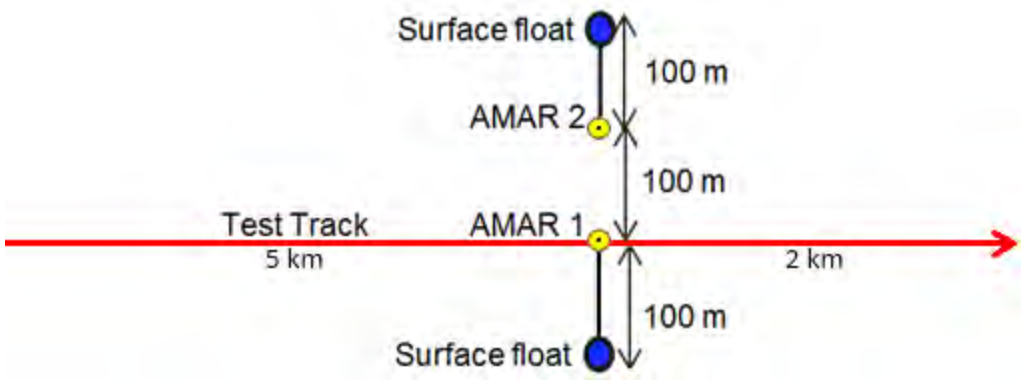

Figure 7-6. Planned recorder deployment locations relative to the test tracks.

7.2.2.1 Sound Source Characterization Scenarios

Ten SSC scenarios were completed along Test Track A at the Shallow Site to measure sound from the vessel (Scenario S1), the interferometric sonar (Scenarios S2 and S3), and the sub-bottom profiler (Scenarios S4 to S10). Six SSC scenarios were completed along Test Track B at the Deep Site for the interferometric sonar (Scenarios D1 and D2) and the sub-bottom profiler (Scenarios D3 to D6) (Figures 7-7 and 7-8). Table 7-4 provides detailed information on the scenarios, including the acoustic source measured, the operational settings of the source, the start and end time of each scenario, and the time of the closest point of approach (CPA). The pulse repetition rates were 151 ms for the interferometric sonar and 250 ms for the sub-bottom profiler, as provided by the equipment operator and recorded in the field logs. The repetition rates as observed in the acoustic data are provided in Section 2.4.4

Navigation data for the sonars were provided by the scientific crew of the *SRVx*. Navigation data for Scenario S1, which measured the noise from the vessel itself, were recorded by JASCO with a handheld GPS receiver (Garmin GPSMap 76SCx) placed on the vessel.

7.2.3 MEASUREMENT TECHNOLOGY

Acoustic energy loss depends on the acoustic path length between a source and receiver. At short range, the acoustic path length is approximately equal to the slant range, which is the geometric distance between the source and receiver (Figure 7-9). The horizontal range is the distance in the horizontal plane from the source to the receiver. The vertical separation between the source and receiver is the water depth minus the source depth and minus the elevation of the hydrophone above the seabed. When the slant range is several times greater than the vertical separation, the slant range and the horizontal range are effectively equal.

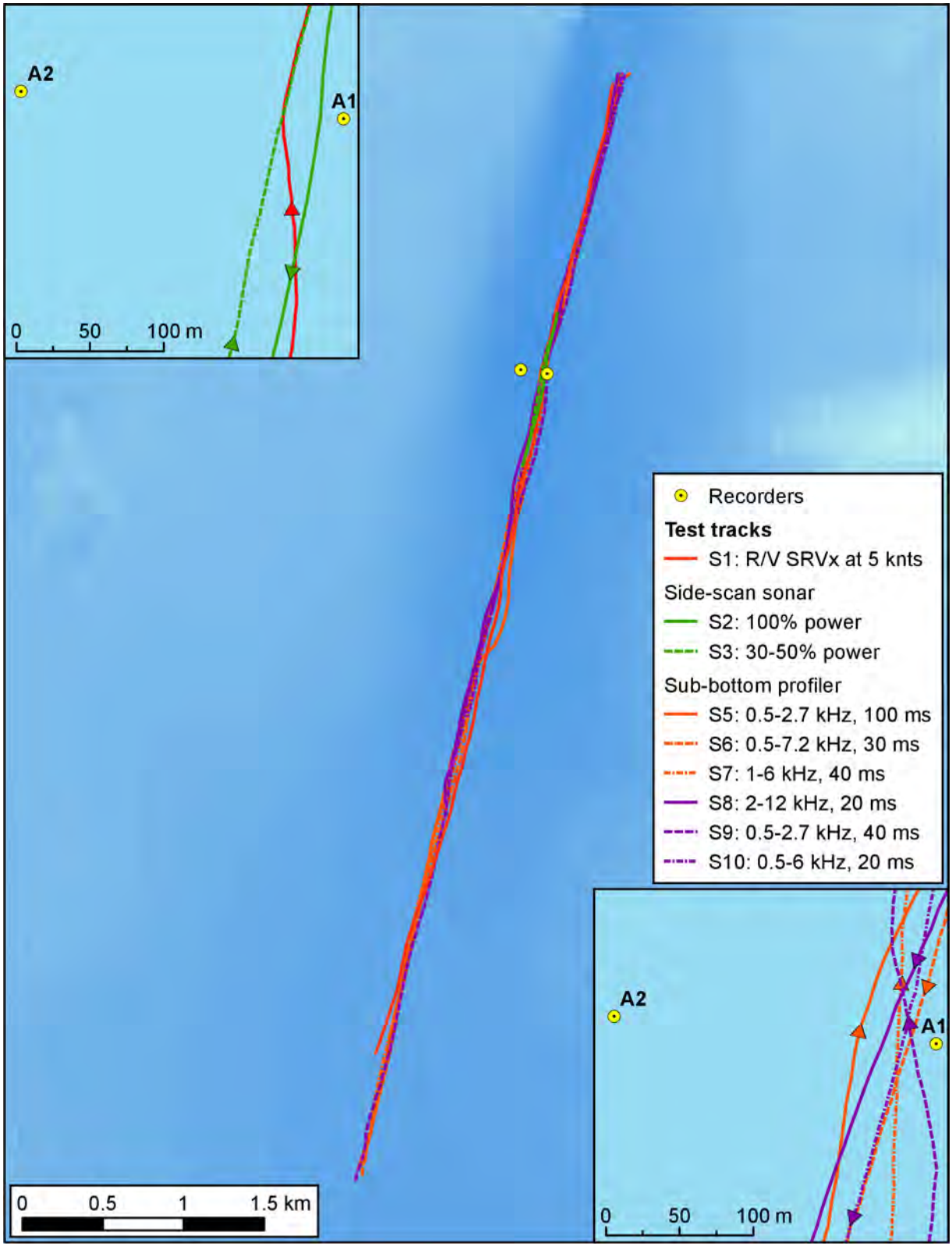

Figure 7-7. Test tracks at the Shallow Site relative to A1 and A2. Arrows indicate the travel direction of each scenario. The recorders are 165 m (541 ft) apart.

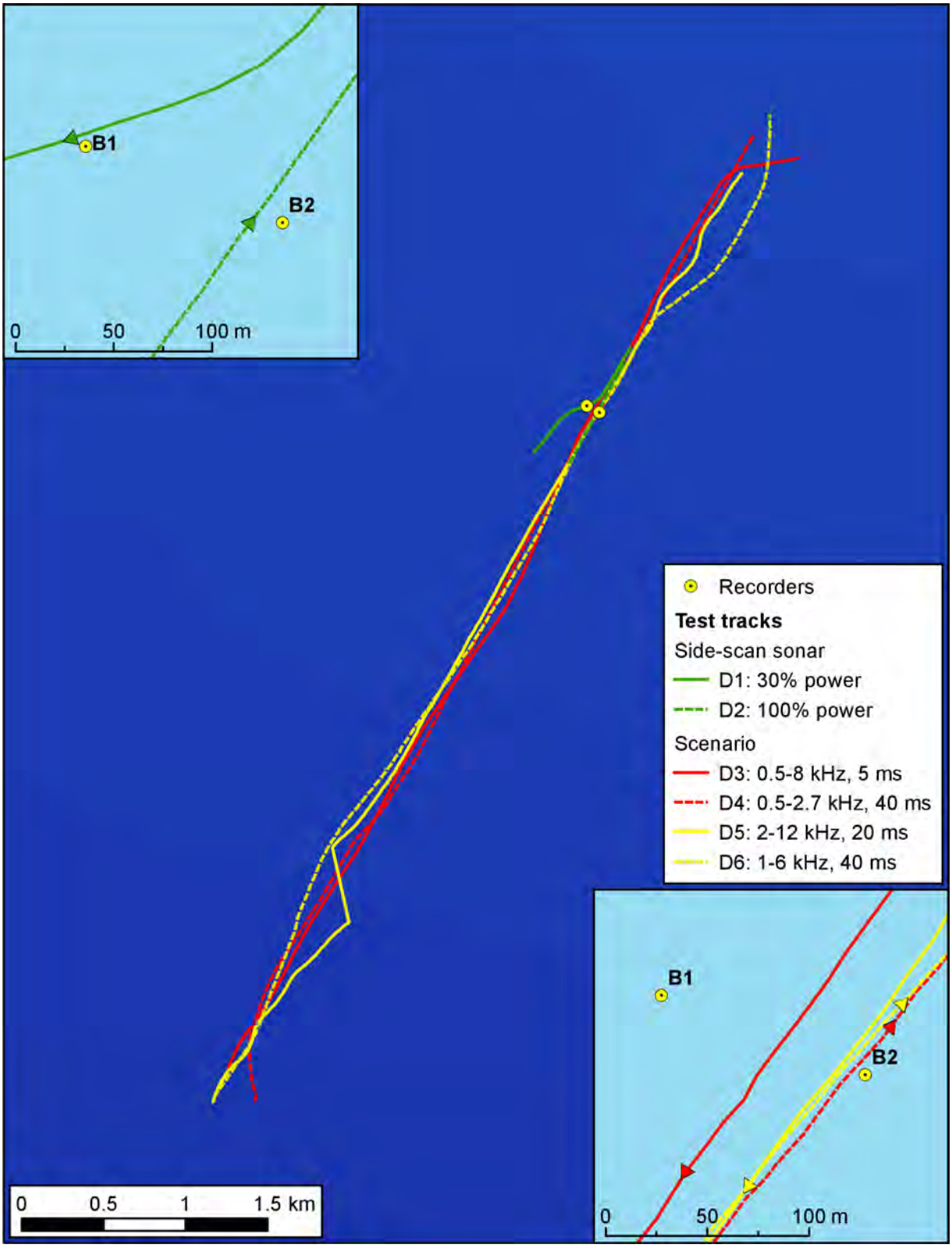

Figure 7-8. Test tracks at the Deep Site relative to B1 and B2. Arrows indicate the travel direction of each scenario. The recorders are 85 m (279 ft) apart.

Table 7-4.
Time (UTC) of the start, closest point of approach (CPA), and end of the test tracks for each source configuration. The horizontal and vertical range from each recorder at the CPA between the source and the hydrophone are indicated. The pulse types are frequency modulated (FM) and wide-band (WB).

Scenario	Source operational setting	Start	CPA	End	Horizontal range at CPA (m)		Vertical separation (m)	
					A1/B1	A2/B2	A1/B1	A2/B2
Shallow Site, 29 August 2012								
S1	*R/V SRVx*, 5 knots	14:59	15:33	15:47	31	135	23.5	22
Interferometric Sonar								
S2	100% output power	15:52	16:04	16:35	12	152	24	22.5
S3	30 to 50% output power	16:37	17:13	17:25	32	133		
Sub-Bottom Profiler								
S4	0.5 to 8 kHz, 5 ms, FM	17:42	17:59	18:29	21	144	22.5	21
S5	0.5 to 2.7 kHz, 100 ms, FM	18:32	18:59	19:09	40	125		
S6	0.5 to 7.2 kHz, 30 ms, FM	19:13	19:25	19:56	13	150		
S7	1 to 6 kHz, 40 ms, FM	20:00	20:25	20:35	19	145		
S8	2 to 12 kHz, 20 ms, FM	20:38	20:51	21:22	27	135		
S9	0.5 to 2.7 kHz, 40 ms, WB	21:27	21:52	22:03	12	147		
S10	0.5 to 6 kHz, 20 ms, WB	22:07	22:19	22:32	17	147		
Deep Site, 30 August 2012								
Interferometric Sonar								
D1	30% output power	12:49	13:00	13:31	6	72	55	55
D2	100% output power	13:41	14:12	14:23	74	11		
Sub-Bottom Profiler								
D3	0.5 to 8 kHz, 5 ms, FM	14:47	15:00	15:27	51	34	53.5	53.5
D4	0.5 to 2.7(4.5) kHz, 40 ms, WB	15:30	15:59	16:11	80	5		
D5	2 to 12 kHz, 20 ms, FM	17:13	17:23	17:54	74	10		
D6	1 to 6 kHz, 40 ms, FM	17:57	18:25	18:36	76	9		

* Provided by the equipment operator and recorded in the field logs.

Endfire and broadside are the principal directions on the horizontal plane, originating at the acoustic source. The endfire direction is along the tow axis (i.e., fore and aft), and the broadside direction is perpendicular to the tow axis (i.e., port and starboard). Multibeam and interferometric sonar beams usually have a narrow main lobe directed perpendicular to the tow axis, so the source level is typically approximately 40 dB higher in the broadside direction than in the endfire direction; therefore, the received levels in both the broadside and endfire directions must be assessed independently. Along the test tracks, the broadside beam was measured at or near the CPA to A2 and B2 and the endfire beam was measured before and after the CPA.

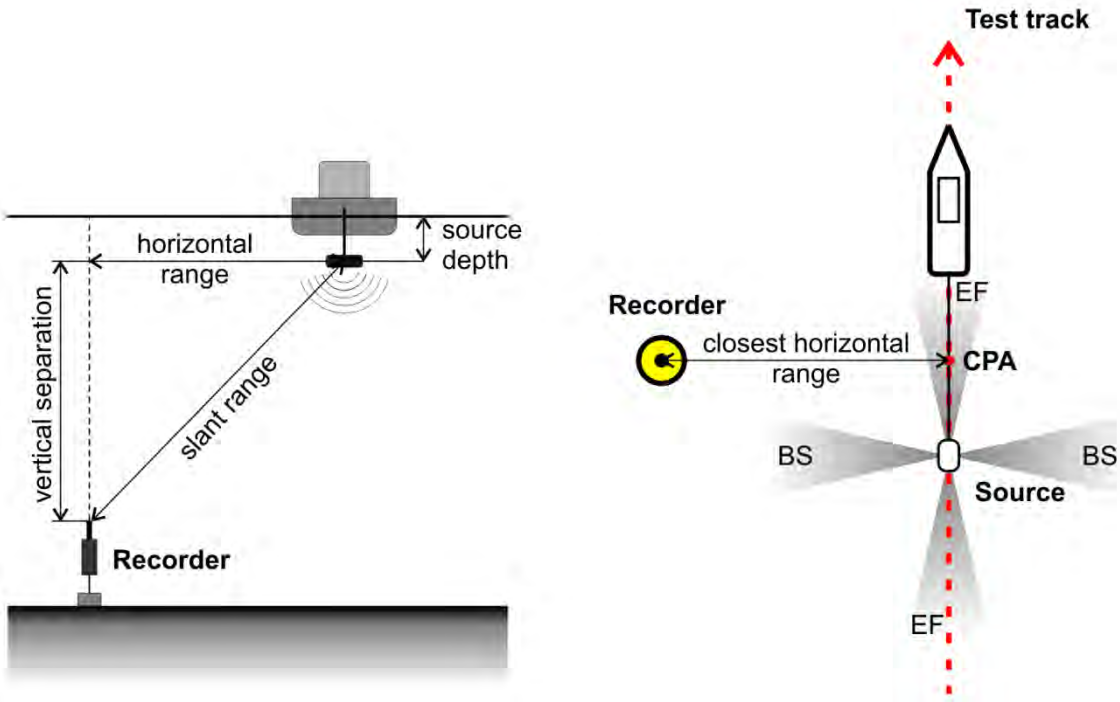

Figure 7-9. Typical geometry of sound source characterization (SSC) measurements and the associated terminology. Abbreviations: BS is broadside, CPA is closest point of approach, and EF is endfire.

7.2.4 DATA ANALYSIS

7.2.4.1 Acoustic Metrics

Underwater sound amplitude is measured in decibels (dB) relative to a fixed reference pressure of p_0 = 1 µPa. Because the loudness of impulsive noise, from the sub-bottom profiler for example, is not generally proportional to the instantaneous acoustic pressure, several sound level metrics are commonly used to evaluate the loudness of impulsive noise and its effects on marine life.

The zero-to-peak SPL, or peak SPL (L_{pk}, dB re 1 µPa), is the maximum instantaneous sound pressure level in a stated frequency band attained by an impulse, $p(t)$:

$$L_{pk} = 10\log_{10}\left(\frac{\max\left(\left|p^2(t)\right|\right)}{p_0^2}\right) \quad (1)$$

The peak SPL metric is commonly quoted for impulsive sounds, but it does not account for the duration or bandwidth of the noise. At high intensities, the peak SPL can be a valid criterion for assessing whether a sound is potentially injurious; however, because the peak SPL does not consider pulse duration, it is not a good indicator of perceived loudness.

The root-mean square (rms) SPL (L_p, dB re 1 µPa) is the rms pressure level in a stated frequency band over a time window (T, s) containing the pulse:

$$L_p = 10\log_{10}\left(\frac{1}{T}\int_T p^2(t)dt \Big/ p_0^2\right) \quad (2)$$

The rms SPL can be thought as a measure of the average pressure or as the "effective" pressure over the duration of an acoustic event, such as the emission of one acoustic pulse. Because the window length, T, is a divisor, pulses more spread out in time have a lower rms SPL for the same total acoustic energy.

In studies of impulsive noise, T is often defined as the "90% energy pulse duration" (T_{90}): the interval over which the pulse energy curve rises from 5% to 95% of the total energy. The SPL computed over this T_{90} interval is commonly called the 90% rms SPL (L_{p90}, dB re 1 µPa):

$$L_{p90} = 10\log_{10}\left(\frac{1}{T_{90}}\int_{T_{90}} p^2(t)dt \Big/ p_0^2\right) \quad (3)$$

The sound exposure level (SEL, dB re 1 µPa^2 s, symbol L_E) is a measure of the total acoustic energy contained in one or more pulses. The SEL for a single pulse is computed from the time-integral of the squared pressure over the full pulse duration (T_{100}):

$$L_E = 10\log_{10}\left(\int_{T_{100}} p^2(t)dt \Big/ T_0 p_0^2\right) \quad (4)$$

where T_0 is a reference time interval of 1 s. The SEL represents the total energy (or sound exposure) received over the duration of an acoustic event at some location. The SEL can be a cumulative metric if calculated over time periods containing multiple pulses.

Because the rms SPL and SEL are both computed from the integral of square pressure, these metrics are related by a simple expression, which depends only on the duration of the 90% energy time window T_{90}:

$$L_E = L_{p90} + 10\log_{10}(T_{90}) + 0.458 \quad (5)$$

where the 0.458 dB factor accounts for the rms SPL containing 90% of the total energy from the per-pulse SEL.

7.2.4.2 Per-Pulse Sound Levels

Each recorded pulse from the sub-bottom profiler and interferometric sonar was analyzed in terms of the three noise metrics described above: peak SPL, 90% rms SPL, and SEL. Each pulse was analyzed as follows:

1. Convert the digital recording units to micropascals (µPa) by applying the hydrophone sensitivity, analog circuit frequency response, and digital conversion gain.
2. If the source-to-receiver range is less than 300 m (984 ft), apply no frequency filtering of the signal; otherwise, apply a band-pass filter to isolate the source signal from the background noise.
3. Determine the start and end time of the pulse with an automated power-threshold detector.
4. Compute the peak SPL (L_{pk}) according to Equation 1.
5. Compute the cumulative energy over the duration of the pulse.

6. Determine the 90% energy pulse duration (T_{90}) and compute the 90% rms SPL (L_{p90}) according to Equation 3.
7. Compute the SEL (L_E) according to Equation 4 over the duration of the pulse.

The limits for the band-pass filter in Step 2 were equal to the pulse band limits for the sub-bottom profiler and 200 to 250 kHz for the interferometric sonar.

Estimating source levels and beam patterns for the sonars required specialized processing of the pulse data to isolate the direct-path signal in the recorded pulse waveforms. The sound received for each sonar pulse consists of the pulse that propagates directly from the source to the receiver (the direct path arrival) and pulses that arrive as a result of reflections off the water surface and the seabed (multipath arrivals). To characterize the direct path arrival of the pulse, its energy was isolated from that of the multipath arrivals using a sliding time window of fixed length. The window length was set to the T_{90} of the direct path arrivals received at the CPA, where the direct path and multipath arrivals did not overlap in time. For each pulse, the rms SPL was calculated within this fixed-length time window starting at each consecutive sample. The maximum rms SPL over all the windows was taken as the rms SPL for that pulse. The direct path signals, extracted in this way, were used for estimating source levels and beam patterns for the sonars.

7.2.4.3 Sonar Bean Patterns

The source levels for the sub-bottom profiler and interferometric sonar are reported as rms SPLs in dB re 1 µPa at the standard reference distance of 1 m (3 ft). Sonars transducers are directional sources and use beam forming techniques to project sound preferentially toward a specific target, such as the seabed. As a result, the source level of a sonar depends on the direction in which sound is radiated. The beam pattern of a sonar describes the source level as a function of beam angle. The vertical and horizontal beam patterns for the sonars were estimated from the rms SPL of the direct-path signals calculated using a sliding time window of fixed length as described in Section 2.4.2.

For each received pulse, the vertical and bearing angles of the direct path from the source to the receiver was calculated from the navigation data of the survey source and the position of the recorder. The received levels were corrected for the transmission loss assuming spherical spreading losses of $20\log(R)$, where R is the slant range (i.e., along the direct path) from the source to the receiver. The received levels for interferometric sonar were also corrected for volumetric absorption in the sea water, which was 89.5 dB/km. The volumetric absorption coefficient was calculated based on equation from Francois and Garrison (1982) for the following conditions: 236 kHz frequency, 20.4°C temperature, 35.7 psu salinity, and 15 m (49 ft) depth. The volumetric absorption at operational frequencies of the sub-bottom profiler were negligible (less than 0.5 dB/km).

Application of the correction for the geometric transmission loss and the volumetric absorption (interferometric data only) yielded the source level at a reference distance of 1 m as a function of the vertical or horizontal angle.

For the sub-bottom profiler, the empirical beam patterns were compared with the theoretical beam pattern for different pulse bandwidth settings. The theoretical beam patterns were calculated based on transducer theory, which mathematically predicts transducer directivity from the size of the transducer and the operational frequency:

$$R(\phi) = \frac{2 \cdot J_1\left(\pi L_\lambda \sin(\phi)\right)}{\pi L_\lambda \sin(\phi)} \quad , \quad L_\lambda = \frac{60}{\theta_{bw}} \tag{6}$$

where L_λ is the transducer dimension in wavelengths, θ_{bw} is the beamwidth in degrees, and ϕ is the angle from the transducer axis (Kinsler 1950, ITC 1993).

7.2.4.4 Background Sound Levels

To document baseline underwater sound conditions at the SSC sites, all data from A1 and B1 were analyzed. The total length of analyzed data was 10 h for the Shallow Site (13:00 to 23:05, 29 August 2012) and 7.5 h for the Deep Site (11:30 to 19:00, 30 August 2012). For each 20 s of data, an average spectrum was calculated and reported as 1/3-octave band levels from 10 Hz to 100 kHz (45 bands) yielding 1709 acoustic spectrum samples for the Shallow Site and 1252 samples for the Deep Site.

The 5th, 25th, 50th, 75th, and 95th exceedance percentiles were calculated for each frequency band and for the broadband level. The 95th percentile curve, for example, describes the frequency-dependent levels exceeded by 95% of the 20-s averages. The 95th percentile represents the quietest noise state measured during the recording period. The 5th percentile typically represents the noise level associated with occasional loud events, such as nearby shipping, extreme weather, or survey sources.

7.3 RESULTS

A total of 16 sound source characterization (SSC) scenarios were conducted on 29 and 30 August 2012 (Table 7-5). Scenarios S1, S2, S3, D1, and D2 were analyzed to assess the noise from the survey vessel, the *R/V SRVx*. Scenarios for the SEA SWATH*plus*-M interferometric sonar with 100% and 30 to 50% output power were conducted at both the Shallow and Deep Sites. For the EdgeTech 3200 SB-0512i sub-bottom profiler, seven scenarios were conducted at the Shallow Site and four at the Deep Site. Results for Scenario S4 are omitted because the detected pulse rate and pulse length varied throughout the scenario, possibly due to changes to the operational settings during the measurement.

7.3.1 *R/V SMALL RESEARCH VESSEL EXPERIMENTAL*

Only Scenario S1 was dedicated to measuring sound from the R/V SRVx. The vessel's acoustic systems were inactive during the scenario. Scenarios S2, S3, D1, and D2 were also analyzed for vessel-noise assessment. These scenarios were completed with only the interferometric sonar operational. The interferometric sonar operates outside the frequency range of the vessel noise, so these two sources do not interfere. In total, data from five scenarios were analyzed to assess the noise from the SRVx (Table 7-6).

The acoustic data were processed in the frequency range from 10 Hz to 100 kHz. For the scenarios during which the interferometric sonar was operational, no additional filtering was necessary since the sonar's operating frequency (236 kHz) is outside the frequency range of interest. The data were processed using a 1 s wide sliding window and a sliding step of 0.5 s. The received levels are plotted to the distance at which the received levels approach the ambient background levels (see Section 3.4): 200 to 300 m (656 to 984 ft) for the Shallow Site (Figure 7-10) and 300 m (984 ft) for the Deep Site (Figure 7-11).

Table 7-5.
Sources and operational parameters of each sound source characterization (SSC) scenario. The pulse types are frequency modulated (FM) and wide-band (WB).

Scenario	Source operational setting	Vessel speed (m/s)	Pulse rate (ms)	Horizontal range at CPA (m)	
Shallow Site				**A1**	**A2**
S1	R/V SRVx, 5 knots (2.6 m/s)	2.1		31	135
Interferometric Sonar					
S2*	100% output power	3.1	230	12	152
S3*	30 to 50% output power	2.9	195	32	133
Sub-Bottom Profiler					
S4†	0.5 to 8 kHz, 5 ms, FM	3.0	160 to 250	21	144
S5	0.5 to 2.7 kHz, 100 ms, FM	3.3	665	40	125
S6	0.5 to 7.2 kHz, 30 ms, FM	2.8	250	13	150
S7	1 to 6 kHz, 40 ms, FM	3.3	265	19	145
S8	2 to 12 kHz, 20 ms, FM	2.8	250	27	135
S9	0.5 to 2.7 kHz, 40 ms,WB	3.4	265	12	147
S10	0.5 to 6 kHz, 20 ms, WB	2.8	250	17	147
Deep Site				**B1**	**B2**
Interferometric Sonar					
D1*	30% output power	2.5 to 3.0	185	6	72
D2*	100% output power	2.9	200	74	11
Sub-Bottom Profiler					
D3	0.5 to 8 kHz, 5 ms, FM	2.8	250	51	34
D4	0.5 to 4.5 kHz, 40 ms, WB	2.7	265	80	5
D5	2 to 12 kHz, 20 ms, FM	3.7	250	74	10
D6	1 to 6 kHz, 40 ms, FM	3.0	265	76	9

* Scenario was also analyzed to assess the noise from the R/V SRVx.
† The operational parameters varied during the measurement, so the results are omitted from this report.

The vessel noise spectra were calculated between 10 Hz and 100 kHz (Figure 7-12). The spectrum for each scenario is from the nearest recorder when the vessel was near the CPA (±15 m [49 ft]). The averaging time for the spectrum calculations was 10 s. The 1/3-octave band spectrum values were corrected for distance using geometrical transmission loss assuming spherical spreading losses of $20\log(R)$, where R is the slant range, to obtain the source level spectrum (Figure 7-12).

Table 7-6 summarizes the source levels from the back-propagation of the received levels at the CPA, similar to the vessel noise spectra calculations. The back-propagation was performed using geometrical transmission loss assuming spherical spreading losses of $20\log(R)$, where R is the slant range. The broadband source levels for all five scenarios are within 3 dB difference.

Table 7-6.
Scenarios analyzing noise from R/V Small Research Vessel experimental (R/V SRVx). The slant range at the closest point of approach (CPA) is given relative to the closest recorder (usually A1 or B2). The estimated source levels are from back-propagation of the received levels at the CPA using a propagation loss of 20logR, where R is the slant range.

Scenario	Depth at CPA (m)	Sailing direction	Vessel speed (m/s)	Slant range at CPA (m)	Source Level (dB re 1 µPa @ 1 m)
Shallow Site					
S1	30	North	2.1	39	161.6
S2	30	South	3.1	27	160.8
S3	30	North	2.9	39	162.2
Deep Site					
D1	60	South	2.8	56	163.6
D2	60	North	2.9	56	160.7

The spectrum obtained for Scenario D1 exhibits elevated levels, compared to other scenarios, for the frequencies above 1 kHz. It is likely due to shows substantially more cavitation noise than in the other scenarios. This difference is likely due to differences in power output that were necessary to counteract wind/current action and maintain the survey speed. Scenario D1 was sailed southward with a headwind, whereas Scenario D2 was sailed northward with a tailwind. Table 7-7 presents the distances to various rms SPL thresholds based on the 90th percentile fit line.

The maximum received rms SPL was 174.4 dB re 1 µPa at 40 m slant range (32 m horizontal range, Scenario S3: 30 to 50% power output). The sonar exhibited strong directivity with a narrow beam extending perpendicular to the vessel track. Only two to five pulses recorded when the vessel was near the CPA (±1 m [3 ft]) exhibited levels similar to the maximum detected level; however, even those differed from the maximum level by 3 to 5 dB. Figure 7-13 and 7-14 show the variability in the received levels at the CPA. The peak SPLs decrease by more than 10 dB for the adjacent pulses (±2 m [7 ft] from the CPA) and by about 30 dB when the vessel is 30 m from the CPA. Adjacent pulses are only 230 ms apart, which equates to 1.5 m [4.9 ft] motion of the tow vessel. These observations are consistent with the sonar's narrow main lobe of 0.55°.

7.3.2 SEA SWATH*plus*-M Interferometric Sonar

Two SSC scenarios for the SEA SWATH*plus*-M interferometric sonar were monitored at each site, with two output power levels: Scenarios S2 (100% output power), S3 (30-50% output power), D1 (30% output power), and D2 (100% output power) (see Table 7-5). The measured pulse rate was not constant, varying between 185 and 231 ms (Figure 7-13). The pulse rate configured by the equipment operator was 151 ms.

Due to strong directivity of the interferometric sonar, few data points for each scenario and recorder are available to describe the acoustic source levels in the broadside direction. The broadside data for the same output power obtained at the Shallow and Deep Sites were combined to increase the number of data points available for data fitting (Figure 7-14). The maximum values detected in the broadside direction are presented in Table 7-8. Distances to various rms SPL thresholds based on the 90th percentile fit lines are provided in Table 7-9 for the Shallow and Deep Sites.

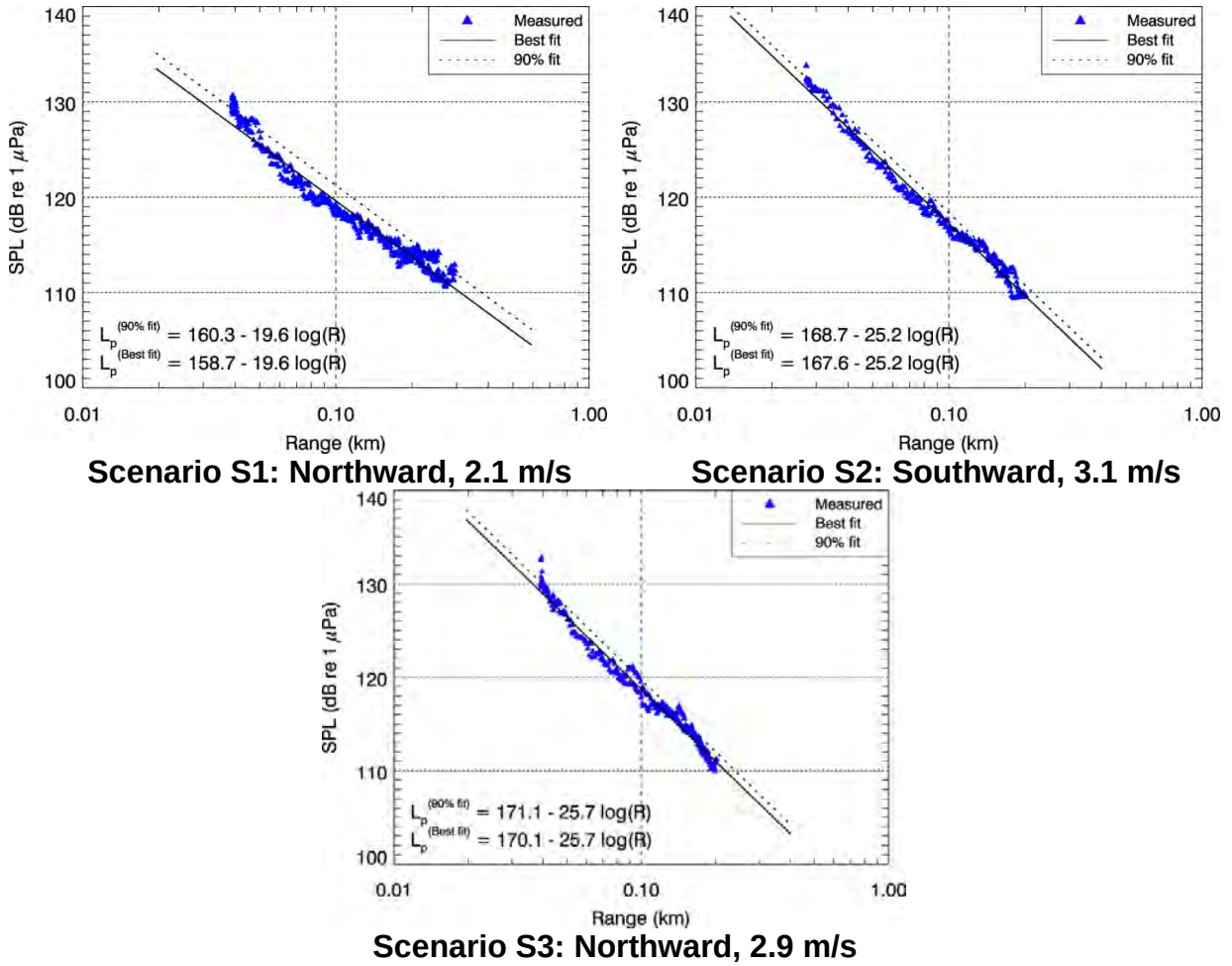

Figure 7-10. R/V Small Research Vessel experimental (R/V SRVx), Shallow Site (30 m [98 ft] water depth): Root-mean-square (rms) sound pressure level (SPL) versus slant range at A1 for Scenarios S1, S2, and S3. The solid line is the best-fit line to the rms SPLs. The dashed line is the 90th percentile fit line: the best-fit line shifted up to exceed 90% of the rms SPLs.

The results for the endfire direction are consistent between the recorders (Figure 7-15). High transmission loss rates with distance for the endfire direction are explained by the fact that very little energy is emitted at or near the horizontal. Most of the energy is directed toward the bottom due to the beam pattern of the sonar. Figure 7-16 shows the waveform of a pulse recorded at the CPA, the pulse spectral density, and the spectral density of the background noise as calculated in between the pulses.

In general, the difference between the rms SPL for 100% and 30 to 50% power output is expected to be 3 to 5 dB. Such a difference is observed between the levels detected for Scenario D1 (B1, 55 m slant range) and Scenario D2 (B2 55 m slant range).

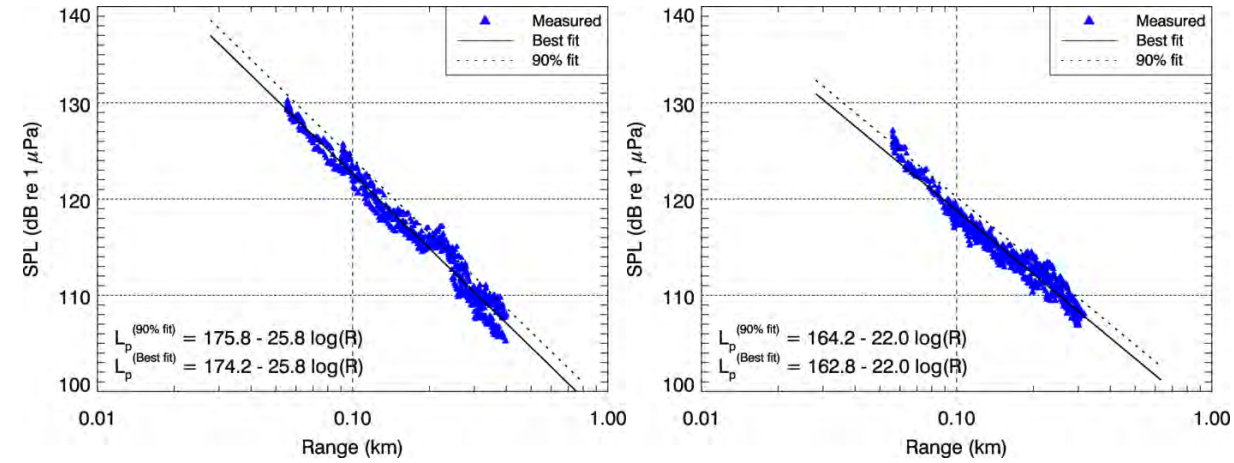

Figure 7-11. R/V Small Research Vessel experimental (R/V SRVx), Deep Site (60 m [197 ft] water depth): root-mean-square (rms) sound pressure level (SPL) versus slant range at B1 and B2 for Scenarios D1 and D2. The solid line is the best-fit line to the 90% rms SPL.

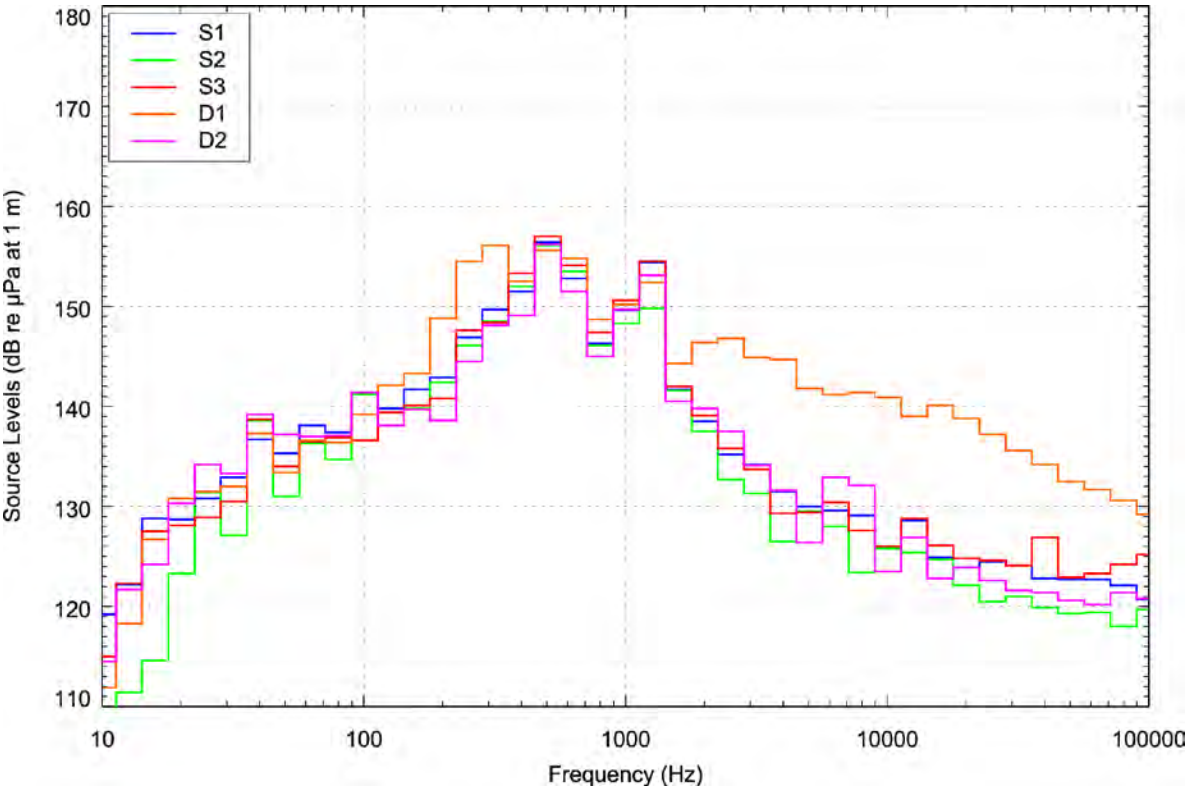

Figure 7-12. R/V Small Research Vessel experimental: Source level spectrum in 1/3-octave bands recorded at the closest point of approach on the nearest recorder (usually A1 or B1) for each scenario. The spectrum values were corrected for distance using the coefficient from the best-fit lines of Figure 7-10 and 7-11. The spectrum for Scenario D1 shows much more high frequency energy which is associated with cavitation noise, likely due to the propulsion system working harder than the other scenarios due a head wind/current during this scenario.

Table 7-7.
R/V Small Research Vessel experimental: Distances (in meters) to 90% root-mean-square (rms) sound pressure level (SPL) thresholds determined from the 90th percentile fit lines in Figures 7-10 and 7-11 for each scenario.

90% rms SPL (dB re 1 µPa)	S1: 2.1 m/s	S2: 3.1 m/s	S3: 2.9 m/s	D1: 2.8 m/s	D2: 2.9 m/s
150	less than10	less than10	less than10	10	less than10
140	11	14	16	24	13
130	36	34	40	60	36
120	116	86	98	146	102
110	375	214	239	356	292

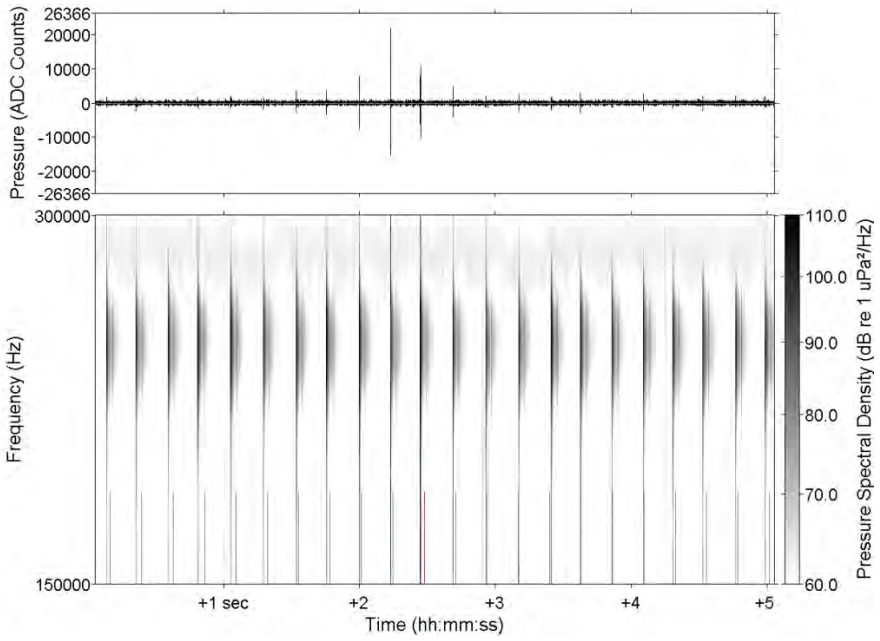

Figure 7-13. Time-series (top) and spectrogram (bottom) of the SWATH*plus*-M signal at closest point of approach (CPA) during Scenario S2. Red and gray vertical bars at the bottom of the spectrogram are evenly spaced at 231 ms. The pulse rate from the sonar varied between 185 and 231 ms.

The measurements for the broadside direction with the slant range between the source and recorder at less than 100 m (328 ft) are not reliable due to the narrow beamwidth of the interferometric sonar. With a beamwidth of 0.55°, the linear width of the beam at 100 m from the source is only 0.9 m (3.0 ft). The distance between the pulses along the track line was about 0.5 m [1.6 ft]. In such conditions, the main lobe of the beam may not be sampled at all for the slant ranges at the CPA less than 100 m (328 ft).

The geometry of the experiment did not permit reliable measurement of the sound levels from the interferometric sonar in broad side direction; therefore, no fits to the data were performed and no threshold radii are reported for the broadside direction of the interferometric sonar. Possible reasons

for the inconsistences include vertical beam variation, beam interference with the vessel hull (see Section 0), roll of the vessel affecting beam-pattern orientation, and pings from the sonar not occurring at the actual CPA to recorder (10 dB peak SPL variations in 230 ms).

Beam pattern analysis was performed to determine the directivity of the interferometric sonar in the horizontal and vertical planes. For this analysis, the rms SPLs were calculated with a fixed rms time window of 200 µs and corrected for spherical spreading loss and volumetric absorption.

For the horizontal directivity (i.e., in the azimuthal plane), the data recorded at the Shallow Site at A2 were used because the direct path from the source to the receiver was closer to the horizontal plane than at the Deep Site. Data for Scenario S2 (100% power output) and S3 (30 to 50% power output) were considered. The azimuthal angle was calculated from the recorder position, the source position was determined from the navigational file and the source towing direction. The angular sampling for the sector close to the broadside direction was 0.2°. The estimated horizontal beam patterns are presented in Figure 7-17. As expected, they show a narrow main lobe. The beamwidth of the main lobe obtained from the data is about 0.5°, which closely matches the sonar specification of 0.55°.

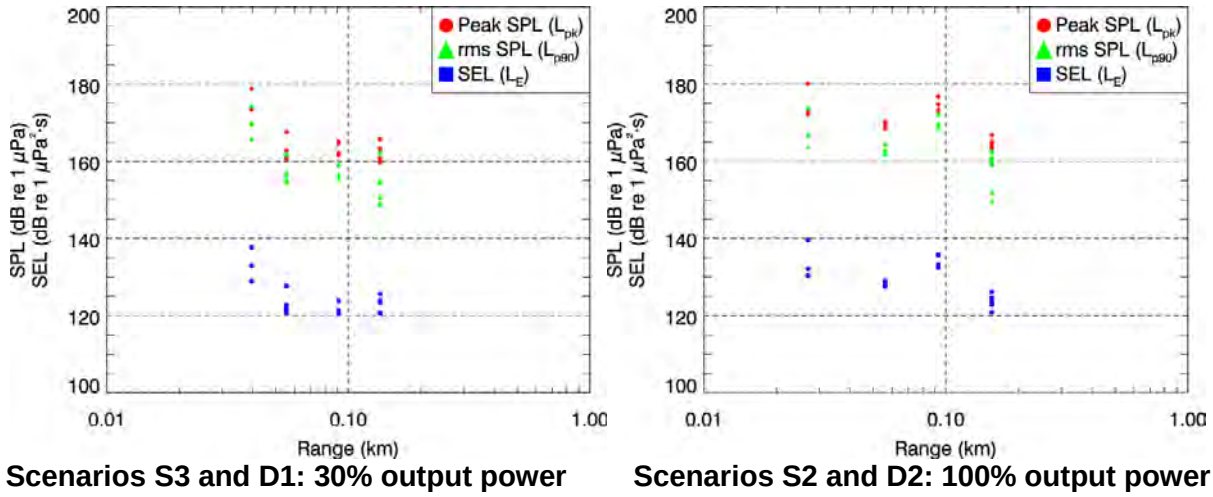

Figure 7-14. SEA SWATH*plus*-M interferometric sonar: Peak sound pressure level (SPL), 90% root-mean-square (rms) SPL, and sound exposure level (SEL) versus slant range in the endfire and broadside directions for two output power levels. Each plot combines data from the Shallow and Deep Sites and from both recorders. The data points with slant range less than 100 m (328 ft) may not sample the levels in the main lobe of the beam because the linear beamwidth was less than 0.5 m (1.6 ft).

The vertical directivity (i.e., in the vertical plane intersecting the survey track) was estimated from the data collected at the Deep Site at B1 for Scenario D1, 30 to 50% output power, and at B2 for Scenario D2, 100% output power (Figure 7-18). The recorder closest to the track was selected to avoid signal variability due to the horizontal beam pattern. The deeper site was selected to increase the resolution of the calculated pattern at near vertical angles. The vertical angle was calculated based on the recorder position and the source position was determined from the navigational file. The angular sampling for the sector close to the vertical direction was 0.6°. The estimated vertical beam patterns support the general expectation of a narrow main lobe. The beamwidth of the main

lobe obtained from the data is about 0.5°, which is a close match with the manufacturer's specification of 0.55.

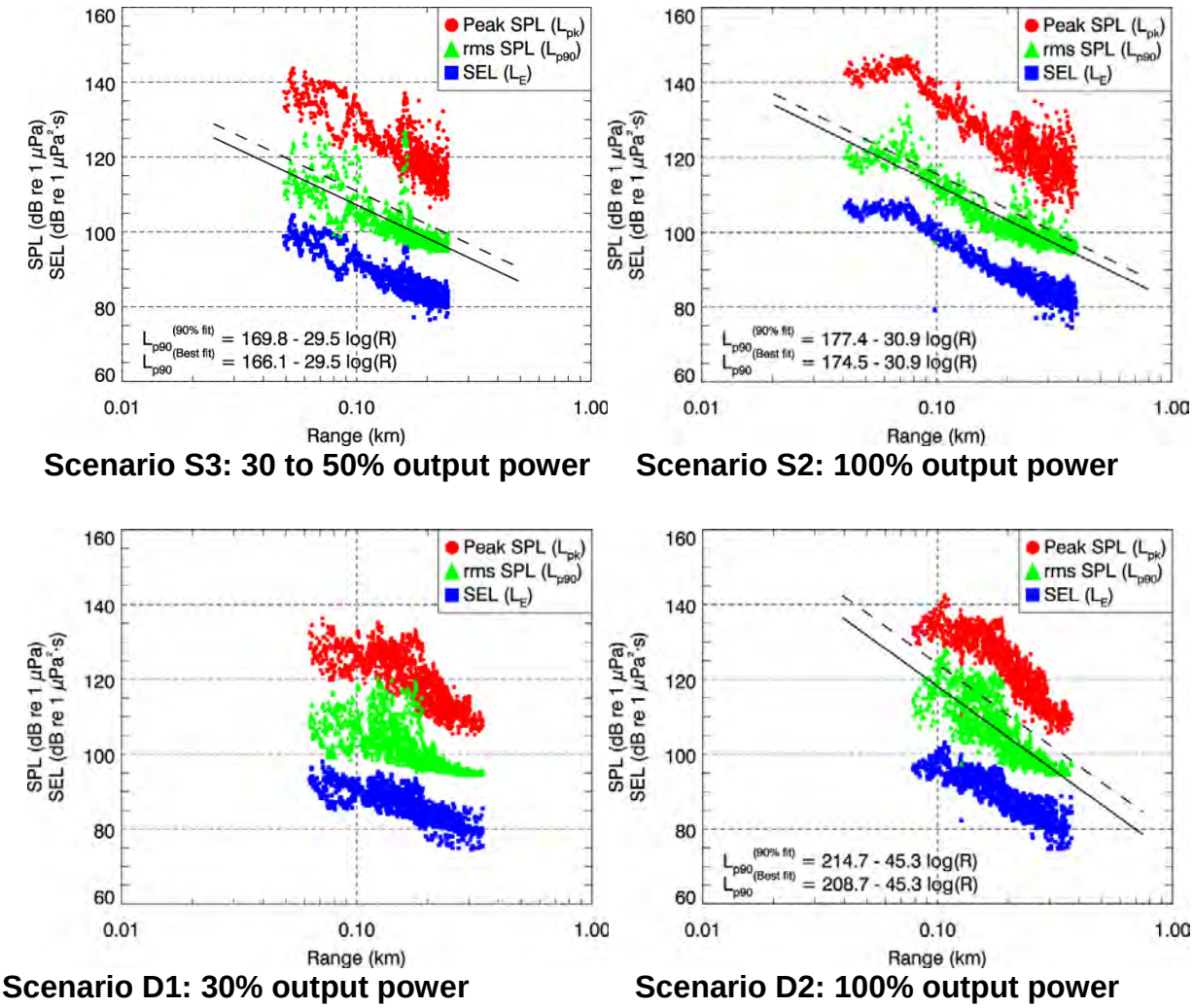

Figure 7-15. SEA SWATH*plus*-M interferometric sonar, endfire direction: Peak sound pressure level (SPL), 90% root-mean-square (rms) SPL, and sound exposure level (SEL) versus slant range for two output power levels. The solid line is the best-fit line to the 90% rms SPLs. The dashed line is the 90th percentile fit line: the best-fit line shifted up to exceed 90% of the 90% rms SPLs. Each plot combines data from both recorders. The signal levels for Scenario D1 were too low for accurate measurement of T90, hence the rms SPL. No regressions are shown.

The vertical angle was calculated based on the recorder position and the source position determined from the navigation data. The angular sampling for the sector close to the vertical direction was 0.4°. The estimated vertical beam patterns are presented in Figures 7-30 through 7-34. Each plot has three additional lines representing theoretical beam patterns for selected angles calculated using standard formulae for the beam pattern of a circular transducer (Kinsler et. al. 1950, ITC 1993).

7.3.4 BACKGROUND SOUND LEVELS

The percentile broadband sound levels of underwater noise recorded during both deployments are provided in Table 7-14. The percentile 1/3-octave band levels of underwater noise at the Shallow and Deep Sites are shown in Figure 7-35 and 7-36, respectively. All data from the deployments were processed. The 5th percentile levels are high because of the signals from the measured sound sources.

Table 7-8.
Maximum sound levels of pulses from the SWATH*plus*-M interferometric sonar at the closest point of approach (CPA) to each recorder: peak sound pressure level (SPL), 90% root-mean-square (rms) SPL, and sound exposure level (SEL). The 90% energy pulse duration (T_{90}) is also shown.

Scenario	Power output	Location	Slant range (m)	Peak SPL (dB re 1 µPa)	90% rms SPL (dB re 1 µPa)	T_{90} (µs)	SEL (dB re 1 µPa)
Shallow Site							
S2	100%	A1	27	180.1	173.9	300	139.5
		A2	154	166.8	162.6	200	126.1
S3	30 to 50%	A1	40	178.8	174.4	190	137.6
		A2	135	165.7	162.3	190	125.6
Deep Site							
D1	30%	B1	55	167.6	161.9	340	127.7
		B2	91	165.1	159.3	260	123.8
D2	100%	B1	92	176.9	172.3	200	135.7
		B2	55	170.3	164.6	250	128.9

Table 7-9.
SEA SWATH*plus*-M interferometric sonar: Distances (in meters) to 90% root-mean-square (rms) sound pressure level (SPL) thresholds determined from the 90th percentile fit line in Figure 7-15 for the endfire direction of various power output settings.

90% rms SPL (dB re 1 µPa)	S3: 30 to 50% power	S2: 100% power	D2: 100% power
170		less than10	10
160	less than10	less than10	16
150	less than10	less than10	27
140	10	16	45
130	22	34	74
120	49	71	123
110	107	150	205

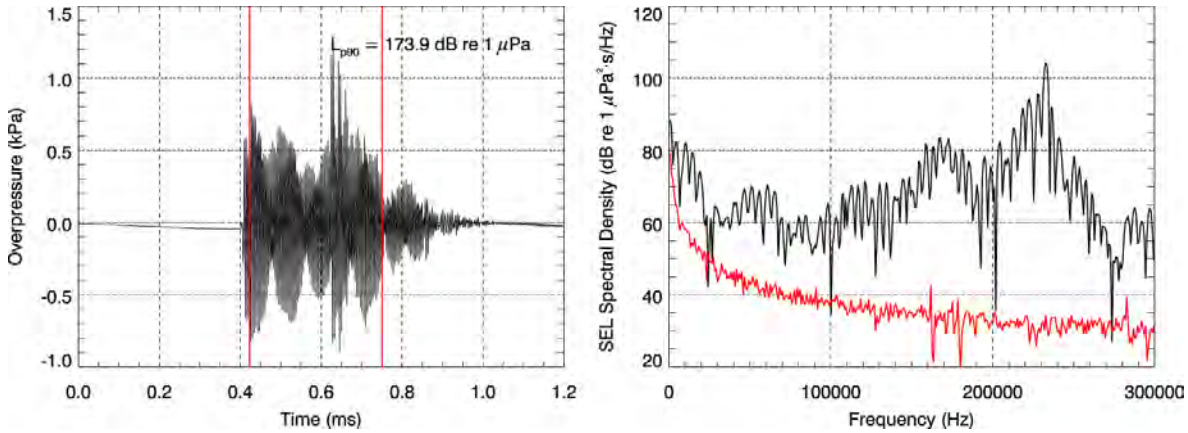

Figure 7-16. SEA SWATH*plus*-M interferometric sonar. (Left) Waveform and (right) corresponding sound exposure level (SEL) spectral density of a pulse (black line) at A1, 27 m (89 ft) slant range (12 m [39 ft] horizontal range) (Shallow Site, Scenario S2). The red bars on the waveform indicate the 90% energy pulse duration, T90. The red line on the spectral density plot shows spectral density of background noise as calculated in between pulses.

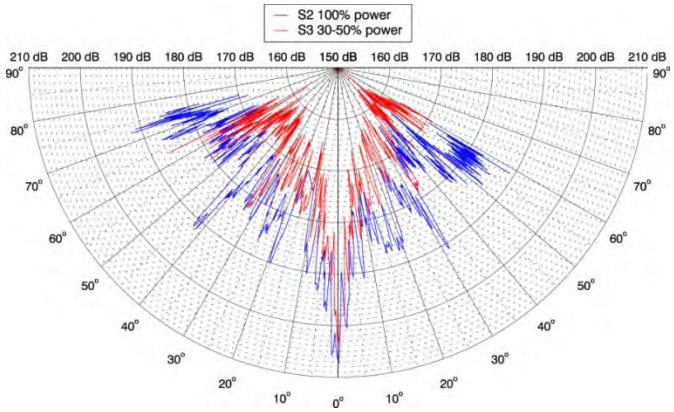

Figure 7-17. SEA SWATH*plus*-M interferometric sonar. Horizontal beam pattern showing source level versus angle from transducer broadside. The tow direction is to the right.

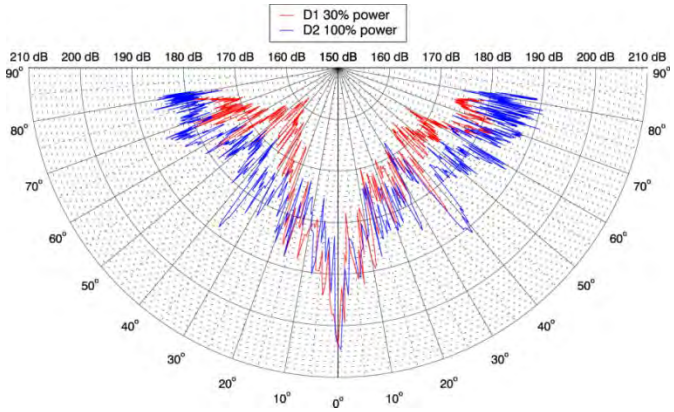

Figure 7-18. SEA SWATH*plus*-M interferometric sonar. Vertical beam pattern showing source level versus angle from vertical. The tow direction is to the right.

7.3.3 EDGETECH 3200 SB-0512I SUB-BOTTOM PROFILER

Scenarios S5 through S10 at the Shallow Site and Scenarios D3 through D6 at the Deep Site were performed with various operational settings of the EdgeTech 3200 SB-512i sub-bottom profiler (Table 7-10). Evaluating of the Scenario S4 data showed the pulse rate and source level differed substantially from the values provided by the operator as well as varying during the

scenario; therefore, results for Scenario S4 are omitted from this report, as they cannot be reliably connected to specific operational settings (see Figure 7-19).

The received peak SPLs exceeded the top end of the dynamic range of the recorders (172.1 and 171.1 dB re 1 µPa) for Scenarios S6, S8, S9, S10, D3, D5, and D6 at 37 to 73 m slant range (29 to 50 m [128 to 164 ft] horizontal range) from the source, resulting in clipped waveforms. Table 7-10 summarizes the results of each scenario, providing the slant range to the recorder hydrophone at the CPA and the sound levels of the loudest pulse.

Figure 7-20 and 7-21 present the variation in the peak SPL, rms SPL, and SEL with slant range for the Shallow Site and Deep Site scenarios, respectively. Best-fit and 90th percentile fit lines were calculated for the rms SPLs. Distances to various rms SPL thresholds based on the 90th percentile fit line are provided in Table 7-11 and 7-12 for the Shallow and Deep Sites, respectively.

The sub-bottom profiler transmits a chirp pulse characterized by an increase in frequency over the duration of the pulse as well as a change in amplitude. Figure 7-22 shows an example waveform of a chirp pulse recorded at the CPA, the pulse spectral density, and the spectral density of the background noise as calculated in between the pulses. Figures 7-23 and 7-24 show the SEL and rms SPL, respectively, for the Shallow Site scenarios. Figure 7-25 and 7-26 show the SEL and rms SPL, respectively, for the Deep Site scenarios.

The analysis determined the variation in the pulse length with range. The measured 90% energy pulse durations (T_{90}) for the sub-bottom profiler pulses for the Shallow and Deep Site scenarios are presented in Figures 7-32 and 7-33, respectively. The minimum T_{90} values for each scenario are summarized in Table 7-13.

The recorded signals were analyzed to obtain the frequency spectrum of the pulses at different settings. The spectrum of the time series was calculated over the time window that includes 10 to 15 pulses. The time window was selected so that it encloses the first unclipped pulses at the closest range to the recording station. The spectrum was calculated for six scenarios at the Shallow Site (Figure 7-29) and four scenarios at the Deep Site (Figure 7-30).

Pulse specifications, such as pulse bandwidth and maximum frequency, as well as the minimum T_{90}, were calculated for each scenario (Table 7-13). The pulse bandwidth and main frequency were derived from the calculated spectra. Two pulse bandwidths are reported as a pair of frequencies at which the spectrum levels drops 10 and 20 dB below the maximum spectrum level. For Scenario S9, three maximum frequencies are reported because the spectrum exhibits three maxima (see Figure 7-29), possibly because both transducers were operating simultaneously.

Table 7-10.
Maximum sound levels of pulses from the EdgeTech 3200 SB-0512i sub-bottom profiler at the closest point of approach (CPA) to each recorder. Peak sound pressure level (SPL), 90% root-mean-square (rms) SPL, and sound exposure level (SEL). Pulse types: frequency modulated (FM) and wide-band (WB). For the scenarios where the signal exceeded the dynamic range of the recorder, the levels for the nearest unclipped pulse are shown.

Scenario	Frequency (kHz)	Pulse period (ms)	Pulse type	Location	Slant (horizontal) range (m)	Peak SPL (dB re 1 µPa)	90% rms SPL (dB re 1 µPa)	SEL (dB re 1 µPa)
Shallow Site								
S5	0.5 to 2.7	100	FM	A1	46(40)	168.2	158.3	144.9
				A2	127(125)	160.0	148.4	136.3
S6*	0.5 to 7.2	30	FM	A1	42(35)	171.8	160.5	145.0
				A2	152(150)	150.8	135.2	123.6
S7	1 to 6	40	FM	A1	29(19)	171.9	161.6	146.2
				A2	147(145)	159.2	144.6	131.0
S8*	2 to 12	20	FM	A1	42(35)	172.1	162.0	145.9
				A2	137(135)	152.0	134.4	124.6
S9*	0.5 to 2.7	40	WB	A1	37(29)	171.7	161.7	145.8
				A2	149(147)	157.7	145.8	132.0
S10*	0.5 to 6	20	WB	A1	46(40)	171.3	159.6	145.1
				A2	149(147)	155.3	138.2	127.1
Deep Site								
D3†	0.5 to 8	5	FM	B1	74(51)	165.5	148.6	128.3
				B2	73(50)	170.9	162.8	137.0
D4	0.5 to 4.5	40	WB	B1	96(80)	155.9	148.5	132.1
				B2	54(5)	164.5	156.1	139.4
D5†	2 to 12	20	FM	B1	92(74)	156.3	145.4	130.0
				B2	66(39)	170.8	163.6	143.4
D6†	1 to 6	40	FM	B1	93(76)	167.4	158.1	139.7
				B2	64(35)	171.0	163.1	144.0

***** The signal exceeded the dynamic range of the recorder of 172.1 dB re 1 µPa for this scenario.
† The signal exceeded the dynamic range of the recorder of 171.1 dB re 1 µPa for this scenario.

Table 7-13 shows that for all scenarios except D4, the upper and lower limits of the measured frequency band are within the frequency band defined by the operational settings of the sonar. The shortest duration T_{90} were retrieved from the per-shot pulse analysis results (see Section 2.4.2).

For Scenario D4, the upper limit of the measured frequency band (3.8 kHz for −20 dB threshold) is about 40% higher than the upper limit for the operational settings for this scenario as documented in the field logs. A possible explanation is that the actual operational settings were different, likely 4.5 kHz for the upper limit. This assumption is made based on the standard bandwidths for the EdgeTech 3200 sub-bottom profiler (Table 7-2).

Beam pattern analysis was performed for the directivity of the sub-bottom profiler transducer in the vertical plane. For the analysis, the rms SPLs were calculated with a fixed time window and

corrected for spherical spreading loss. The width of the time window was set to the minimum T_{90} value observed for the scenario. The rms SPLs for clipped pulses were excluded from the analysis.

The vertical directivity was estimated from the data collected at the Deep Site at B1, which was closest to the track for all four sub-bottom profiler scenarios. The closest recorder was selected to remove the variability of the signal due to the horizontal beam pattern. The deeper site was selected to increase the resolution of the calculated pattern at near vertical angles.

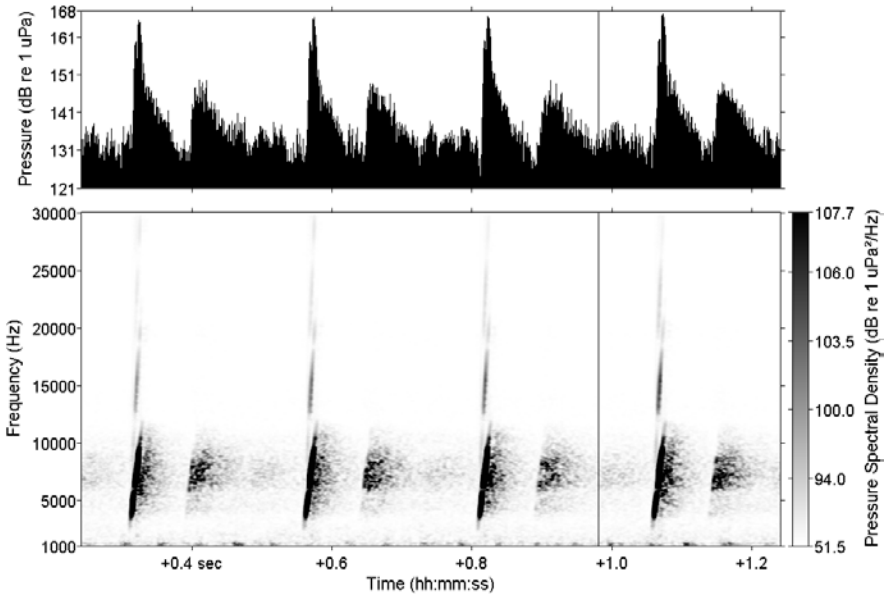

Figure 7-19. One second of received pressure level (top) and spectrogram (bottom) of the SB-0512i sub-bottom profiler at CPA for Scenario D5. Significant sideband energy is visible in the spectrogram at higher frequencies. This is also shown in Figure 7-22.

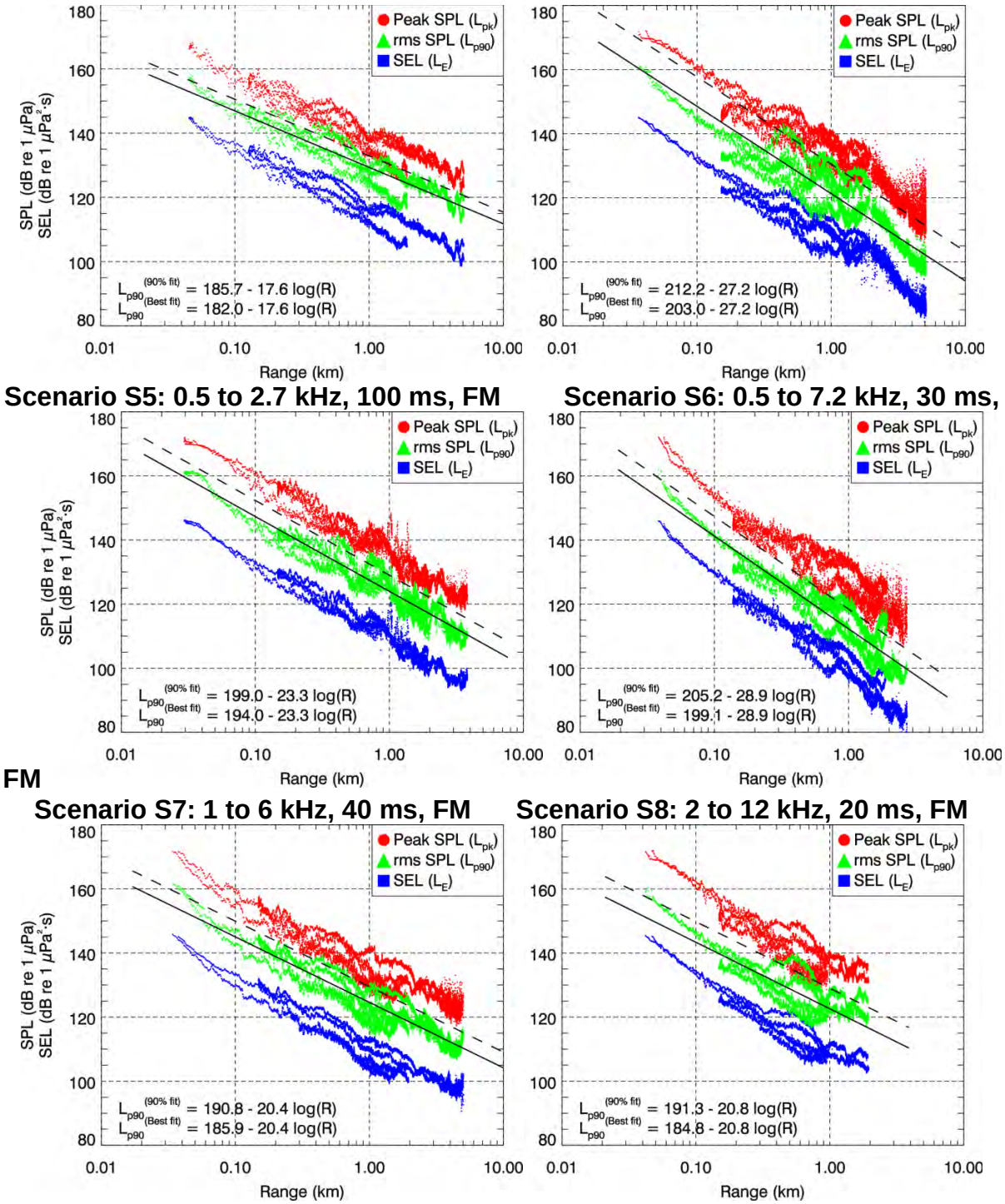

Figure 7-20. EdgeTech 3200 SB-0512i sub-bottom profiler, Shallow Site. Peak sound pressure level (SPL), root-mean-square (rms) SPL, and sound exposure level (SEL) versus slant range for various pulse settings. The solid line is the best-fit line to the 90% rms SPLs. The dashed line is the best-fit line shifted up to exceed 90% of the 90% rms SPLs. Data from both A1 and A2 are shown. Data for clipped pulses are excluded.

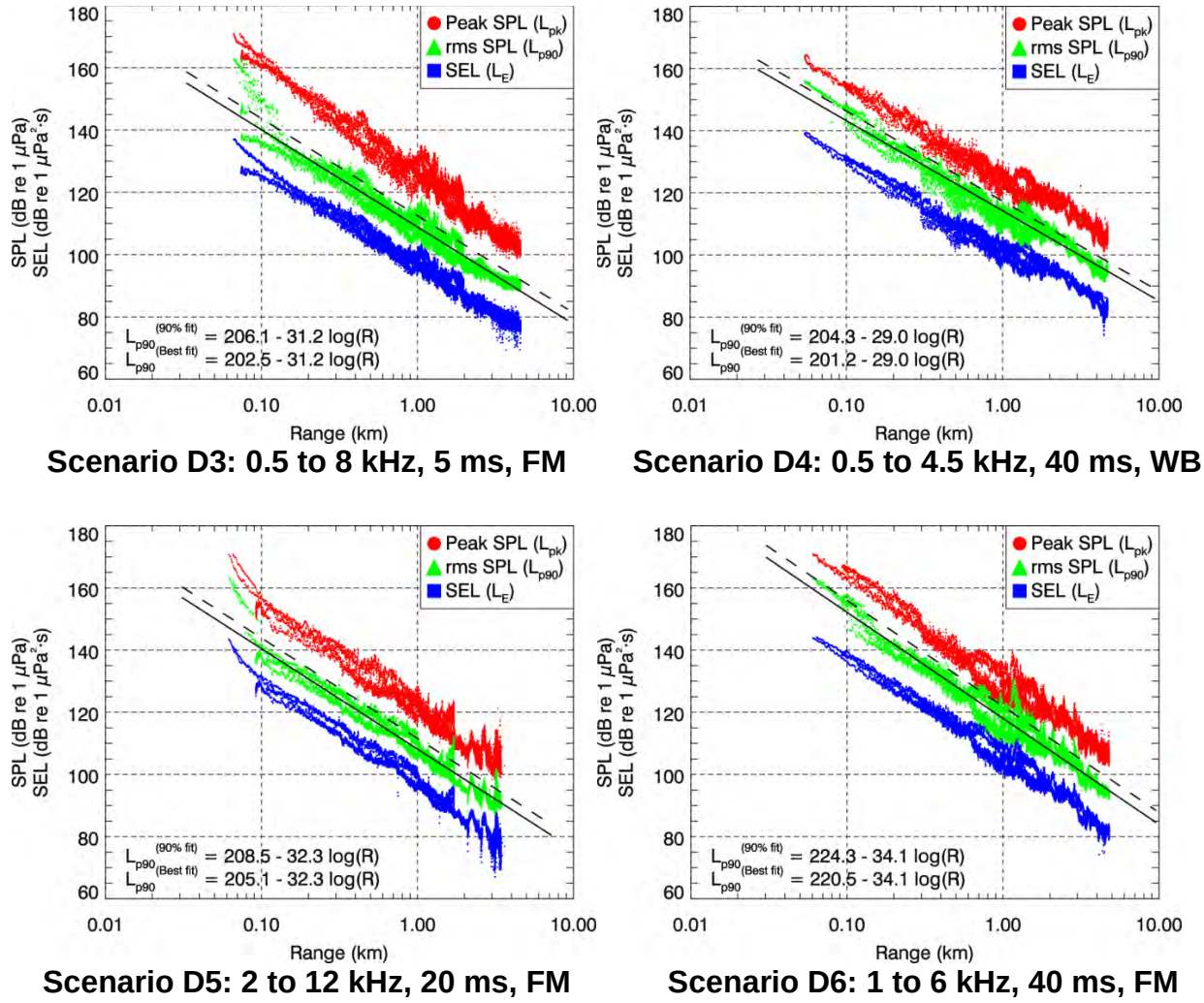

Figure 7-21. EdgeTech 3200 SB-0512i sub-bottom profiler, Deep Site. Peak sound pressure level (SPL), root-mean-square (rms) SPL, and sound exposure level (SEL) versus slant range for various pulse settings. The solid line is the best-fit line to the 90% rms SPLs. The dashed line is the best-fit line shifted up to exceed 90% of the 90% rms SPLs. Data from both B1 and B2 are shown. Data for clipped pulses are excluded.

Table 7-11.
EdgeTech 3200 SB-0512i sub-bottom profiler, Shallow Site. Distances to 90% root-mean-square (rms) sound pressure level (SPL) thresholds determined from the 90th percentile fit lines in Figure 7-20 for each SSC scenario.

90% rms SPL (dB re 1 µPa)	Scenario S5	Scenario S6	Scenario S7	Scenario S8	Scenario S9	Scenario S10
190		less than10				
180	less than10	15	less than10	less than10	less than10	less than10
170	less than10	35	17	16	10	11
160	29	82	47	37	32	32
150	107	192	126	81	99	97
140	397	447	338	179	306	295
130	1472	1040	908	398	944	894
120	5461	2422	2436	881	2914	2713

Table 7-12.
EdgeTech 3200 SB-0512i sub-bottom profiler, Deep Site. Distances to 90% root-mean-square (rms) sound pressure level (SPL) thresholds determined from the 90th percentile fit lines in Figure 7-21 for each sound source characterization (SSC) scenario.

90% rms SPL (dB re 1 µPa)	Scenario D3	Scenario D4	Scenario D5	Scenario D6
190				10
180	less than10	less than10	less than10	20
170	14	15	16	39
160	30	34	32	77
150	63	75	65	150
140	131	165	132	295
130	274	365	269	579
120	574	809	549	1137

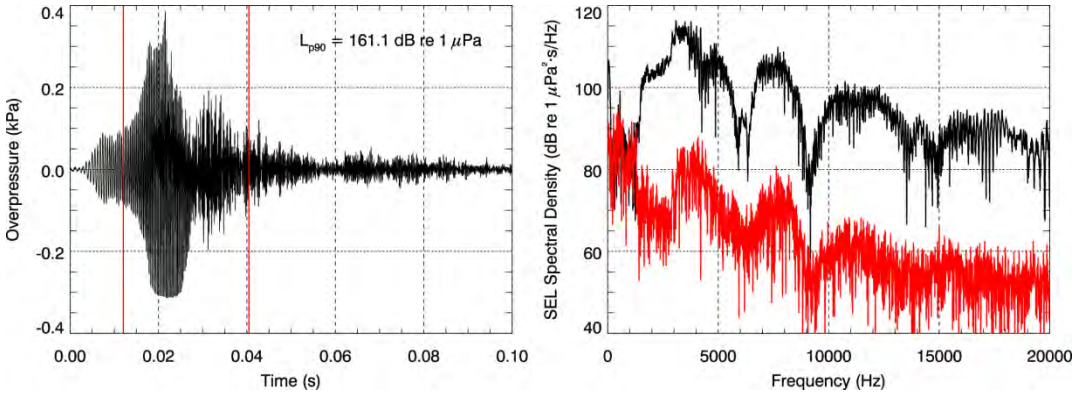

Figure 7-22. EdgeTech 3200 SB-0512i sub-bottom profiler, 1 to 6 kHz, 40 ms. (Left) Waveform and (right) corresponding sound exposure level (SEL) spectral density of a pulse (black line) at A1 at 29 m (95 ft) slant range (19 m [62 ft] horizontal range) (Shallow Site, Scenario S7). The red bars on the waveform indicate the 90% energy pulse duration, T90. The red line on the spectral density plot shows spectral density of background noise as calculated in between pulses.

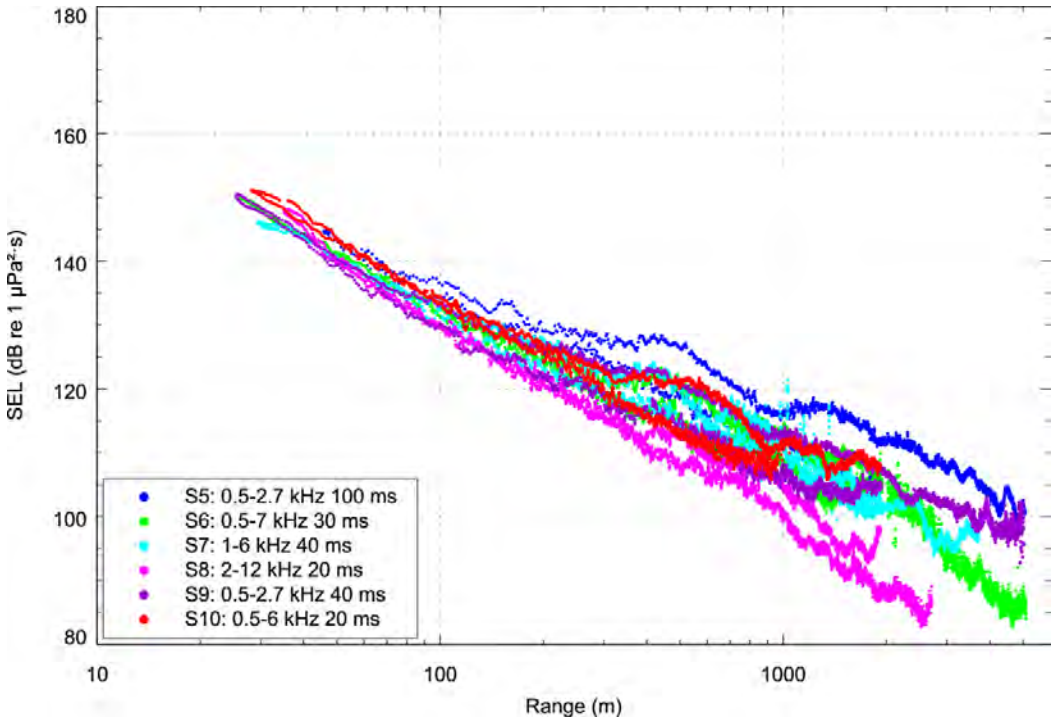

Figure 7-23. EdgeTech 3200 SB-0512i sub-bottom profiler, Shallow Site. Sound exposure level (SEL) versus slant range for various pulse settings. Data from the closest recorder (A1) are shown.

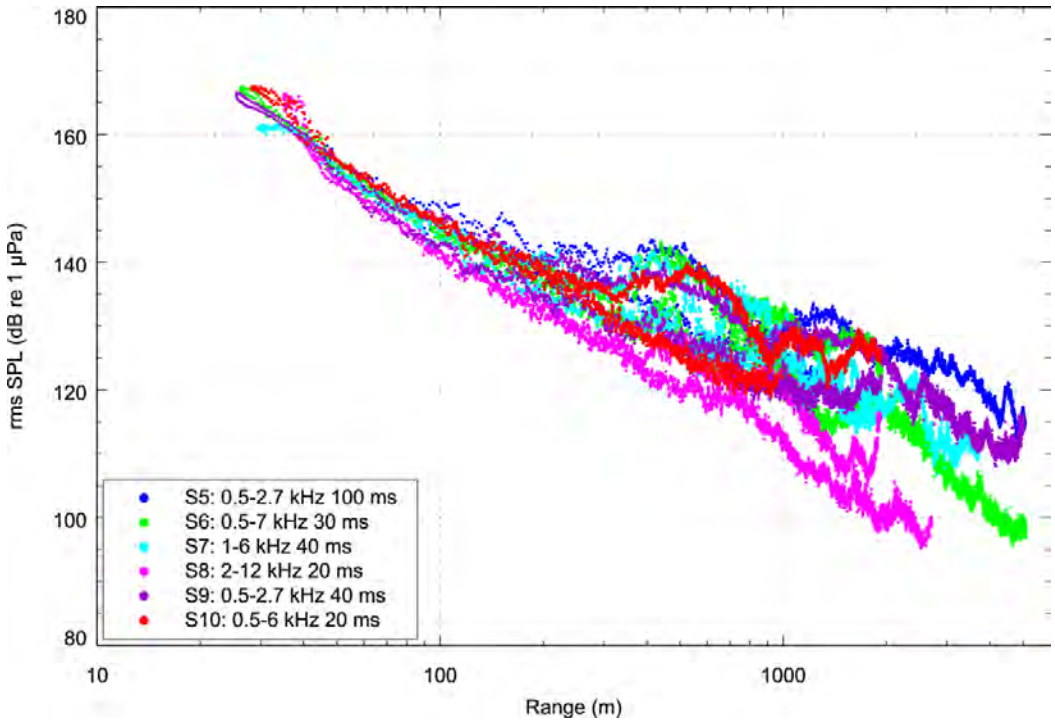

Figure 7-24. EdgeTech 3200 SB-0512i sub-bottom profiler, Shallow Site. 90% rms sound pressure level (SPL) versus slant range for various pulse settings. Data from the closest recorder (A1) are shown.

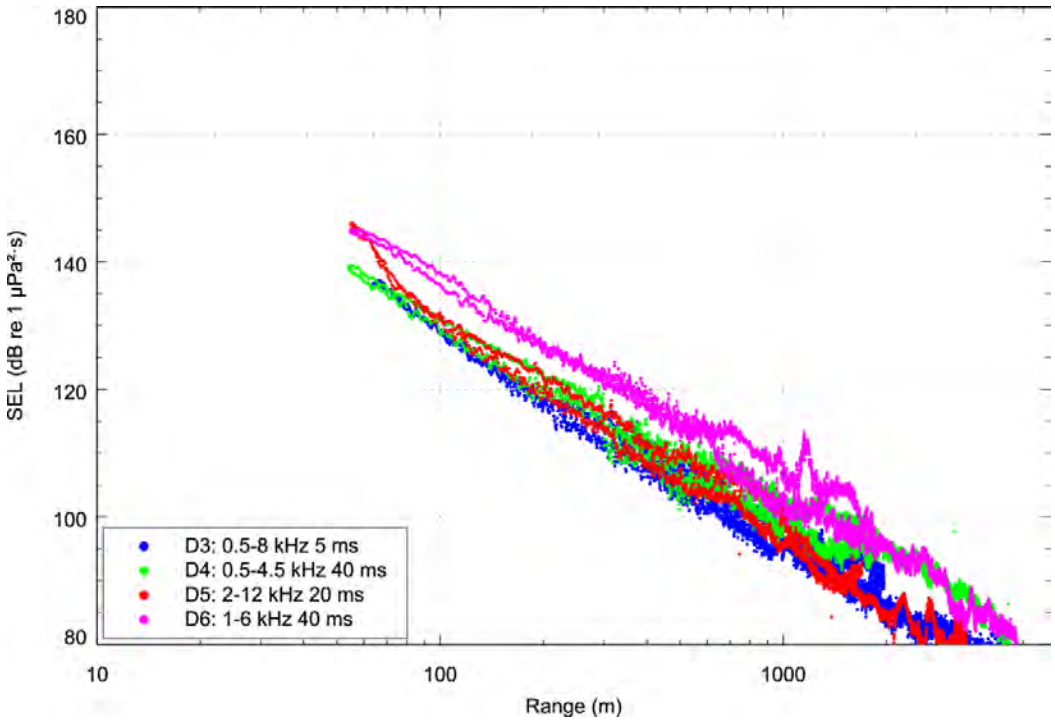

Figure 7-25. EdgeTech 3200 SB-0512i sub-bottom profiler, Deep Site. Sound exposure level (SEL) versus slant range for various pulse settings. Data from the closest recorder (B2) are shown.

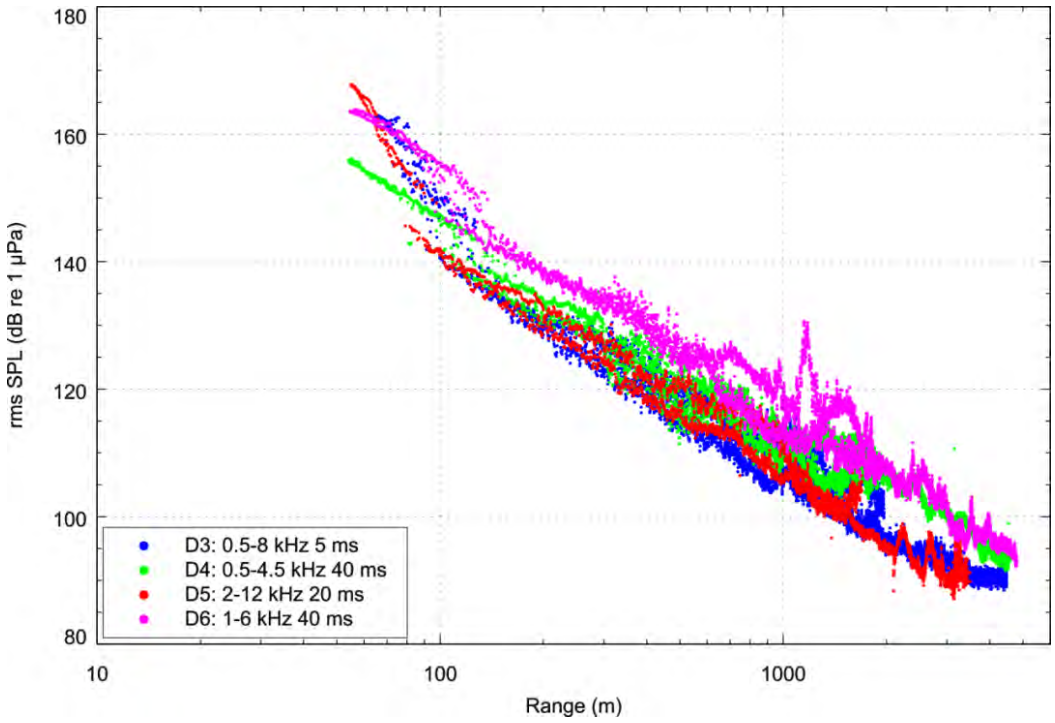

Figure 7-26. EdgeTech 3200 SB-0512i sub-bottom profiler, Deep Site. 90% rms sound pressure level (SPL) versus slant range for various pulse settings. Data from the closest recorder (B2) are shown.

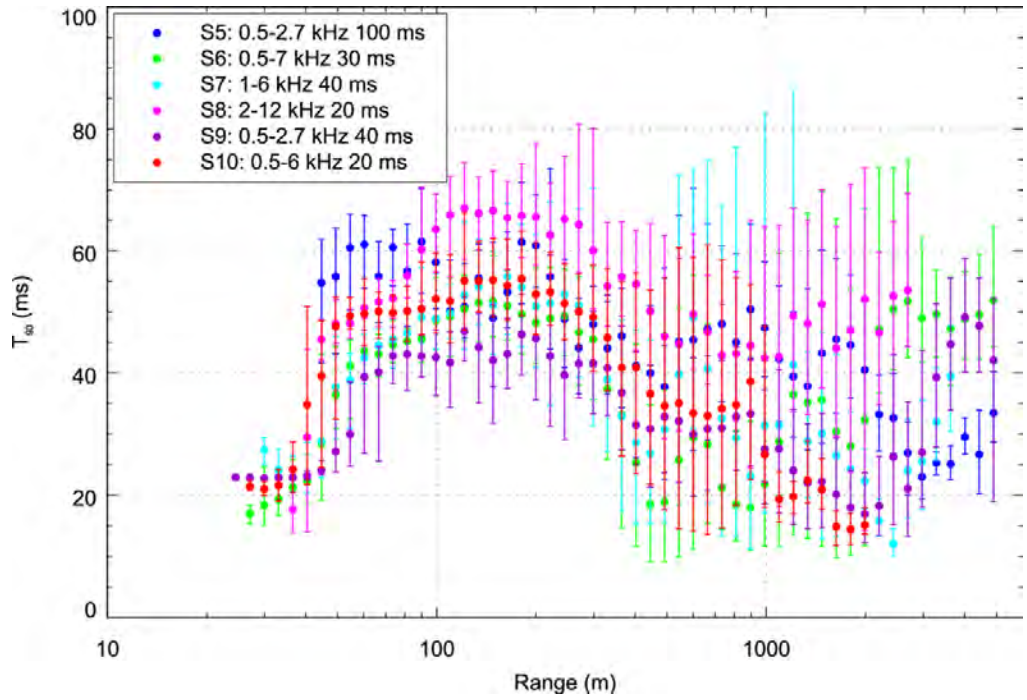

Figure 7-27. EdgeTech 3200 SB-0512i sub-bottom profiler, Shallow Site. The 90% energy pulse duration (T90) vs. slant range for various pulse settings. The error bars indicate 5th and 95th percentile value in each bin.

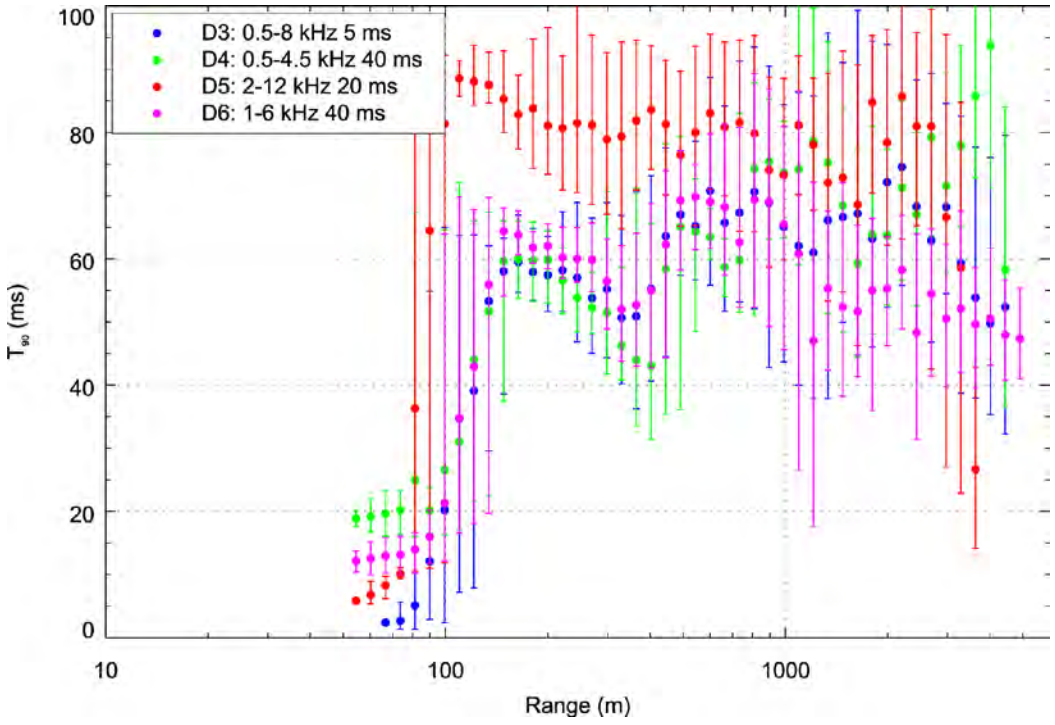

Figure 7-28. EdgeTech 3200 SB-0512i sub-bottom profiler, Deep Site. The 90% energy pulse duration (T90) vs. slant range for various pulse settings. The error bars indicate 5th and 95th percentile value in each bin.

Table 7-13.
Edgetech 3200 SB-512i sub-bottom profiler. Operational settings and measured pulse parameters for each sound source characterization (SSC) scenario.

Scenario	Frequency setting (kHz)	Pulse length setting (ms)	F_{max}	-10 dB bandwidth (kHz)	-20 dB bandwidth (kHz)	Min T_{90} (ms)
Shallow Site						
S5	0.5 to 2.7	100	1.8	1.2 to 2.0	0.4 to 2.3	50
S6	0.5 to 7.2	30	3.6	2.0 to 5.8	1.2 to 6.5	15
S7	1 to 6	40	3.7	2.6-4.5	1.5 to 5.5	20
S8	2 to 12	20	6.6	4.6 to 9.5	3.0 to 10.5	14
S9	0.5 to 2.7	40	1.9	1.1 to 2.1	0.9 to 2.5	19
S10	0.5 to 6	20	2.0, 4.1, 5.8	1.1 to 6.5	0.8 to 6.5	10
Deep Site						
D3	0.5 to 8	5	4.3	3.2 to 5.5	3.0 to 6.0	2.2
D4	0.5 to 4.5	40	2.7	1.5 to 3.5	1.0 to 3.8	12.5
D5	2 to 12	20	6.5	4.0 to 9.0	3.3 to 9.5	5.3
D6	1 to 6	40	3.9	2.2 to 4.8	2.0 to 5.0	10

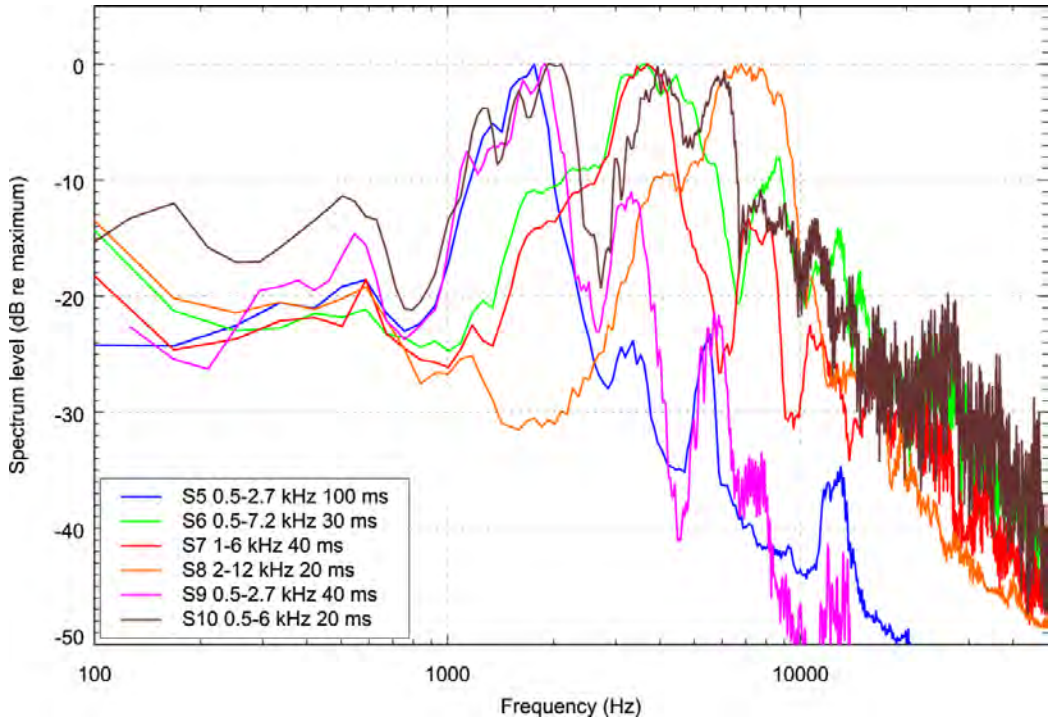

Figure 7-29. Spectra of pulses from the EdgeTech 3200 SB-512i sub-bottom profiler at the Shallow Site.

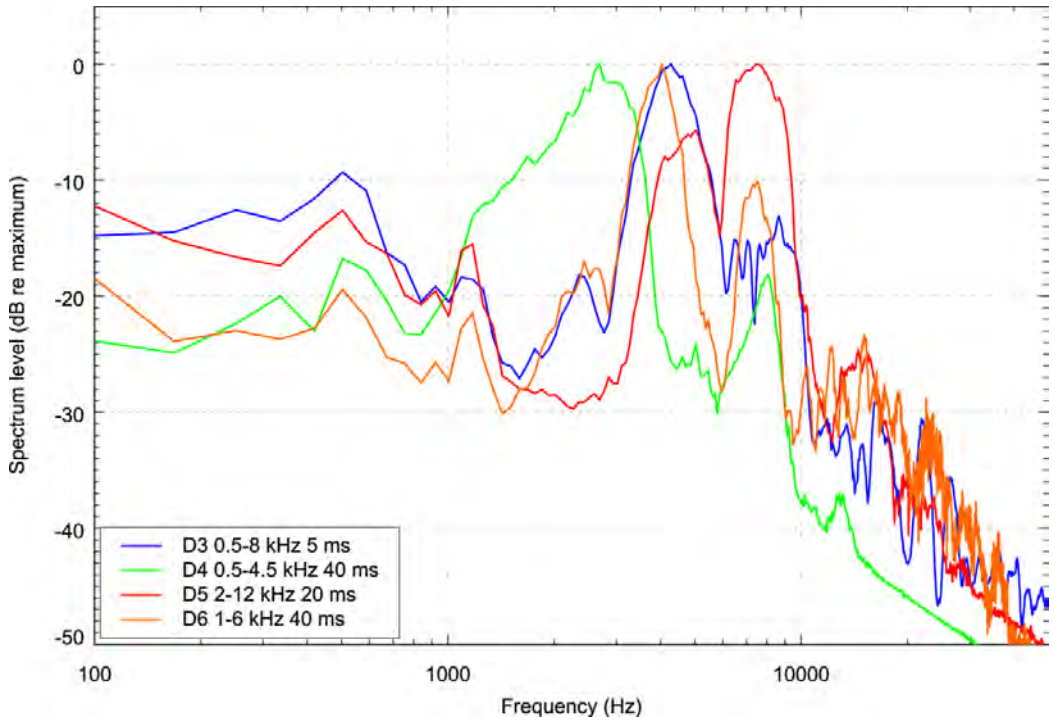

Figure 7-30. Spectra of pulses from the EdgeTech 3200 SB-512i sub-bottom profiler at the Deep Site.

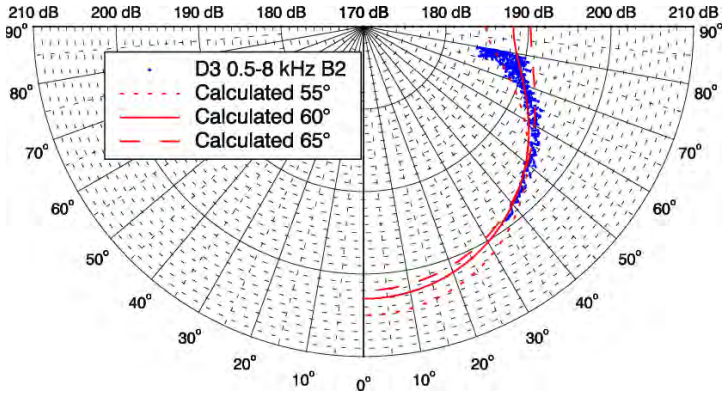

Figure 7-31. EdgeTech 3200 SB-0512i sub-bottom profiler. Vertical beam pattern for the 0.5 to 8 kHz setting measured during Scenario D3 and calculated for transducer beamwidths of 55°, 60°, and 65°. The tow axis is into the page.

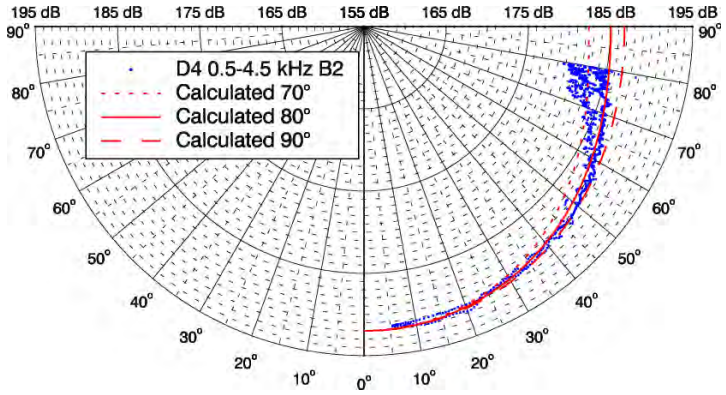

Figure 7-32. EdgeTech 3200 SB-0512i sub-bottom profiler. Vertical beam pattern for the 0.5 to 4.5 kHz setting measured during Scenario D4 and calculated for transducer beamwidths of 70°, 80°, and 90°. The tow axis is into the page.

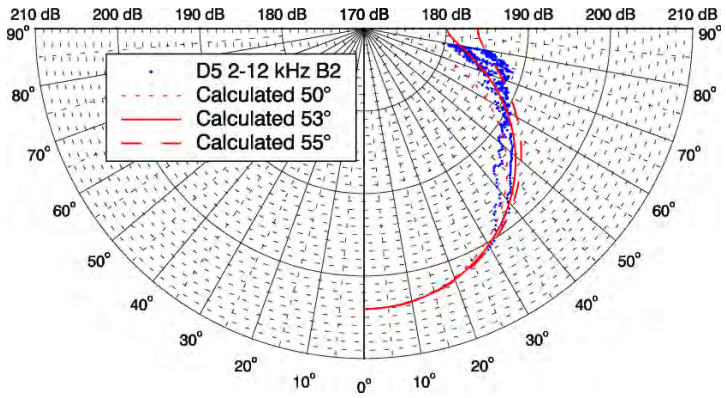

Figure 7-33. EdgeTech 3200 SB-0512i sub-bottom profiler. Vertical beam pattern for the 2 to 12 kHz setting measured during Scenario D5 and calculated for transducer beamwidths of 50°, 53°, and 55°. The tow axis is into the page.

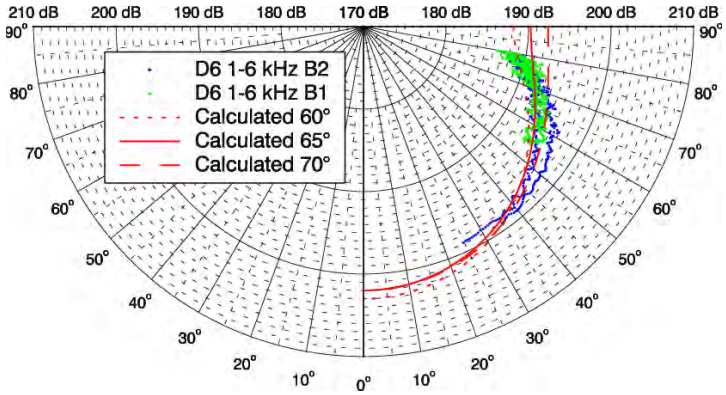

Figure 7-34. EdgeTech 3200 SB-0512i sub-bottom profiler. Vertical beam pattern for 1 to 6 kHz frequency band setting measured during Scenario D6 and calculated for transducer beamwidths of 60°, 65°, and 70°. The tow axis is into the page.

Table 7-14.
Exceedance percentiles of 20 s average broadband rms SPLs of underwater noise.

Percentile	Broadband rms SPL (dB re 1 µPa)	
	Shallow Site	Deep Site
5th	130.5	126.7
25th	120.0	110.5
50th	114.7	105.7
75th	110.2	103.8
95th	106.2	102.3

7.4 DISCUSSION

The received peak sound pressure levels (SPLs) for the sub-bottom profiler exceeded the top end of the dynamic range of the recording system (172.1 and 171.1 dB re 1 µPa) for several scenarios at horizontal ranges less than 40 m (131 ft) from the source. As a result, the signal waveform was clipped for pulses recorded when the EdgeTech 3200 SB-0512i sub-bottom profiler was near the closest point of approach (CPA).

According to the 90th percentile fit lines, the largest range from the EdgeTech 3200 SB-0512i to the 160 dB re 1 µPa threshold is 83 m (272 ft) for Scenario S6 (0.5 to 7.2 kHz, 30 ms, FM) and to the 120 dB re 1 µPa received level was 5,461 m (17,917 ft) for Scenario S5 (0.5 to 2.7 kHz, 100 ms, FM) (Table 7-11).

The highest spectral density frequency for the EdgeTech 3200 SB-0512i was approximately in the center of the operational frequency band. The spectral density distribution inside the operational band can be approximated with Gaussian distribution function. The spectral density at the low and high end of the band was about 25 to 35 dB less than for the central frequency. The detected central operational frequency for the SEA SWATH*plus*-M interferometric sonar was about 232 kHz. The operational frequency band (-10 dB from the maximum level) was about 5 kHz or 2.1%.

7.4.1 PULSE LENGTH FOR THE SUB-BOTTOM PROFILER

The 90% rms SPL of a pulse depends on the total amount of acoustic energy received (i.e., the SEL) and on the 90% energy pulse duration (T_{90}) over which the energy arrived (see Equation 2). Due to multipath scattering, the T_{90} varies more with distance than does the SEL, which makes the rms SPL more difficult to predict. The T_{90} of the pulse depends on the relative energy levels of the direct path arrival, the various multipath arrivals (i.e., reflections and refractions), and the time delays between those arrivals. The measured T_{90} for the sub-bottom profiler pulses are presented in Figures 7-27 and 7-28 for the Shallow and Deep sites, respectively.

At closer ranges, the T_{90} values are about half the set pulse length. At those ranges, the acoustic energy of the direct path arrival dominates the other arrivals. At ranges of about 30 m (98 ft)for the Shallow Site and about 80 m (262 ft) for the Deep Site (approximately equal to the water depth), the total pulse length that includes the multipath arrivals increases dramatically: 2 to 3 fold for short pulses (20 to 40 ms settings) and 10 to 15 fold for very short pulses (5 ms setting). The total pulse length for the long pulse (100 ms setting) changes little with range. For all settings, the total pulse length ranges from 40 to 60 ms at distances of 150 to 300 m (492 to 984 ft). Beyond 300 m (984 ft) range, the variation in the total pulse length increases, independent of the original pulse length.

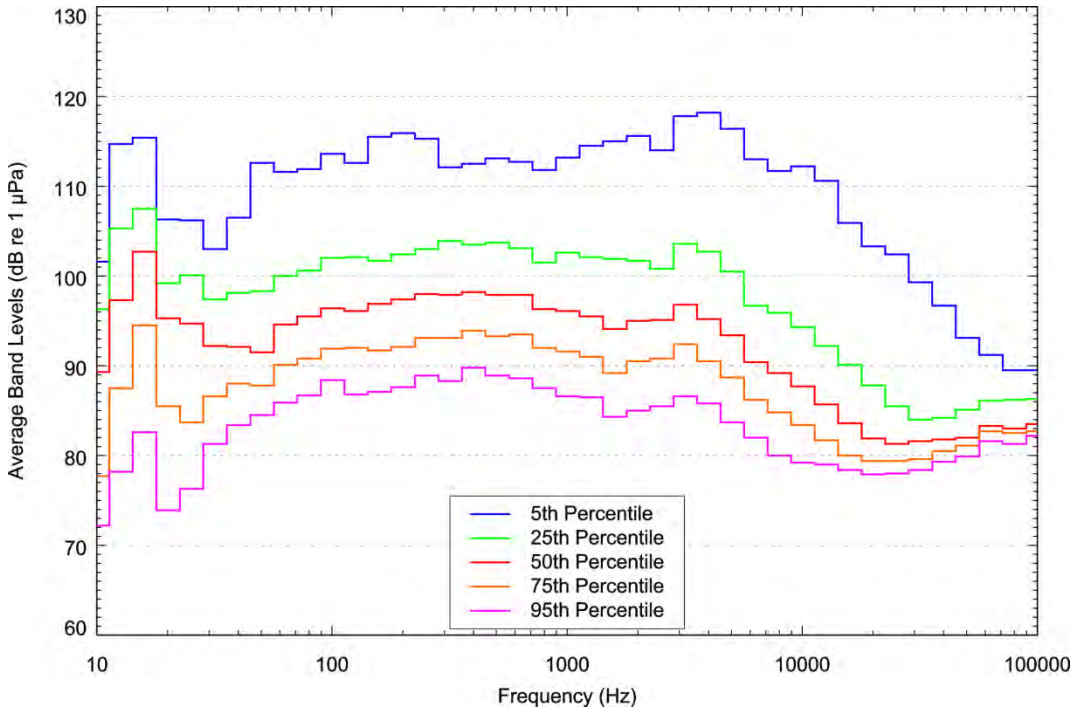

Figure 7-35. Underwater noise at the Shallow Site. Percentiles of 20 s average 1/3‑octave band sound pressure levels of underwater noise at A1, 13:05–23:15, 29 August 2012.

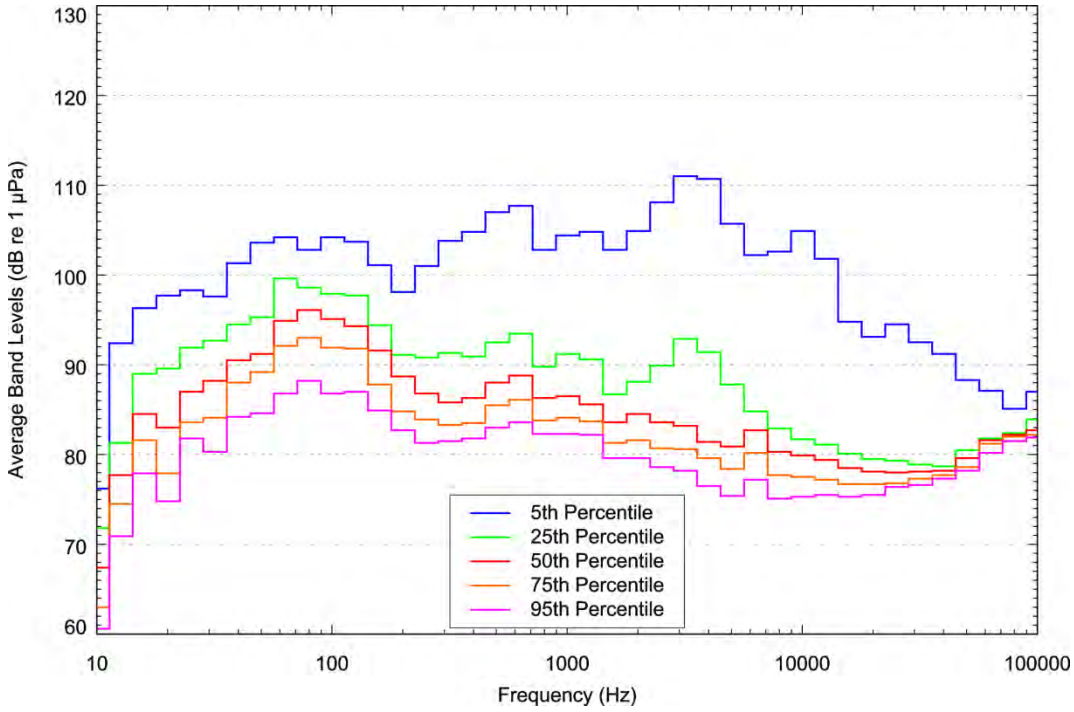

Figure 7-36. Background noise at the Deep Site. Percentiles of 20 s average 1/3‑octave band sound pressure levels of underwater noise at B1, 11:30–19:00, 30 August 2012.

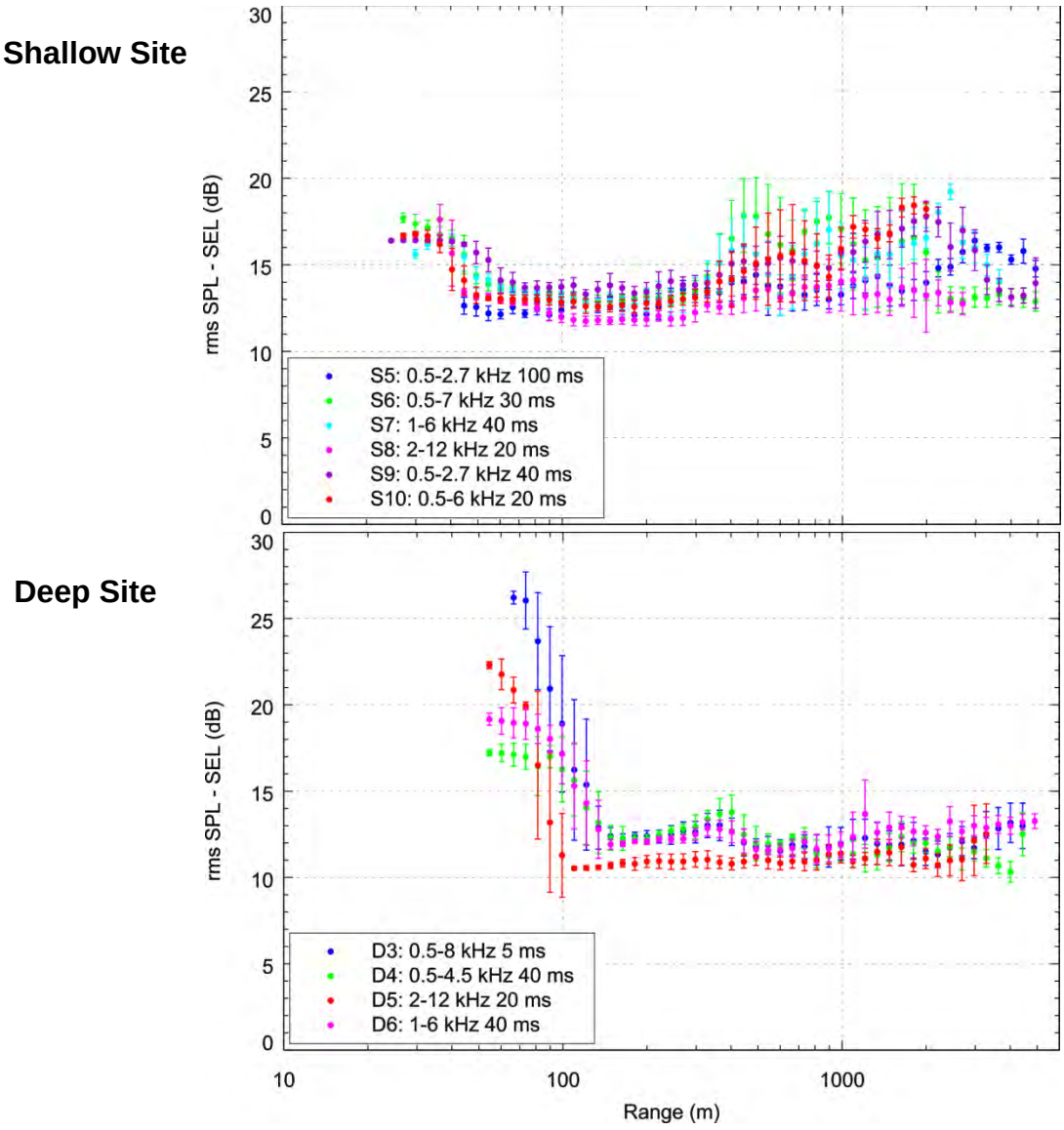

Figure 7-37. EdgeTech 3200 SB-0512i sub-bottom profiler. Difference (±SD) between per-pulse root-mean-square (rms) sound pressure level (SPL) and sound exposure level (SEL) vs. slant range for each scenario at the Shallow and Deep Sites.

Most T_{90} values observed at the Deep Site were greater (at ranges greater than150 m [492 ft]) than at the Shallow Site. With greater separation between the two reflecting surfaces (the sea surface and the bottom), the time delay between the direct path arrival and the multipath arrivals is also greater, which causes the acoustic energy to spread in time and reduce the rms SPL. The variation in the difference between the per-pulse rms SPL and SEL are presented in Figure 7-37 for the Shallow and Deep Sites. The difference between the per-pulse rms SPL and SEL detected at the Shallow Site was 11 to 19 dB, virtually independent of the pulse operational settings. At the Deep Site the difference was 17 to 27 dB at shorter ranges (less than150 m [492 ft]), where the scenarios with shorter pulse settings provided greater difference. At longer ranges, the rms SPL-SEL difference is 10 to 15 dB independent of the pulse setting.

The variability in the T_{90} pulse length is largely responsible for the spread of rms SPLs shown in Figure 7-20 and 7-21.

7.4.2 BEAM PATTERNS

The beam pattern was estimated for both electromechanical sources and the results agree with those expected from the source specifications.

7.4.2.1 SWATHplus-M Interferometric Sonar

Both the horizontal (Figure 7-17) and along-track vertical (Figure 7-18) beam patterns for the interferometric sonar exhibit a narrow main lobe with an angular width of about 0.5 to 0.6°, which is close to the specifications of 0.55°. The source levels are about 10 dB less for the second- and third-order lobes. Some energy leaked to higher order lobes; however, the source levels for the sector 5° to 45° from the main lobe axis are 15 dB below the maximum or lower, and for angles more than 45°, 30 dB less than the source level of the main lobe or lower. As expected the beam patterns did not significantly change with the output power settings of the sonar.

7.4.2.2 EdgeTech 3200 SB-0512i Sub-Bottom Profiler

The beam pattern of the sub-bottom profiler was expected to be uniform in the horizontal plane; therefore, only the vertical beam pattern was estimated. Table 7-15 summarizes the results of Figure 7-31 through 7-34. The beamwidth estimated from the field measurements agrees with the theoretical value, especially for the 0.5 to 8.0 kHz and 1.0 to 6.0 kHz band settings.

Table 7-15.
Estimated beamwidths of the EdgeTech 3200 SB-0512i sub-bottom profiler at various frequency settings.

Scenario	Frequency (kHz)	Measured F_{max} (kHz)	Beamwidth	
			Empirical	Theoretical (for F_{max})
D3	0.5 to 8.0	4.3	60°	62°
D4	0.5 to 4.5	2.7	80°	98°
D5	2.0 to 12.0	6.5	53°	41°
D6	1.0 to 6.0	3.9	65°	68°

The plot of SEL versus range for Scenario D5 (Figure 7-21) is the best example of the effect of the beam pattern on the received levels. The steeper slope for the SEL data trend at close ranges (less than 80 m [262 ft]) is caused by the receiver being "illuminated" by a sector of the beam with higher source levels. Scenario S8 (Figure 7-20) provides another example of the beam pattern effect though not as distinct due to the shallow water depth.

Whereas the sub-bottom profiler was expected to radiate uniformly in the horizontal plane (i.e., source level independent of azimuth), the source levels differ somewhat between the left and right sides. Comparison of the relative sound levels between recorders for the Shallow Site scenarios (Figure 7-20) reveals that for the tracks sailed northward (Scenarios S5, S7, and S9) the levels at A1 (right of the source) are lower than at A2 (left of the source) by 1 to 2 dB for the same source-to-receiver range. For the tracks sailed southward (Scenarios S6, S8, and S10) the levels at A1 (left of the source) are lower than at A2 (right of the source) by 4 to 5 dB. The source levels on the right side of the EdgeTech 3200 SB-0512i sub-bottom profiler are 2 to 4 dB higher than on the left side.

7.4.3 Comparison of Operational Settings of the EdgeTech 3200 Sub-Bottom Profiler

7.4.3.1 Shallow Site

At the Shallow Site, the difference in per-pulse SEL between the operational settings of the EdgeTech 3200 SB-0512i sub-bottom profiler is less than 5 dB at the closest distance (25 to 40 m [66 to 131 ft] slant range; see Figure 7-23). This difference is more or less preserved to about 100 m (328 ft) slant range. Beyond 100 m (328 ft), the SELs differ more between scenarios. The highest transmission loss occurred for Scenario S8 (2 to 12 kHz, 20 ms, FM), and the lowest transmission loss occurred for Scenario S5 (0.5 to 2.7 kHz, 100 ms, FM). The lower frequency and longer pulse duration of Scenario S8 likely contributed to the higher received levels at longer distances. The average difference in the received levels between Scenarios S5 and S8 increases to approximately 15 dB at 1 km from the source and to more than 20 dB at 2.5 km (1.3 nm) from the source.

The rms SPLs, which also depend on the 90% energy pulse duration, T_{90}, follow the general trend of the SELs. There are small (approximately 5 dB) differences in the received levels between different pulse settings at small slant ranges (less than 80 m [262 ft]). The differences increase with slant range to approximately 20 dB at 1 km and approximately 30 dB at 2.5 km (1.3 nm).

7.4.3.2 Deep Site

At the Deep Site, the highest received SELs from the sub-bottom profiler were detected for Scenario D6 (1 to 6 kHz, 40 ms, FM). They are about 7 dB higher than for Scenarios D3 (0.5 to 8 kHz, 5 ms, FM) and D4 (0.5 to 4.5 kHz, 40 ms, WB). This difference increases to about 15 dB at 3 km (1.6 nm). The SEL trends differ more between pulse settings at the Deep Site than at the Shallow Site.

The rms SPLs have more scatter at the Deep Site than at the Shallow Site, mainly due to greater variation of the T_{90}. The difference between scenarios in the rms SPL at the CPA is about 12 dB. The scenarios with the shortest pulse length settings exhibit the highest rms SPLs.

The received SELs and rms SPLs are compared between the Shallow and Deep sites in Figures 7-38 and 7-39, respectively. On average, the received levels are higher for the Deep Site scenarios than for the Shallow Site scenarios within 200 m of the source, whereas the opposite is true beyond 300 m (984 ft) from the source. The difference in levels between Shallow- and Deep-Site scenarios within 200 m (656 ft) of the source can be related to the beam pattern of the profiler: at the Deep Site the illumination area of the main beam is greater. The higher received levels beyond 300 m (984 ft) from the source at the Shallow Site can be explained by the acoustic energy spreading over a smaller volume, as the water depth is half that of the Deep Site. Also, the greater difference in the rms SPL compared to SEL can be attributed to the smaller T_{90}: at the Shallow Site the distance between two reflectors (sea surface and the bottom) is smaller, and the reflected acoustic energy arrives closer to the direct path pulse effectively reducing the T_{90} of the overall pulse.

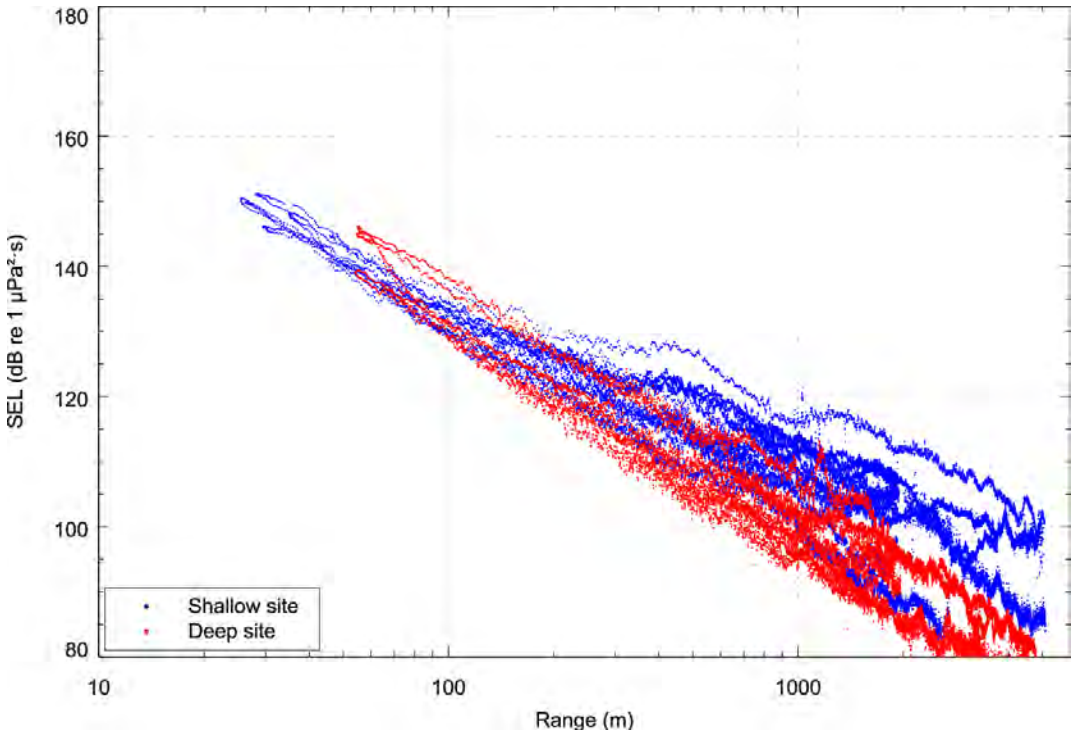

Figure 7-38. EdgeTech 3200 SB-0512i sub-bottom profiler. Comparison of sound exposure level (SEL) versus slant range between the Shallow Site and Deep Site scenarios.

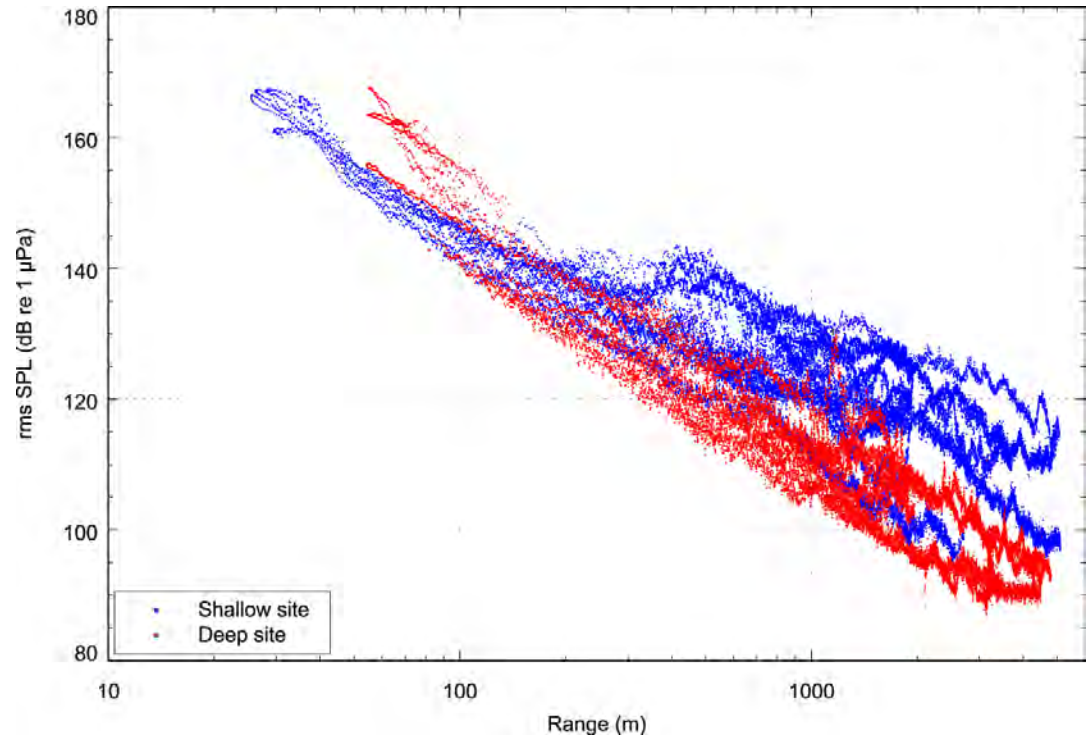

Figure 7-39. EdgeTech 3200 SB-0512i sub-bottom profiler. Comparison of 90% root-mean-square (rms) sound pressure level (SPL) versus slant range between the Shallow Site and Deep Site scenarios.

7.4.4 COMPARISON WITH MODEL RESULTS

In 2010, sound propagation modeling was performed for geophysical survey equipment at multiple sites in the Atlantic (Zykov et al. 2012). The modeling report was included as Appendix D in the *Atlantic OCS Proposed Geological and Geophysical Activities Mid-Atlantic and South Atlantic Planning Areas Draft Programmatic Environmental Impact Statement* by BOEM. The modeled Knudsen Chirp 3260 sub-bottom profiler is comparable to the EdgeTech 3200 SB-0512i sub-bottom profiler.

The Knudsen 3260 includes three transducers with resonance frequencies of 2.5, 12, and 200 kHz, respectively. The profiler was modeled operating all three transducers simultaneously with a combined source level of 225.2 dB_{rms} re 1 µPa @ 1 m (Table 7-16). The EdgeTech 3200 system has a lower source level of just 210 dB_{rms} re 1 µPa @ 1 m (Table 7-16). Compared with the estimated 50° to 80° for the EdgeTech 3200, at 30° the beamwidth of the Knudsen Chirp 3260 sub-bottom profiler modeled for the PEIS is much narrower.

Table 7-16.
Specifications for the modeled Knudsen Chirp 3260 and the measured EdgeTech 3200 SB-0512i sub-bottom profilers. The sound pressure levels (SPLs) are given in dB re 1 µPa @ 1 m, and the sound exposure levels (SEL) are given in dB re 1 µPa2•s @ 1 m.

Profiler	Frequency (kHz)	Beam	Power output (kW)	rms SPL	Peak SPL	SEL	Max. pulse duration (ms)	Total rms SPL
Knudsen Chirp 3260	3.5	Circular, 30°	3	222	225	210.1	64	225.2
	12	Rectangular, 26°×38°	3	222	225	210.1	64	
	200	Circular, 8°	0.5	215.2	218.2	191.2	4	
EdgeTech 3200	0.5 to 12	Circular, 19° to 130°	2	210	213	n/a	100	210

To compare the modeled and measured results, the sources must have similar specifications; therefore, the model results for the Knudsen Chirp 3260 sub-bottom profiler were re-processed with a new source level of 210 dB_{rms} re 1 µPa @ 1 m (3 ft; that of the EdgeTech 3200) and excluding the 12 and 200 kHz transducers. The model results were reported as maximum-over-depth (MoD) sound levels, i.e., the received level at a surface sampling location was taken as the maximum value that occurs over all samples within the water column below. For this comparison, the modeled received levels were instead taken at the depth of the recorder hydrophone, 3 m (10 ft) above the seafloor or 27 m (89 ft) below the sea surface.

The modeling was performed at multiple sites in the Mid- and South Atlantic. The results from modeled Scenario 22 were considered for the comparison because it has a water depth of 30 m (98 ft) and a sandy bottom, similar to the conditions at the Shallow Site. Figure 7-40 compares the measurements for the EdgeTech 3200 sub-bottom profiler for all the Shallow Site scenarios to the following model results for the Knudsen Chirp 3260 sub-bottom profiler:

- the MoD received levels from the original model results (i.e., the received levels from the 3.5, 12, and 200 kHz pulses combined with a combined source level of 225 dB_{rms} re 1 µPa @ 1 m);
- the MoD received levels for the 3.5 kHz pulses adjusted to a source level of 210 dB re 1 µPa @ 1 m to match that of the EdgeTech 3200; and

- the received levels at 27 m (89 ft) depth for the 3.5 kHz pulse adjusted to a source level of 210 dB re 1 µPa @ 1 m to match that of the EdgeTech 3200.

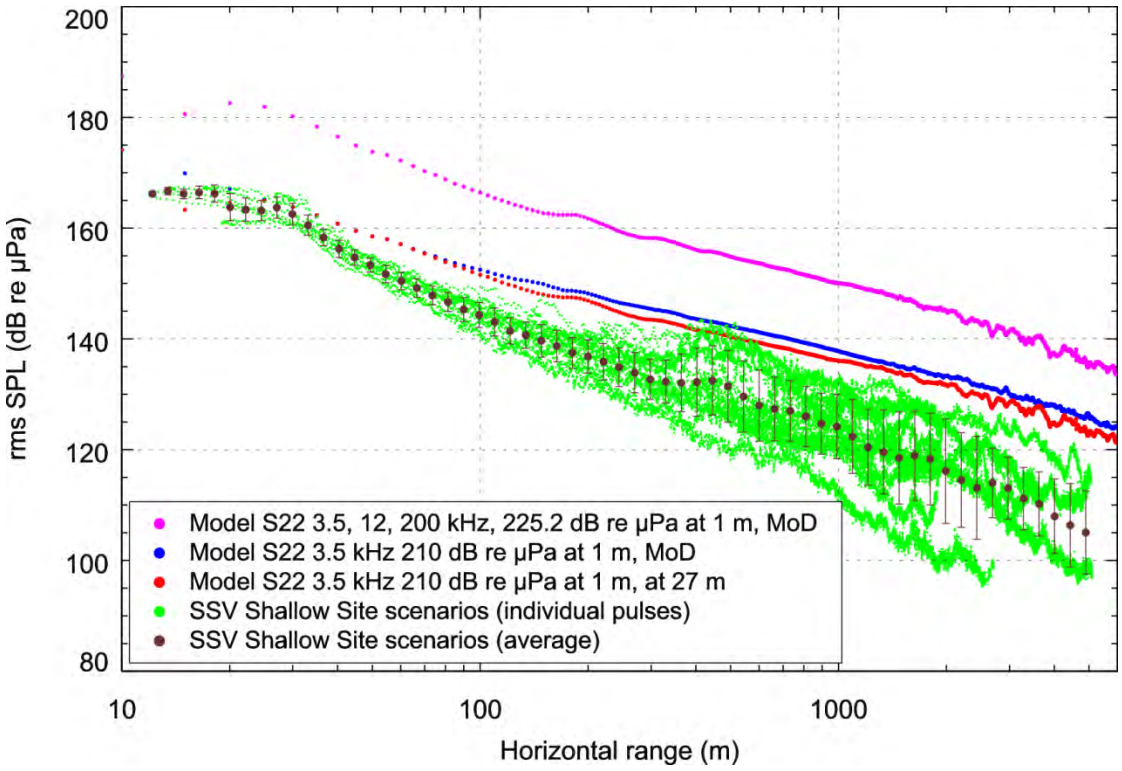

Figure 7-40. Sub-bottom profilers. Comparison of 90% root-mean-square (rms) sound pressure level (SPL) with horizontal range between the model results for the Knudsen Chirp 3260 (for various settings and depths) and the measurements of the EdgeTech 3200 SB-0512i (individual pulses and the average ± SD).

Figure 7-40 shows that the modeling provides conservative results, i.e., the observed received levels are below the model estimates with few exceptions. Table 7-17 compares the predicted and measured distances to sound level thresholds. The test scenario that exhibited the highest received levels during the field measurements (Scenario S5: 0.5 to 2.7 kHz, 100 ms, FM) was selected for the comparison.

The Knudsen Chirp 3260 sub-bottom profiler is designed for deep-water applications and can be operated at significantly higher source levels compared to other instruments of this type intended for shallow-water environment. The modeling results presented in the PEIS for the Knudsen Chirp 3260 sub-bottom profiler cannot be used directly for the impact assessment of other sources of this type, as it would provide significantly overestimated values. The results of this Sound Source Characterization study showed that after proper adjustment for the source level difference, the modeling results for the Knudsen Chirp 3260 sub-bottom profiler can be applied to other sub-bottom profiler sources.

Table 7-17.
Sub-bottom profiler, comparison with model results. Distances to 90% root-mean-square (rms) sound pressure level (SPL) thresholds based on the best-fit lines to 3200 SB-0512i measurements (Scenario 5) and the model results for the Knudsen Chirp 3260. The source levels (SL) are given in dB_{rms} re 1 µPa @ 1 m (3 ft).

90% rms SPL (dB re 1 µPa)	EdgeTech 3200 SB-0512i	Knudsen Chirp 3260		
	0.5 to 2.7 kHz, 100 ms, FM SL=210 dB	3.5 kHz SL=210 dB		3.5, 12 & 200 kHz SL=225.2 dB
	90th perc. fit	Rmax at 27 m	Rmax MoD	Rmax MoD
190	1	0	0	12
180	2	0	0	32
170	8	10	14	136
160	29	42	42	808
150	107	128	152	2863
140	397	662	778	6250
130	1472	3272	3570	12971
120	5461	9815	10777	>20000

The analysis presented in this report showed that the maximum sub-bottom profiler frequency spectrum is approximately at the middle frequency of the operational frequency band. The measured beam pattern closely matches the theoretical beam pattern at the middle frequency of the operational frequency band as well. These two facts support the modeling approach used in the PEIS, in which all the acoustic energy is assigned to a single frequency and the propagation modeling is performed for only that single frequency. In the acoustic modeling, propagation modeling is commonly performed for only the middle frequency of a frequency band (e.g., modeling central frequency of 1/3-octave bands). The variation of the propagation conditions for the acoustic waves of different frequencies within the sweep frequency band is negligible; therefore, the approach of performing propagating modeling for just a single frequency that carries the main characteristics of the source (source level and beam pattern) is valid.

7.4.5 RECOMMENDATIONS

JASCO suggests adopting the following procedures when operating the sub-bottom profiler and interferometric sonar to reduce the ensonification of the surrounding environment:

- use the highest frequency band possible for the sub-bottom profiler. The beam of the sub-bottom profiler is narrower at high frequency and therefore emits less acoustic energy toward the horizontal;
- while short pulses (5 to 20 ms) can result in higher rms SPLs than longer pulses, short-duration pulses have lower SEL and are perceived as less loud by mammals than long-duration pulses (Au and Hastings 2008); therefore, JASCO recommends using the shortest possible pulse length; and
- the Cumulative Sound Exposure Levels (cSEL) calculated over a specific period of the survey can be reduced by lowering the pulse rate (pings per second). Changes to the pulse rate do not affect rms SPL or SEL calculated over each pulse. The effect on the cSEL values can be estimated by the following formula: $\Delta cSEL = 10 \cdot \log(R/R_0)$, where $\Delta cSEL$ is the change in the cumulative SEL, R and R_0 are the desired and original pulse rates (number of pings per second) respectively.

The following are recommended for future sound source characterization measurements:

- for the sources with the beam pointing downward (e.g., the sub-bottom profiler) it is important to obtain data for the horizontal position of the source as close as possible to the recorder in order to obtain the measurement for the main lobe of the beam;
- there is no benefit of driving the source as close as possible to the recorder for the systems, which beams are pointing to the sides (e.g., the interferometric sonar). The received levels directly below the source will not be the maximum levels;
- more than two samples must be collected in the main beam for highly directive sources such as the interferometric sonar. More off-track recorders could be deployed or more test tracks could be used with various CPA distances. Choose a CPA range that ensures recorders receive at least one ping from the sonar's main-lobe;
- satisfactory results for omnidirectional in the horizontal plain sources (e.g., sub-bottom profiler, vessel) can be achieved with just two recorders. Detailed source characterizations require more data. Using only one recorder is not recommended; and
- the dynamic range of the recorders should extend at least 10 dB above the anticipated maximum received levels to ensure accurate assessment of peak sound levels.

7.5 CONCLUSION

The report provides the analysis results and findings of the sound source characterization data collected in Rhode Island Sound on 29 and 30 August 2012. Three acoustic noise sources were targeted: research vessel (R/V *SRVx*), interferometric sonar (SEA SWATH*plus*-M), and sub-bottom profiler (EdgeTech 3200 SB-0512i). The data were collected at two sites with different water depths (30 and 60 m [98 to 197 ft]) for the survey equipment operating at various settings. The variation of the per pulse SEL, 90% rms SPL, and peak SPL with distance was successfully established for ten measured scenarios of sub-bottom profiler and three scenarios of interferometric sonar. The beam patterns of the sub-bottom profiler and of the spectrum of the signal were successfully obtained. The most important findings are:

- for the sub-bottom profiler, the threshold distance to 160 dB re 1µPa rms SPL does not extend further than 100 m (328 ft) from the source for any measured operational settings or water depth;
- for the sub-bottom profiler, the threshold distances to 120 dB re 1µPa rms SPL tend to be larger in the shallower environment: generally 2.4 to 3 km in 30 m (98 ft) of water compared to 0.5 to 1.1 km (0.3 to 0.6 nm) in 60 m (197 ft) of water;
- for the sub-bottom profiler, the operational settings with a lower frequency band and a longer pulse produce greater threshold distances to 120 dB re 1µPa rms SPL: 5.5 km for 0.5 to 2.7 kHz band and a 100 ms pulse length compared to 2.4 to 3 km (1.3 to 1.6 nm) for higher frequency bands and a 20 to 40 ms pulse length;
- for the side to scan sonar, the threshold distances to 120 dB re 1µPa rms SPL in the endfire direction do not extend further than 200 m (656 ft) from the source and drop below the ambient noise levels at 300 to 400 m (984 to 1,312 ft) range;
- the frequency spectrum of the sub-bottom profiler has a bell-like shape with the maximum approximately at the middle frequency of the set frequency band; and
- the measured vertical beam pattern for the sub-bottom profiler fits the theoretical beam pattern calculated for the middle frequency of the set frequency band.

Unfortunately, due to very narrow beamwidth (approximately 0.5°) of the instrument, the broadside beam characteristics for the interferometric sonar could not be accurately measured.

CHAPTER 8

MAGNETIC SENSING FOR ARCHAEOLOGICAL RESOURCES

The following chapter on magnetic sensing for submerged archaeological resource identification was prepared by John Bright and David Conlin of the National Park Service Submerged Resources Center.

A secondary goal of the survey was to evaluate the capabilities of a marine magnetometer in terms of the detection of archaeological resources. This body of data formed the basis for reviewing BOEM's current standards for geophysical and archaeological survey in the *Guidelines*. Much of this assessment, however, required a conceptual review of the physical and mathematical principles underpinning magnetic remote sensing and, therefore, did not require as complex of a fieldwork component as the acoustic testing.

A Geometrics G-882 magnetometer was towed in tandem with the acoustic instruments and collected magnetic data throughout the WEA and over a known shipwreck outside of the WEA. The data from these surveys helped illustrate the importance of magnetic survey design on magnetic survey results.

This chapter provides an introduction to the theory of magnetism and magnetic sensing (in Section 8.2), followed by a discussion of how magnetic data are filtered and processed to determine the presence and location of magnetic objects within the survey area (See Section 8.3). These discussions are intended to illustrate the relationship between object mass and distance from sensor as the driving factor of an object's detectability, which in turn demonstrates the necessity of accounting for this relationship during the design of a given survey to ensure adequate coverage of an area. Factors affecting processing and interpretation of magnetic surveys are addressed in Section 8.4; in Section 8.5, factors affecting confidence levels are discussed. In Section 8.6, magnetometer surveys conducted on the WEA are compared with surveys over a known shipwreck site outside of the WEA. Recommendations for magnetometer surveys are provided in Section 8.7.

8.1 MAGNETIC SENSING OVERVIEW

Magnetic remote sensing is applied throughout a broad array of geophysical survey operations, including the search for submerged cultural materials. This type of remote sensing offers unique utility to archaeologists in its ability to detect ferrous objects and cultural material that may go undetected with acoustic systems. Specifically, ferrous objects embedded in or below the seabed, or those located on the surface amidst geological formations with enough relief to camouflage man-made objects, might escape detection with conventional acoustic survey systems. Yet, these objects are detectable through proper magnetic survey.

8.1.1 ACOUSTIC SENSING COMPARED TO MAGNETIC SURVEYS

Acoustic remote sensing provides visual output as it is acquired and requires relatively little processing to achieve a finalized dataset. In contrast, the output from a magnetic survey is tabular

data that requires mathematical and geospatial processing to create visual outputs. For this reason, the integrity of a magnetic survey relies upon careful survey design to ensure desired objects are detected and proper post-processing and visualization to ensure accurate depiction. Both require a proper understanding of the physical principles at work during data acquisition and processing.

Unlike sonar, where a particular frequency and swath width are set and survey tracklines are planned to ensure adequate overlap, magnetic systems do not have a set range or resolution, *per se*, that dictate survey planning in every case. Instead, the detectability of an object is a function of the object's mass, magnetic moment, and distance from the magnetic sensor, which must be quantified and accounted for in the survey design. Each of these factors are individually complex interactions of the metallic properties of the various ferromagnetic materials comprising an object, such as a shipwreck, as well as the interaction of larger scale forces on the earth's magnetic field. It is the composite of all these forces with the earth's ambient magnetic field that is being read by the magnetic sensor and must later be interpreted to determine the presence and location of potential cultural materials.

Thus, there are many variables within a magnetic survey of a given survey area. The necessity of data processing and visualization, furthermore, imposes specific limitation on magnetic surveys that must be recognized and managed.

8.1.2 LIMITATIONS OF MAGNETIC SURVEYS

The usefulness of magnetometer surveys is constrained by physical and human factors. Physical factors that can affect the usefulness of magnetometer surveys include the object's size, the distance between the sensor and the object, and the object's magnetic moment (force of the object's magnetic field). These physical parameters place quantifiable limitations on magnetic survey capabilities that can be mitigated through appropriate survey design.

Human factors also limit magnetic survey capabilities. Human factors manifest during data processing and during data interpretation and are less quantifiable than are physical limitations. These factors are managed through appropriate standards for the collection, processing, interpreting, and reporting of data.

These physical and human limitations can be overcome, for the most part, with the appropriate magnetic survey management requirements. Physical limitations can be handled through the use of correct survey trackline spacing, sensor altitude (height off bottom) and careful data management to preserve data integrity when processing data from marine magnetic surveys.

These additional considerations speak to possible revisions of BOEM's *Guidelines for Providing Geological and Geophysical, Hazards, and Archaeological Information Pursuant to 30 CFR Part 285*, as well as the standards for the presentation of magnetic data in survey reports (see Chapter 9).

8.2 THEORY OF MAGNETIC SENSING TO DETECT ARCHAEOLOGICAL MATERIAL

Local disturbances in the earth's magnetic field are caused by the presence of ferromagnetic objects, like geological formations and certain cultural materials. These disturbances can be detected and

used as a means to locate these objects, given that the survey is adequately designed to detect them. This section provides a brief background discussion of magnetic fields, magnetic field disturbances, and how disturbances are detected.

8.2.1 Nature of Magnetic Fields

Magnetism is measured as the force of magnetic intensity generated between the poles of an object. Much like a locomotive (i.e. moving) force, magnetic force has a magnitude and direction. Generally, magnetic force moves parallel to the axis of the object's magnetic poles, varying in intensity depending upon distance from the poles. The origin of magnetic fields, however, is quite dissimilar between the earth and relatively smaller objects. Whereas the earth's magnetic field is generated from circulating electric currents at the planet's core, smaller objects gain magnetism through specific elemental properties inherent in the material's formation, as well as through interaction with other magnetic fields, chiefly the earth's (Ingham 1975, Weymouth 1976, Breiner 1999a, 1999b).

8.2.2 Magnetic Field of the Earth

Earth's magnetic field is generated by circulating electrical currents at the planet's core that produce a geomagnetic field between the planet's polar axis. The earth's magnetic field behaves in a predictable manner, conforming to various physical laws that occur in predictable cycles (Ingham 1975, Weymouth 1976, Breiner 1999a, 1999b).

The earth's ambient magnetism, essentially the 'background' of a magnetic survey, is not a constant force. Instead, it is in a constant state of flux through time and space. Large geological substrates and certain materials in earth's crust, as well as the cyclic interaction of solar and lunar forces, cause the earth's ambient magnetic field to constantly, though predictably, vary.

Measurements of ambient magnetism in a given area, therefore, vary significantly over periods of hours, days, and years; what is referred to as secular and diurnal variation. Secular variation originates from the shifting forces within the planet's core that generate the field, and occur on the scale of years. Interactions with solar and lunar forces, mainly the impact of charged particles broadcast by the sun against the earth's atmosphere, are responsible for daily diurnal changes in the intensity of the ambient magnetic field.

Irregularity also exists when measuring the magnetic field over large distances, independent of time. The strength of magnetic force between poles is not constant. Instead, differing latitudes will experience different levels of magnetic force. The presence of magnetic geological substrates, which can span large areas, also creates spatial variability. Therefore, though earth's magnetic field can be accurately measured, naturally occurring forces introduce wide variability into observed magnetic data through space and time (Ingham 1975, Weymouth 1976, Breiner 1999a, 1999b).

8.2.3 Earth's Magnetic Field Variation and Cultural Anomalies

Geologic formations also can locally distort the earth's magnetic field. Detecting archaeological materials amidst the background of secular, diurnal, and geologically induced variation is possible due to the differences in the scale of magnetic intensity and duration between them. That is to say,

iron or other magnetic cultural materials are small, comprised of concentrated magnetic substances, and therefore induce high-intensity variations over short durations. Geological variation may produce a magnetic shift on the order of tens to hundreds of gammas, but these shifts occur over miles and are usually observed as gradual changes. Similarly, diurnal and secular variations occur through the span of days and years, respectively, on the order of tens of gammas. In contrast, magnetic cultural materials can exhibit flux from tens to hundreds, if not thousands of gammas, depending on size. These changes, furthermore, happen in the span of tens of meters, or over hundreds of meters for very large magnetic objects. Thus, the characteristic signature of cultural material which distinguishes it from other forms of natural variation is high-intensity magnetic flux over short distances (Ingham 1975, Weymouth 1976, Breiner 1999a, 1999b).

8.2.4 INDUCED AND REMNANT MAGNETISM

The magnetic field of the earth and that of a small magnetic object are essentially the same in their basic behavior. Small objects manifest two types of magnetism at varying degrees: induced and remnant.

8.2.4.1 Induced Magnetism

Induced magnetization is described as:

> …the combined effect of a magnetic property of the material (permeability), the earth's magnetic field, and the shape and orientation of the object in the earth's magnetic field. If the magnetic permeability (or a related property called magnetic susceptibility) is very high, the material is described as being ferromagnetic….these factors cause the material to act as a magnet in the presence of the earth's magnetic field; [which is] a stronger magnet (Breiner 1999b:3).

In short, a susceptible object, when in the presence of the earth's magnetic field, will take on a magnetic field of its own. The amount of susceptibility varies between materials. Furthermore, "the shape and orientation of an object also tends to enhance induced magnetism; the longer the object and more nearly parallel to the earth's magnetic field, the stronger the magnet" (Breiner 1999b:3).

8.2.4.2 Remnant Magnetism

Remnant, or permanent magnetization, on the other hand, exists independent of any applied magnetic field. Instead, this form of magnetization results from forces applied during the formation of a particular material, forces such as heat and the alignment and intensity of earth's magnetic field at the time, which could be millions of years ago. Heat in particular can also cause an object to lose its remnant magnetization—a fact that accounts for the theoretical detectability of ceramic materials, such as pottery, by a magnetometer. Therefore, the level of remnant magnetization will be unique for any given substance. Nevertheless, permanent magnetization can exert a magnetic force an order of magnitude stronger than induced magnetization. As a result, permanent magnetism "…sometimes represents the predominant magnetic property useful in searching for such an object" (Breiner 1999b:3). Modeling and predicting permanent magnetism for a cultural object, however, can be considerably difficult since its specific formational history dictates the level of permanent magnetization the object retains; different substances obtain and retain permanent magnetism to varying degrees.

8.3 DETECTING MAGNETIC ARCHAEOLOGICAL RESOURCES IN MAGNETIC FIELDS

When seeking to locate submerged magnetic archaeological resources, it is necessary to design the survey so that the right amounts and types of information are collected. First, it is necessary to identify the types of items you are seeking. A survey that is seeking to locate a 100,000 US ton steel vessel in shallow water is designed differently than a survey seeking small pieces of iron in deep water.

This section discusses the factors that affect survey design, including:

- the predicted size of the archaeological objects of interest;
- the predicted magnetic field anomaly produced by the archaeological artifacts being sought;
- the effect of the sensor's proximity (survey trackline width and sensor height) on detection; and
- the certainty of unintentional deviations in survey lines.

8.3.1 CALCULATING GAMMA VALUES USING THE NPS ESTIMATED CONSTANT

It is possible to predict the observable magnetic flux (anomaly) produced by a given object. The most basic relationship to model is an object's induced magnetism, as observed in gauss and converted to gammas. This relationship assumes the object is "a concentrated mass of iron, all of whose dimensions are shorter than its distance to the magnetometer [and therefore] behave as a magnetic dipole" (Breiner 1999b:7). This relationship describes that:

> the magnetic anomaly for such an object would vary inversely as a cube of the distance between the magnetometer and the object, and directly with the weight of the ferromagnetic object, i.e.,
>
> $$T = \frac{M}{r^3}$$
>
> where T is the anomaly in gauss (1 gauss = 105 gammas), M is the dipole moment [a derivative of magnetic susceptibility] in cgs [centimeter-gram-seconds] units and r is the distance in centimeter (Breiner 1999b:7).

Converting between gauss and gammas is a simple scalar function, as are converting distance from centimeters to ft or m. Magnetic moment is a constant for a given material described per unit mass. In the equation above, grams are used; a simple scaling factor converts to kilograms or pounds. The actual constant, however, varies depending on the substance. Briener (1999b:7) states that "for such discrete objects made typically of iron or steel, the magnetic moment, M, is between 10 and 100 cgs units per ton."

As a basis for modeling the magnetic moment of submerged cultural materials, a constant of 14.4 cgs units has consistently proven useful during several years of experimentation conducting magnetometer surveys in National Parks. It is a conservative estimate of the moment of ferrous materials, and therefore prevents over-estimation of predicted anomaly size (i.e. it is a worst-case scenario for the anticipated magnetic moment of cultural materials), and is also generally accurate at predicting anomaly size of objects that are only partly ferromagnetic, such as a wooden shipwreck with iron fasteners and rigging. The resulting equation, adjusted for more helpful units, is:

$$\gamma = \frac{((kg*.001)*14.4^5)}{(r*.01)^3} \quad *10^5$$

where γ is gammas, mass is in kg, and distance, r, is in cm. Thus, a 1,000 kg (1.1 US ton) iron object 5 cm (2 inches [in]) from the magnetic sensor should give an induced magnetic anomaly (deviation from ambient) of approximately 495 gammas.

Applying this equation across a broad range of archaeological material shows how survey design should be modified to accommodate objects of varying sizes. Using the equation above with the estimated constant from NPS, the magnetic anomaly (in gammas) of an object can be calculated, based on the size of the ferrous object being sought, and its distance from the sensor.

8.3.2 Effect of Predicted Object Size on Detectability

Object size has a pronounced effect on detectability. Smaller iron or steel objects will generate smaller magnetic anomalies than larger ones. It is possible to calculate the expected magnetic anomaly size for a given archaeological objects based on known factors, such as the amount of iron and steel the object is likely to contain.

Objects of various masses are evaluated in terms of their predicted γ anomaly values in Tables 8-1 and 8-2. In both tables, the offset (half of the survey trackline spacing) stays constant at 15 m (49 ft). The differences are in sensor height and in object mass. Both tables show that, as object mass increases, gamma values increase. In addition, a comparison between similar-sized objects in the two tables shows that, as distance from the sensor increases, gamma values decrease sharply.

Thus, modeling the predictability of magnetic material according to this equation shows that some small objects may not be detectable with a magnetometer. In particular, small Paleoindian and Archaic period artifacts may be very difficult, if not impossible to locate. Artifacts typical of the precontact period—stone and bone tools, as well as organic materials—have a theoretical magnetic moment, though it is so miniscule that these objects are not actually detectable in the offshore environment with a marine magnetometer. This is due to two factors. First, the size of the objects themselves and second the anticipated Holocene overburden separating them vertically from the surface. Thus, though they may be identified in a terrestrial environment with the appropriate instrument, artifacts from the precontact period would not be detectable in the offshore environment with a marine magnetometer, regardless of trackline spacing utilized.

8.3.3 Effect of Survey Trackline Spacing on Detectability

When comparing Table 8-2 with Table 8-1, note the reduction in predicted anomaly size for these objects despite reducing the sensor altitude. In fact, many of the anomalies listed in Table 8-1 would not be detectable at the survey trackline spacing in Table 8-2 because the gamma values are of the same magnitude as the normal background noise of most commonly used magnetometers, 1-2 gammas. In Table 8-2, the 1,000 kg (1.1 US ton) object produces a magnetic anomaly of 286.65 gamma when sensor the passes directly over it, but only 3.64 gamma when the sensor passes 25 m (82 ft) to its right or left in a 50 m (164 ft) survey trackline spacing.

Noting the minimum standards listed in BOEM's (2012) *Guidelines* require a maximum survey trackline spacing of 30 m (98 ft) and a towfish altitude of no more than 6 m (20 ft). Yet, at these

distances, these data suggest smaller material culture items would not likely be detected by a magnetometer.

Table 8-1.
Predicted anomaly sizes for various maritime-related objects using 30 m (98 ft) survey trackline spacing.

Object	Mass (kg)	Sensor Alt (m)	Offset (m)	γ
Compound Steam Engine (588 lb)	267	6	15	3.92
Wright R-1820-40 Cyclone Radial Engine (0.6 US ton)	537	6	15	7.89
18th cent. Iron 4 pounder (0.63 US ton)	572	6	15	8.40
Small 3x Expansion Engine (1.05 US ton)	952	6	15	13.98
Wright R-3350 Duplex Cylone Radial Engine (1.34 US ton)	1212	6	15	17.80
Small (4th bower) 17th Cent. Anchor (1.4 US ton)	1270	6	15	18.65
CFM56-3B-2 Jet Engine 2.15 US ton)	1950	6	15	28.63
18th cent. Iron 24 Pounder 2.4 US ton)	2177	6	15	31.97
18th cent. Iron 42 Pounder (2.77 US ton)	2511	6	15	36.87
Large 17th Century Anchor (3.085 US ton)	2794	6	15	41.03
Large Admiralty Bower (4.54 US ton)	4115	6	15	60.43
Large Water Tube Boiler (4.83 US ton)	4386	6	15	64.41
Early Stockless Anchor (10.64 US ton)	9652	6	15	141.73
Large 3x Expansion Engine (16.07 US ton)	14582	6	15	214.13
600 ft. (182 m) Anchor Chain (18.25 US ton)	16561	6	15	243.19
Modern Stockless Anchor (20 US ton)	18143	6	15	266.42
Single-End Scotch Boiler (40 US ton)	36287	6	15	532.85
Note: Distances are calculated from the hypotenuse of a 6 m (20 ft) sensor altitude and 15 m (49 ft) offset from the survey tracklines. Predicted anomaly is in gamma (γ).				

Table 8-2.
Difference in predicated anomaly size between 1000 kg (1.1 US ton) iron object resting exactly between two survey tracklines and a sensor passing directly over the object..

Survey Line Spacing	50 m		30 m		20 m		15 m	
Object Offset from Survey Trackline	25 m	0 m	15 m	0 m	10 m	0 m	7.5 m	0 m
Gamma	3.64	286.65	14.68	286.65	39.04	286.65	69.88	286.65

Adjusting survey parameters by bringing the survey trackline spacing closer and reducing sensor altitude makes many smaller ferrous objects theoretically detectable. Tables 8-3 and 8-4 show the difference in the calculated gamma values for small maritime cultural objects when detected by a magnetic survey with a survey trackline spacing at 30 m (98 ft) (the maximum in the BOEM standard) and at 20 m (65 ft). The sensor altitude was kept at 3 m (10 ft). In this case, the gamma values for six of the eleven objects was greater than background noise at a 30 m (98 ft) spacing, so they would be theoretically detectible, yet many of the small objects would still escape detection.

Table 8-3.
Predicted anomaly sizes for smaller maritime-objects using 30 m (98 ft) survey trackline spacing.

Object	Mass (kg)	Sensor Alt (m)	Offset (m)	γ
Iron Projectile (3 lb)	1.3	3	15	0.02
Historic Long Gun (12 lb)	5.4	3	15	0.09
Iron Projectile (24 lb)	10.8	3	15	0.19
Iron Projectile (42 lb)	19.1	3	15	0.33
Iron object (100lb)	45.3	3	15	0.78
100 ft 1-inch Iron Rigging Wire (1.5lbs/ft) (150 lb)	68	3	15	1.18
Iron object (250 lb)	113.3	3	15	1.96
Iron object (500 lb)	226.7	3	15	3.92
100 ft 2-inch Steel Hawser (6.2lbs/ft)	281	3	15	4.86
Iron object (750 lb)	340.19	3	15	5.88
Iron object (1500 lb)	680.3	3	15	11.77
Notes: Distances are calculated from the hypotenuse of 3 m (9.8 ft) sensor altitude and 30 m (98 ft) survey trackline spacing. Anomalies are given in gammas (γ).				

Table 8-4.
Predicted anomaly sizes for smaller maritime objects using 20 m (65 ft) survey trackline spacing.

Object	Mass (kg)	Sensor Alt. (m)	Offset (m)	γ
Iron Projectile (3 lb)	1.3	3	10	0.07
Historic Long Gun (12 lb)	5.4	3	10	0.29
Iron Projectile (24 lb)	10.8	3	10	0.59
Iron Projectile (42 lb)	19.1	3	10	1.04
Iron object (100lb)	45.3	3	10	2.46
100 ft 1-inch Iron Rigging Wire (1.5lbs/ft) (150 lb)	68	3	10	3.70
Iron object (250 lb)	113.3	3	10	6.16
Iron object (500 lb)	226.7	3	10	12.33
100 ft 2-inch Steel Hawser (6.2lbs/ft)	281	3	10	15.29
Iron object (750 lb)	340.19	3	10	18.51
Iron object (1500 lb)	680.3	3	10	37.01
Notes: Distances are calculated from the hypotenuse of 3 m (10 ft) sensor altitude and 20 m (65 ft) survey trackline spacing. Anomalies are given in gammas (γ).				

The effect of using an even narrower survey trackline spacing (8 m [29 ft]) and lower sensor height (1 m [3 ft]) is shown in Table 8-5. These values were selected to show a sensor altitude and survey trackline spacing which makes every object theoretically detectable. The feasibility of such tight survey pattern is discussed further in Section 8.7, yet the theoretical threshold of detection for a very small ferrous object requires the magnetometer to pass almost exactly over the object.

At the other end of the spectrum, when examining very large magnetic objects, such as entire ferrous shipwrecks, a dense survey design is not necessary. Table 8-6 shows the predicted anomalies for large shipwrecks using 30 m (98 ft) survey trackline spacing and an altitude of 6 m (20 ft). If one

was seeking these objects of this size, expanding the survey trackline spacing outward would allow a much wider survey to be conducted with relative assurance of locating these large objects.

Table 8-5.
Survey parameters adjusted to make every object theoretically detectable.

Object	Mass (kg)	Sensor Alt. (m)	Offset (m)	γ
Iron Projectile (3 lb)	1.3	1	4	1.15
Historic Long Gun (12 lb)	5.4	1	4	4.77
Iron Projectile (24 lb)	10.8	1	4	9.54
Iron Projectile (42 lb)	19.1	1	4	16.87
Iron object (100lb)	45.3	1	4	40.02
100 ft 1-inch Iron Rigging Wire (1.5lbs/ft) (150 lb)	68	1	4	60.07
Iron object (250 lb)	113.3	1	4	100.08
Iron object (500 lb)	226.7	1	4	200.26
100 ft 2-inch Steel Hawser (6.2lbs/ft)	281	1	4	248.22
Iron object (750 lb)	340.19	1	4	300.51
Iron object (1500 lb)	680.3	1	4	600.95
Note: Anomalies measured in gammas (γ).				

Table 8-6.
Predicted anomaly sizes for larger maritime-related objects using 30 m (98 ft) survey trackline spacing.

Object	Mass (kg)	Sensor Alt. (m)	Offset (m)	γ
Norman Fishing Vessel (400 US tons; 50 of Iron	45359	6	15	666.06
Frigate *Boston* (514 US tons; assume 64 of iron)	58059	6	15	852.55
HMS *Victory* (2162 US tons; assume 250 of iron)	226796	6	15	3330.33
WWII Type VIIC U-Boat (860 US tons)	780179	6	15	11456.34
USS *Monitor* (987 US tons)	895391	6	15	13148.14
City of Glasgow (1609 US tons)	1459660	6	15	21434.01
WWII *Fletcher* Class Destroyer (2500 US tons)	2267962	6	15	33303.32
HMS *Warrior* (9137 US tons)	8288947	6	15	121716.95
HMS *Dreadnought* (10,886 US tons)	9875613	6	15	145015.95
USS *Enterprise* (19,875 US tons)	18030297	6	15	264761.35
SS *America* (33,532 US tons)	29937096	6	15	439603.73
Notes: Distances are calculated from the hypotenuse of a 6 m (20 ft) sensor altitude and 30 m (98 ft) survey trackline spacing. Anomalies measured in gammas (γ).				

Table 8-7 shows the predicted anomaly sizes with 100 m (328 ft) survey trackline spacing and a sensor altitude of 10 m. Even within these parameters, the vessels larger than 1,814 metric tons (2,000 US tons) yield large induced magnetic flux. Wider survey design would likely be able to locate these types of sites, but obviously at the cost of detecting smaller items.

Table 8-7.
Predicted anomaly sizes for ship-sized objects using 100 m (328 ft) survey trackline spacing.

Object	Mass (kg)	Sensor Alt. (m)	Offset (m)	γ
Norman Fishing Vessel (400 US tons; 50 of Iron)	45359	10	50	21.18
Frigate Boston (514 US tons; assume 64 of iron)	58059	10	50	27.12
HMS Victory (2162 US tons; assume 250 of iron)	226796	10	50	105.92
WWII Type VIIC U-Boat (860 US tons)	780179	10	50	364.37
USS Monitor (987 US tons)	895391	10	50	418.18
City of Glasgow (1609 US tons)	1459660	10	50	681.72
WWII Fletcher Class Destroyer (2500 US tons)	2267962	10	50	1059.22
HMS Warrior (9137 US tons)	8288947	10	50	3871.26
HMS Dreadnought (10,886 US tons)	9875613	10	50	4612.29
USS Enterprise (19,875 US tons)	18030297	10	50	8420.84
SS America (33,532 US tons)	29937096	10	50	13981.77
Notes: Distances are calculated from the hypotenuse of a 10 m (32.8 ft) sensor altitude and 100 m (328 ft) survey trackline spacing. Anomalies are measured in gammas (γ).				

Encompassing the spectrum from small Native American artifacts and maritime material culture, to large steel-hulled ships, this predictive modeling demonstrates the need to understand the relationship between object mass, magnetic moment, and proximity to the detection sensor in order to design a proper survey. The main implication, therefore, is that survey design is a function of anticipated finds. Were the goal of a survey to locate large ferrous shipwrecks, a survey trackline spacing of 100 m (328 ft) and sensor altitude of 10 m (32.8 ft) would be more than sufficient. Locating small artifacts, such as an historic anchor, on the other hand, would require 20 to 30 m (65 to 98 ft) survey trackline spacing and a sensor height of no more than 6 m (20 ft), with tighter survey trackline spacing and sensor closer to the bottom being preferable. Smaller artifacts, such as an historic barrel, or small personal items, would require an even tighter design.

8.3.3.1 Survey Trackline Spacing and Sensor Height versus Detection

Extrapolating predicted anomaly sizes for various sized objects at varying distances reveals the powerful effect of proximity to strength of detection. Breiner (1999a, 1999b) described this relationship as an inverse cube, meaning that for a single unit change in distance, measured magnetic flux changes by an exponent of three. Table 8-1 (above) depicts various maritime-related objects, showing their masses, distance from the magnetometer sensor, and predicted anomaly size in gammas. For this calculation, distance was given as the hypotenuse (also called slant line) of sensor altitude and the object's distance from the survey trackline (see Figure 8-1).

Several important associations are represented in this diagram. First, the positioning of the object is exactly between the two planned survey lines. In any given survey design, the worst case scenario would be an object which rests exactly between two survey lines; as far as possible from each adjacent sensor pass. Given that observed intensity of magnetic flux decreases as a cube function of

distance, the area between lines represents the position where an object will yield minimum possible return.

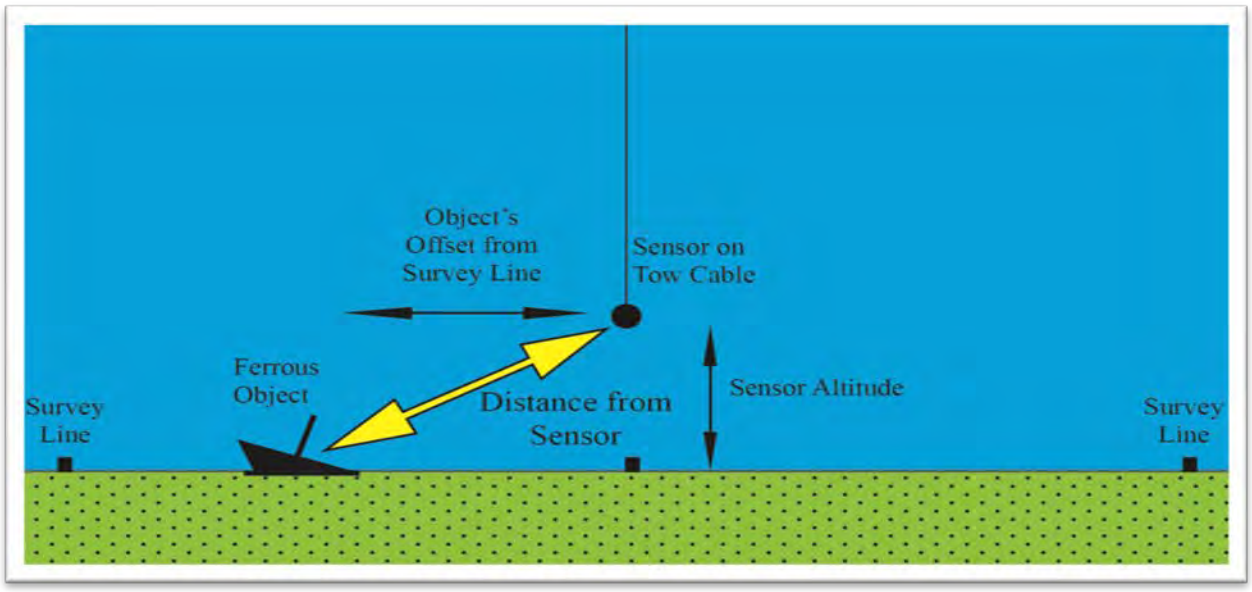

Figure 8-1. Diagram showing the relationship of sensor altitude and object offset from survey trackline as related to the object's distance from the magnetometer. Actual distance is hypotenuse of offset and sensor altitude (source: J. Bright, NPS-SRC).

Table 8-2 (above) depicts the difference in predicted anomaly size when a 1,000 kg (1.1 US ton) object rests exactly between two adjacent survey lines versus the sensor passing directly overhead. Therefore, the model generates predictions assuming that every object is exactly between planned survey lines, the worst case scenario.

In addition to the object's offset from the survey line, the altitude of the sensor, also factors into the sensor's distance from the object. The higher the sensor, the farther from an object, regardless of whether the object is offset or directly on the path of the survey line; and the closer the sensor to the bottom the closer it will be to magnetic objects. Thus, the sensor altitude showed also factor into survey planning. Though variations in bottom topography make maintaining a constant sensor altitude difficult in certain areas, as well as the fact that certain makes of magnetometer are not equipped with an altimeter or depth sensor, the survey operator is ultimately in control of the towfish's depth and the model, therefore, assumes consistent altitude.

The distance between the sensor and the object detected is also affected by variations in survey trackline spacing caused by sea conditions. Wind and currents inevitably cause the ship to drift off course slightly during a survey. These deviations are not predictable and their magnitude is only evident during post-processing, but deviations from survey trackline spacing can have a significant effect on the detectability of an object. This factor is related both to magnetic survey design and the confidence placed in the final survey results. A detailed discussion of deviations from survey lines is found in Section 8.5.2.

8.3.3.2 Effects of Induced and Remnant Magnetic Fields

Induced magnetism is that created when a magnetically susceptible object is placed within another magnetic field (such as when a magnet is touched to an iron nail and this reorients the nail's magnetic flux to that of the magnet). The result is a localized field parallel to that of the inducing field, which would yield a nearly identical observed magnetic trace to a magnetometer.

Remnant magnetism, on the other hand, exists independently of an inducing force, and is oriented parallel to the magnetic poles of the object. When an object is heated beyond a certain temperature, the magnetic molecules of that object orient themselves in accordance to the magnetic field that surrounds that object at the time (e.g., iron, steel or pottery in a furnace or kiln). When these objects are removed from their place of creation, their remnant magnetism is usually oriented differently from that of the new ambient field in which the object resides. Should these poles rest at an angle askew to earth's ambient field, they create a complex interference pattern with one another. Similar to the interaction of electromagnetic radiation, the convergence of magnetic forces of different magnitude and directions results in a sort of vector addition. The portion of the object's magnetic field oriented antiparallel to Earth's magnetic field will create a local reduction, whereas the portion oriented parallel will have an additive effect to the local field. If every observed magnetic field were parallel to earth's, then the shape of the magnetic flux would be the same, with only the amplitudes varying according to object size and distance from sensor. Figure 8-2, however, demonstrates the effect of a remnant field an angle askew to earth's magnetic field. The resulting observed trace is the combination of magnetic force vectors from both fields which produces an uneven flux.

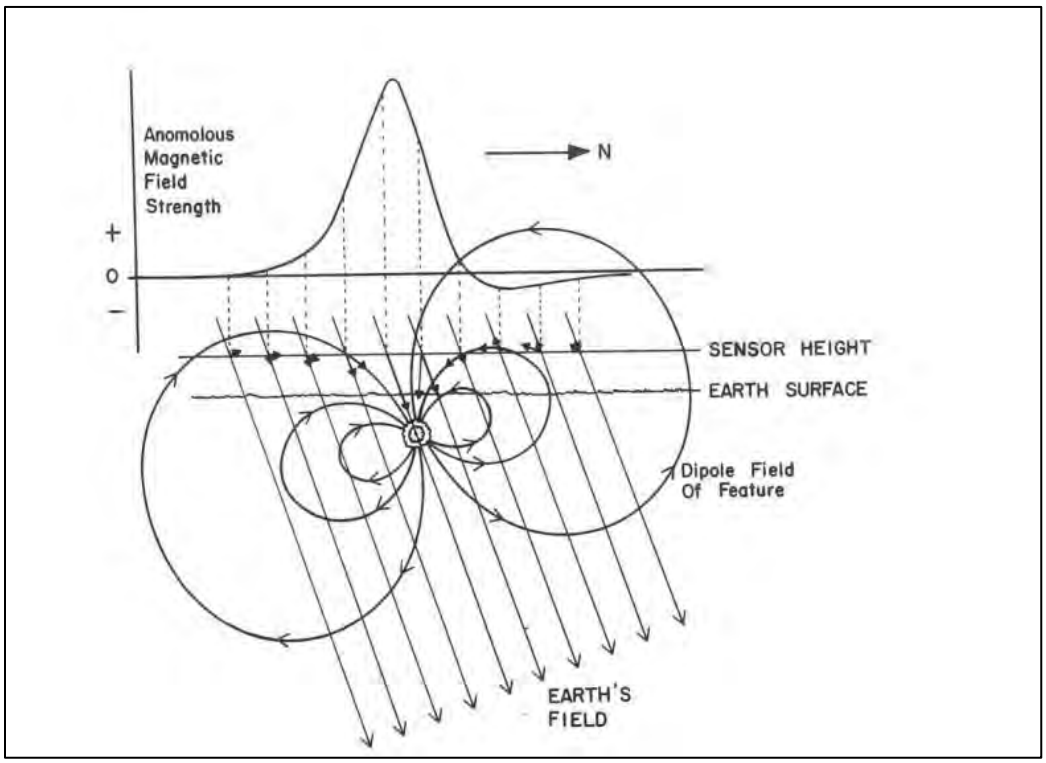

Figure 8-2. Diagram depicting interaction of earth's magnetic field with ferromagnetic object showing the constructive and destructive interference of fields which result in an observed dipole (Source: Weymouth 1976:7).

As was previously stated, this model does not account for the effects of remnant magnetism when predicting the amplitude of an observed anomaly. As Breiner (1999b:) noted, for a given ferromagnetic object the remnant magnetism is often much stronger than its induced field, by as much as an order of magnitude. Yet, since the amount of remnant magnetism is dependent upon the formation and metallurgic history of a substance, it is much more difficult to predict. Nevertheless, by modeling only for induced magnetic flux, the model essentially underestimates the actual observed flux, which ensures a form of redundancy similar to overlapping acoustic survey tracklines. Though it is not incorporated into the model, however, remnant magnetism does conspicuously manifest in the data record.

Using the magnetic moment equation (described in Section 8.3.1 above) as the basis for predicting the detectability of various sized objects allows for methodical survey planning, as opposed to arbitrarily designated survey trackline spacing and sensor height. Understanding the physical relationships underlying magnetic properties enables the surveyor to account for the limitations of the survey system and to customize the parameter for the desired results.

8.4 PROCESSING OF MAGNETIC SURVEY DATA

Survey design is only one of many components to an effective survey. Once data are collected in accordance with the planned parameters, the manner in which the data are processed is equally important to ensuring proper coverage and interpretation. Thus, a discussion of magnetic data processing is necessary.

Interpreting the magnetic data record in real time, as the magnetic trace develops across the user interface, is a difficult and learned skill which requires the user to understand the function of object size, shape, and distance on the formation of monopoles and dipoles (Briener 1999a), yet it is nearly impossible to view the magnetic landscape across an entire survey area by simply looking at the raw data. Rather, the real work of interpreting magnetic data takes place during data processing. The results of data processing form the basis for identifying anomalies, identifying archaeological material, and disseminating the data set to interested parties.

Multiple data processing methodologies exist. The choice of methodology depends mainly on data format and software, as well as user preference for certain processing operations. Nevertheless, the mathematical principles underlying magnetic data processing are fairly ubiquitous. Thus, the present discussion addresses these principles more hypothetically than specifically to any hardware/software platform.

8.4.1 PRIMARY MATHEMATICAL PROCESSES USED ON MAGNETIC SURVEY DATA

The three main types of mathematical operations used with magnetic survey datasets are terrain modeling, interpolation, and gradient processing.

8.4.1.1 Terrain Mapping

Terrain mapping is perhaps the least complex of the mathematical operations used on magnetic datasets. Also known as terrain modeling, the process involves one of several geospatial functions to construct a terrain model, using magnetic readings as elevation values, thus creating a visual

magnetic 'landscape.' Whereas interpolation and gradient processing filter data through an algorithm, terrain modeling translates raw magnetic data into a three-dimensional surface. A well-suited version of terrain modeling involves building a Triangular-irregular network (TIN). TIN modeling provides a quick means of generating an unfiltered spatial output. Yet, it is also not totally accurate. Since each triangular node is an actual data point and no interpolation occurs to solve for magnetic intensity between points, the TIN therefore fails to capture the true nature of the local field. Instead, the TIN will only render based upon the data gathered, thus if the sensor did not pass through the highest or lowest point of magnetic flux, the TIN model will not accurately represent the size of the anomaly. Nevertheless, it is an efficient means to model raw magnetic data, and to locate cultural materials on the seafloor.

The TIN model uses measured magnetic field strength as an elevation value where each individual reading serves as a node. The matrix of nodes is connected via an overlapping network of triangles as shown in Figure 8-3. When color-coded for gamma values, as in Figure 8-3, the two-dimensional representation also reveals a conspicuous local variation. When viewed three dimensionally, as in Figure 8-4, the terrain map reveals the large dipole created by the presence of a shipwreck at this location.

The surface of the TIN also serves as the basis for drafting contour lines; a more traditional means of viewing magnetic data (see Figure 8-5). Each contour line serves as an isoline of a user-determined gamma level in the same manner as a traditional contour map uses isolines of altitude to denote topographical changes in a particular area. Thus, if the user specifies contouring along a 10 gamma interval, each isoline will represent a change of 10 gammas. Similarly, if the contouring is specified along a 20, 50, 100, or 200 gamma interval, the visual output will be represented at these respective intervals

8.4.1.2 Interpolation

Another mathematical operation used with magnetic data is interpolation, which is one of the most common methods used. This process uses a distance-weighted algorithm to infer magnetic field strength between the known data points.

Interpolation does a more effective job than terrain mapping at rendering the true shape of the magnetic field. Many different formulas for interpolation exist, but all have a similar function. That is, "all interpolation algorithms…estimate the value at a given location as a weighted sum of data values at surrounding locations" (Bohling 2005:3). The most commonly used interpolation function for magnetic data is kriging. Developed for geophysical sampling, kriging is ideal for remote sensing by mitigating the effects of data clustering by decreasing the weighting assigned to points within a cluster, such as a survey tracklines, while still performing a distance-based function (Bohling 2005).

When performed as a geospatial operation, kriging results in a continuous raster surface representing the magnetic field in a given area. Since each point in the surface is generated as a weighted function of surrounding known points, the surface is a much more accurate representation of overall magnetic levels within the survey area, as opposed to the TIN model. Figures 8-6, 8-7 and 8-8 show the kriging output generated from the Buzzards Bay dataset at a 10-gamma, 50-gamma, and 200-gamma contour interval, respectively. Rendering the raster image in color reveals the same large anomaly

discovered in the TIN model. Similar to the TIN model, surface contours can also be generated from the raster kriging surface.

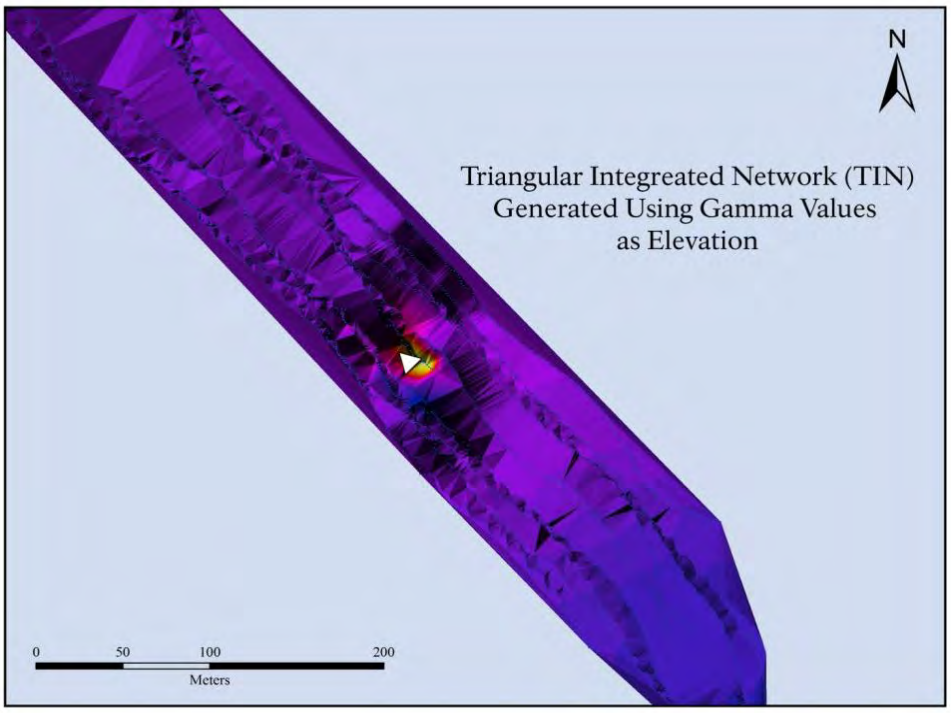

Figure 8-3. A triangular-irregular network (TIN) generated from a section of the MA WEA Baseline Survey Data.

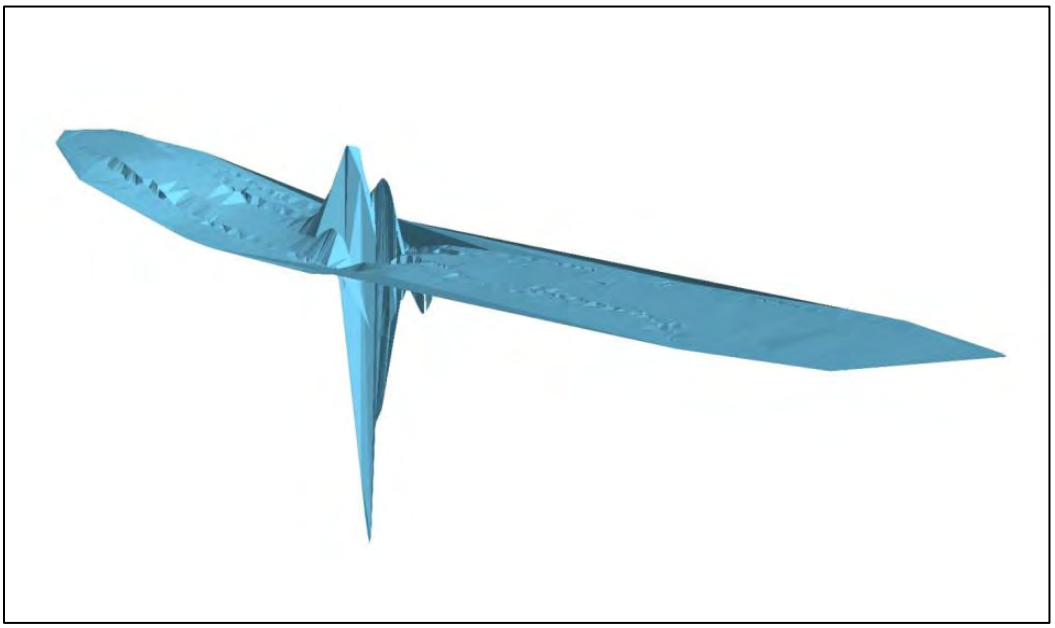

Figure 8-4. Three-dimensional rendering of the triangular-irregular network (TIN) magnetic data; the magnetic anomaly is the large feature in the middle, in this case a shipwreck (source: J. Bright, NPS-SRC).

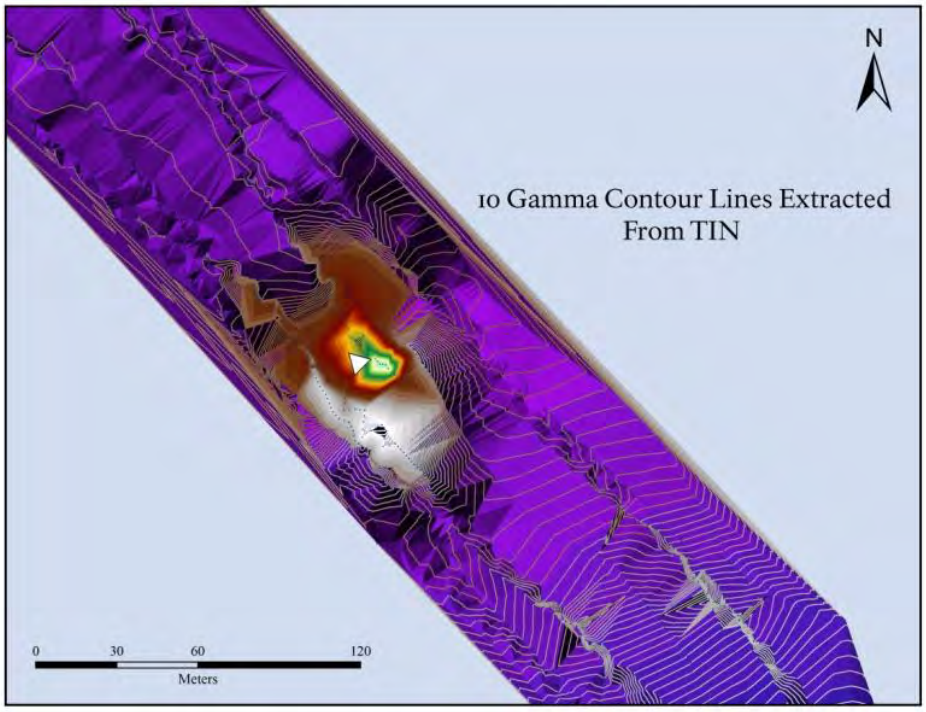

Figure 8-5. Ten gamma contour lines generated from the triangular-irregular network (TIN) terrain map of the Buzzards Bay dataset (source: J. Bright, NPS-SRC).

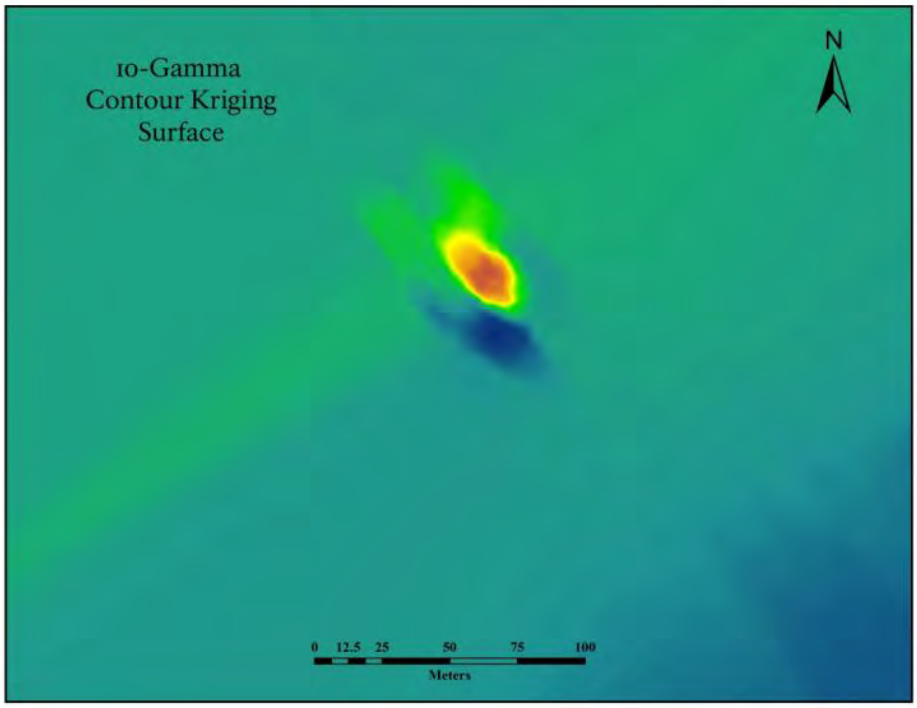

Figure 8-6. Ten-gamma interval kriging output for Buzzards Bay survey block (source: J. Bright, NPS-SRC).

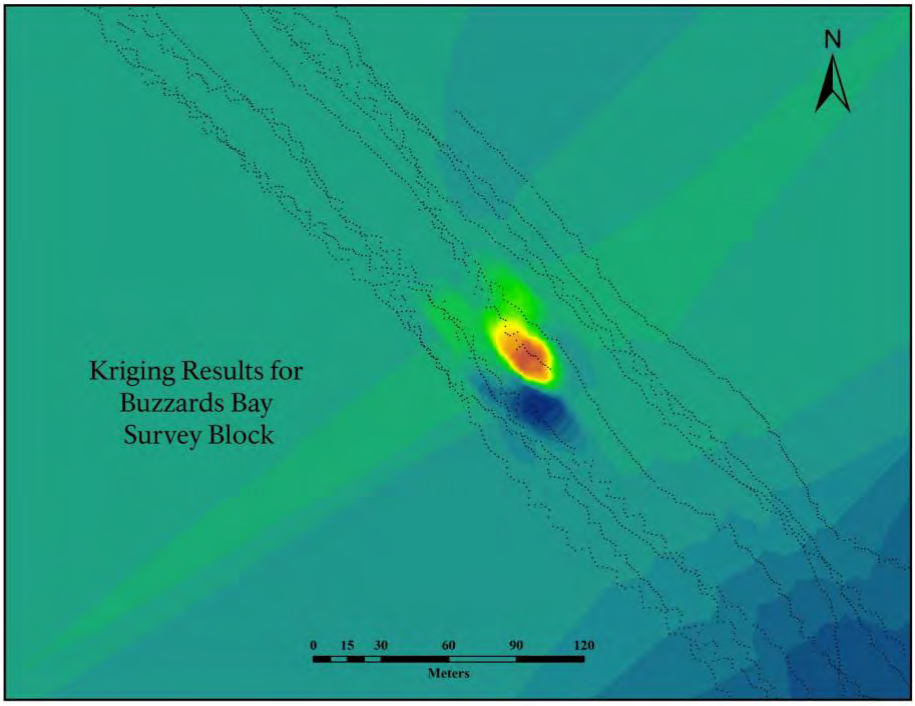

Figure 8-7. Fifty-gamma interval kriging output for Buzzards Bay survey block; raw data points shown in black (source: J. Bright, NPS-SRC).

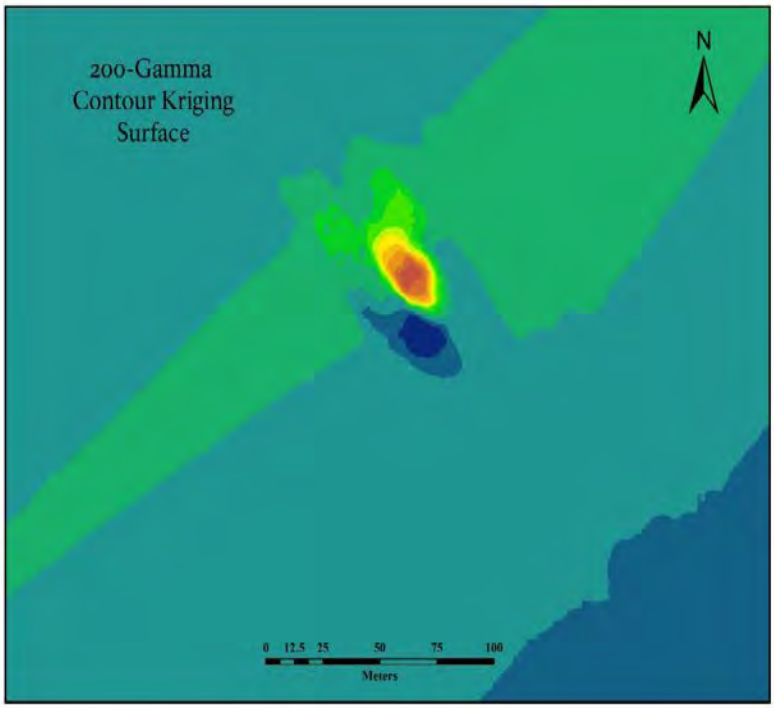

Figure 8-8. Two hundred-gamma interval kriging output for Buzzards Bay survey block (source: J. Bright, NPS-SRC).

The symbology of the kriging surface, however, presents the same contour interval issue as the vector TIN contour. The color-coding of the raster surface can be designated at any contour interval (see Figures 8-7 and 8-8), or as vector isolines extrapolated from the kriging surface (see Figures 8-9 and 8-10). As was the case with the TIN model, changing the symbology of the contour interval does not change the data, only the manner in which it is presented to the viewer. This can affect the interpretation of the data because, as the contour interval increases, smaller magnetic fluxes disappear into the space between isolines (see Figure 8-11), making the magnetic anomaly increasingly less visible. For a site with a strong anomaly, like the Buzzard's Bay survey block, this effect is not as noticeable as at a site with a weaker anomaly.

8.4.1.3 Gradient Processing

As discussed earlier, visualizing data via TIN terrain modeling and spatial interpolation shows a full field magnetic surface, complete with diurnal and geological variations. Such variation is apparent throughout both methods, as shown in Figures 8-3 through 8-11; the best example shown in Figure 8-7, where the geological variation along the glacial moraine created a slow, but dramatic change in total magnetic field intensity.

Gradient processing is a third type of mathematical operations used with magnetic survey datasets. Gradient processing uses derivatives to calculate localized rates of change within the magnetic field, capturing the short, high-intensity fluxes produced by the presence of magnetic materials, and is built into the operating system of specialized magnetometer array known as a gradiometer.

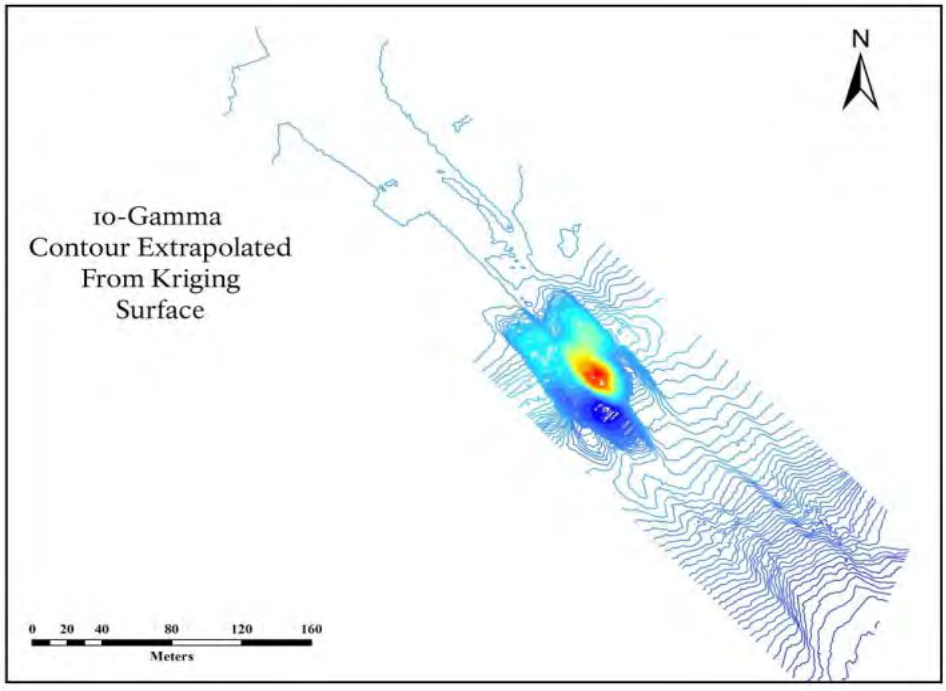

Figure 8-9. Ten-gamma vector isolines extracted from kriging output for Buzzards Bay survey block (source: J. Bright, NPS-SRC).

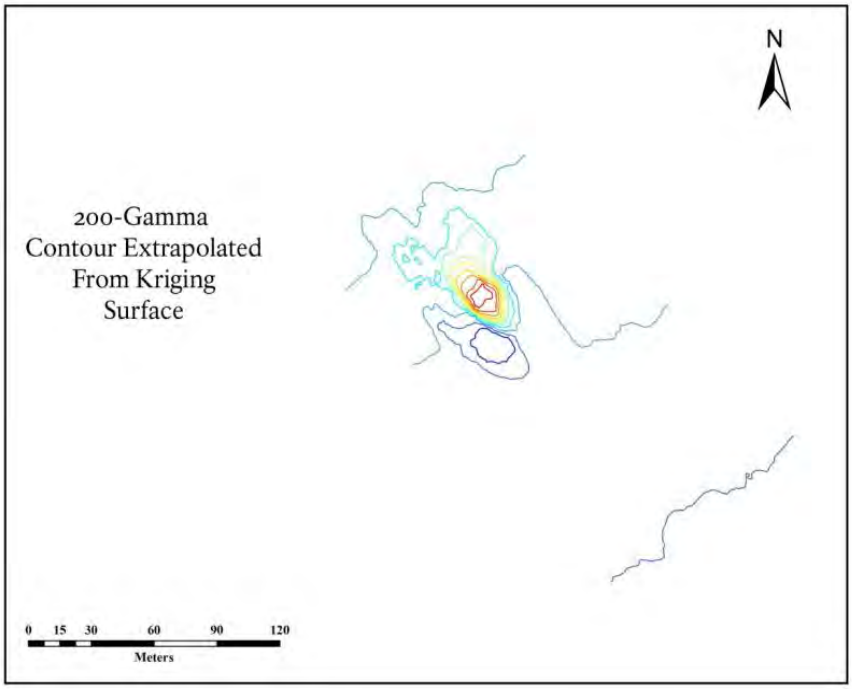

Figure 8-10. Two hundred-gamma vector isolines extracted from kriging output for Buzzards Bay survey block (source: J. Bright, NPS-SRC).

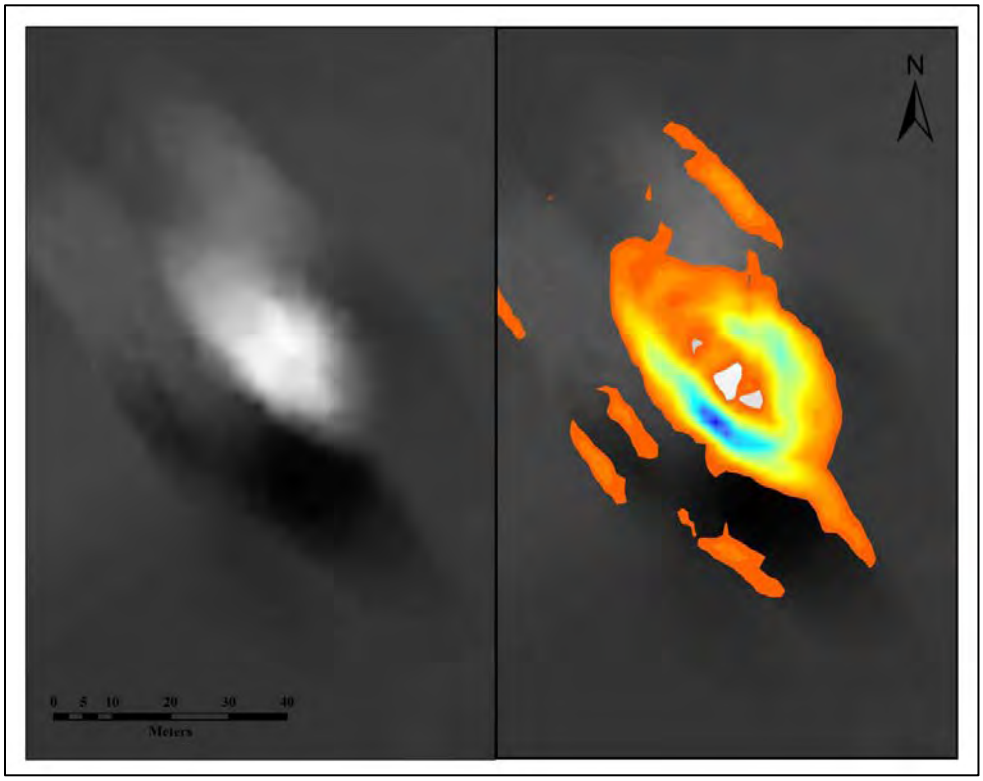

Figure 8-11. Ten-gamma contour raster slope calculation performed on full-field interpolated surface (source: J. Bright, NPS-SRC).

Gradient contour analysis originally arose from the NPS's experience with hundreds of surveys and the physical principle that wherever the magnetic flux changes most dramatically (i.e. where the gradient is the steepest) is the source of the magnetic field (the area between the polarized lobes of the magnetic field) and, therefore, where the physical object responsible for the magnetic anomaly is located.

Gradient processing applies a mathematical function which cancels out long-range spatial and temporal variability within the data set, filtering geological and diurnal variation to an extent that is impossible with terrain modeling and interpolation. In this way, gradient processing offers another method to filter and present raw magnetic data.

Instead of generating a surface representative of magnetic values, gradient processing calculates rates of change between individual data points. In particular,

> the basis of gradient processing of magnetometer data is to look for changes in the magnetic field over short distances. Because of various geologies, the magnetic field can change significantly over the span of one survey block. Gradient processing can, [therefore], be described as a selective filter (Shope 2011:1).

In a purely mathematical sense, two types of gradient processing are possible with magnetic data: first- and second-order derivatives of the magnetic field. In a basic form, these functions are as follows:

First-Order Gradient

$$Gradient_1 = \frac{\partial H}{\partial r}$$

Second-Order Gradient

$$Gradient_2 = \frac{\partial^2 H}{\partial r^2}$$

The first-order gradient calculates the rate of magnetic change, i.e. the velocity versus distance. The second-order gradient uses the second-order derivative to calculate the rate of change in the gradient, i.e., acceleration, as a function of distance (Shope 2011).

Yet, visualizing these data as a continuous surface is not possible. First- and second-order derivatives represent the magnitude of change between sequential data points. If transferred into a graph, they would be linear in nature, a representation of the rate of change over distances, similar to a parabolic curve. Raw magnetic data, on the other hand, is a matrix of samples from a continuous surface, the actual magnetic landscape. Interpolation between these samples, therefore, accurately approximates the disposition of this landscape. Derivative calculations between data points, however, are a determination of change between discrete points sampled from the continuous surface. Thus, an alternative means of executing the derivative function is necessary**.**

When executed, interpolation algorithms produce a continuous raster surface. Actual or interpolated magnetic field strengths are assigned to each raster cell. Executing a slope calculation by determining the proportion of change between one raster cell and each adjacent cell, produces the same kind of result as mathematical gradient processing; it isolates areas of short, high-intensity magnetic flux within the dataset. Figure 8-11 shows the krig surface (black and white) overlaid with the color-coded slope calculation. The higher slope values (those shown in blue) occur right at the shift from positive to negative dipoles: precisely where anomaly investigation would target (and where the physical object is on the seafloor, as shown by sonar data). The slope surface also eliminates all of the background noise produced by geological and diurnal shifts in the dataset, such as those apparent in Figures 8-3 through 8-5 (above) since the only data value of interest is the net change from one data collection point to another.

Thus, gradient processing in the form of raster slope calculation offers the "selective spatial filer" described by Shope (2011:1). Using the higher ratios of magnetic field strength change, it becomes much easier to pinpoint the center of discrete magnetic field flux and, therefore locate the objects producing these fields. In essence, gradient processing enhances anomaly identification and location, providing a more precise means to interpret magnetic data beyond the visualization of full-field surface mapping.

8.4.2 SOURCES OF ERROR

From a management perspective, the primary issue with data processing is that human interface with these systems can potentially induce error. An examination of these processes, therefore, highlights critical management and regulation issues which have yet to be officially addressed in BOEM's published standards.

8.4.2.1 Non-Obvious Cultural Material

In earlier chapters, an acoustic survey was shown to produce an image of the bottom in which cultural material is usually fairly conspicuous. Specifically, acoustic data processing produces a mosaic from the composite of individual survey track lines; thus, if the acquired data are good, the mosaicked images are good as well.

Magnetic systems, on the other hand, require much more data manipulation and interpretation. Most currently available software programs will export magnetic data as a series of points, coding raw data readings with their respective geographical location, as shown in Figure 8-12.

Visualized raw magnetic survey data does not indicate the presence of magnetic materials; instead, it merely shows were data points were collected. Thus, the researcher does not know prior to processing where an anomaly might occur or how large or small it might be.

8.4.2.2 Mathematical Processing Error

Manipulation and interpretation of the raw data during processing can in result in the loss or obscuring of data. For example, the commonly-used magnetic processing software Hypack offers the user the ability to edit raw data prior to processing and visualization. This feature is intended to allow the user to remove bad data, such as a false anomaly produced by the sensor hitting the

bottom. However, it is also possible for the user to remove actual magnetic anomalies, and thus omit them from later processing. Errors like these are possible throughout the entire work-flow of magnetic data processing, regardless of the specific methodology employed.

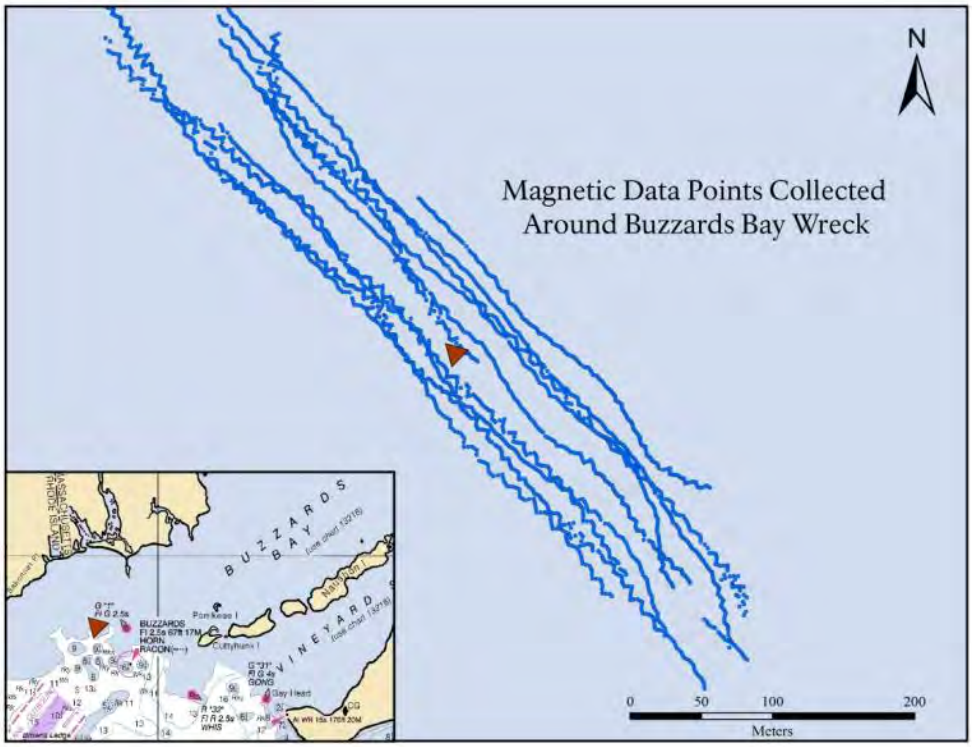

Figure 8-12. Unprocessed magnetic data points, produced in Hypack 2012 and visualized in ArcGIS, from the MA WEA Baseline Survey (source: J. Bright, NPS-SRC).

In the raw data from a magnetic survey, each data point is a discrete measurement of ambient magnetism, coupled with a geographic location. As discussed earlier, magnetic fields generated by cultural objects are continuous, localized phenomena, which exhibit relatively large levels of flux. Thus, data points acquired while moving through these fields serve as isolated samples of the complete field. To visualize and quantify the field in its totality, and therefore pinpoint archaeological material, a mathematical solution is necessary.

8.4.2.3 Improper Gamma Contour Selection

Designating different contour intervals affects the manner in which the subsequent visualization presents magnetic information, as evident in Figures 8-13 through 8-15. In general, the smaller the contour interval, the larger an anomaly will appear, however this is not always desirable due to the effect of background noise. In the case of this particular dataset, where a single anomaly was detected, setting a higher contour interval helps reduce some of the background noise without obscuring the magnetic spike. This object, however, produced an anomaly in excess of one thousand gammas. Smaller objects, or those farther from the sensor, would yield a much smaller hit or might be completely obscured by a large contour interval.

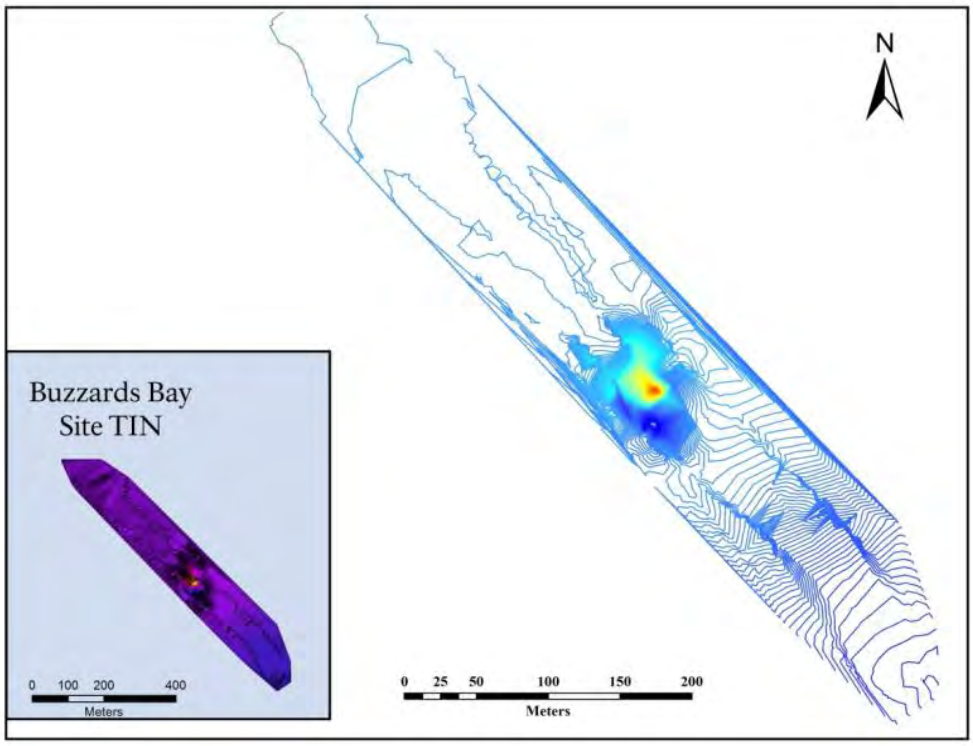

Figure 8-13. Ten-gamma contour generated from the Buzzards Bay TIN (source: J. Bright, NPS-SRC).

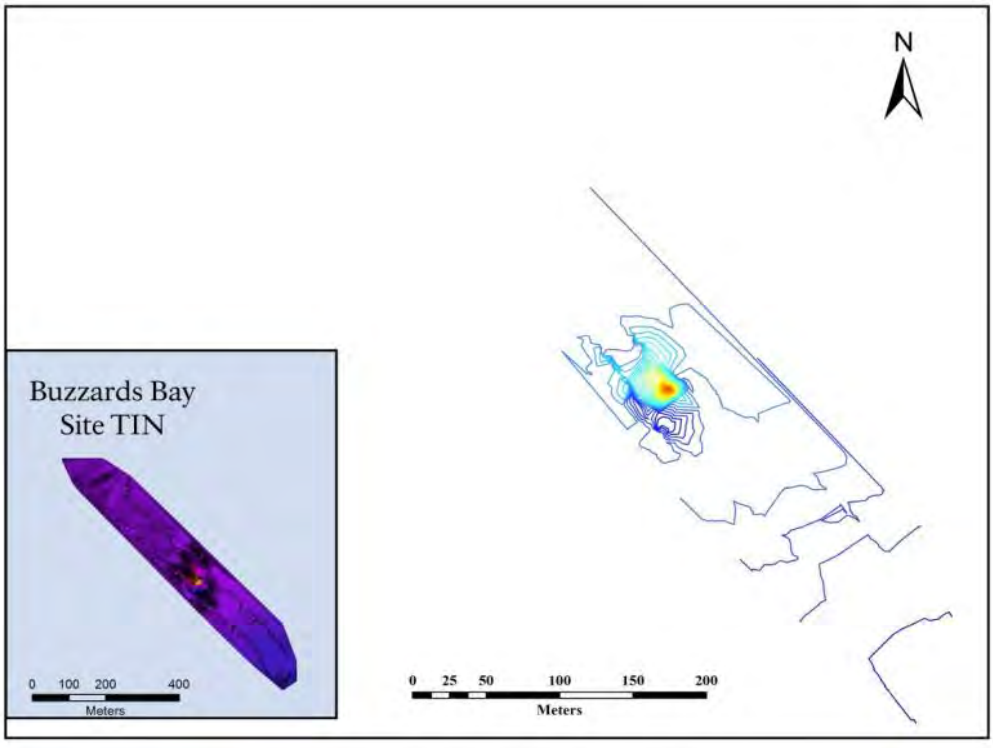

Figure 8-14. One hundred-gamma contour generated from the Buzzards Bay TIN (source: J. Bright, NPS-SRC).

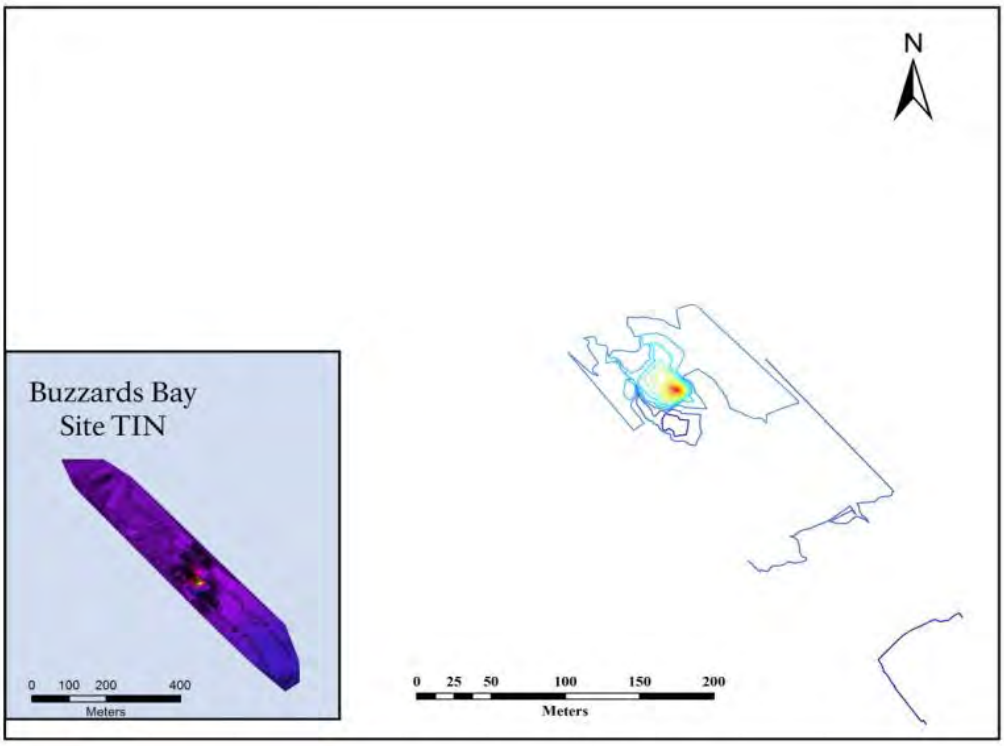

Figure 8-15. Two hundred-gamma contour generated from the Buzzards Bay TIN (source: J. Bright, NPS-SRC).

Given that even a 5 to 10-gamma hit is detectable above ambient levels with a modern magnetometer, using a 100-gamma contour, or even a 10-gamma contour for that matter, would fail to represent smaller anomalies that may be produced by objects of interest. Thus, the designated contour level is an integral factor in the processing of the data. Using the model presented in the previous section, magnetic surveys can be designed to ensure detection of smaller objects, or for the sake of expediency, made such that desired objects are theoretically detectable at wider spacing or higher sensor altitudes. In either case, such planning is only effective if the data are processed accordingly. Thus, contours should be generated in accordance with the smallest anticipated anomaly. Conversely, specifying a very tight contour interval may indicate magnetic anomalies that are the result of cultural materials not of interest for the specific research design, or, in the worst case, be specious anomalies generated by instrument noise or diurnal variations that occur over the course of the survey effort.

8.4.2.4 Summary of Error Sources

Apparent throughout processing of the data stream from a magnetic survey, is the need for the user to consciously control the degree of data filtering and the parameters of visualization. Without purposeful control of these processes, archaeological assessments based upon magnetic data sets are neither systematic nor reliable.

The potential for data processing manipulation is very high and should be addressed in BOEM's requirements. Intentional errors, or unintentional errors, such as accepting the default settings and default symbologies, will change the visual appearance of the map. "Default symbology" is a GIS

term describing how visual output is rendered by a software program. It includes colors, contours, line thinness, point size, et cetera. The use of default settings and symbologies will not change the actual data, just its appearance and could produce a visualization that does not reflect the true nature of a survey area.

8.5 CONFIDENCE REPORTING

A final step in the evaluation of magnetic survey data is confidence reporting. To determine the completeness of a given data set, it is necessary to identify possible sources of error and to estimate the range of those errors in terms of the sizes of objects that could have been missed.

8.5.1 ARCHAEOLOGICAL CONTEXT

One factor to consider when evaluating the meaning of a given set of archaeological data is its archaeological context. The science of archaeology investigates contexts—the relationships between and among the physical remains of past human activity. The delineation and characterization of these relationships is the first step in a more complex chain of reasoning that attaches meaning and value to these physical remains. A compliance survey for the identification of archaeological resources, therefore, needs to evaluate magnetic anomalies both in and of themselves, and also as they relate to other nearby anomalies in larger groupings and clusters. In other words, the archaeological significance of an object depends in part upon the context in which the object exists. Given certain survey parameters, however, additional artifacts—contextual information—may go undiscovered. Understanding the limitations of a given survey and the potential types of artifacts which could have been missed are integral to determining the archaeological context and significance of items discovered during magnetic survey. Confidence reporting allows for quantitative review of a given magnetic dataset to better understand the types of artifacts (if any) that were missed during a magnetic survey and therefore results in more accurate statements regarding archaeological context.

8.5.2 DEVIATIONS FROM SURVEY LINES

Deviations from planned survey lines are inevitable and introduce an inherent amount of error into a dataset. Where a survey may have been designed to a certain set of parameters, the actual coverage throughout an area is entirely dependent on the actual data acquisition process. Figures 8-16 (below) and 8-12 (above) demonstrate how a survey vessel can, and inevitably will, deviate from planned survey lines. Figure 8-16 is a hypothetical illustration depicting a typical course made good by a vessel, while Figure 8-12 depicts the actual course traversed in a survey block from this study. Though deviation from survey tracklines is an inevitable occurrence, these deviations affect the detectability of potential archaeological material; wide deviations introduce gaps in the surveyed area where small ferromagnetic objects may go undetected. Though most archaeological surveys fail to generate information regarding the completeness of their coverage, quantification of these gaps is essential to establishing confidence in a magnetic dataset.

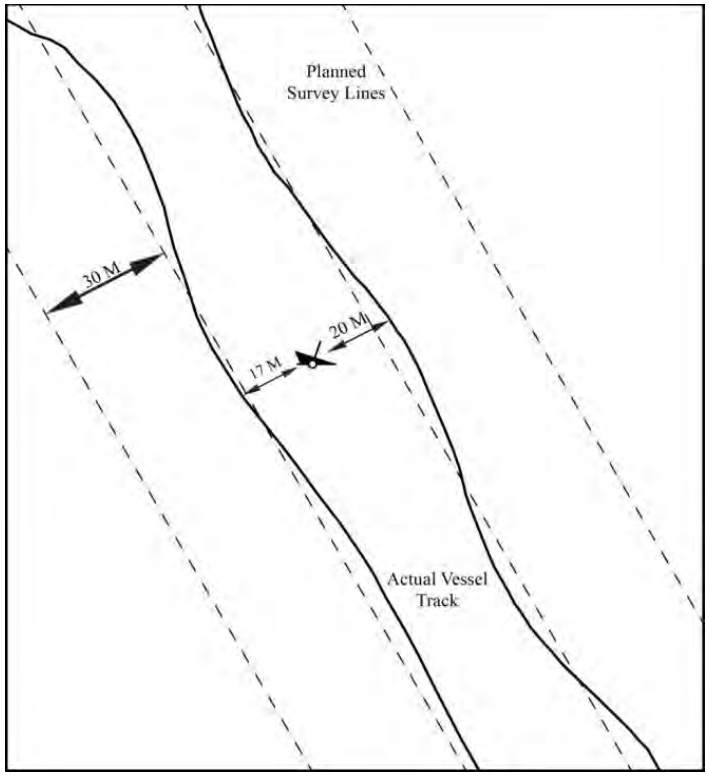

Figure 8-16. Unavoidable deviation from planned survey tracklines can increase distance between object and magnetometer sensor (source: J. Bright, NPS-SRC).

The assumption with this model is that the sensor is moved precisely along the planned survey tracklines. Deviation from planned survey tracklines, which regularly occurs due to the difficulty of piloting a vessel, currents, winds, and sea state, moves the sensor closer or farther from on object on either side of the survey line, thereby altering the "ideal" picture of survey design. This can decrease the distance between object and sensor, and likewise increase the distance beyond the planned maximum. For example, if while piloting survey tracklines spaced at 30 m, the operator deviates 5 m (16 ft) to the left of the line, an object 15 m (49 ft) to the right of the survey tracklines will actually be 20 m (66 ft) from the sensor, as shown in Figure 8-16. Similarly, if on the adjacent line the vessel deviates away from the object and additional space is placed between the sensor and object, the object could potentially escape detection. Nevertheless, since planning for deviations due to environmental conditions and boat handling is nearly impossible, survey design will always assume the magnetic sensor travels exactly along the planned survey tracklines.

In operational reality, however, deviations from the planned survey tracklines will occur. Thus, though a survey may be planned such that objects of a certain size are detected, without re-evaluating the data set post-acquisition, no such certainty actually exists. Confidence reporting, therefore, re-processes the acquired data to map areas of actual detection and identifies specific gaps within the acquired data set that may require re-visiting.

The process is fairly straightforward. Using the detection algorithm, and knowing the average sensor altitude during the survey and the mass of the smallest target object, a dissolved spatial buffer is created around the imported raw data points to represent the area of actual coverage within the

survey block. Figures 8-17 and 8-18 show these buffers for the two survey blocks completed during the present study. Each buffer is modeled based upon a sensor altitude of 10 m (33 ft), the average altitude of the magnetic sensor during these survey operations, and a detection threshold of 10 gammas.

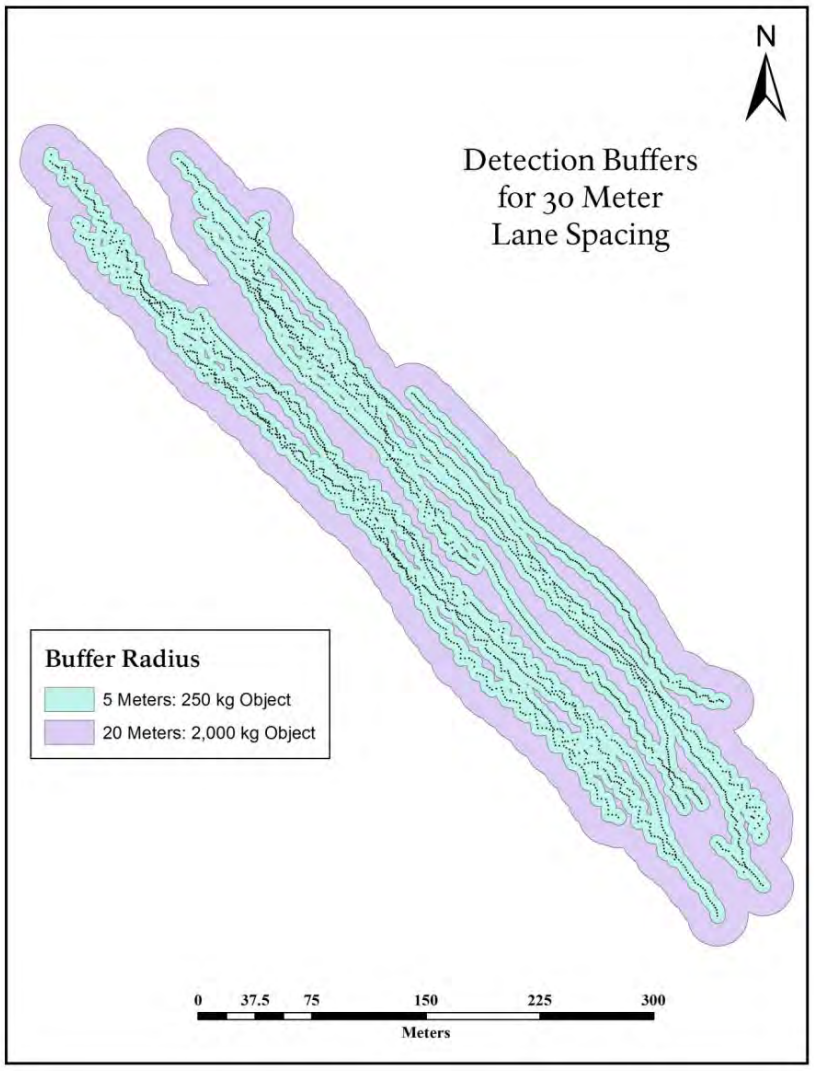

Figure 8-17. Spatial buffers representing theoretical area around sensor path where 250 kg (551 lb) and 2,000 kg (2.2 US ton) magnetic objects would produce a 10-gamma anomaly (source: J. Bright, NPS-SRC).

In Figure 8-17, the purple areas between the turquoise lines show areas where a 250 kg (551 lb) object would not have produced a 10 gamma anomaly because it was too far from the sensor. If 10 gammas was the detection limit on the equipment used, the anomalies from a 250 kg (551 lb) object in those areas would have been missed. There would not be high confidence that objects about 250 kg (551 lb) in weight were detected in this survey. However, if the object weighed 2,000 kg (2.2 US ton), anything with the purple area would have produced a 10 gamma anomaly, and confidence in detecting 2,000 kg (2.2 US ton) objects would be high.

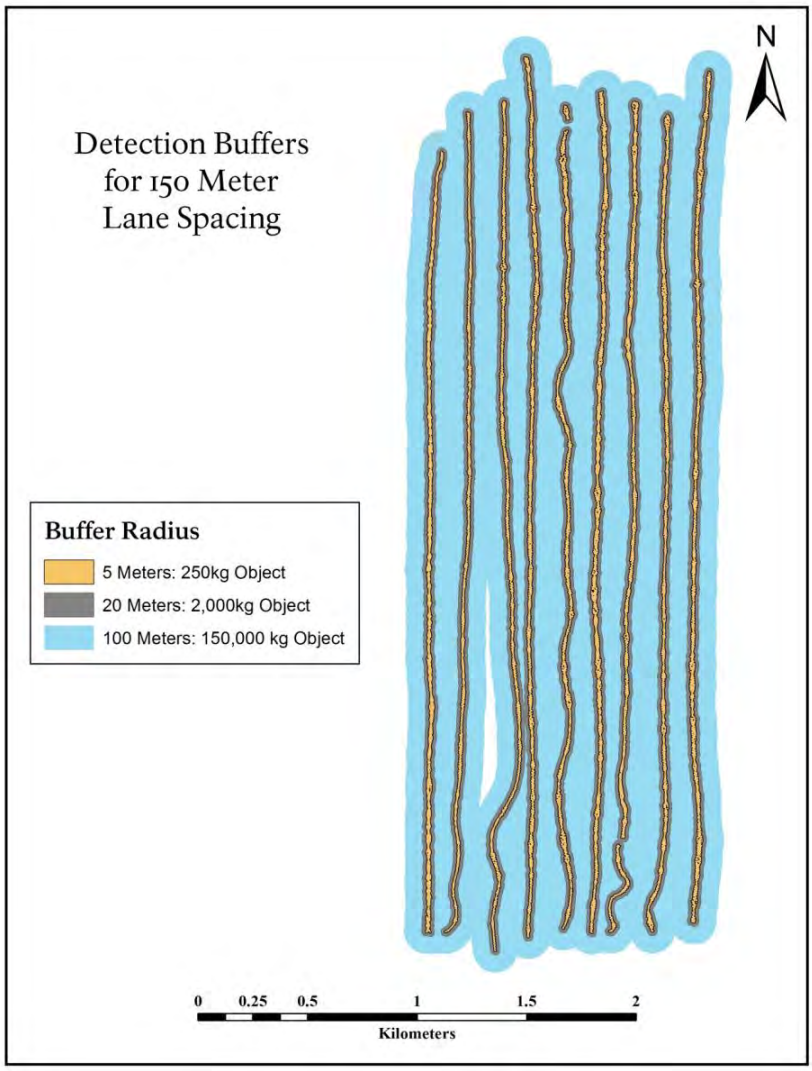

Figure 8-18. Spatial buffers representing theoretical area around sensor path where 250 kg (551 lb), 2,000 kg (2.2 US ton), and 150,000 kg (165.3 US ton) magnetic objects would produce a 10-gamma anomaly with much wider line spacing (source: J. Bright, NPS-SRC).

The larger survey trackline spacing represented in Figure 8-18 is a considerable exaggeration, as most magnetic sensing operations use spacing of 50 m (164 ft) or less. The example, however, does illustrate how quickly thresholds of detection diminish as survey trackline spacing increases.

These types of post-processing analyses are valuable from a management perspective because they indicate the object sizes that were sought, the object sizes (if any) that were detected, the areas that were surveyed (and those that were missed) and the degree of confidence the surveyors can place on the data and analyses they generated.

When reviewed in this way, each survey data set reveals significant gaps in regards to detection of smaller objects. For example, in the area surveyed with a planned survey trackline spacing of 30 m (98 ft), a total survey area of 0.0802 km^2 (0.0234 nm^2) was covered, with 0.04 km^2 (0.116 nm^2)

within the 5 m (16 ft) buffer and 0.0801 km^2 0(0.0233 nm^2) in the 20 m (66 ft) buffer. Therefore, a 250 kg (551 lb) magnetic object could have been found in less than half of the area covered. In the area surveyed with a planned survey trackline spacing of 150 m (492 ft) and a total survey area of 5.67 km^3 (1.65 nm^2), this is the percent coverage expected: 5.64 km^2 (1.64 nm^2) (99%) of the area would be within the 100 m (328 ft) buffer, 1.71 km^2 (0.49 nm^2) (30%) of the area would be within the 20 m (66 ft) buffer, and 0.589 km^2 (0.172 nm^2) (10%) of the area would be within the 5 m (16 ft) buffer. As a result, for 99% of the entire survey area, the smallest theoretically detectable object in a worst-case scenario where the object lay exactly between two survey lines, was 150,000 kg, approximately the mass of a 16.5 US ton steel ship.

As is shown in Figure 8-17, even close survey trackline spacing still results in gaps when considering the detectability of small ferromagnetic objects. In that case, a 250 kg (55a lb) object—approximately the mass of a small steam engine—could have escaped detection within the area.

Each survey block is different; varying in survey trackline spacing, sensor altitude, the ferromagnetic mass of target objects, and the chosen contour interval for analysis. Thus, these thresholds will be unique, depending on each survey set, especially those with large deviations from planned survey lines. Confidence reporting therefore is the only quantifiable way to verify a theoretical minimum level of coverage within a magnetic data set.

8.6 COMPARISON OF MAGNETIC SURVEYS CONDUCTED AT A KNOWN SHIPWRECK SITE AND ON THE MA WEA

A majority of research conducted during the MA WEA baseline survey focused on evaluation of acoustic sending packages. During these experiments, as well as during reconnaissance survey, a Geometrics G-882 magnetometer was deployed in tandem with the NPS SRC's Klein 3000H side scan sonar to collect magnetic data. These deployments included data collection during the sub-bottom profiling transects planned by URI-GRO and during comparative assessment between the interferometric and side scan sonar systems over known and possible shipwreck sites. The resulting data provided operational feedback regarding the theoretical principles outlined in the Sections 8.1 through 8.5 pertaining to anomaly prediction, levels of detection, data processing, and confidence reporting. While operational feedback on these protocols offers useful insight regarding regulatory and management requirements of magnetic sensing in federally-managed areas, magnetic testing during this study was by no means a complete or exhaustive exploration of these issues. Instead, these data stand as preliminary results that can inform future magnetic research.

Magnetic survey data were collected during several long reconnaissance transects and during two multiple-pass surveys, one over a known shipwreck site, and one within the WEA (Figure 8-19). The magnetometer was run during the long transects to test a tandem towing configuration with the side scan sonar for the purpose of streamlining both acoustic and magnetic data collection during subsequent survey. Magnetic survey data collected during the reconnaissance transects was of little use since single-track data cannot be processed into magnetic fields. We had anticipated that, for this reason, magnetic data collected during the survey would not be useful to identify cultural material; only magnetic survey data from multiple, parallel lines provides adequate sampling to model magnetic fields and to identify anomalies. Instead, the two multi-pass survey blocks are of interest. These two surveys were intended to compare imaging resolutions of two sonar systems, rather than

to test the magnetometer or collect magnetic data. Using a number of wreck and obstruction databases, two potential shipwreck sites were chosen, and survey blocks were therein established. Having configured the G-882 magnetometer to run in tandem with the Klein 3000H side scan sonar, magnetic data were collected at both locations.

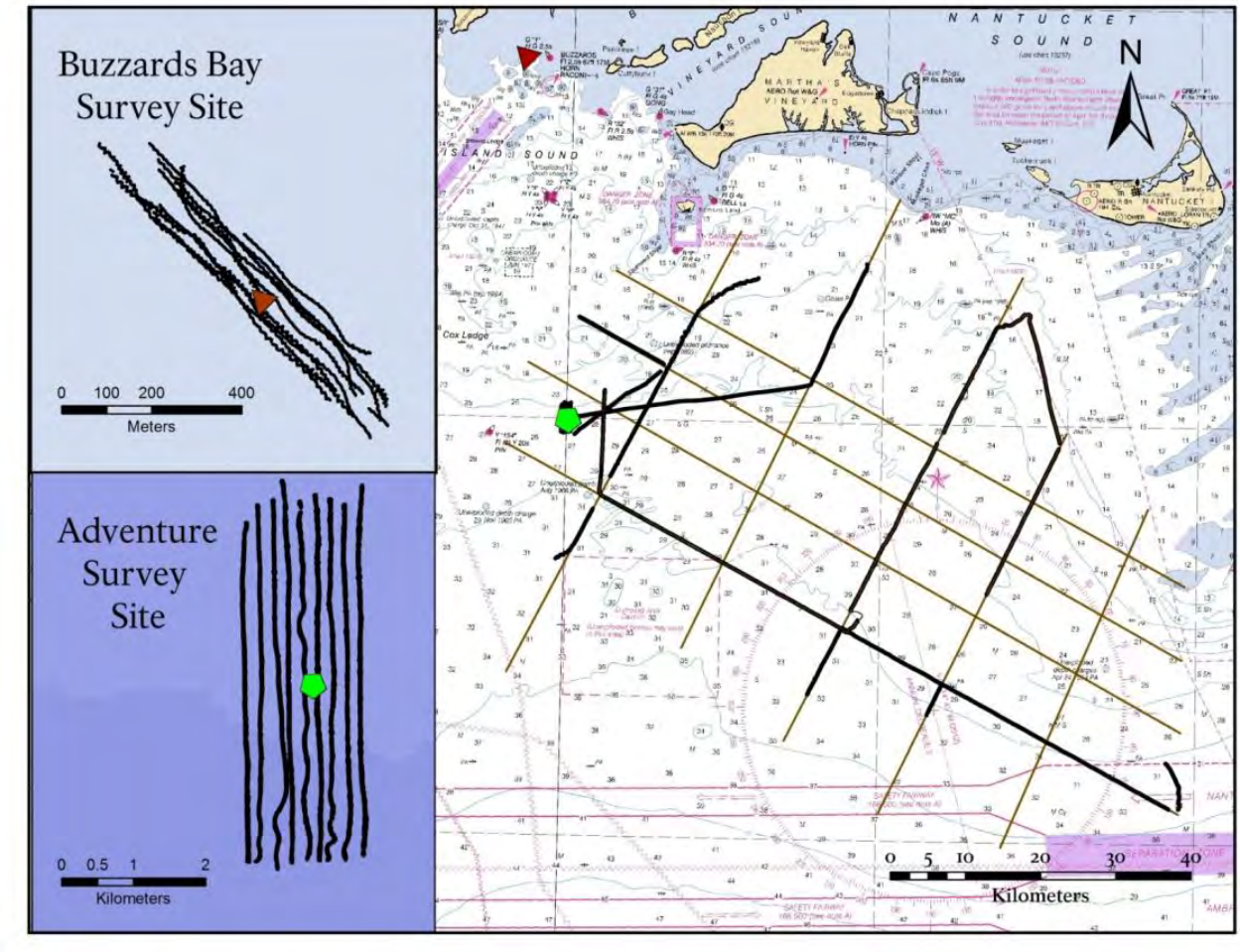

Figure 8-19. Locations of all magnetic data collected during the 2012 MA WEA Baseline Survey; two wreck imaging sites and several long transect lines (source: J. Bright, NPS-SRC).

8.6.1 Magnetic Survey at a Shipwreck Site in Buzzard's Bay

At the first site, a shipwreck off Cuttyhunk Island in Buzzards Bay, survey tracklines were planned at 30 m (98 ft) and run opportunistically to optimize sonar image acquisition. (The survey tracklines run during this survey are shown in Figure 8-4 above). The presence of a shipwreck at this location was known, having been previously visited by the USGS.

Survey operations, therefore, were immediately focused on the site without the need for systematic sweeps to pinpoint the target. In this respect, this survey block was atypical of most surveys, especially surveys preceding archaeological clearance work. Methodical planning to determine

survey trackline spacing and sensor altitudes was unnecessary, and since the target was a single object expected to be large and conspicuous, predictive modeling was likewise unnecessary.

Nevertheless, magnetic data from this survey block provides useful observations, including:

- narrow survey trackline spacing (30 m [98 ft]) allows detection of medium-sized and larger magnetic objects;
- using magnetic imaging and side scan sonar together allows one to make an estimate of the size and mass of the objects detected; and
- with the appropriate survey trackline spacing and sensor altitude, large metallic objects will be detected using this type of survey.

8.6.1.1 Survey Trackline Spacing at the Buzzards Bay Shipwreck

Even though the vessel deviated from the planned survey tracklines, the narrow survey trackline spacing offered relatively complete magnetic coverage of large- and medium-sized magnetic objects. The example shown in Figure 8-17 (above) shows the confidence reporting for the Buzzards Bay survey block. This reporting indicated the survey would have found any magnetic object larger than 2,000 kg (2.2 US ton), which, if cross-referenced with Tables 8-1 through 8-3, shows the survey would have located most large- and medium-sized material cultural items. Smaller items, however, would not have been detected if they rested between the areas encompassed by the 5 m (16 ft) buffer in Figure 8-17.

8.6.1.2 Estimated Mass and Material of Buzzards Bay Shipwreck

Second, the size and mass of the detected objects can be estimated by using acoustic data in tandem with magnetic data. For example, the observed anomaly within the survey block induced a reading of approximately 1,600 gammas at a range of 10 m (33 ft) and a sensor height of 10 m. The same equation used to model predicted anomaly size can also be re-worked to estimate object mass from observed anomaly amplitude and range. In this case, the equation indicates the object contained 75,000 kg, or 83 US ton, of magnetic material. Imaging data from the side scan sonar indicates the vessel was 40 m long (131 ft) by 10 m (33 m) in beam. A steel ship of similar dimensions, the 38-m (125-ft) class of United States Coast Guard Cutters, have a length of 38.1 m, beam of 7 m (22 ft), and mass of 210 metric tons (232 US tons). These were lightly armed vessels, thus most of the mass was comprised of hull and machinery. Such a vessel would have produced an anomaly of 4,607 gammas. Being slightly larger in overall dimensions, yet containing considerably less magnetic material, the wreck imaged at Buzzards Bay likely contains large amounts of non-magnetic material, probably wood. Understanding the physical relationship between size and measured magnetic field strength allows for quantitative assessments of the anomaly prior to more targeted investigation.

8.6.1.3 Data Processing Relative to the Buzzards Bay Shipwreck

The Buzzards Bay survey block prompts some discussion of data processing. User-defined contour intervals and raw data manipulation are the primary means of human-induced error, regardless of the specific processing methodology. Defining the correct minimum resolution, i.e. gamma contour intervals, is necessary to assure proper interpretation of individual datasets. Given the magnitude of anomaly generated by the object imaged in Buzzards Bay, changing the contour interval of the

survey block by 10's to 100's of gammas would not have prevented its visibility in the processed data set. However, if the object in Buzzards Bay had been smaller, it may have gone undetected if the contour interval were too large.

Similarly, the number of passes taken past the object resulted in numerous survey lines recording the field it generated. This made inadvertent deletion of the trace from the raw data unlikely; unless the user intentionally deleted each trace. Raw data manipulation can introduce error, which is much more likely if there are fewer traces registering the anomaly as opposed to more, such as when the survey lines are few or widely spaced. The interpretation of the Buzzard's Bay data illustrates the appearance of a conspicuous large magnetic anomaly in the data record with the appropriate line spacing and sensor altitude.

8.6.2 MAGNETIC SURVEY AT WEA SITE

The second survey site, on the other hand, offered a demonstrative negative example of magnetic survey. At this location, the presence of a wreck was uncertain, and ultimately nothing was found. Data on the potential wreck, such as size or identity, was scant amongst the various wreck and obstruction databases at the project's disposal. Nevertheless, a hypothetical figure, such as a small 9071 kg (10 US ton) vessel, could have been used as an input into the modeling algorithm to determine the appropriate survey trackline spacing.

8.6.2.1 Survey Trackline Spacing at WEA Site

Survey trackline spacing, sensor altitude, and wreck mass determine the detectability of a shipwreck. For example, a small 9071 kg (10 US ton) metal wreck would generate a minimum 9.6 gamma anomaly within a 75 m (246 ft) survey trackline spacing and sensor altitude of 10 m (33 ft); using 50 m (164 ft) survey trackline spacing would generate a minimum 29 gamma anomaly.

In the magnetic survey at the WEA site, the maximum swath width of the low-frequency sonar gear, 150 m (492 ft), was used. At a survey trackline spacing of 150 m (492 ft), a 9,071 kg (10 US ton) vessel would only generate a 1.3 gamma anomaly if situated between two adjacent lines; not at all detectable when the data are contoured at a 10-gamma interval. At this spacing, the minimum-sized object detectable throughout the survey area would have a magnetic object mass totaling 149 metric tons (165 US tons), or more (see Figure 8-18). In comparison, the frigate *Boston* weighed 489 metric tons (540 US tons), and an assumed 58 metric tons (64 US tons) of that was iron. A frigate of that size would not have been detectible at the WEA, given the 150 m (492 ft) survey trackline spacing.

8.6.2.2 Results of the Initial Magnetic Survey at the WEA Site

No large or medium-sized objects were detected at the WEA site. However, the magnetic data set for this site is incapable of negating the possibility of a wreck or other large object within the survey area. The possibility of a small shipwreck in the survey area cannot be discounted on the basis of these survey data. To fill these gaps, additional magnetic data would be needed.

8.6.2.3 Analysis of the Initial Magnetic Survey at the WEA Site

The WEA survey was designed to test acoustic gear only, so the survey tracklines spacing was set at intervals of 150 m, rather than the 30 m (98 ft) used at the Buzzards Bay survey site.

The results of this particular survey area neatly illustrate deficiencies created in a magnetic data set, should the surveyor fail to account for the limitations caused by magnetic survey trackline spacing. By spacing the survey tracklines based on the limits of acoustical instruments, rather than on the limits of the magnetic instruments, the surveyor greatly decreases the value of the magnetic survey. If the goal of the survey is to detect metallic objects, then the determining factor for survey trackline spacing should be the detection thresholds of the magnetic instruments for desired target objects, rather than the capabilities of the acoustic instruments. Since the survey trackline spacing used in the second survey block was too wide to generate a reliable magnetic record, data processing essentially becomes moot. Kriging the data resulted in a relatively smooth surface, shown in Figure 8-20, yet this surface is deficient since the kriging was forced to interpolate across large areas of no data. Though no magnetic anomalies are present in this data set, archaeological material could still be present in the area. Thus, this visualization is essentially useless from an archaeological standpoint.

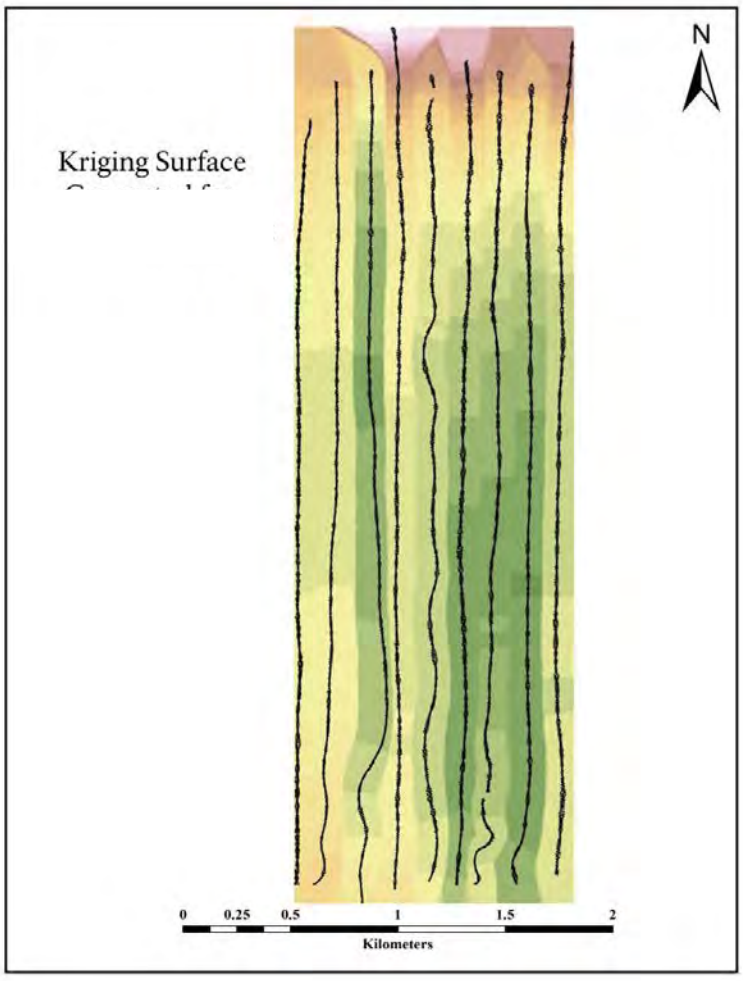

Figure 8-20. Kriging results for a magnetic dataset collected at the MA WEA (source: J. Bright, NPS-SRC).

8.6.3 Conclusions Based on the WEA Site Magnetic Survey

The magnetic data collected during the survey offers preliminary, but valuable, exploration of the scientific underpinning governing regulations, and BOEM enforcement standards for remote sensing data in federally managed areas.

8.6.3.1 Predictive Algorithm Needs Refinement

The dipole moment constant in the predictive algorithm used for designing and assessing magnetic surveys need further refinement, so that it reflects variations in real-world conditions. The physical laws describing the behavior of magnetic objects are immutable. Our interpretation and utilization of these laws, however, require constant evaluation. The predictive modeling algorithm is based upon simple physics, yet the dipole moment used to approximate anomaly size needs further refinement.

For example, it is certain that an iron object corrodes in seawater. As it corrodes, its magnetic moment diminishes; therefore the magnetic anomaly produced by the object also diminishes. For modeling purposes, the NPS assumes a magnetic moment of 14.4 cgs for ferrous material, but clearly this is a simplification that does not take into account the potentially heterogeneous constituents of various ferrous materials, nor the effects of corrosion over time. The existing algorithm should be adjusted, based on empirical observations of anomaly amplitude when crossing objects of known size and known distance.

8.6.3.2 Additional Data Needed for Interpolation

Similarly, data processing methods are based on sound statistical and mathematical formulae. However, the applicability of certain interpolative functions relative to others remains a matter of debate. Acquiring more datasets of distinct character can refine the utility of these methods for various research designs.

Types of datasets needed include: those with larger geological interference, those with large amounts of small amplitude flux, datasets covering varying geographic areas, terrain modeling, and gradient processing through a similar range of processing scenarios.

Within each dataset, the bottom line is determining the optimal methods and the correct mathematical parameter to extrapolate reliable and comprehensive anomaly information from a magnetic dataset for the purpose of identifying archaeological materials of interest as specified in an explicit research and survey design.

8.6.3.3 Confidence Reporting Needs More Specificity

Finally, revisions made to the predictive algorithm would increase the specificity of confidence reporting. This often-omitted facet of magnetic remote sensing is essential for quantifying the limitations of a particular data set for locating archaeological material. For archaeological resource management, this information is imperative. The absence of anomalies in a magnetic dataset is not necessarily evidence of the absence of archaeological material in the survey area.

8.7 RECOMMENDATIONS FOR MAGNETIC SURVEY FOR ARCHAEOLOGICAL RESOURCES

Under Section 106 of the National Historic Preservation Act, BOEM is required to consider the effects of development upon archaeological materials in areas managed by the agency. One of the core scientific methods for detecting archaeological resources, particularly historic shipwrecks, is the collection and analysis of magnetic data.

BOEM-funded studies (e.g., Pearson et al. 2003), as well as independent studies (e.g., Camidge et al. 2009), recommended a 30 m (98 ft) survey trackline spacing for magnetometer survey coverage to improve the reliability that archaeological resources with a magnetic signature are identified and avoided.

8.7.1 BOEM'S CURRENT MAGNETOMETER SURVEY GUIDELINES

BOEM (2012:3) incorporates these study results in its guidelines as a specified minimum survey trackline spacing:

> Line spacing for HRG [high-resolution geophysical] survey for archaeological resource assessment should not exceed a primary line spacing of 30 m throughout the project area. Perpendicular tie-lines spaced at 900 m should be surveyed. A minimum of at least three equidistant tie-lines should be surveyed; this may mean in some instances that tighter line spacing is necessary for the tie-lines.

BOEM (2012:5) also provides survey guidelines to developers for the collection of this data, as follows:

> For HRG survey conducted in water depths of 200 m or less, a proton precession, overhauser, or Cesium total field magnetometer should be employed to detect ferrous metals or other magnetically susceptible materials. The magnetometer should be towed as near as possible to the seafloor (but no more than 6 m above the seafloor) and in a way that minimizes interference from the vessel hull and the other survey instruments. A depth sensor should be used to ensure the proper altitude of the magnetometer and each survey line should be annotated with the tow sensor height above the seafloor and with start of the line and end of the line times. Magnetometer sensitivity should be one gamma (γ) or one nano-Tesla (nT) or less, and the data sampling interval should not exceed one (1) second. Background noise level should not exceed a total of 3 γ peak to peak.

In these guidelines, BOEM recommends a singular survey design, irrespective of predictive modeling—a specified survey trackline spacing and sensor altitude—and requires developers to provide:

> A table of the magnetic anomalies with the OCS block, SP [shot-point], and survey line location (corrected for sensor offset); gamma intensity; lateral extent (duration); whether the anomaly is characterized by a dipolar, monopolar, or complex signature; the magnetometer sensor tow height above the seafloor; the appropriate decimal degree coordinates of the center of each unidentified anomaly; and the recommended avoidance zone. The following table is an example, including sample information, for listing unidentified magnetic anomalies (BOEM 2012:15).

8.7.2 ISSUES WITH CURRENT BOEM GUIDELINES

Although these guidelines are a good beginning, there are some areas that could be improved. In particular, BOEM has no ability at present to evaluate the quality of magnetic data or the degree of

coverage received from developers. This section will discuss the problems. The following section will suggest solutions.

As described in Section 8.4.2 the potential for error—either accidental or intentional—exists throughout the acquisition, processing, post-processing, and interpretation of a magnetic survey dataset. Without more specific guidelines for each step, this error cannot be quantified.

8.7.2.1 No Standard for Minimum Contour Intervals

Under the current BOEM guidelines, the processing methods, such as the minimum contour interval allowed—are not explicit. Contour intervals are used to identify magnetic anomalies. As shown in Section 8.4.2.3, the selection of too large a contour interval can obscure data on small metallic objects in the surveyed area.

8.7.2.2 No Requirement to Report Deviations from Survey Trackline Spacing and Sensor Height

In addition, the current BOEM guidelines do not require quantitative reporting of the efficacy and actual coverage of a given survey. Planning survey trackline spacing and sensor altitude to ensure detection of desired objects, regardless of size, assumes the magnetic sensor travels exactly along the planned survey tracklines and at the planned altitude. As we have seen from this study, that does not happen even in the best of cases. Section 8.5.2 shows that even a careful survey can result in areas that were not surveyed, due to unavoidable deviations from the planned survey trackline spacing.

Deviations from survey lines and deviations from altitude of the sensor above the seafloor affect the detectability of potential archaeological materials. These deviations introduce gaps in the surveyed area where ferromagnetic objects of varying sizes may go undetected. Because of this, an area is not 'covered' by a magnetic survey simply by towing a magnetic sensor across a survey grid.

Most archaeological survey reports fail to generate information regarding the completeness of their coverage; however, quantification and characterization of these gaps is essential to establishing confidence in a magnetic dataset and in developing appropriate avoidance mitigation strategies. Although a survey may be conducted such that ferrous objects of a certain size are thought to be detected, without re-evaluating the data set post-acquisition, no such certainty actually exists.

8.7.2.3 No Tools for Verifying Magnetic Survey Data or for Monitoring Guideline Effectiveness

Without data on deviations from planned survey trackline spacing and sensor height, and without the raw data with which to assess the effect of contour interval on the visibility of smaller anomalies, BOEM does not currently have the tools to independently verify the reliability of this data after it is collected, nor does it have the ability to inform the analysis of the magnetic survey results included with plans. BOEM also has no method to monitor the effectiveness of the guidelines based on the real-world survey data submitted by developers.

8.7.3 RECOMMENDATIONS FOR STRENGTHENED GUIDELINES

Guidelines that address data processing and confidence reporting – which are integral factors to understand the coverage and quality of a magnetic survey dataset – will allow BOEM to assess the quality of the data being submitted and the effectiveness of their own magnetic survey standards.

8.7.3.1 Require Submittal of Processed and Raw Magnetic Survey Data

One recommendation is that BOEM include a provision whereby magnetometer data are provided to the agency in multiple forms:

1) As processed maps, tables and narrative text, along with recommendations for avoidance/mitigation, that adheres to published agency standards; and
2) As raw data that includes locational data, measured magnetic intensity and sensor height over bottom in electronic format that can be independently analyzed and checked through a Quality Assurance/Quality Control (QA/QC) process by BOEM staff or other contractors.

8.7.3.2 Require Confidence Reporting

Confidence reporting reprocesses the acquired data to map areas of actual detection and it identifies specific gaps within the acquired dataset that need to be treated differently from the rest of the survey area. The conclusion of a magnetic survey should include a description of the survey in terms of possible archaeological material left undetected as a result of survey design and as a result of course made good (the course actually achieved on the chart [map], after making allowances for wind direction and currents).

8.7.3.3 Review Subset of Magnetometer Survey Data

Because of the potential for error in data processing and in confidence reporting, review by BOEM archaeologists of at least a sample of the magnetometer data submitted by developers should be an essential component in the 106 compliance portion of any and all lease block developments.

Because the amount of data that comes in may quickly overwhelm BOEM staff, it is not recommended that all data be double checked, rather a representative sub-set of the surveyed area be examined as a method to determine overall confidence in the dataset as a whole.

8.7.3.4 Reassess Effectiveness of Magnetometer Survey Requirements to Protect Archaeological Resources

BOEM needs to quantitatively assess the magnetometer data received to ensure that the bureau is making an appropriate level of effort in the identification and protection of archaeological resources.

With modern technology, rapid automated processing by computer programs—in particular GIS—BOEM can significantly improve the effectiveness and confidence of marine magnetic survey. In other words, BOEM needs a method of automating the assessment of magnetometer coverage and confidence; potentially an open-source software platform which streamlines the geoprocessing functions outlined throughout the chapter. This will allow BOEM to quickly and independently verify the quality of the survey data as the agency moves to address its management responsibilities.

Developing the capability to assess the reliability of this data also allows BOEM to monitor the effectiveness of its guidelines and to adjust survey recommendations and reporting standards, as needed, to ensure data quality standards are met and are clearly communicated between the bureau and developers.

8.7.3.5 Verify Estimated Magnetic Moment Accuracy

Presented in this chapter was a mathematical algorithm used to model magnetic moment and predicted anomaly amplitude. This algorithm, however, is a theoretical representation with limited empirical input to verify its validity and applicability to real-world magnetometry. Operational testing, therefore, is needed to review and revise the parameters of this model so it more accurately depicts the relationship between submerged magnetic objects in a marine environment. Ultimately, this will result in more effective survey design and confidence reporting. Until such data are collected, however, these quantitative assessment protocols are merely theoretical.

The bottom line is that there is a need to determine the optimal methods and the most accurate mathematical parameters to extrapolate reliable and comprehensive anomaly information from a magnetic dataset so that archaeological materials of interest can be identified. This should be specified in an explicit research and survey design. Much work remains to produce a comprehensive body of research on marine magnetic sensing. We recommend that BOEM test this algorithm by conducting magnetic surveys over known archaeological sites and magnetic objects of known size to verify and adjust the modeling algorithm as needed.

CHAPTER 9

RECOMMENDATIONS

The following set of recommendations was prepared by multiple authors working in collaboration. The discussion of paleolandscape reconstructions was authored by David Robinson of the University of Rhode Island Graduate School of Oceanography. The discussions concerning the effectiveness of interferometric sonar and applications for magnetic sensing for the purposes of identifying archaeological resources were prepared by John Bright and David Conlin of the National Park Service Submerged Resources Center. Finally, the recommended procedures when operating the sub-bottom profiler and interferometric sonar to reduce the ensonification of the surrounding environment were prepared by Mikhail Zykov and Jeff MacDonnell of JASCO Applied Sciences.

In its management of the exploration and development of the nation's offshore resources, BOEM seeks to balance economic development, energy independence, and environmental protection. BOEM's overarching strategic goal is to achieve expeditious and orderly development of resources, while minimizing impacts on the environment and developing and employing sound science and partnerships. With this goal and stakeholder concerns regarding a lack of data for the MA WEA in mind, one of the objectives BOEM sought to achieve through the study was to obtain the baseline data that could help inform its decision making processes that are focused on minimizing impacts and its responsibilities under the National Historic Preservation Act (NHPA). Additionally, BOEM sought to independently verify the accuracy and effectiveness of its own and others' recommendations for conducting surveys for archaeological information. The following sections summarize recommendations from the various chapters.

9.1 PALEOLANDSCAPE RECONSTRUCTIONS

9.1.1 INTRODUCTION

This section examines the approach taken by this study to reconstruct the submerged paleolandscape within the MA WEA as a means for identifying areas with a high probability of containing preserved submerged ancient Native American cultural resources. The approach followed the recommended steps currently outlined in BOEM's November 2012 revised *Guidelines*. Conclusions drawn from this process, as well as recommendations for possible enhancements to it for use during future investigations within the MA WEA and elsewhere, are also provided.

9.1.2 SUMMARY OF APPROACH UTILIZED

The research approach utilized during this study generally adhered to the strategy outlined in the BOEM's November 2012 revised *Guidelines*, which references and follows closely the stages of submerged paleolandscape research and reconstruction presented in Westley, et al. (2011). In summary, the individual steps of the recommended research approach, as applied during this study, involved:

- review of relevant literature on late Pleistocene and Holocene geology, paleogeography, marine and coastal prehistory, and previous archaeological resource reports for the area, as they were available;
- detailed pre-survey analysis and reconstruction of sea level rise (i.e., a series of maps depicting relative sea level rise and the modeled evolution of the shoreline at various time intervals within the MA WEA and a discussion of the sea level rise curve used in the analysis;
- discussion of relict geomorphic features that could exist in the MA WEA, the archaeological potential of these features, and the potential for these landscape features to have survived marine transgression;
- discussion of the potential to identify and evaluate precontact sites that may be present, based on the capabilities of current technology, the thickness and composition of overlying sediments, or other factors;
- analysis of sub-bottom profiler data to determine if elements of the past landscape are buried beneath more recent seabed sediments. Identification, as possible, of buried geomorphic features and any buried layers that may require further sampling to conclusively determine their nature; and
- provision of a sample of sub-bottom profiler data for each type of relict landform identified with horizontal and vertical scales.

The guidelines and Westley, et al. 2011 also recommend the acquisition and analysis of geotechnical samples (e.g., grab samples, gravity cores, vibracores, etc.) for correlation with the acoustic reflectors in the sub-bottom data. These samples also may provide visual evidence of intact paleosols, subsampling of organics for paleoenvironmental analysis, temporal dating for building transgressive chronologies and other applicable analyses. Geotechnical sampling was not an element of this study.

Data acquired through the research process outlined above can be used, if the data allows, for the ultimate purpose of creating a diachronic model of the submerged landscape of the survey area, as well as for the development of a geo-referenced model of the formerly terrestrial paleolandscape depicting it as a continuous land surface. The latter of these two plots can then be used to generate: a) a map of archaeological potential based on landscape attributes that were favored by past humans, given what is known from terrestrial sites, and; b) landscape settings that have the greatest potential for preservation of archaeological deposits, based on what is known of seabed geology and transgressive processes. These data would be available through the same existing survey activities conducted – and data collected – during site specific survey activities.

In the case of the MA WEA, existing geophysical and geotechnical data derived from background research and geophysical data acquired during the 2012 baseline survey ultimately proved insufficient for creating a continuous surface model of the formerly subaerial paleolandsurface. There simply was not sufficient sub-bottom geomorphological structure resolved in the sub-bottom data to perform cross-correlations between the surveyed track lines, though given the limited time available for data collection, this was not an unexpected outcome. Furthermore, without that land surface model, generating a map of archaeological potential based on landscape attributes favored by past humans also was not possible. Again, this was not an unexpected outcome. Given that this was the case, the question then becomes, "What *can* be concluded from the data that was generated by

the background research and field survey?" and from these conclusions, "What, if any, recommendations regarding the accuracy and effectiveness of the BOEM guidelines for conducting surveys for archaeological information can be made?" "Can the process be improved?" and, if so, "How can it be improved?" and "What areas should be the focus of future investigations within the MA WEA?"

9.1.3 Conclusions Based on the Available Data

From the literature search and detailed pre-survey analysis and reconstruction of sea level rise within the MA WEA, the first conclusion that may be drawn is that the entire MA WEA, which lay south of the terminus of the Wisconsin glaciation, was subaerially exposed up until around 13,000 yBP before it was completely submerged around 10,000 yBP, and that elements of this formerly sub-aerial paleolandscape do appear to be preserved below the surface of the sea floor. Given that the oral histories of regional tribes indicate occupation of the continental shelf in the southern New England region predates significantly the 11,200 yBP date of the earliest archaeological evidence of human habitation in southern New England (Leveillee, personal communication, 2013), as well as the complete submergence of the MA WEA by 10,000 yBP, it may also be concluded that is probable that human inhabitants once occupied and interacted with – for at least a 1,000 year period and possibly much longer – the formerly exposed paleocultural landscape comprising elements of the present sea floor within the MA WEA.

Although no provenienced finds of archaeological materials within the MA WEA have been reported to date, bottom-trawling commercial fishing vessels working off the coast of Massachusetts on George's Bank, located northeast of the MA WEA, have periodically recovered large masses of freshwater "peats" (Emery et al. 1965, 1967), as well as faunal remains of late Pleistocene-early Holocene terrestrial megafauna (e.g., mammoth teeth and a tusk). The presence of such remains suggests that elements of the broad continental shelf off the coast of southern New England, including the MA WEA, do contain elements of the formerly terrestrial environment once dominated by grassland/steppe ecotones. These ecotones were suitable for supporting large grazing and herd animals, such as the mammoth, caribou, deer, etc., that were known to be exploited by ancient Native Americans.

The principal reason why no similar ancient remains of the paleolandscape, or ecofacts, or even artifacts have been discovered to date within the MA WEA may be answered by the results from previous geophysical and geotechnical investigations as well as by the results of the present study. These survey results indicate that the Holocene sedimentary regime within the MA WEA is one that has been predominantly depositional in nature (Bothner et al. 1981; Knott and Hoskins 1968; Seigel et al. 2012). In contrast to a predominantly erosional situation, which leads to exposure and destruction of submerged paleolandscape features, depositional conditions bury and preserve elements of the paleolandscape and any cultural sites they may contain. By being situated below the maximum depth of impacts from commercial fishing bottom trawl gear, any chance for the serendipitous recovery of artifacts or ecofacts by bottom-fishing activities is greatly reduced or eliminated within the MA WEA; thus no such finds are known from the area. It may be concluded, therefore, that the chance finds of ecofacts and elements of the formerly subaerial landscape in an exposed, open-ocean environment, such as of George's Bank, similar to that of the MA WEA, and the comparatively preservative depositional sedimentary environment that prevails within the MA

WEA, would both be indicators that elements of an archaeologically sensitive paleolandscape are likely to be preserved, buried beneath the sediments comprising the relatively flat and featureless sea floor within it.

The identification of five acoustic reflectors of "archaeological interest" (see "E," "F," "H," "J," and "M" in Figure 4-1) within the MA WEA survey data from the examination of the present study's sub-bottom profiler data, confirms the conclusion above that there is a strong potential for archaeologically sensitive, stratigraphically intact paleolandforms to be preserved within the MA WEA. These reflectors are suggestive of intact elements of the former subaerially exposed paleolandscape (primarily buried paleochannels and/or shallow lacustrine features in each of these five cases) that are buried between approximately 5 and 10 m (16 and 31 ft) below the surface of the sea floor. Other geomorphological features likely to be preserved under the Holocene sediments within the MA WEA include those that would be typical of a low-relief coastal plain (e.g., shorelines/beaches, coastal ponds and lagoons, braided river and streambeds, wetlands, etc.). Identification of such features will require more intensive (i.e. tightly constrained) survey with a more powerful sub-bottom profiler that is able to resolve the substrate more fully, which would allow for cross-survey trackline correlation of acoustic reflectors and reconstruction of paleolandsurfaces, as well as geotechnical sampling (e.g., vibracoring or deep borings) to confirm the interpretation of the geophysical data and provide information for paleo-environmental characterization, refinement of the local sea level rise model, and dating of subaerial exposure and subsequent inundation. Low-lying features such as these would more likely have survived the marine transgression sequence intact, as they have a higher potential for having been inundated and buried in-place and protected from the erosional forces of wind-driven waves and tidal currents. The margins of such features would have the greatest archaeological sensitivity, as it is in these areas where ancient humans would have interacted with the water and discarded their refuse.

The potential to identify and evaluate precontact archaeological sites that may be present within the MA WEA is limited by the capabilities of current technology, the costs of performing a large-scale, detailed regional survey, limitations in the physical accessibility of the paleolandscape and any archaeological deposits it may contain because of the thickness and composition of overlying sediments, and other factors. Geophysical instruments can be satisfactory tools for identifying relatively large, discrete archaeological deposits, such as shipwrecks (in a best-case scenario), but are not particularly well-suited for the identification of the more subtle signatures that would be associated with comparatively much smaller submerged ancient Native American archaeological deposits. Shell middens, stone fish-weirs, ceremonial stone arrangements, log-boats, and, perhaps, large-scale burial sites, are among the few different types of ancient Native American submerged cultural resources that could be resolved by a detailed, site-specific geophysical survey (Figure 9-1); however, these, and virtually all other known types of ancient Native archaeological sites, would be indiscernible in the data records produced by preliminary surveys conducted on either a regional scale or using BOEM's currently recommended *Guidelines* for site-specific geophysical survey parameters. Data produced by the BOEM-recommended parameters is useful, however, for identifying and defining the preserved remains of stratigraphically-intact submerged paleolandscape where archaeological sites and cultural remains still in meaningful contexts may be present and identified through sub-surface archaeological testing.

The depth at which a paleolandscape is buried beneath the sea floor is *the* controlling factor in the techniques that are available for sub-surface archaeological testing to determine presence/absence of

cultural deposits. If the buried paleolandscape's surface lies below the vertical Area of Potential Effect (APE) of a proposed project, then testing for presence-absence is unnecessary. However, if the buried paleolandscape's surface lies within the vertical APE, then sub-surface archaeological testing to determine presence/absence of cultural deposits is necessary. For paleolandscape surfaces buried under less than a meter or two of marine sediments, conventional archaeological diver- or ROV-guided dredge-testing would be the recommended approach. Archaeological sub-surface testing of paleolandscapes buried more than a meter or two below the seafloor would require mechanical, industrial-scale techniques, such as barge-mounted sand/gravel aggregate harvesting equipment or, for shallow-water situations, barge-mounted bucket excavators, capable of reaching 3 to 5 m (10 to 16 ft) below the surface. For sub-surface testing of deeper deposits, the only remaining options are geotechnical coring and boring, which produce very small-diameter samples (ca. 10 cm [3.9 in]), but can reach far greater depths (e.g., up to about 10 m [32.8 ft] for coring and more than 50 m [164 ft] for boring).

Figure 9-1. Contact-period Native American log-boats or dug-out canoes (called "mishoonash" by the local Nipmuc Nation Tribal people) imaged using a high-resolution EdgeTech 4125 dual-frequency (400/900 kHz) chirp side scan sonar system (image courtesy of Project Mishoon).

9.1.4 RECOMMENDATIONS

Given the results of the present study and conclusions above that were drawn from them, the following is recommended:

- future geophysical surveys performed in the MA WEA by BOEM or developers should employ a more powerful sub-bottom profiling system (e.g., a seismic "boomer" or bubble-pulser) capable of penetrating the sea floor surface and fully resolving the substrate's geomorphology to, at a minimum, the depth of the late Pleistocene/subaerially exposed paleolandsurface, so that cross-survey trackline correlations can be drawn and the paleolandscape's surface reconstructed and modeled;
- selective geotechnical sampling of sub-bottom profiler acoustic reflectors of interest should be performed to: a) confirm interpretations of the geophysical record and the presence of archaeologically sensitive stratified paleosols; b) characterize paleoenvironmental conditions

at the sample location and across the MA WEA; c) date organic remains in the sample; d) refine the local sea level rise model; and e) reconstruct the paleolandscape; and

- opportunities for synergistic collaboration between industry, science, tribal and governmental agencies to jointly fund and perform high-resolution regional baseline geophysical surveys, ground-truthed by geotechnical sampling should be aggressively pursued, particularly in areas like the MA WEA. The active participation of tribal partners – the descendent communities of the ancient people whose submerged cultural resources we are attempting to identify offshore – will serve to inform the identification, interpretation, and our mutual connection to the past. Such collaboration will create a win-win scenario wherein multiple users would enjoy the benefits from the data produced and the sharing of the significant costs associated with offshore survey. Such regional survey efforts will produce detailed baseline data sets, such as three-dimensional maps of bathymetry, maps of surface-conditions, benthic habitat maps, plots and profiles of substrate geomorphology, plots of identified submerged cultural resources (i.e., shipwrecks), and reconstructions of formerly subaerial paleolandscapes characterized as likely to contain submerged ancient Native American cultural resources, all of which could be used by industry, science and governmental agencies in the development, research, and marine spatial planning on the continental shelf.

A model for the methodology and resolution of such a high-resolution regional baseline geophysical survey is one completed recently by the U.S. Geological Survey (USGS) (Ackerman et al. 2012). The USGS investigation produced precisely the kind of data that allowed for the production of a map of the detailed pre-inundation paleolandscape that can then be used by archaeologists to model archaeological sensitivity in the same manner as they would while working in a terrestrial environmental context on shore (Figure 9-2). Such mapping will also help guide decisions about where to perform geotechnical sampling to identify intact paleolandscapes and stratified, contextually intact paleosols that could then be subjected to interpretation by tribal research partners, as well as inform and prioritize archaeological sub-surface testing to determine presence/absence of culturally sensitive areas and archaeological deposits.

9.2 INTERFEROMETRIC SONAR FOR THE IDENTIFICATION OF ARCHAEOLOGICAL RESOURCES

Under BOEM's current guidelines, conventional (towed) side scan sonar arrays are recommended for use during archaeological resource assessments. During the present study, an interferometric system and side scan sonar were run simultaneously to facilitate a side-by-side comparison to determine the efficacy of interferometric sonar at detecting submerged cultural materials. Findings from this portion of the study include:

- the SWATH*plus* interferometric sonar system, operating at 234 kHz, yielded comparable resolution to the Klein 3000H side scan sonar at 445 kHz and 900 kHz under the ranges, water depths, environmental conditions, and other operational parameters of the study;
- the interferometric system was capable of swath-widths greater than those used during the study testing, greater than both the 445 kHz and 900 kHz ranges of the side scan sonar system, which could potentially increase survey efficiency;

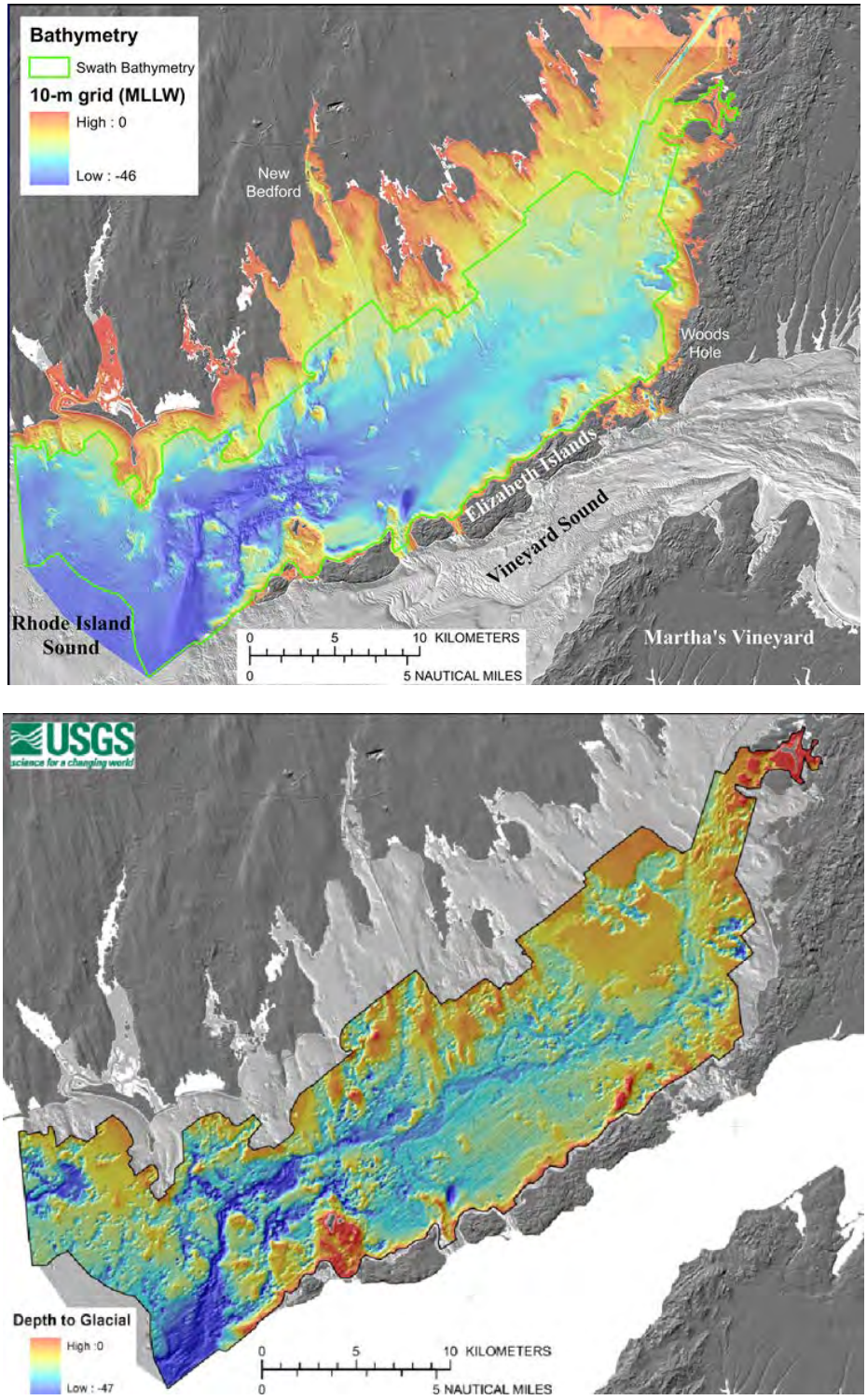

Figure 9-2. USGS plots of baseline geophysical data acquired at a 100 m trackline spacing showing multibeam bathymetry (top image) and the depth to the glacial surface (with the Holocene marine sediments stripped out) revealing a buried paleochannel and adjacent associated elements of the archaeologically sensitive paleolandscape buried and preserved beneath the surface of the seafloor (bottom image) (source: images courtesy of USGS).

- cultural materials, when present, were better visualized with side scan sonar due to the lower grazing angles which created pronounced acoustic shadows behind the object as it was ensonified;
- the output from interferometric sonar survey had greater geo-locational reliability than that from a towed side scan system, especially when used in conjunction with a motion-reference unit and regular CTD sampling; and
- it is unlikely that either interferometric or side scan systems will be able to detect artifacts smaller than 0.5 to 1 m (1.6 to 3.3 ft) on the sea floor, such as Native American material culture, or to distinguish larger objects (less than 5 m [16 ft]) in areas with heterogeneous geology.

Interferometric testing during the study built off similar testing conducted by NOAA's Office of Coast Survey in 2004 and 2006 (see Gostnell 2004 and Gostnell et al. 2006). In their first study, Gostnel utilized a Geoacoustics GeoSwath system at 250 kHz to conduct preliminary testing and found that this system was capable of resolving discrete objects with a diameter as small as 2 m (7 ft) and sand ripples as narrow as 0.1 m (0.3 ft) apart. Testing was conducted in Portsmouth Harbor in water depths up to 25 m (82 ft), conditions similar to the MA WEA. Their acquired dataset, however, was processed and compared against two shallow-water multi-beam systems, not side scan sonar systems. Interestingly, they also determined that interferometric data co-located with side scan coverage was a more effective visualization tool than interferometric coverage alone (see Gostnell 2004).

NOAA's next study focused on the efficacy of interferometric sonar for shallow water survey (average depth during testing: 7 m [23 ft]). Though this survey design is not reflective of the deeper, offshore areas managed by BOEM, their findings are nonetheless relevant. Along the Patuxent River in Maryland, they deployed three interferometric systems: the GeoAcoustics GeoSwath, SEA SWATH*plus*, and Teledyne Benthos C3D. These were compared against two multi-beam systems and one side scan sonar system (Klein 5500) currently in use by NOAA hydrographic teams. Within their survey parameters, all systems were capable of sub-meter resolution. Confirming also that interferometric systems consistently achieved twice the coverage of the multi-beam systems, the study prompted NOAA to begin interferometric system integration into shallow water (less than 15 m [49 ft]) survey platforms.

Clearly demonstrating the general effectiveness of interferometric systems, the NOAA studies prompted BOEM to begin testing this technology with respect to the detection of archaeological resources. Operating in depths up to 200 m (656 ft), however, and tasked with protecting submerged archaeological resources, be it historical shipwrecks or Native American cultural materials, BOEM required additional field research to confirm the operational capabilities of an interferometric system beyond the shallow-water bathymetric survey tests conducted by NOAA. If deemed acceptable, furthermore, BOEM would also need to consider appropriate standards for the use of interferometric sonar in archaeological resources assessments.

For example, the most recent NOAA field procedures manual (April 2013), which sets the standard operating procedures for hydrographic charting by the Office of Coast Survey, indicate that interferometric systems do not meet charting standards based, in part, on ability to resolve discrete objects and, in part, on processing. While this determination is important to note, BOEM would need

to consider independently under what specifications and appropriate processing of data the instrumentation is appropriate for its purposes The relevant section is included here in its entirety.

> Note on Phase Measuring Bathymetric Sonars (PMBS): NOAA's extensive investigation of PMBS systems (also known as interferometric sonars, or Phase Differencing Bathymetric Sonars) has shown that the discrete soundings generated by these systems have unacceptably high uncertainty for use in nautical charting and that available systems are incapable of resolving features to the standards required in this manual. NOAA has also found that statistical processing of these raw data to a gridded depth product is not currently practical due to the exceptionally high sounding density and lack of a validated uncertainty model. Therefore, bathymetry generated from PMBS systems shall not be utilized in products intended to support nautical charts unless specifically authorized by the Chief, NOS Office of Coast Survey Hydrographic Surveys Division. (NOAA 2013: 81).

The MA WEA covers a large area south of Martha's Vineyard and Nantucket with depths ranging between 32 and 65 m (105 and 213 ft). Characterized by a glacial moraine near shore, transitioning into flat, sandy substrate offshore, testing within the WEA allowed the interferometric system to be evaluated in two distinct environments, homogenous and heterogeneous geological substrates, as well as across a range of depths. In fact, the system was also deployed over a target site inshore of the WEA, at a depth of 18 m (59 ft), as well as offshore of the WEA, at depths of up to 70 m (230 ft). Testing was conducted over known shipwreck sites and within the glacial moraine to qualitatively evaluate imaging characteristics as well as to quantitatively determine the resolution and depth capability of the interferometric system.

The system deployed during this study was a SWATH*plus* interferometric sonar, running at 234 kHz. During testing, this system was consistently capable of resolving objects less than 1 m (3 ft), often as small as 0.5 m (1.6 ft), including discrete objects within moraine debris, or individual features within a shipwreck site. Limited by the range of the 445 kHz side scan sonar, testing was only conducted out to 75 m (246 ft) swath width, though the interferometric system is theoretically capable of ranges 7 to 10 times the depth of water. Thus, in the shallow portions of the WEA, the system should be capable of 210 to 300 m (689 to 984 ft) swath width. Transverse and range resolutions, however, were only tested out to 75 m (246 ft), thus additional testing is needed to determine if this resolution is consistent throughout the full range.

Another concern raised by during testing was depth limitations. Noted as efficient shallow water survey tools, interferometric systems have a theoretical depth limit where the broadcasted signal deteriorates as energy is dissipated into the surrounding water. Most of the testing during the Baseline Survey was conducted in the 20 to 40 m (66 to 131 ft) range, so performance in deeper depths is still inconclusive. Qualitative observations made while operating the system in depths up to 70 m (23 ft; over a flat, sandy, featureless bottom) indicated the system may lose resolution at greater depths. Another depth-related consideration is the performance of the system in stratified waters where sound velocity varies through the water column. Additional testing in deeper water is perhaps the most pressing need to evaluate the capabilities of interferometric systems for targeted archaeological survey in offshore federally managed areas.

Though the interferometric system performed comparably to medium and high frequency side scan sonar during testing, several qualitative observations were made as a result of the comparison. By virtue of its design, the interferometric system was far superior to side scan sonar in terms of the quality of navigation data and geo-locational reliability. Pole mounted on the survey vessel, and

processed to correct for sound-velocity and vessel motion, position data gathered by the interferometric system eliminated the inaccuracy inherent with towed systems (cable-out, layback, and sensor altitude). The visual output of the interferometric system, on the other hand, was not as intuitive as the side scan sonar, making discrete objects more difficult to identify. The proximity of the side scan sonar to the seafloor results in lower grazing angles between the broadcasted sound waves and the ensonified object. This produces a more noticeable acoustic shadow behind the object, creating a more obvious signature for the sonar operator.

Based upon these preliminary test results, the 234 kHz interferometric system utilized was capable of resolving cultural materials in the depth ranges tested (18 to 40 m [50 to 131 ft], averaging 30 m [98 ft]), at line intervals of 75 to 100 m (246 to 328 ft). Additional testing is needed to assess the performance of the system at similar depths, with wider swaths, as well as in deeper water (up to 200 m [656 ft]). Based upon this testing, however, this specific system proved adequate for targeted archaeological survey within these given survey parameters. In short, based on the survey results collected by this project, interferometric sonar systems provide adequate resolution and coverage to be used as an alternative to a towed-array system for water depths of up to 40 m (131 ft) and with survey lane spacing of 75 to 100 m (246 to 328 ft; depending on water depth) for the purposes of conducting surveys for identification under Section 106 of the NHPA.

For deeper water and wider lane spacing, in light of the theoretical capability of interferometric systems to achieve drastically increased swath widths when compared to side scan sonars, a capability which translates into a significant economic benefit to surveyors and applicants, the agency should continue testing the viability of interferometric sonar throughout the range of conditions present in areas managed by BOEM. Theoretical limits to interferometric systems hold considerable promise for wider swath width in deeper water; however, this study did not verify the actual resolution of these systems in deeper water and at extended ranges greater than 100 m (328 ft). Should the agency determine interferometric systems inadequate for deeper-water survey, they should still consider them as a viable tool for shallow water environments. Though not an objective of this study, these test results indicate that interferometric sonar may also be a useful to for high-resolution geophysical survey.

BOEM's current guidelines for acoustic survey during archaeological resource assessments are tailored to towed side scan sonar arrays. Given that interferometric systems operate in a fundamentally different manner, BOEM would need to consider re-drafting its *Guidelines* should they deem these systems acceptable for use. Specifically, the *Guidelines* detail survey line spacing distances and sensor altitudes not appropriate for boat-mounted interferometric systems. Instead, BOEM should consider a separate set of recommendations which would amend their current guidelines for side scan sonar. These could include a range of effective frequencies, swath widths, sound-velocity testing intervals, processing requirements for motion reference data and tide corrections, as well as a maximum recommended depth of water for deployment of the system.

9.3 MAGNETIC SURVEY FOR THE IDENTIFICATION OF ARCHAEOLOGICAL RESOURCES

Guidelines that address data processing and confidence reporting – which are integral factors to understanding the coverage and quality of a magnetic survey dataset – will allow BOEM to assess the quality of the data being submitted and the effectiveness of their own magnetic survey standards.

One recommendation is that BOEM include in future versions of the *Guidelines* a provision whereby magnetometer data are provided to the agency in multiple forms: as processed maps, tables and narrative text, along with recommendations for avoidance/mitigation, that adheres to published agency standards; and as raw data that includes locational data, measured magnetic intensity and sensor height over bottom in electronic format that can be independently analyzed and checked through a Quality Assurance/Quality Control (QA/QC) process by BOEM staff or other contractors.

Additionally, BOEM should conduct confidence reporting. Confidence reporting reprocesses the acquired data to map areas of actual detection and it identifies specific gaps within the acquired dataset that need to be treated differently from the rest of the survey area. The conclusion of a magnetic survey should include a description of the survey in terms of possible archaeological material left undetected as a result of survey design and as a result of course made good (the course actually achieved on the chart [map], after making allowances for wind direction and currents.).

Because of the potential for error in data processing and in confidence reporting, review by BOEM archaeologists of at least a sample of the magnetometer data submitted by developers should be an essential component in the 106 compliance portion of any and all lease block developments.

Moreover, BOEM needs to quantitatively assess the magnetometer data received to ensure that the bureau is making an appropriate level of effort in the identification and protection of archaeological resources. With modern technology, rapid automated processing by computer programs—in particular GIS—BOEM can significantly improve the effectiveness and confidence of marine magnetic survey. In other words, BOEM needs a method of automating the assessment of magnetometer coverage and confidence; potentially an open-source software platform which streamlines the geoprocessing functions outlined throughout the chapter. This will allow BOEM to quickly and independently verify the quality of the survey data as the agency moves to address its management responsibilities.

Developing the capability to assess the reliability of this data also allows BOEM to monitor the effectiveness of its guidelines and to adjust survey recommendations and reporting standards, as needed, to ensure data quality standards are met and are clearly communicated between the bureau and developers.

Operational testing, therefore, is needed to review and revise the parameters of the algorithmithic model so it more accurately depicts the relationship between submerged magnetic objects in a marine environment. Ultimately, this will result in more effective survey design and confidence reporting. Until such data is collected, however, these quantitative assessment protocols are merely theoretical.

In summary, there is a need to determine the optimal methods and the most accurate mathematical parameters to extrapolate reliable and comprehensive anomaly information from a magnetic dataset so that archaeological materials of interest can be identified. This should be specified in an explicit research and survey design. Much work remains to produce a comprehensive body of research on marine magnetic sensing. BOEM should test this algorithm by conducting magnetic surveys over known archaeological sites and magnetic objects of known size to verify and adjust the modeling algorithm as needed.

9.4 CONSIDERATIONS REGARDING ACOUSTIC EFFECTS DURING THE OPERATION OF GEOPHYSICAL SURVEY EQUIPMENT

This report provides the analysis, results, and findings of the sound source characterization data collected in Rhode Island Sound on 29 and 30 August 2012. Three acoustic noise sources utilized in the present study were targeted: the research vessel (R/V *SRVx*), the interferometric sonar (SEA SWATH*plus*-M), and the sub-bottom profiler (EdgeTech 3200 SB-0512i). The data were collected at two sites with different water depths (30 and 60 m [98 to 197 ft]) with the survey equipment operating at various settings

In 2010, sound propagation modeling was performed for geophysical survey equipment at multiple sites in the Mid- and South-Atlantic (Zykov et al. 2012). The results from one of the model's scenarios (Scenario 22) were comparable to the present study's scenarios because it had a water depth of 30 m (98 ft) and a sandy bottom, similar to the conditions at the Shallow Site. The test scenario that exhibited the highest received levels during the field measurements (Scenario S5: 0.5 to 2.7 kHz, 100 ms, FM) was selected for the comparison. After comparing the predicted and measured distances to sound level thresholds, the researchers concluded that the modeling provided conservative results, i.e., the observed received levels are below the model estimates with few exceptions.

The analysis presented in this report showed that the maximum sub-bottom profiler frequency spectrum is approximately at the middle frequency of the operational frequency band. The measured beam pattern closely matches the theoretical beam pattern at the middle frequency of the operational frequency band as well. These two facts support the modeling approach used, in which all the acoustic energy is assigned to a single frequency and the propagation modeling is performed for only that single frequency. In the acoustic modeling, propagation modeling is commonly performed for only the middle frequency of a frequency band (e.g., modeling central frequency of 1/3-octave bands). The variation of the propagation conditions for the acoustic waves of different frequencies within the sweep frequency band is negligible; therefore, the approach of performing propagating modeling for just a single frequency that caries the main characteristics of the source (source level and beam pattern) is valid.

JASCO suggests adopting the following procedures when operating a sub-bottom profiler or an interferometric sonar to reduce the ensonification of the surrounding environment:

- use the highest frequency band possible for the sub-bottom profiler. The beam of the sub-bottom profiler is narrower at high frequency and therefore emits less acoustic energy toward the horizontal;

- while short pulses (5 to 20 ms) can result in higher root-square-mean (rms) sound pressure levels (SPL) than longer pulses, short-duration pulses have lower sound exposure level (SEL) and are perceived as less loud by mammals than long-duration pulses (Au and Hastings 2008); therefore, JASCO recommends using the shortest possible pulse length; and
- the Cumulative Sound Exposure Levels (cSEL) calculated over a specific period of the survey can be reduced by lowering the pulse rate (pings per second). Changes to the pulse rate do not affect rms SPL or SEL calculated over each pulse. The effect on the cSEL values can be estimated by the following formula: $\Delta cSEL = 10 \cdot \log(R/R_0)$, where $\Delta cSEL$ is the change in the cumulative SEL, R and R_0 are the desired and original pulse rates (number of pings per second) respectively.

The following are recommended for future sound source characterization measurements:

- for the sources with the beam pointing downward (e.g., the sub-bottom profiler) it is important to obtain data for the horizontal position of the source as close as possible to the recorder in order to obtain the measurement for the main lobe of the beam;
- there is no benefit of driving the source as close as possible to the recorder for the systems which feature beams pointing to the sides (e.g., the interferometric sonar). The received levels directly below the source will not be the maximum levels;
- more than two samples must be collected in the main beam for highly directive sources such as the interferometric sonar. More off-track recorders could be deployed or more test tracks could be used with various distances. Choose a range that ensures recorders receive at least one ping from the sonar's main-lobe;
- satisfactory results for omnidirectional in the horizontal plain sources (e.g., sub-bottom profiler, vessel) can be achieved with just two recorders. Detailed source characterizations require more data. Using only one recorder is not recommended; and
- the dynamic range of the recorders should extend at least 10 dB above the anticipated maximum received levels to ensure accurate assessment of peak sound levels.

Bibliography

Ackerman, Seth D., Brian D. Andrews, David S. Foster, Wayne E. Baldwin, and William C. Schwab. 2012. *High-Resolution Geophysical Data from the Inner Continental Shelf: Buzzards Bay, Massachusetts*. U.S. Geological Survey Open-File Report 2012-1002.

Aerodata International. 1987. *U.S. Navy Carrier Fighters of World War II*. Squadron/Signal Publishers, Carrollton, TX.

Albion, Robert B., William A. Baker, Benjamin W. Labaree, and Marion V. Brewington. 1972. *New England and the Sea*. Wesleyan University Press, Middletown, Connecticut.

Au, W., and M. Hastings. 2008. *Principles of Marine Bioacoustics*. Springer, NY. ISBN 978-0-387-78364-2.

Automated Wreck and Obstruction Information System, NOAA Office of the Coast Survey 2012. http://www.nauticalcharts.noaa.gov/hsd/awois.html Accessed in 2012.

Barber, R. J. 1979. A summary and analysis of cultural resource information on the continental shelf from the Bay of Fundy to Cape Hatteras. Final Report, Vol. II, Archaeology and Paleontology. Cambridge, MA: Institute for Conservation Archaeology, Harvard University.

Bard, E., Hamelin, B., and Delanghe-Sabatier, D., 2010, Deglacial meltwater pulse 1B and Younger Dryas sea levels revisited with boreholes at Tahiti. *Science*, v. 327, p. 1235-1237.

Barnhardt, W.A., Gehrels, R., and Kelley, J.T., 1995, Late Quaternary relative sea-level change in the western Gulf of Maine: Evidence for a migrating glacial forebulge: *Geology*, v. 23, p. 317-320.

Bauer, Jack K. 1988. *A Maritime History of the United States: The Role of America's Seas and Waterways*. University of South Carolina Press, Columbia, South Carolina.

Belknap, D.F., Anderson, B.A., Anderson, R.S., Anderson, W.A., Borns Jr., H.W., Jacobson, G.L., Kelley, J.T., Shipp, R.C., Smith, D.C., Stuckenrath Jr., R., Thompson, W.B., and Tyler, D.A., 1987, Late Quaternary sea-level changes in Maine, *in* Nummedal, D., ed., Sea-level fluctuation and coastal evolution: Society of economic paleontologists and mineralogists Special Publication Volume 41, p. 71-85.

Bell, Edward L. 2009. Cultural Resources on the New England Coast and Continental Shelf: Research, Regulatory, and Ethical Considerations from a Massachusetts Perspective. Coastal Management 37(1) 17 — 53.

Bohling, G. 2005. *Kriging*. Kansas Geological Survey, Lawrence, KS. Accessed 20 Sept. 2012.

Boothroyd, Jon C. and Peter V. August. 2008. Chapter 1: "Geologic and Contemporary Landscapes of the Narragansett Bay Ecosystem Science for Ecosystem-based Management." In *Science for Ecosystem-based Management*, edited by Alan Desbonnet and Barry A. Costa-

Pierce. pp. 1-33. Springer Series on Environmental Management. David E. Alexander, general editor. Springer, New York.

Bourque, B. J. 1979. A summary and analysis of cultural resource information on the continental shelf from the Bay of Fundy to Cape Hatteras. Final Report, Vol. III, Historic Shipping. Cambridge, MA: Institute for Conservation Archaeology, Harvard University.

Bothner, M.H., E.C. Spiker, P.P. Johnson, R.R. Rendigs, and P.J. Aruscavage, 1981. Geochemical Evidence for Modern Sediment Accumulation on the Continental Shelf off Southern New England. *Journal of Sedimentary Petrology* 51(1):281-292.

Bowers, Peter M. 1999. *Boeing B-29 Superfortress*. Specialty Press Publishers and Wholesalers, North Branch, NM.

Breiner, S. 1999a Magnetic Search in the Marine Environment. Geometrics, San Jose, CA less than ftp://geom.geometrics.com/pub/mag/Literature/MarineSearch.pdf greater than. Accessed 10 Sept. 2012.

Breiner, S. 1999b. *Applications Manual for Portable Magnetometer*. Geometrics, San Jose, CA less thanftp://geom.geometrics.com/pub/mag/Literature/AMPM-OPT.PDFgreater than. Accessed 10 Sept. 2012.

Bureau of Ocean Energy Management (BOEM). 2012. *Guidelines for Providing Geological and Geophysical, Hazards, and Archaeological Information Pursuant to 30 CFR Part 585*. Office of Alternative Energy Programs, US Department of the Interior, Bureau of Ocean Energy Management, Regulation and Enforcement, Herndon, VA.

Camidge, K., P. Holt, C. Johns, L. Randall, and A. Schmidt. 2009. *Developing Magnetometer Techniquest to Identify Submerged Archaeological Sites: Rev. 02, Final Report*. Historic Environment, Environment, Planning & Economy; Cornwall Council. Cornwall, UK. 121 pp.

Caruana, A. B. 1994. *The History of English Sea Ordnance 1523-1875*, Volume I: 1523-1715 The Age of Evolution. Jean Boudriot Publications, East Sussex, England.

Caruana, A. B. 1997. *The History of English Sea Ordnance 1523-1875*, Volume II: 1715-1815 The Age of the System. Jean Boudriot Publications, East Sussex, England.

CFM International. 2010. *CFM56-3 Technology*. CFM International website. less thanhttp://www.cfmaeroengines.com/_engines/cfm56-3greater than. Accessed 22 Oct. 2012.

Chesapeake Technology Inc., 2012. SonarWiz5, accessed July 1, 2012, http://www.chesapeaketech.com/products.html.

Coleman, D.F., 2008, Archaeological and Geological Oceanography of Inundated Coastal Landscapes, an Introduction, *in* Ballard, R.D., ed., Archaeological Oceanography, Princeton University Press.

Coleman, Dwight. F., and Kevin McBride, 2008. Underwater Prehistoric Archaeological Potential of the Southern New England Continental Shelf off Block Island. In *Archaeological Oceanography* (Ballard, Robert D. ed.), pp. 200-223. Princeton University Press, Princeton, NJ.

Cultural Resources Committee. 1990. Maritime Cultural Resources of Massachusetts Bay: The Present State of Identification and Documentation. Massachusetts Bay Marine Studies Consortium: Boston, Massachusetts.

Curryer, Betty Nelson. 1999. *Anchors: An Illustrated History*. Naval Institute Press, Annapolis, MD.

Dresser, Thomas. 2011. *The Wampanoag Tribe of Martha's Vineyard: Colonization to Recognition*. The History Press, Charlestown, SC.

Donnelly, J.P., and Bertness, M.D., 2001, Rapid shoreward encroachment of salt marsh cordgrass in response to accelerated sea-level rise: Proc. Natl. Acad. Sci. U.S.A, v. 98, p. 14214-14223.

Dyke, A.S., and Peltier, W.R., 2000. Forms, response times and variability of relative sea-level curves, glaciated North America: *Geomorphology*, v. 32, p. 315-333.

Dyke, A.S., and Prest, V.K., 1987, Late Wisconsinan and Holocene history of the Laurentide ice sheet: Geographie physique et Quaternaire, v. 41, p. 237-263.

EdgeTech. 2009. 3200-XS Sub-Bottom Profiling System: User's Manual. Document No. 990-0000026-1000, Rev. 2.3

EdgeTech, 2012. EdgeTech: Sub-bottom profiler descriptions, accessed July 1, 2012, available online at http://www.edgetech.com/edgetech/gallery.

Emery, K. O., R. L. Wigley, and Meyer Rubin, 1965. A Submerged Peat Deposit Off the Atlantic Coast of the United States. *Limnology and Oceanography*, Supplement: Alfred C. Redfield 75th Anniversary Volume 10:97-102.

Emery, K. O., R. L. Wigley, Alexandra S. Bartlett, Meyer Rubin, and E. S. Barghoorn, 1967. Freshwater Peat on the Continental Shelf. *Science*, New Series, 158(3806):1301-1307.

Fairbanks , R.G., 1989, A 17,000 year glacio-eustatic sea level record: influence of glacial melting rates on the Younger Dryas event and deep ocean circulation: Nature, v. 342.

Faught, M.K. 2002. Submerged Paleoindian and Archaic sites of the Big Bend, Florida. *Journal of Field Archaeology*, Volume 29, Numbers 3-4, pp. 273-290.

Faught, M.K. 2004. The underwater archaeology of paleolandscapes. *American Antiquity*, Volume 69, Number, pp. 275-289.

Fedje, D. and H. Josenhans. 2000. Drowned forests and archaeology on the continental shelf of British Columbia, Canada. *Geology* 28: 99-102.

Ferris, Donald L. 1994. *Exploring the Waters of Cape Cod: Shipwrecks and Dive Sites*. Bailey Press, Boston, MA.

Fischer, Anders, 1997. People and the Sea – Settlement and Fishing along the Mesolithic Coasts. Chapter 2.2 in *The Danish Storebaelt Since the Ice Age – Man, Sea and Forest*, eds. Lisbeth Pedersen, Anders Fischer, and Bent Aaby. A/S Storebaelt Fixed Link, Kalundborg Regional Museum, The National Forest and Nature Agency, and the National Museum of Denmark, Copenhagen, DK.

Fish, J.P. and H.A. Carr. 1990. *Sound Underwater Images: A Guide to the Generation and Interpretation of Side Scan Sonar Data*. Lower Cape Publishing, Orleans, MA.

Francois R.E. and G.R. Garrison. 1982. Sound absorption based on ocean measurements: Part II: Boric acid contribution and equation for total absorption. JASA 72:1879-1890.

Gafney, V.F., K. Thomson, and S. Fitch (eds) 2007. *Mapping Doggerland: The Mesolithic Landscapes of the Southern North Sea*. BAR British Series 31: Oxford, Archaeopress.

Garrison, L., 1967. *Cretaceous-Cenozoic Development of the Continental Shelf South of New England.* Unpublished doctoral thesis, University of Rhode Island Graduate School of Oceanography, Narragansett, RI.

Garrison, Ervan. G., Jeffrey L. Holland, Alice R. Kelley, Joseph T. Kelley, Darrin Lowery, Daria E. Merwin, David S. Robinson, Christopher A. Schaefer, Brian W. Thomas, Larissa A. Thomas, and Gordon P. Watts, 2011. *Prehistoric Site Potential and Historic Shipwrecks on the Atlantic Outer Continental Shelf*. Final Report prepared under MMS Contract GS-10F-0401M M09PD00024 by TRC Environmental Corporation, Norcross, GA. Published by U.S. Department of the Interior Bureau of Ocean Energy Management, Regulation and Enforcement, Atlantic OCS Region, Herndon, VA.

Gibbons, Tony (editor). 2001. *The Encyclopedia of Ships: Over 1,500 Military and Civilian Ships from 5000 B.C. to the Present Day*. Thunder Bay Press, San Diego, CA.

Goldsmith, R., 1982, Recessional moraines and ice retreat in southeastern Connecticut: Dubquene, Kendall - Hunt, 61-76 p.

Gostnell, C. 2004. Efficacy of interferometirc sonar of hydrograhic surveying: Do interferoneters warrant an in-depth examination? Report by Hydrographic Survey Division, Office of Coast Survey, National Ocean Service, National Oceanic and Atmospheric Administration, Silver Spring, MD. Available from: http://www.nauticalcharts.noaa.gov/hsd/docs/SW_techpaper_gostnell.pdf. Accessed May 2012

Gostnell, C., J. Yoos, and S. Brodet. 2006. NOAA Test and Evaluation of Interferometric Sonar Technology. Report by Hydrographic Survey Division, Office of Coast Survey, National Ocean Service, National Oceanic and Atmospheric Administration, Silver Spring, MD.

Gramly, Richard M., 1982. The Vail Site: A Palaeo-Indian Encampment in Maine. *Bulletin of the Buffalo Society of Natural Sciences* (Vol. 30), Buffalo, NY.

Graumont, Raoul and John Hensel 1994 *Splicing Wire & Fiber Rope.* Cornell Maritime Press, Centreville, MD.

Henkart, P., 2011. SIOSEIS – The introduction: software package sponsored by the National Science Foundation and the Scripps Industrial Associates., URL http://sioseis.ucsd.edu/index.html ; accessed July 1, 2011.

Hughes, Charles H. 1917. *Handbook of Ship Calculations, Construction and Operation*. D. Appleton and Company, New York, NY.

Knott, S.T., and H. Hoskins, 1968. Evidence of Pleistocene Events in the Structure of the Continental Shelf off the Northeastern United States. Marine Geology 6:5-43.Ingham, A.E. 1975. *Sea Surveying*. John Wiley & Sons, New York, NY.

ITC. 1993. *Application Equations for Underwater Sound Transducers* (pamphlet). International Transducer Corporation, Santa Barbara, CA.

Kinsler, L.E., A.R. Frey, A.B. Coppens, and J.V. Sanders. 1950. *Fundamentals of Acoustics*. John Wiley & Sons Inc., New York.

Knott, S.T., and H. Hoskins, 1968. Evidence of Pleistocene Events in the Structure of the Continental Shelf off the Northeastern United States. *Marine Geology* 6:5-43.

Koteff, C., and Larsen, F.D., 1989, Postglacial uplift in western New England: geologic evidence for delayed rebound, *in* Gregersen, S., S. Basham, ed., Earthquakes at North-Atlantic passive margins: Neotectonics and postglacial rebound 105-123.

Koteff, C., Robinson, G.R., Goldsmith, R., and Thompson, W.B., 1993, Delayed postglacial uplift and synglacial sea levels in coastal central New England: *Quaternary Research*, v. 40, p. 46-54.

Leverington, D.W., Teller, J.T., and Mann, J.D., 2002, A GIS method for reconstruction of late Quaternary landscapes from isobase data and modern topography: *Computers & Geosciences*, v. 28, p. 631-639.

Liu, J.P., and Milliman, J.D., 2004. Reconsidering meltwater pluses 1A and 1B: Global impacts of rapid sea level rise. *Journal of Oceans University of China* 3:183-190.

Massa, D.P. 1999. *Choosing and ultrasonic sensor for proximity or distance measurement; part 2: Optimizing sensor selection*. *Sensors*. March 1, 1999. http://www.sensorsmag.com/

Massachusetts Executive Office of Energy and Environmental Affairs (MA EOEEA). 2009. Massachusetts Ocean Management Plan. (Volumes I and II) December 2009. Online at http://www.mass.gov/eea/ocean-coastal-management/mass-ocean-plan/final-massachusettsocean-management-plan.html. Accessed March 7, 2012.

Macalaster, G. 2013. Fisherman Finds Mammoth Tooth in Load of Scallops. New Hampshire Union Leader, February 21, 2013. http://www.newhampshire.com/article/20130221/NEWS01/130229729/1006/news03).

Marine Protected Areas Federal Advisory Committee. 2011. Committee Recommendations for Integrated Management Using a Cultural Landscape Approach in the National MPA System. http://www.mpa.gov/pdf/helpful-resources/mpafac_rec_cultural_landscape_12_11.pdf.

Massachusetts Historical Commission (MHC). 1987. *Historic and Archaeological Resources of Cape Cod and the Island: A Framework for Preservation Decisions*. Massachusetts Historical Commission, Office of the Secretary of State, Boston.

Massachusetts Ocean Resource Information System (MORIS) n.d: Massachusetts Office of Coastal Zone Management (MA CZM) Online Mapping Tool at: http://www.mass.gov/czm/mapping/index.htm. Accessed March 2012.

Massachusetts Office of Coastal Zone Management (MA CZM). n.d.(a). Coastal Public Access Sites. Online at: http://maps.massgis.state.ma.us/czm_access_locator/viewer.htm. Accessed March 12, 2012.

Mastone, Victor T. 2002. Massachusetts: The Devil to Pay and No Pitch Hot! In International Handbook of Underwater Archaeology, C.V. Ruppe and J.F. Barstad, editors, pages 145-157. New York: Kluwer Academic/Plenum Publishers.

Mather and Jensen. 2010. Investigations into Block Island's Submerged Cultural Sites and Landscapes for the Rhode Island Ocean Special Area Management Plan 2010 (Technical Report #5). Online at: http://seagrant.gso.uri.edu/oceansamp/pdf/appendix/05-Mather-Jensen-Cultural%20Resources.pdf. Accessed April 24, 2012.

Mazel, C. 1985. *Side Scan Sonar Record Interpretation*. Klein Associates Manual.

McKay, John. 1987. *100-gun Ship Victory*. Conway Maritime Press, London, England.

McLoughlin, William G. 1978. *Rhode Island: A Bicentennial History.* W.W. Norton & Company, Inc., New York.

McMaster, Robert L. 1984. Holocene Stratigraphy and Depositional History of the Narragansett Bay System, Rhode Island, U.S.A. *Sedimentology* 31, 777-792.

Merwin, Daria E. 2001. Preliminary Investigation of Submerged Prehistoric Resources in the Mid-Atlantic Bight. Paper presented at the Society for Historical Archaeology 35th Conference on Historical and Underwater Archaeology, Mobile, Alabama.

Merwin, Daria E. 2003. The Potential for Submerged Prehistoric Archaeological Sites off Sandy Hook. Bulletin of the Archaeological Society of New Jersey 57: 1-10.

Merwin, Daria E. 2010. *Submerged Evidence of Early Human Occupation in the New York Bight*. Doctoral dissertation, Department of Anthropology, Stony Brook University, Stony Brook, NY.

Merwin, Daria E. and David J. Bernstein. 2003. A GIS-Based Model for Predicting the Location of Submerged Prehistoric Archaeological Sites in New York Harbor. Section VII: 24 pp. In Final Reports to the Tibor T. Polgar Fellowship Program, 2002, edited by J.R. Waldman and W.C. Nieder. Hudson River Foundation, New York.

Merwin, Daria E., Daniel P. Lynch, and David S. Robinson. 2003. Submerged Prehistoric Sites in Southern New England: Past Research and Future Directions. Bulletin of the Archaeological Society of Connecticut 65:41-56.

Miller, Edward M. 1978. *U.S.S. Monitor: The Ship That Launched A Modern Navy*. Leeward Publications, Annapolis, MD.

Morison, Samuel Eliot. 1961. *The Maritime History of Massachusetts: 1730-1860*. Northeastern University Press, Boston, MA.

NAVD88 North American Vertical Datum of 1988, National Geodetic Survey http://www.ngs.noaa.gov/PUBS_LIB/NAVD88/navd88report.htm

NGDC, 1999, U.S. Coastal Relief Model - Northeast Atlantic, Volume 1, National Geophysical Data Center, NESDIS, NOAA, U.S. Department of Commerce, Washington, DC.

NOAA Office of Coast Survey 2013. NOS Hydrographic Specifications and Deliverables. Updated April 2013.

Oakley, B.A. and J.C. Boothroyd, 2012. Reconstructed topography of Southern New England prior to isostatic rebound with implications fo total isostatic depression and relative sea level. *Quaternary Research* vol. 78 issue 1 July, 2012. P. 110-118.

Oldale, R.N., and O'Hara, C.J., 1980, New radiocarbon dates from the inner continental shelf off southern Massachusetts and a local sea-level rise curve for the past 12,000 years: Geology, v. 8, p. 102-106.

Paasch, H. 1885. *Paasch's Illustrated Marine Dictionary*. Lyons & Burford, New York, NY. Reprinted 1997 by Conway Maritime Press, London, England.

Pearson, C.E., S.R. James, Jr., M.C. Krivor, S.D. El Darragi, and L. Cunningham. 2003. *Refining and Revising the Gulf of Mexico Outer Continental Shelf Region High-Probability Model for Historic Shipwrecks: Final Report*. Volume II: Technical Narrative. U.S. Dept. of the Interior, Minerals Management Service, Gulf of Mexico OCS Region, New Orleans, LA OCS Study MMS 2003-061, 195 pp., 3 vol.

Peck, John A. and Robert L. McMaster. 1991. Stratigraphy and Geologic History of Quaternary Sediments in Lower West Passage, Narragansett Bay, Rhode Island. *Journal of Coastal*

Research. SPECIAL ISSUE NO. 11. Quaternary Geology of Long Island Sound and Adjacent Coastal Areas: Walter S. Newman Memorial Volume: 25-37.

Peltier, W.R., and Fairbanks, R.G., 2006, Global glacial ice volume and Last Glacial Maximum duration from an extended Barbados sea level record. *Quaternary Science Reviews* 25:3,322-3,337.

Perdue, Theda. 1985. *Native Carolinians: The Indians of North Carolina*. North Carolina Division of Archives and History, Department of Cultural Resources, Raleigh.

Phelps, David Sutton. 1983. Archaeology of the North Carolina Coast and Coastal Plain, in *The Prehistory of North Carolina: An Archaeological Symposium*, Mark A. Mathis and Jeffery J. Crow, editors. North Carolina Division of Archives and History, Department of Cultural Resources, Raleigh.

Reid, J. M., Reid, J. A., Jenkins, C. J., Hastings, M. E., Williams, S. J., and Poppe, L. J., 2005. usSEABED: Atlantic coast offshore surficial sediment data release: U.S. Geological Survey Data Series 118, version 1.0. Online at http://pubs.usgs.gov/ds/2005/118/.

Rhode Island Coastal Resources Management Council (RICRMC). 2010. *Rhode Island Ocean Special Area Management Plan (SAMP), Volumes 1 and 2.* Prepared by the Coastal Resources Center, 260 University of Rhode Island, Narragansett, RI for the Coastal Resources Management Council. Providence, RI. 1021 pp.

Rhode Island Shipwreck Database. n.d. Rhode Island Historical Preservation & Heritage Commission. Private database. Accessed March 7, 2012.

Ridge, J.C., 2004, The Quaternary glaciation of western New England with correlations to surrounding areas, in Ehlers, J., and Gibbard, P.L., eds., *Quaternary glaciations - extent and chronology: Part II: North America. Developments in Quaternary Science, Volume 2B.* Amsterdam, Elsevier, p. 163-193.

Robinson, David S., Ben Ford, Holly Herbster, and Joseph N. Waller, Jr. 2003. Marine Archaeological Sensitivity Assessment: Cape Wind Energy Project, Nantucket Sound, Massachusetts. Submitted to Cape Wind Associates, LLC, Boston, Massachusetts by PAL, Pawtucket, Rhode Island.

Robinson, D. S., B. Ford, H. Herbster, J. N. Waller, Jr., J. Bailey, S. K. Faldetta, and J. King, 2004. *Marine Archaeological Reconnaissance Survey, Cape Wind Energy Project, Nantucket Sound, Massachusetts*. Submitted to Cape Wind Associates, Inc., by the Public Archaeology Lab (PAL), Pawtucket, RI. PAL Report 1485.

Schafer, J.P., and Hartshorn, J., 1965, The Quaternary of New England, *in* Wright, J., and Frey, D., eds., The quaternary of the United States: Princeton, N.J., Princeton University Press, p. 113-127.

Shope, S.M. 2011. *Magnetic Gradient Processing*. Report to National Park Service Submerged Resources Center, Lakewood, CO, from Sandia Research Corporation, Mesa, AZ.

Siegel, Jacob, Brandon Dugan, Daniel Lizarralde, Mark Person, Whitney DeFoor, and Nathanial Miller, 2012. Geophyical evidence of a late Pleistocene glaciation and paleo-ice stream on the Atlantic Continental Shelf offshore Massachusetts, USA. *Marine Geology* 303-306:63-74.

Society of Exploration Geophysicists ("SEG"), 2012. Technical standards, available online at http://www.seg.org/documents/10161/77915/seg_y_rev1.pdf.

Stanford, Dennis and Bruce Bradley. 2012. *Across Atlantic Ice: The Origin of America's Clovis Culture*. University of California Press, Berkeley.

Stanford, S.D., 2010, Onshore record of Hudson River drainage to the continental shelf from the late Miocene through the late Wisconsinan deglaciation, USA: synthesis and revision. *Boreas*, v. 39, p. 1-17.

Stright, Melanie J. 1986. Human Occupation of the Continental Shelf during the Late Pleistocene/Early Holocene: Methods for Site Location. *Geoarchaeology*. Vol. 1, No. 4, 347-64.

Systems Engineering and Assessment Ltd. (SEA). 2010. SWATH*plus* (pamphlet). Data sheet OD DS SWATH*plus* 091222 revision 0. Systems Engineering & Assessment Ltd. http://www.sea.co.uk/Docs/Offshore/SWATHPLUS%202PP%20DATA%2022%202.pdf

Tarrant, V.E. 1989. *The U-Boat Offensive 1914-1945*. Sterling Publishing Co, New York, NY.

TRC Environmental Corporation (TRC). 2012. *Inventory and Analysis of Archaeological Site Occurrence on the Atlantic Outer Continental Shelf*. U.S. Dept. of the Interior, Bureau of Ocean Energy Management, Gulf of Mexico OCS Region, New Orleans, LA. OCS Study BOEM 2012-008. 324 pp. Accessed May 2012.

van de Plassche, O., van der Borg, K., and de Jong, A.F.M., 1998, Sea level-climate correlation during the past 1400yr: Geology, v. 26, p. 319-322.

Hendricks, Marcus, and David Weeden, Mashpee Wampanoag Cultural Resource Monitors, and Ramona Peters, Tribal Historic Preservation Officer. Multiple conversations with Brandi Carrier of the Bureau of Ocean Energy Management, Office of Renewable Energy Programs on Wampamog oral traditions, July, August, and September, 2012.

West, William R., and Betty West Morris. 2004. Native Americans in Tyrrell County, in *The Heritage of Tyrrell County North Carolina*, Volume 1, Gwen A. White and Virginia C. Haire, editors. Tyrrell County Genealogical and Historical Society in Cooperation with County Heritage, INC, Waynesville, NC, pp. 128-132.

Westley, K., Bell, T., Plets, R., and Quinn, R., 2011. Investigating Submerged Archaeological Landscapes: a Research Strategy Illustrated with Case Studies from Ireland and Newfoundland, Canada. Chapter 11 in *Submerged Prehistory*, eds. Benjamin, J., Bonsall, C., Pickard, C., and Fischer, A. Oxbow Books, Oxford, UK.

WGS84 World Geodetic System, U.S. National Geospatial-Intelligence Agency. http://earth-info.nga.mil/GandG/wgs84/index.html

Wetmore, John F. 1975. *First on the Land: The North Carolina Indians*. John F. Blair, Publisher, Winston Salem, NC.

Weymouth, John W. 1976. *A Magnetic Survey of the Walth Bay Site (39WW203)*. Manuscript, National Park Service, Midwest Archaeological Center, Lincoln, NE.

Whitmore, F.C., Jr., K.O. Emery, H.B.S. Cooke, and D.J.P. Swift, 1967. Elephant teeth from the Atlantic Continental Shelf. *Science* 156:1477–1481.

Wigley, Roland L., and A. D. McIntyre, 1964. Some Quantitative Comparisons of Offshore Meiobenthos and Macrobenthos South of Martha's Vineyard. *Limnology and Oceanography* 9(4):485-493.

Zykov, M., T. Deveau, and N. Chorney. 2012. Acoustic Modelling Report. (Appendix D) In: *Atlantic OCS Proposed Geological and Geophysical Activities Mid-Atlantic and South Atlantic Planning Areas Draft Programmatic Environmental Impact Statement.* Bureau of Ocean Energy Management, Gulf of Mexico OCS Region. Prepared by JASCO Applied Sciences for Continental Shelf Associates International Inc.

APPENDIX A
SYNOPSES OF AGENCY AND COLLABORATIVE PARTNERS

This appendix lists the collaborative partners in the study.

A.1 NATIONAL PARK SERVICE SUBMERGED RESOURCES CENTER

In 1980, the Submerged Cultural Resources Unit was formed and staffed by underwater archeologists and photographers to provide the expertise required by managers of national parks with submerged lands. Renamed the Submerged Resources Center in 1999 to include natural resources, the core mission of the program has remained the same: the Submerged Resources Center supports stewardship for the protection, preservation, public access and interpretation of submerged resources. The Submerged Resources Center provided the archaeological lead for the project and participated in the survey.

12795 West Alameda Pkwy., Lakewood, CO 80228 | 303-969-2665
http://www.nps.gov/submerged/

Archaeological Lead: David Conlin
MA Aegean and Underwater Archaeology, Oxford University
PhD Anthropology and Archaeology, Brown University

Dr. Conlin's career at the NPS began on detail with the US Navy during which he helped plan and execute the recovery of the world's first successful combat submarine, the Confederate submersible *H.L. Hunley,* lost in 1864. After working on the *Hunley* project, Conlin returned to work on submerged cultural resources in the national parks, eventually becoming Chief of the Submerged Resources Center. Recent projects have included searching for John Paul Jones' ship *Bonhomme Richard*; diving on the wreck of a B-29 Superfortress bomber that crashed into Lake Mead on a secret, high-altitude research mission for the Air Force; diving the wreck of the USS *Arizona* in Pearl Harbor; and diving World War II German U-boats lost off Cape Hatteras National Seashore. For this collaboration, Dr. Conlin led the archaeological data collection and analysis of side scan sonar data and the interpretation of the applicability of interferometric sonar testing for identification of archaeological resources (see Appendix C).

A.2 UNITED STATES GEOLOGICAL SURVEY SEAFLOOR MAPPING OPERATION GROUP, WOODS HOLE SCIENCE CENTER

The Woods Hole Coastal and Marine Geology Team is one of three marine teams that conduct research within the USGS Coastal and Marine Geology Program. Within the team, the Seafloor Mapping operational group provides the technical expertise and innovations to plan, acquire, process, interpret, archive, and publish products to support coastal, and inner-continental shelf geology, sediment transport, environmental geoscience, and energy/tectonics research programs. The Seafloor Mapping group provided the geophysical lead for the project and participated in the survey.

84 Woods Hole Road, Quissett Campus, Woods Hole, MA 02543-1598 | 508-548-8700

http://woodshole.er.usgs.gov/operations/sfmapping/staff.htm

Geophysical Lead: William Schwab
MS Geology/Geophysics, University of Rhode Island
PhD Marine Geology, Duke University

Dr. Schwab's research in sedimentology and geophysics is focused on the dynamics of shelf-sediment transport, the formative processes controlling the evolution of submarine sediment deposits, and the relation of shelf sediment transport to coastal change. He has lead cooperative research efforts with other agencies and is the Supervisory Geophysicist for the Woods Hole Science Center Seafloor Mapping Group. For this collaboration, Dr. Schwab led the geophysical data collection and analysis for sub-bottom profiling and interferometric sonar testing (see Appendix C).

A.3 NATIONAL OCEANIC AND ATOMSPHERIC ADMINISTRATION (NOAA) OFFICE OF NATIONAL MARINE SANCTUARIES

The mission of NOAA's National Marine Sanctuaries is to serve as the trustee for the nation's system of marine protected areas, to conserve, protect, and enhance their biodiversity, ecological integrity and cultural legacy. The Northeast regional office protects not only the USS Monitor but natural and cultural resources at Stellwagen Bank, and a vast collection of Great Lakes wrecks in Thunder Bay. Stellwagen Bank, located approximately 50 miles due north of the project area, was designated by Congress in 1992 to protect the primary summer feeding grounds of the endangered North Atlantic right whale and other important marine features. Both the Northeast and Great Lakes Regional Office and the Monitor National Marine Sanctuary assisted BOEM by providing an appropriate vessel, their SRVx (see Appendix C, Figure 2) and Stellwagen Bank National Marine Sanctuary provided technical advice on archaeological, marine biological, and acoustic elements of the research design.

Stellwagen Bank National Marine Sanctuary
175 Edward Foster Road, Scituate, MA 02006 | 781-545-8026
http://stellwagen.noaa.gov

Northeast and Great Lakes Region
10 Ocean Science Circle, Savannah, GA 31411 | 912-598-2437

A.4 UNIVERSITY OF RHODE ISLAND GRADUATE SCHOOL OF OCEANOGRAPHY

The University of Rhode Island (URI) Graduate School of Oceanography (GSO) of the University of Rhode Island offers instruction leading to the Doctor of Philosophy (PhD), the Master of Science (MS) and the Master of Oceanography (MO) degrees in oceanography. At the Bay Campus, researchers conduct more than 200 projects, with a combined budget of approximately $30 million in federal, state, and private funds. GSO serves a community of scientists who are conducting research in all areas of marine science. Research ranges from advancing our understanding of fundamental processes, to the development of new technologies for research and economic development, to the immediate practical application of knowledge to the solution of the problems of modern society. GSO research is conducted around the globe. This global expertise is also applied to studies in the

local waters of Rhode Island and Narragansett Bay. GSO faculty, marine research scientists, and professional staff collectively generate more than $30 million each year in external funding, which accounts for nearly 1/3 of the University's total. URI-GSO prepared the sections of the report authored by Brian Oakley and by David Robinson.

215 South Ferry Road, Narragansett, RI 02882 | 401-874-6222
http://www.gso.uri.edu/

A.5 NOAA NATIONAL MARINE FISHERIES SERVICE (NMFS) NORTHEAST FISHERIES SCIENCE CENTER (NEFSC)

Marine mammals and many fishes are highly adapted for producing and perceiving sound in the ocean. In an environment where vision is limited, hearing has become one of the most important senses. These animals rely on sound for many purposes, such as navigating, maintaining social interactions, establishing dominance, attracting mates, avoiding predators, and finding food. The Passive Acoustic Research group at NEFSC is interested in understanding the sounds these animals make, on a variety of spatial and temporal scales. Ultimately, the group seeks to evaluate the impacts of various human-produced sounds on acoustically sensitive marine mammals, to aid in management, education, and conservation efforts. The NEFSC Passive Acoustic Research group provided technical advice, particularly on the preparation of the research design for acoustic data collection.

166 Water Street, Woods Hole, MA 02543 | 508-495-2119
http://www.nefsc.noaa.gov/psb/acoustics/index.html

A.6 MASSACHUSETTS BOARD OF UNDERWATER ARCHAEOLOGICAL RESOURCES

Established in 1973, the MA Board of Underwater Archaeological Resources (BUAR) is the sole trustee of the Commonwealth's underwater heritage, promoting and protecting the public's interests in these resources for recreational, economic, environmental, and historical purposes. Under Massachusetts General Law Chapter 6, sections 179-180, and Chapter 91, section 63, the Board is charged with the responsibility of encouraging the discovery and reporting, as well as the preservation and protection, of underwater archaeological resources. The BUAR provided technical advice, particularly on the preparation of the preliminary paleolandscape reconstruction.

251 Causeway Street, Suite 800, Boston, MA 02114-2199 | 617-626-1141
http://www.mass.gov/czm/buar/

A.7 MASHPEE WAMPANOG TRIBE

The Mashpee Wampanoag people are the People of the First Light, a federally-recognized tribe of MA located on Cape Cod. Mashpee oral traditions maintain that, for at least 10,000 years, the Wampanoags occupied southeastern MA between the eastern shore of Narragansett Bay in RI to the western end of Cape Cod, including the coastal islands of Martha's Vineyard and Nantucket. The Wampanoag people spoke an Eastern Algonquian dialect of *Massachusett*, and pursued a traditional,

semi-sedentary economy based on fishing and agriculture. After an arduous 30+ year process, the Mashpee Wampanoags were re-acknowledged as a federally recognized tribe in 2007 and retain full tribal sovereignty rights. Today, the Mashpee Wampanoags number more than 1,400 members represented by a tribal council seeking an initial reservation in Mashpee and Taunton, MA in the federal process for land-in-trust. The reservation would allow the Tribe to provide services to the nation, including housing, health care, education, job training, cultural preservation and more in Mashpee. The Mashpee Wampanoag Tribe provided technical advice, particularly on the preparation of the preliminary paleolandscape reconstruction.

A.8 JASCO APPLIED SCIENCES

JASCO Applied Sciences is an international company with over 25 years of experience performing acoustic research, noise and vibration assessment, and data acquisition services. JASCO's team has collected terabytes of acoustic and vibration data and its capabilities include spectral and temporal analysis of data collected in the field and the modeling of acoustic and noise sources and propagation. JASCO has experience in the creation of transducer arrays for the detection and localization of sound sources, including triangulation and beam-forming techniques and research on responses of marine fauna to anthropogenic noise. JASCO's scientists and bioacousticians record and assess the physical properties of sound as they relate to distance, time, depth, and nature of environment. Information obtained from biological analysis or observation is then matched to the acoustic measurements, effectively defining the range of noise considered necessary to minimize impacts to wildlife. JASCO prepared the sound source verification chapter of the report and conducted the sound source verification work aboard the survey vessel. Suite 202, 32 Troop Ave., Dartmouth, NS B3B 1Z, Canada | 902-405-3336

http://www.jasco.com

APPENDIX B
SCIENTIFIC AND ADVISORY PERSONNEL

Last Name	First Name	Position	Organization	Email
Baldwin	Wayne	Geologist	USGS (WHSC)[1]	WBaldwin@usgs.gov
Bergeron	Emile	Marine Technologist	USGS (WHSC)	EBergeron@usgs.gov
Boatman	Mary	Studies Chief	BOEM (OREP)[2]	Mary.Boatman@boem.gov
Bright	John	Archaeologist	NPS SRC[3]	John_Bright@nps.gov
Carr	Scott	Chief Executive Officer, Acoustician	JASCO	Scott.Carr@jasco.com
Carrier	Brandi	Archaeologist	BOEM (OREP)	Brandi.Carrier@boem.gov
Conlin	David	Archaeologist, Chief	NPS (SRC)	David_Conlin@nps.gov
Danforth	Bill	Geologist	USGS (WHSC)	BDanforth@usgs.gov
Hall	Callie	Oceanographer	BOEM (OREP)	Callie.Hall@boem.gov
Hoffman	William	Archaeologist	BOEM (OREP)	William.Hoffman@boem.gov
Hooker	Brian	Marine Biologist	BOEM (OREP)	Brian.Hooker@boem.gov
Jordan	Brian	Archaeologist	BOEM (DEA, FPO)[4]	Brian.Jordan@boem.gov
Lawrence	Matthew	Archaeologist	NOAA[5] (Stellwagen Bank National Marine Sanctuary)	Matthew.Lawrence@noaa.gov
Mastone	Victor	Archaeologist	MA Board of Underwater Archaeological Resources	Victor.Mastone@state.ma.us
Moore	James	Archaeologist	BOEM (DEA)[6]	James.Moore@boem.gov
Mouy	Xavier	Acoustician	JASCO	Xavier.Mouy@jasco.com
O'Brien	Tom	Marine Technologist	USGS (WHSC)	TOBrien@usgs.gov
Peters	Ramona	Tribal Historic Preservation Officer	Mashpee Wampanoag Tribe	RPeters@mwtribe.com
Schwab	William	Geophysicist	USGS (WHSC)	BSchwab@usgs.gov
Van Parijs	Sophie	Acoustician	NOAA (NMFS, NEFSC)[7]	Sofie.VanParijs@noaa.gov

[1] United States Geological Survey Woods Hole Science Center
[2] Bureau of Ocean Energy Management, Offshore Renewable Energy Program
[3] National Park Service Submerged Resources Center
[4] Bureau of Ocean Energy Management, Division of Environmental Assessment, Federal Preservation Officer
[5] National Oceanic and Atmospheric Administration
[6] Bureau of Ocean Energy Management, Division of Environmental Studies
[7] National Oceanic and Atmospheric Administration National Marine Fisheries Service, North East Fisheries Science Center

APPENDIX C
EQUIPMENT

Office of National Marine Sanctuaries
National Oceanic and Atmospheric Administration

Photo: Credit: Unknown Source

Research Vessel *SRVx*

Specifications

Design: Fiberglass sandwich core hull

Length: 85 feet

Beam: 23 feet

Draft: 5 feet, 6 inches

Speed at Best Efficient Power: 13 knots

Speed at Full Power: 35 knots

Max Displacement: 88 tons

Fuel capacity: 3,500 gallons diesel

Range (Efficient Power): 1,500 nautical miles

Power: (2) 2,735 hp MTU World Engines

Propulsion: Fixed-pitch propellers

Ship Service Generator: (2) 32Kw

Waste Water Capacity: 300 Gallons

Fresh Water Capacity: 550 Gallons

Max Day Scientists: 15

Max Overnight Scientists: 8

Crew: 3 (4 for 24-hour operations)

As stewards of our nation's special places in the ocean and Great Lakes, NOAA's Office of National Marine Sanctuaries (ONMS) must always search for better ways to protect, conduct research and monitor the resources of the National Marine Sanctuary System. As a result, ONMS has launched a new class of small research vessel (SRV) to support its ocean conservation missions. Vessels in this class can serve a wide range of ONMS resource protection missions, especially in sanctuaries with remote areas or where higher sea states occur throughout the year. SRVs have the potential to fill a gap between missions suitable for other classes of sanctuary vessels and those performed using larger NOAA multipurpose coastal research vessels.

Missions for which the *SRVx* is designed:

- Coastal and open sea operations for multiple science disciplines including physical and chemical oceanography, biological surveys, habitat mapping, and maritime heritage.
- Supporting diverse science payloads such as water sampling, ROVs, AUVs, and mooring buoy deployments.
- Rapid response to natural events and emergencies requiring heavy-weather transits at speed.
- Patrols to monitor compliance with sanctuary regulations and permit conditions.
- Student, teacher, and public education missions, directly and via telepresence.

Deck Equipment

- Winch with 800 meters of 0.375” wire rope
- Winch with 450 meters of Rochester 0.322” conducting wire
- A-frame with block for 4,500 pounds at sea state 5; 12.5-foot clearance over cockpit deck; LCI-90 wire-out readout
- Knuckle boom crane for boat handling and cargo: 900 pounds of lift at full extension of 20feet; 4,000 pounds at close range
- Hydraulic “quick-connects” and deck mounts for use with itinerant winches and other equipment
- Electrical Power: 440/208 volt three-phase; 110 volt single-phase (15 amp)
- Saltwater and freshwater outlets

The *SRVx* serves not only to advance ONMS missions, but also to support evolving technologies that enhance sanctuary research, and to encourage collaborations within NOAA and with the public and private sector. This new innovative research platform is ready to take on the challenges of understanding and conserving our nation’s ocean environments and maritime heritage.

For questions regarding scheduling or partnership opportunities, please contact David Alberg, Sanctuary Superintendent, Monitor National Marine Sanctuary at 757-591-7326.

G-882 MARINE MAGNETOMETER

- ***CESIUM VAPOR HIGH PERFORMANCE – Highest detection range and probability of detecting all sized ferrous targets***
- ***NEW STREAMLINED DESIGN FOR TOW SAFETY – Low probability of fouling in lines or rocks***
- ***NEW QUICK CONVERSION FROM NOSE TOW TO CG TOW – Simply remove an aluminum locking pin, move tow point and reinsert. New built in easy carry handle!***
- ***NEW INTERNAL CM-221 COUNTER MODULE – Provides Flash Memory for storage of default parameters set by user***
- ***NEW ECHOSOUNDER / ALTIMETER OPTION***
- ***NEW DEPTH RATING – 4,000 psi !***
- ***HIGHEST SENSITIVITY IN THE INDUSTRY – 0.004 nT/√Hz RMS with the internal CM-221 Mini-Counter***
- ***EASY PORTABILITY & HANDLING – no winch required, single man operation, only 44 lbs with 200 ft cable (without weights)***
- ***COMBINE TWO SYSTEMS FOR INCREASED COVERAGE – Internal CM-221 Mini-Counter provides multi-sensor data concatenation allowing side by side coverage which maximizes detection of small targets and reduces noise***

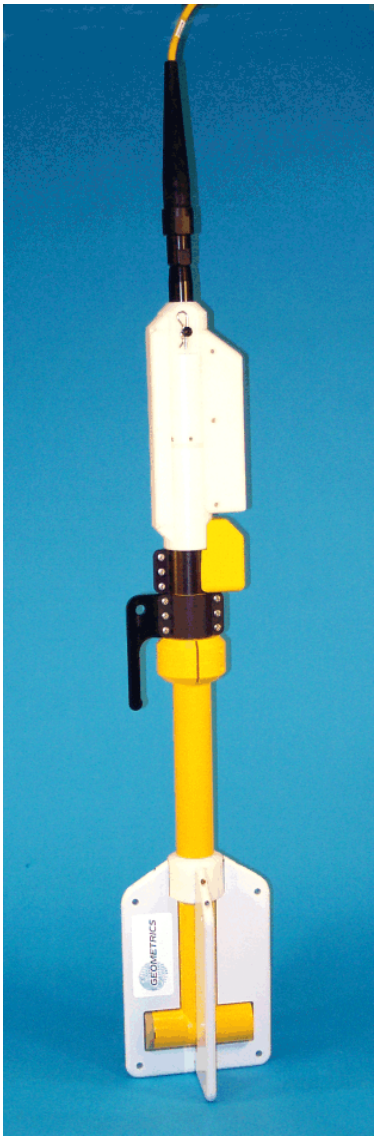

G-882 with Weight Collar Depth Option & Altimeter

Very high resolution Cesium Vapor performance is now available in a low cost, small size system for professional surveys in shallow or deep water. High sensitivity and sample rates are maintained for all applications. The well proven Cesium sensor is combined with a unique and new CM-221 Larmor counter and ruggedly packaged for small or large boat operation. Use your computer and standard printer with our MagLogLite™ software to log, display and print GPS position and magnetic field data. The G–882 is the lowest priced high performance full range marine magnetometer system ever offered.

The G-882 offers flexibility for operation from small boat, shallow water surveys as well as deep tow applications (4,000 psi rating, telemetry over steel coax available to 10Km). The G-882 also directly interfaces to all major Side Scan manufacturers for tandem tow configurations. Being small and lightweight (44 lbs net, without weights) it is easily deployed and operated by one person. But add several streamlined weight collars and the system can quickly weigh more than 100 lbs. for deep tow applications. Power may be supplied from a 24 to 30 VDC battery power or the included 110/220 VAC power supply. The tow cable employs high strength Kevlar strain member with a standard length of 200 ft (61 m) and optional cable length up to 500m with no telemetry required.

A rugged fiber-wound fiberglass housing is designed for operation is all parts of the world allowing sensor rotation for work in equatorial regions. The shipboard end of the tow cable is attached to an included junction box or optional on-board cable for quick and simple hookup to power and output of data into any Windows 98, ME, NT, 2000 or XP computer equipped with RS-232 serial ports.

The G-882 Cesium magnetometer provides the same operating sensitivity and sample rates as the larger deep tow model G-880. MagLogLite™ Logging Software is offered with each magnetometer and allows recording and display of data and position with Automatic Anomaly Detection and automatic anomaly printing on Windows™ printer! Additional options include: MagMap2000 plotting and contouring software and post acquisition processing software MagPick™ (free from our website.)

The G-882 system is particularly well suited for the detection and mapping of all sizes of ferrous objects. This includes anchors, chains, cables, pipelines, ballast stone and other scattered shipwreck debris, munitions of all sizes (UXO), aircraft, engines and any other object with magnetic expression. Objects as small as a 5 inch screwdriver are readily detected provided that the sensor is close to the seafloor and within practical detection range. (Refer to table at right).

The design of this high sensitivity G-882 marine unit is directed toward the largest number of user needs. It is intended to meet all marine requirements such as shallow survey, deep tow through long cables, integration with Side Scan Sonar systems and monitoring of fish depth and altitude.

Typical Detection Range For Common Objects

Ship 1000 tons	0.5 to 1 nT at 800 ft (244 m)
Anchor 20 tons	0.8 to 1.25 nT at 400 ft (120 m)
Automobile	1 to 2 nT at 100 ft (30 m)
Light Aircraft	0.5 to 2 nT at 40 ft (12 m)
Pipeline (12 inch)	1 to 2 nT at 200 ft (60 m)
Pipeline (6 inch)	1 to 2 nT at 100 ft (30 m)
100 KG of iron	1 to 2 nT at 50 ft (15 m)
100 lbs of iron	0.5 to 1 nT at 30 ft (9 m)
10 lbs of iron	0.5 to 1 nT at 20 ft (6 m)
1 lb of iron	0.5 to 1 nT at 10 ft (3 m)
Screwdriver 5 inch	0.5 to 2 nT at 12 ft (4 m)
1000 lb bomb	1 to 5 nT at 100 ft (30 m)
500 lb bomb	0.5 to 5 nT at 50 ft (16 m)
Grenade	0.5 to 2 nT at 10 ft (3 m)
20 mm shell	0.5 to 2 nT at 5 ft (1.8 m)

MODEL G-882 CESIUM MARINE MAGNETOMETER SYSTEM SPECIFICATIONS

OPERATING PRINCIPLE:	Self-oscillating split-beam Cesium Vapor (non-radioactive)
OPERATING RANGE:	20,000 to 100,000 nT
OPERATING ZONES:	The earth's field vector should be at an angle greater than 6° from the sensor's equator and greater than 6° away from the sensor's long axis. Automatic hemisphere switching.
CM-221 COUNTER SENSITIVITY:	<0.004 nT/ √Hz rms. Up to 20 samples per second
HEADING ERROR:	±1 nT (over entire 360° spin)
ABSOLUTE ACCURACY:	<2 nT throughout range
OUTPUT:	RS-232 at 1,200 to 19,200 Baud
MECHANICAL:	
Sensor Fish:	Body 2.75 in. (7 cm) dia., 4.5 ft (1.37 m) long with fin assembly (11 in. cross width), 40 lbs. (18 kg) Includes Sensor and Electronics and 1 main weight. Additional collar weights are 14lbs (6.4kg) each, total of 5 capable
Tow Cable:	Kevlar Reinforced multiconductor tow cable. Breaking strength 3,600 lbs, 0.48 in OD, 200 ft maximum. Weighs 17 lbs (7.7 kg) with terminations.
OPERATING TEMPERATURE:	-30° F to +122°F (-35°C to +50°C)
STORAGE TEMPERATURE:	-48° F to +158°F (-45°C to +70°C)
ALTITUDE:	Up to 30,000 ft (9,000 m)
WATER TIGHT:	O-Ring sealed for up to 4,000 psi (9000 ft or 2750 m) depth operation
POWER:	24 to 32 VDC, 0.75 amp at turn-on and 0.5 amp thereafter
ACCESSORIES:	
Standard:	View201 Utility Software operation manual and ship kit
Optional:	Telemetry to 10Km coax, gradiometer (longitudinal or transverse), reusable shipping case
MagLog Lite™ Software:	Logs, displays and prints Mag and GPS data at 10 Hz sample rate. Automatic anomaly detection and single sheet Windows printer support

SPECIFICATIONS SUBJECT TO CHANGE WITHOUT NOTICE ***12/06***

GEOMETRICS INC. 2190 Fortune Drive, San Jose, California 95131, USA
Tel: 408-954-0522 – Fax: 408-954-0902 – Email: sales@geometrics.com

GEOMETRICS EUROPE 20 Eden Way, Pages Industrial Park, Leighton Buzzard LU7 4TZ, UK
Tel: 44-1525-383438 – Fax: 44-1525-382200 – Email: chris@georentals.co.uk

GEOMETRICS CHINA Laurel Technologies, Ste 1807-1810, Kun Tai Int'l Mansion, #12B, Chaowai St., Beijing 100020, China
Tel: 86-10-5879-0099 – Fax: 86-10-5879-0989 – Email: laurel@laureltech.com.cn

Klein Associates, Inc.

KLEIN SYSTEM 3000H

DIGITAL Side Scan Sonar

The System 3000H System presents the latest technology in digital side scan sonar imaging. The dual-frequency operation is based on new transducer designs, as well as the high-resolution circuitry recently developed for the Klein multi-beam focused sonar. The System 3000H performance and price is directed to the commercial, institutional and governmental markets, and features 445 and 900 kHz frequencies for a variety of applications, including those requiring high resolution operation.

KEY FEATURES

- Advanced signal processing and transducers produce superior imagery
- Cost-effective, affordable
- PC-based operation with SonarPro® software, dedicated to Klein sonars
- Small, lightweight and simple designs — easy to run and maintain
- Easily adapted to ROVs and custom towfish
- Meets IHO & NOAA Survey specifications

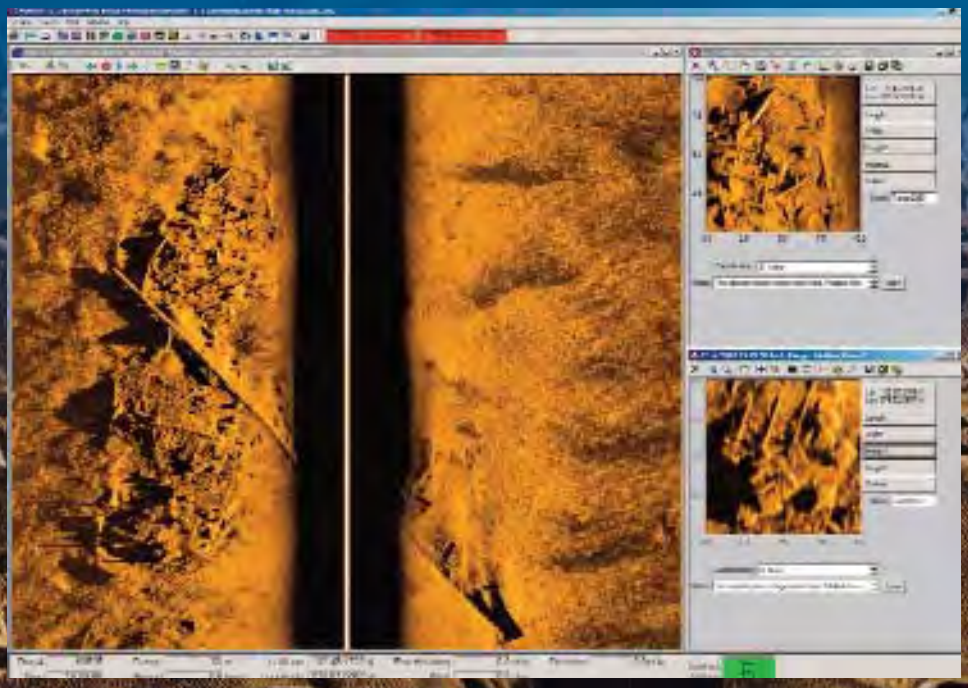

Old Shipwreck, 30m range @ 900 kHz

THE DIFFERENCE
IS IN THE IMAGE

L3

C³ISR > GOVERNMENT SERVICES > AM&M > SPECIALIZED PRODUCTS

Klein Associates, Inc.

SYSTEM 3000H

DIGITAL Side Scan Sonar

Towfish Specifications

Frequencies	445 kHz 900 kHz
Transmission pulse	Tone burst, operator selectable from 25 to 400 µsecs. Independent pulse controls for each frequency
Beams: Horizontal Vertical	 0.21° @ 445 kHz, 0.21° @ 900 kHz 40°
Beam tilt	5, 10, 15, 20, 25° down, adjustable
Range scales	15 settings — 25 to 1,000 meters
Maximum range	150 meters @ 445 kHz 50 meters @ 900 kHz
Depth rating	200 meters standard
Construction	Stainless steel
Body length	122 cm (48 in)
Body diameter	8.9 cm (3.5 in)
Weight (in air)	29 kg (63.9 lbs)
Standard sensors:	Roll, pitch, heading
Options	Magnetometer, pressure, acoustic positioning

Transceiver Processor Unit (TPU) Specifications

Operating system	VxWorks® with custom application
Basic hardware	Standard 19-inch rack or table mount, VME bus structure
Outputs	100 Base-T_X, Ethernet LAN
Navigation input	NMEA 0183
Power (includes towfish)	120 watts @ 120/240 VAC, 50/60 Hz
Interfacing	Interfaces to all major sonar data processors
Options	Splash-proof packaging option available

Tow Cable

Klein offers a selection of coaxial, Kevlar® reinforced, lightweight cables, double armored steel cables, and interfaces to fiber optic cables. All cables come fully terminated at the towfish end.

SonarPro® Software

Custom developed software by users and for users of Klein side scan sonar systems operating on Windows XP®. Field-proven for many years. SonarPro® is a modular package combining ease of use with advanced sonar features.

Basic modules	Main program, data display, information, target management, navigation, data recording & playing, and sensor display.
Multiple display windows	Permits multiple windows to view different features as well as targets in real time or in playback modes. Multi-windows for sonar channels, navigation, sensors, status monitors, targets, etc.
Survey design	Quick and easy survey set up with ability to change parameters, set tolerances, monitor actual coverage, and store settings.
Target management	Independent windows permitting mensuration, logging, comparisons, filing, classification, positioning, time & survey target layers, and feature enhancements. Locates target in navigation window.
Sensor window	Displays all sensors in several formats (includes some alarms) and responder set up to suit many frequencies and ping rates.
Networking	Permits multiple, real time processing workstations via a LAN including "master and slave" configurations.
"Wizards"	To help operator set up various manual and default parameters.
Data comparisons real time	Target and route comparisons to historical data.

Klein Associates, Inc.
11 Klein Drive
Salem, NH 03079-1249 USA
Phone: 603.893.6131
Fax: 603.893.8807
Klein.Mail@L-3com.com
www.L-3Klein.com

L3 Klein Associates, Inc.

L-3. Headquartered in New York City, L-3 Communications employs over 64,000 people worldwide and is a prime contractor in aircraft modernization and maintenance, C³ISR (Command, Control, Communications, Intelligence, Surveillance and Reconnaissance) systems and government services. L-3 is also a leading provider of high technology products, subsystems and systems.

Digital Precision Altimeters

PA200 and PA500

Features

- Analogue only outputs
- Digital only output
- Simultaneous analogue and digital outputs
- Noise immunity
- Can be field reconfigured for different applications
- Free-running outputs
- Interrogated outputs
- Low operating voltage options
- 4000 metre standard depth rating

Applications

- ROV and AUV auto-altitude and under-ice measurement
- Integration to CTD & oceanographic sensor packages
- Low-cost hydrographic surveying of rivers and canals
- Integration to bathymetric packages
- Touchdown monitoring of subsea structures
- Wave height measurement
- Monitoring of scouring around bridge supports

Tritech PA200 and PA500 Digital Precision Altimeters are based on the same high performance electronics found in the proven, industry standard SeaKing sonar and profiler systems.

The range of compact Tritech PA200 and PA500 Digital Precision Altimeters provide exceptionally accurate height off seabed and subsea distance measurements.

Full digital synthesis of transmit and receive frequencies, together with greatly improved input dynamic range, offer unsurpassed levels of performance from a compact unit.

The units may be supplied with simultaneous analogue and digital outputs allowing them to be interfaced to a wide range of PC devices, data loggers, ROV telemetry systems and multiplexers.

OEM configurations including low magnetic signature, rigid polyurethane housings or right-angled heads are available on request.

Control of the altimeters may be performed in many ways including :

- Direct from a PC running DOS
- Direct from a PC running Windows
- Direct from a suitable control system
- Part of a multidrop network

Specifications

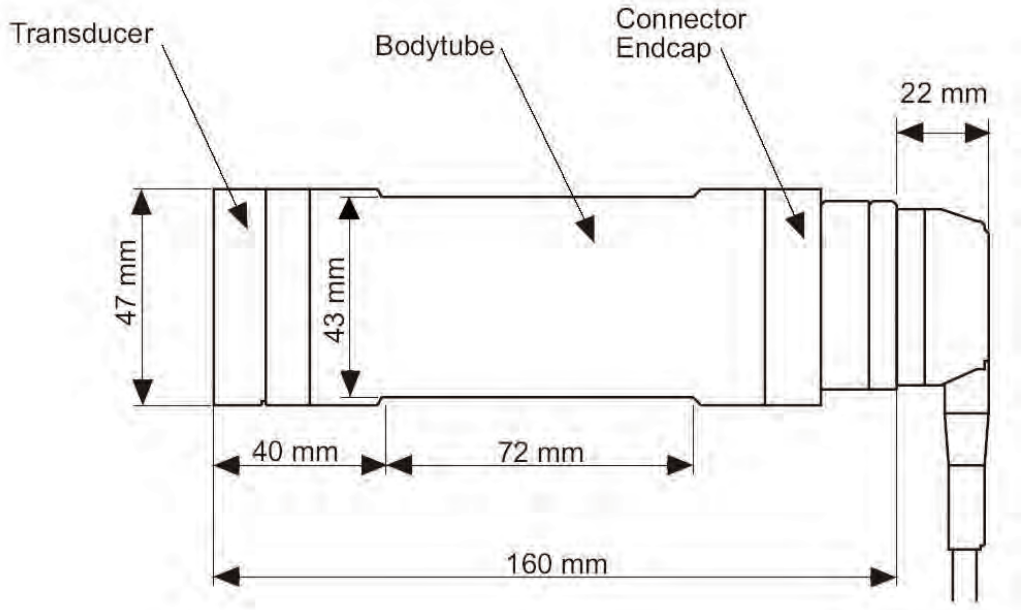

All measurements in mm

	PA200-20	PA500-6
Operating frequency	200 kHz	500 kHz
Beamwidth	20° Conical	6° Conical
Operating range	1 to 100 metres 0.7 to 50 metres	0.3 to 50 metres 0.1 to 10 metres
Standard power supply	24 VDC @ 80 mA, or 12 VDC @ 160 mA	
Standard analogue output	0 to 10 VDC (24 VDC units oly) 0 to 5 VDC or 4 - 20 mA	
Digital resolution	1mm on all ranges	
Analogue resolution	0.025% of range	
Data communication options	Serial RS232, or Serial RS485	
Output modes	Free running Interrogated, or multidrop network	
Serial output format	ASCII, 9600, 1, 8, n, 1	
Length	160mm	
Diameter	47mm	
Standard depth rating (stainless steel body)	4,000 m	
Optional depth ratings	700m and 6,800m	
Weight in air	1.1 kg	
Weight in water	0.8 kg	
Operating temperature range	-10 to +40 °C	
Dry storage temperature range	-20 to +70 °C	

All specifications are subject to change in line with Tritech's policy of continual product development.

Ref: EDS-ALT-002.14

Tritech International Limited
Peregrine Road • Westhill Business Park • Aberdeen
AB32 6JL • United Kingdom

T: +44 (0)1224 744111
F: +44 (0)1224 741771
E-mail: sales@tritech.co.uk
Website: www.tritech.co.uk

Marketed by:

EdgeTech
An Affiliate of ORE Offshore

3200
SUB-BOTTOM PROFILING SYSTEM

FEATURES

- Choice of 3 towfish depending on the application
- Low frequency for greater penetration
- Pole mount option for shallow water surveys

APPLICATIONS

- Geological Surveys
- Geohazard Surveys
- Sediment Classification
- EEZ Resource Development
- Buried Object Location
- Bridge/Shoreline Scour Surveys
- Mining/Dredging Surveys

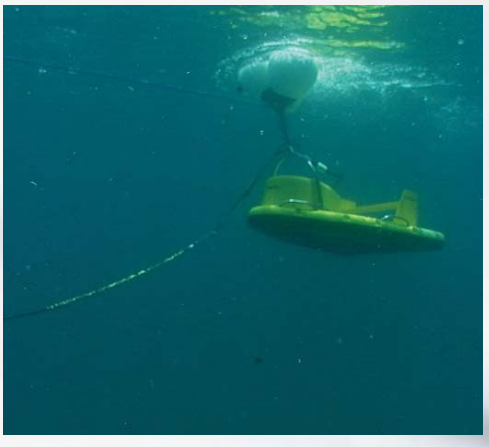

The EdgeTech 3200 Sub-bottom Profiling System is a wideband Frequency Modulated (FM) sub-bottom profiler utilizing EdgeTech's proprietary Full Spectrum CHIRP technology. The 3200 generates high resolution images of the sub-bottom stratigraphy in oceans, lakes, and rivers and provides penetration of up to 200m.

The 3200 comes available with a choice of three stable, low drag towfish that operate at different frequencies and can be used at depths of up to 300m. The selection of towfish depends on the sub-bottom characteristics as well as the resolution and penetration requirements.

Along with a towfish, a standard 3200 system comes with a topside processor running EdgeTech's DISCOVER sub-bottom acquisition & processing software as well as a customer-specified length of tow cable. Additional optional sensors are also available.

EdgeTech
An Affiliate of ORE Offshore

3200
SUB-BOTTOM PROFILING SYSTEM

KEY SPECIFICATIONS

TOWFISH	SB-0512i	SB-216S	SB-424
Frequency Range	500 Hz–12 kHz	2-16 kHz	4-24 kHz
Vertical Resolution (depends on pulse selected)	8–20 cm	6-10 cm	4-8 cm
Penetration (typical)			
In coarse calcareous sand	20 meters	6 meters	2 meters
In clay	200 meters	80 meters	40 meters
Length	160 cm	105 cm	77 cm
Width	124 cm	67 cm	50 cm
Height	47 cm	40 cm	34 cm
Weight in Air	204 kg	76 kg	45 kg
Weight in Water	68 kg	32 kg	18 kg
Depth Rating	300 meters		
TOPSIDE PROCESSOR			
Hardware	Standard 19 inch rack mount with portable aluminum enclosure for transport		
Operating System	Windows XP		
Display	High resolution 21 inch flat panel display		
Archive	Hard drive and/or DVD-R/W		
File Format	Native JSF or SEG-Y		
Output	Ethernet		
Power Input	120/220 VAC		
SYSTEM OPTIONS			
	Integrated depth sensor, USBL acoustic tracking system		

SB-0512i

SB-216S

SB-424

For more information please visit EdgeTech.com

info@EdgeTech.com | USA 1.508.291.0057

SV Plus^{v2}

Setting the Standard for Sound Velocity Profiling

Updated in 2004, the SV Plus was released in 1996 as the first-ever time-of-flight sound velocimeter. By directly measuring the time-of-flight of an acoustic ping, the SV Plus improves sound velocity accuracies by a factor of five. Field accuracy is 0.05m/s; precision is 0.03m/s. In contrast, instruments that calculate sound velocity using Chen & Millero or Del Grosso offer accuracies of 0.25m/s at best.

Applied Microsystems has manufactured more than 3000 invar-rod sound velocity sensors, making the SV Plus a proven field partner. Used by surveyors worldwide and recommended by leading multi-beam manufacturers, the SV Plus is the industry standard for reliable sound velocity measurement.

Customers choose the SV Plus for reliability and accuracy. Each sound velocity sensor receives 700 individual calibration points carefully distributed over the sensor's full range. We do not extrapolate our calibrations. Extrapolated calibrations are often out of spec at individual sound velocities even if the instrument – on average - meets accuracy requirements. Anomalies of this type lead to error.

Standard Features:

- Time-of-flight sound velocity precision of 0.03m/s
- 0.05%FS pressure sensor, temp compensated (0.01%FS optional)
- 0.05°C temperature sensor (0.005°C optional)
- USB port for high-speed data download
- User selectable sampling to 25Hz
- 64Mb non-volatile memory (expandable)
- User configurable comms settings (RS232 or RS485) & baud rates
- Dual power (battery and external)
- Aluminium 6061-T6 hard-anodized housing (to mil spec) for profiling to 5000m depths (deeper on request)
- Programmable sampling parameters
- Plug and play sensor capability

Comes Complete With:

- Aluminium shipping case
- 2m data / power pigtail
- Spares kit
- Sensor protection cage
- Dummy & shorting plugs
- Software & manuals

SV Plus^{v2}

Sound Velocimeter for Profiling

The SV Plus^{v2} is available with either our hi-tech composite sensor (top in photo located below) or traditional invar-rod sensor. Invented in 2000, composite sensors eliminate path-length change due to corrosion and vibration, resulting in longer periods between calibrations. Temperature response time is immediate and range extends to 1600 m/s. On some applications, no zincs are required.

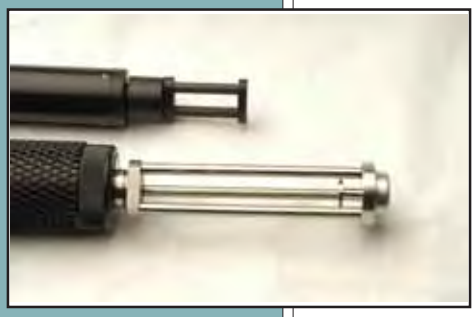

Electrical:

- 64 Mb non-volatile memory
- 16 bit analog to digital resolution (65,536 counts)
- Up to 25 scans per second
- Real time clock
- User configurable comm settings (RS232 or RS485)
- Optional additional channels (10 analog or 5 digital)
- Auto shut-down in low battery conditions

Power Options:

- 8 to 24VDC (external)
- 9 D cell Alkaline batteries
- 3, 6, or 9 D cell Lithium batteries
- 9 D cell Ni-Cad rechargeable batteries

Sampling Modes:

- Continuous, defined increments of time, at specific pressures, or upon request

Mechanical:

- Hard anodized 6061-T6 Aluminium housing, rated to 5000m (optional 7075-T6 Aluminium to 6000m)
- 100mm / 4.0" (diameter) x 881 mm / 34.9" (end-to-end, logger version) or 653 mm / 25.9" (end-to-end, real-time version)
- Connectors: Subconn Micro 8 wet pluggable
- Environmental: Storage, -40°C to 60°C; Usage, -20°C to 45°C

Accessories:

- Instrument suspension bar
- Instrument suspension bar with protective cage

Additional Information:

- The SV Plus is available in various configurations; visit our website for details. Specifications subject to change without notice. Document version 1.06

		Range	Precision	Accuracy	Response	Resolution
Standard Sensors	Sound Velocity (Invar Rod)	1400 to 1550 m/s	+/-0.03 m/s	+/-0.05 m/s	145 microseconds	0.015m/s
	Temperature	-2 to 32°C	+/-0.003°C	+/-0.05°C	1 second	0.001°C
	Pressure (Strain Gauge, Temp Compensated)	Various to 6000m	+/-0.03%FS	+/-0.05%FS	10 milliseconds	0.005%FS
Optional Upgrades	Sound Velocity (Composite)	1350 to 1600 m/s	+/-0.03 m/s	+/-0.05 m/s	47 microseconds	0.015m/s
	Temperature	Various to 45°C	+/-0.003°C	+/-0.005°C	500 milliseconds	0.001°C
	Temperature	Various to 45°C	+/-0.003°C	+/-0.005°C	350 milliseconds	0.001°C
	Pressure (Quartz Crystal)	Various to 7000m		+/-0.01%FS	Varies	0.000001%FS
Calculated Parameters	Salinity	0 to 40 psu		+/-0.035 psu		

APPLIED MICROSYSTEMS Because it's not just H_2O

2071 Malaview Avenue, Sidney B.C. Canada Tel: +1-250-656-0771
info@AppliedMicrosystems.com www.AppliedMicrosystems.com

1 SYSTEM DESCRIPTION

The MVP30 system is a self-contained profiling system capable of sampling water column profiles to 30m depth from a vessel moving at up to 12 knots, and deeper depths at slower speeds. The system provides vertical profiles of oceanographic data such as Sound Velocity and CTD for various operations including the calibration of multibeam sounder systems for hydrographic operations. The MVP30 is completely autonomous and can be controlled by computer without the requirement for personnel on deck. The system consists of a single sensor free-fall fish (fish), an electric winch, an over boarding sheave and a remotely located user interface controller. The MVP30 is shown in Figure 1. The system block diagram is shown in Figure 2.

Figure 1: MVP 30

The interferometric sonar system of choice for acquiring co-registered, very wide swath, high-resolution bathymetry and seafloor imagery.

SWATH*plus*

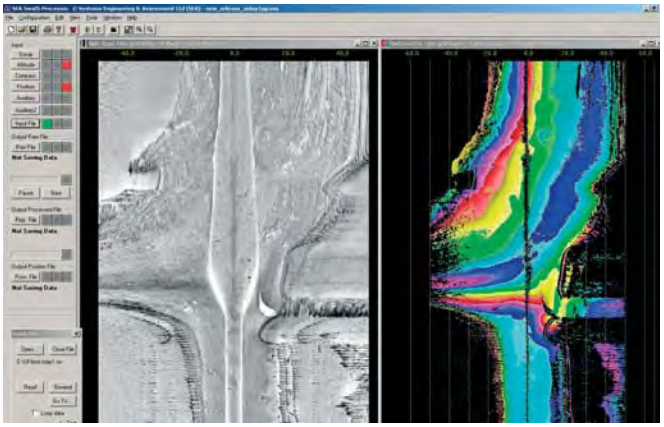

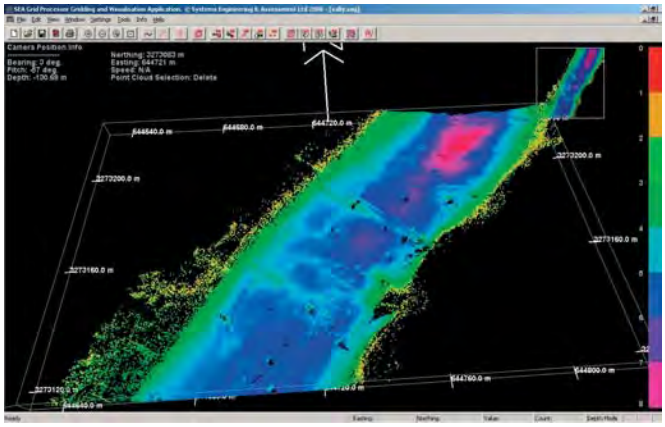

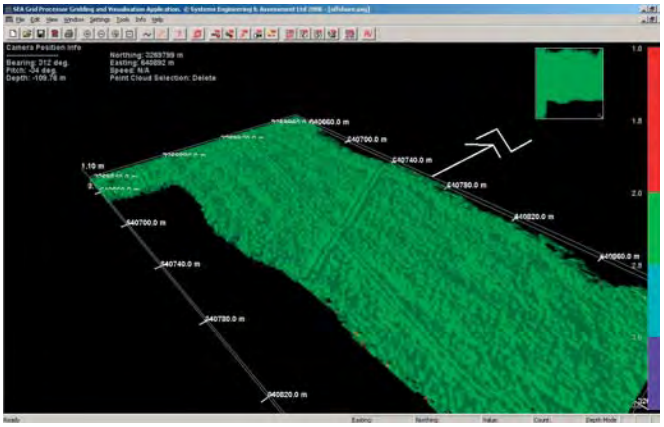

- Meets international survey data standards, such as IHO requirements.
- Co-registered, high-quality bathymetry and seafloor imagery over a very wide swath width in shallow water or at low altitude:

  USGS: "Operating swath of the bathymetric system ranged from 15 to 20 times water depth in depths less than 15 m."
- High data count gives high spatial resolution up to the swath edge.
- Low cost of ownership compared with most beam-forming multibeam systems.
- Simultaneous pinging doubles productivity and along-track coverage over alternate pinging systems – reduced in-field survey and data turn-around efforts.
- Data exportable to industry-standard applications, such as CARIS and QINSy.
- Lightweight, compact, robust and highly portable facilitating simple and rapid deployment.
- Does not require rack mounting; low power requirements – less than 25 W.

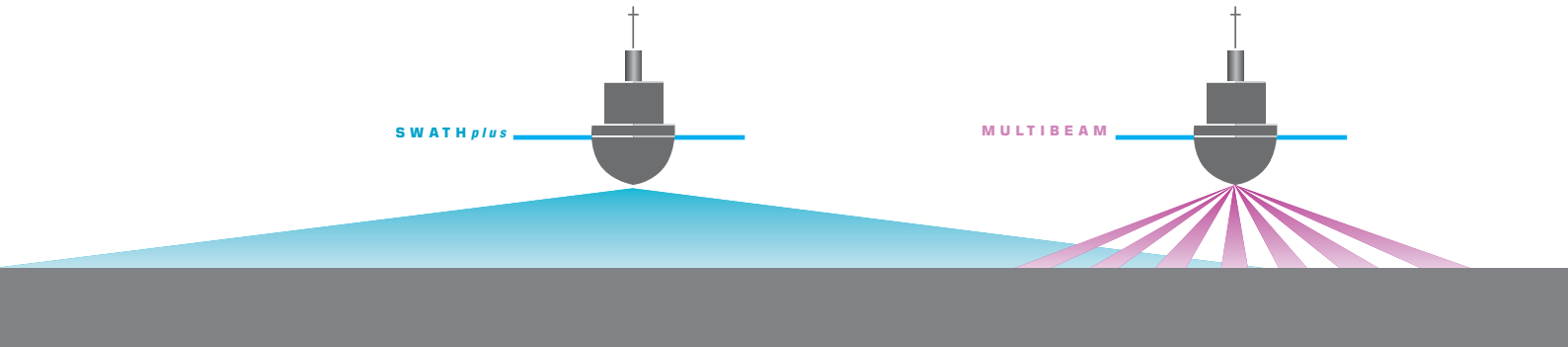

No two hydrographic surveys are the same. But all surveys have the same goals – effective performance, rapid and accurate data acquisition and processing, and reliable outputs.

SWATH*plus*

- Three frequency variants are offered – SWATH*plus*-L, SWATH*plus*-M and SWATH*plus*-H; offered in a standard or splash-proof configuration.
- The 468 kHz system is available for ROV/AUV/ASV deployment.
- System comprises two transducers, a Transducer Interface Unit, universal mounting kit and a laptop with data acquisition (swath processor) and data processing (grid processor) software.
- Interfaces to third party, industry-standard acquisition and processing software systems such as QINSy, CARIS, Hypack, Fledermaus, Starfix and PDS2000.
- Features double-sided pinging; and USB interfacing.
- Users/Applications: Research/education (habitat mapping). Survey companies (navigable depth, route/site surveys, construction/dredging support, pipeline inspections). Utility companies (cable and pipeline surveys/ inspections). Civil engineering (infrastructural surveys).

Technical Specifications

Parameter	SWATH*plus*-L	SWATH*plus*-M	SWATH*plus*-H
Sonar frequency	117 kHz	234 kHz	468 kHz
Maximum Water Depth	350 m	200 m	80 m
Recommended Maximum Working Depth	300 m	100 m	50 m
Across-track resolution	5 cm	2 cm	1 cm
Azimuth Beam Width (2-way)	0.85°	0.55°	0.55°
Transmit Pulse Length	17 µs to 1 ms	8.5 µs to 500 µs	4.3 µs to 250 µs
Transducer dimensions	235 x 550 x 90 mm	160 x 350 x 60 mm	100 x 215 x 42 mm
Transducer Weight in Air	13 kg	6 kg	1 kg
Transducer Weight in Water	1.6 kg	0.9 kg	0.1 kg
Total Cable Length	20 m	20 m	15 m
Transducer Interface Unit Dimensions		125 x 294 x 285 mm	
Transducer Interface Unit Weight		6.4 kg	

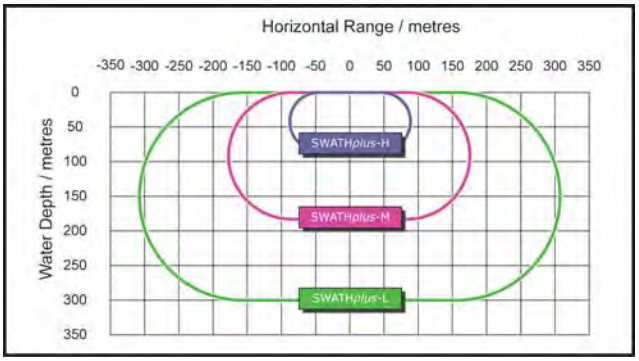

Horizontal ranges for the three sonar versions, against water depth
The swath width, and so the distance between survey lines, is double the horizontal range shown

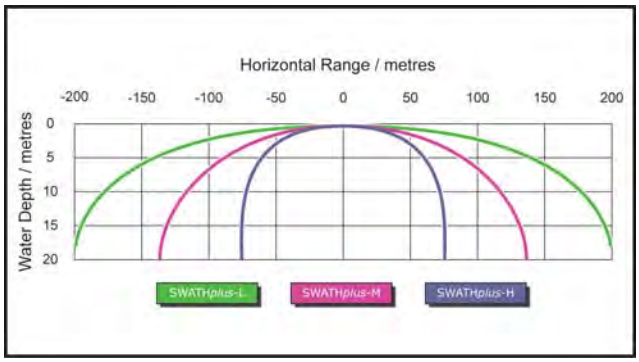

Horizontal Range vs. Water Depth, first 20 metres depth
SWATH*plus* provides outstanding coverage in very shallow water

Note: parameters are for guidance and may vary according to survey conditions such as ambient noise level and seabed type

Systems Engineering & Assessment Ltd
SEA House, Building 450, Bristol Business Park, Coldharbour Lane, Bristol, UK, BS16 1EJ
Telephone: +44 (0) 1373 852000; Fax: +44 (0) 117 937 5088; www.sea.co.uk

S·E·A

APPENDIX D
PREVIOUSLY IDENTIFIED WRECKS, OBSTRUCTIONS, OR OBJECTS OF UNKNOWN CHARACTER WITHIN ONE NAUTICAL MILE OF THE MASSACHUSETTS WIND ENERGY AREA, AND ADDITIONAL COMMENTS

Vessel Name	Vessel Number	Water Depth (m)	Data Source and Comments
Peter Rickmers	7602	-63	N/A
Princess	7609	-37	AWOIS history cl669/69--5/8/69; DOI, Bureau of Commercial Fisheries, Safety Office; List Of Commercial Fishing Vessels Lost at Sea over The Previous Few Years with Approximate Position Aad Loran A Coordinates; F/V Princess located in; charted on wreck chart only and as a non-dangerous wreck. (entered MSD 6/91) AWOIS description: 18 unknown obst. hung by trawl fisherman, NAD27 GP converted from Loran C, observed rates (approx. 1979).
Captain Bill II (outside of WEA)	7610	-39	AWOIS description: 18 unknown obst. hung by trawl fisherman, NAD27 GP converted from Loran C, observed rates (approx. 1979).
Object Airplane	7613	-53	AWOIS description: 18 airplane; hung by trawl fisherman, NAD27 GP converted from Loran C, observed rates (approx. 1979).
Unknown	7615	-55	AWOIS description: 18 unknown obst. hung by trawl fisherman, NAD27 GP converted from loran c, observed rates (approx. 1979).
Star of the Sea	7616	-52.5	AWOIS history CL669/69--5/8/69; DOI, Bureau of Commercial Fisheries, Safety Office; List of Commercial Fishing Vessels Lost at Sea over the Previous Few Years with Approximate Position and Loran A Coordinates; F/V Star of the Sea located in; charted on wreck chart only and as a nondangerous wreck. (entered MSD 6/91) AWOIS description: 18 unknown obst. hung by trawl fisherman, NAD27 GP converted from Loran C, observed rates (approx. 1979).
Unknown	7617	-44	AWOIS description: 18 unknown obst. hung by trawl fisherman, NAD27 GP Converted from Loran C, observed rates (approx. 1979).
St. John	7621	-48	AWOIS description: 18 unknown obst. hung by trawl fisherman, NAD27 GP converted from Loran C, observed rates (approx. 1979).
Adventure II	7623	-46	AWOIS description: 24 no.875; trawler, 119 gt, sunk 3/13/43 by Marine Casualty; pos. accuracy uncertain 61 3/13/43.
L. & W.B. Co. 11	7624	-46	AWOIS description: 24 no.876; barge, 862 gt; sunk 1/12/45 by Marine Casualty; position accur. uncertain 61 1/12/45.
Unknown	7625	-45.5	AWOIS description: 18 unknown obst. hung by trawl fisherman, NAD27 GP converted from Loran C, observed rates; (approx. 1979).
Pat & Judy	7629	-41	AWOIS history h6447/39--137 ft depths exist in vicinity. AWOIS description: 18 Pat & Judy, hung by trawl fisherman, NAD27 GP converted from Loran C, observed rates (approx. 1979).
Unknown Object (outside WEA)	7637	-40	AWOIS history H6446/39--133 ft depth exist in vicinity (updated 11/91 RWD) NM6/51--a yellow spherical object, 3 ft. in diameter, with projections and with a cable mooring to a heavy anchor, is submerged in 20 fathoms of water in PA; believed to be a drill mine and is considered to be a menace to navigation (explosive). (entered MSM 3/89) AWOIS description: 24 no.1216; position accuracy within 1 mile.

Vessel Name	Vessel Number	Water Depth (m)	Data Source and Comments
Skipper	7747	-44	AWOIS History cl669/69--5/8/69; DOI, Bureau Of Commercial Fisheries, Safety Office; List of Commercial Fishing Vessels Lost at Sea over the Previous Few Years with approximate position and Loran A coordinates; F/V Skipper located in; charted on wreck chart only and as a nondangerous wreck. (entered MSD 6/91).
Olive M. Williams (outside WEA)	7748	-38	AWOIS history h6446/39--129 ft depths exist in vicinity. cl669/69--5/8/69; DOI, Bureau of Commercial Fisheries, Safety Office; List of Commercial Fishing Vessels Lost at Sea over the Previous Few Years with approximate position and loran a coordinates; F/V Olive M. Williams located charted on wreck chart only and as a nondangerous wreck. (entered MSD 6/91).
JoAnne	7750	-39.5	AWOIS history lNm43/80--1st CGD; 9/23/80; fishing vessel, JoAnne, is reported sunk in 32 fathoms in PA. (entered MSD 6/91).
David C. Winslow	7761	-44	AWOIS history LNM40/84--A 60 ft tug, David C Winslow, has sunk in PA (NAD27); Applied to wreck charts only. (entered MSD 6/91).
Object UXO	7766	-55	AWOIS history NM49/65--A submerged torpedo has been reported in PA in 31 fathoms of water. (entered MSD 6/91).
Unknown	8911	-51	Source: US Navy's Non-Submarine Contact List - Wreck Features.
Unknown (outside WEA)	8919	-38	Source: US Navy's Non-Submarine Contact List - Wreck Features.
Adventure II	9031	-46	Source: US Navy's Non-Submarine Contact List - Wreck Features.
L. & W.B. Co. II	9032	-46	Source: US Navy's Non-Submarine Contact List - Wreck Features.
Unknown	9215	-53	Source: US Navy's Non-Submarine Contact List - Wreck Features.
Viking	9277	-39	Source 256: Search Requirements Comments Survey only in Conjunction with AWOIS Item 1805 AWOIS history H6447/39--134 ft depths exist in vicinity. (updated 3/92 RWD) CL669/69--5/8/69; DOI, Bureau Of Commercial Fisheries, Safety Office; List of Commercial Fishing Vessels Lost at Sea over the Previous Few Years with approximate position and Loran A coordinates; F/V Viking located in; charted on wreck chart only and as a nondangerous wreck. (ENTERED MSD 6/91).
Unknown	9282	-47	Source: US Navy's Non-Submarine Contact List - Wreck Features.
PT 200	10009	-46	AWOIS description: 24 no.1116; patrol, 33 gt; sunk 2/22/44 by Marine Casualty; pos. accuracy 3-5 miles.
Pat & Judy	10019	-51	AWOIS history CL669/69--5/8/69; DOI, Bureau Of Commercial Fisheries, Safety Office; List of Commercial Fishing Vessels Lost at Sea over the Previous Few Years with approximate position and Loran A coordinates; F/V Pat & Judy located in; charted on wreck chart only and as a nondangerous wreck. (entered MSD 6/91).
Doreen Lee	10168	-53.5	AWOIS history NM42/68-- CL669/69--5/8/69; DOI, Bureau of Commercial Fisheries, Safety Office; List of Commercial Fishing Vessels Lost at Sea over the Previous Few Years with approximate position and Loran Acoordinates; F/V Doreen Lee located in; charted on wreck chart only and as a nondangerous wreck. (entered MSD 6/91).

Vessel Name	Vessel Number	Water Depth (m)	Data Source and Comments
Alert	10345	-40	AWOIS history H6447/39--133 ft depths exist in vicinity. NM46/42--located southward of Martha's Vineyard AWOIS description: 24 NO.293; trawler; sunk 10/10/42 by Marine Casualty; position accuracy 1-3 miles; fisherman; sunk 10/10/42; a non-dangerous wreck of a small vessel reported southward of Martha's Vineyard. According to Source 156: New Bedford Customs, Wreck reports, 1914-1942.

APPENDIX E
CALIBRATION INFORMATION FOR M8E HYDROPHONES USED DURING SOUND SOURCE CHARACTERIZATIONS

E.1 LOW-FREQUENCY CALIBRATION

The calibrations of the M8E hydrophones in terms of the total system gain used for the analysis are shown in Table E-1, below. Figure E-1 shows the frequency response of the hydrophone. The calibrated sensitivity is used to adjust this curve up / down during analysis.

Table E-1.
Nantucket SSV calibration data.

AMAR ID / Location	Hydrophone ID	Time (UTC, 2012)	Calibrator ID	Full System Gain (dB re 1 FS / µPa)
071- Deep Site	247	09:42 30 Aug	42AC 53719	-172.2
071- Shallow Site	247	10:06 29 Aug	42AC 53719	-172.7
059- Shallow Site	248	10:17 29 Aug	42AC 53719	-173.2
Hydrophone 248 was not calibrated at the Deep Site due to concerns about the fit between the pistonphone calibrator adapter and the hydrophone.				

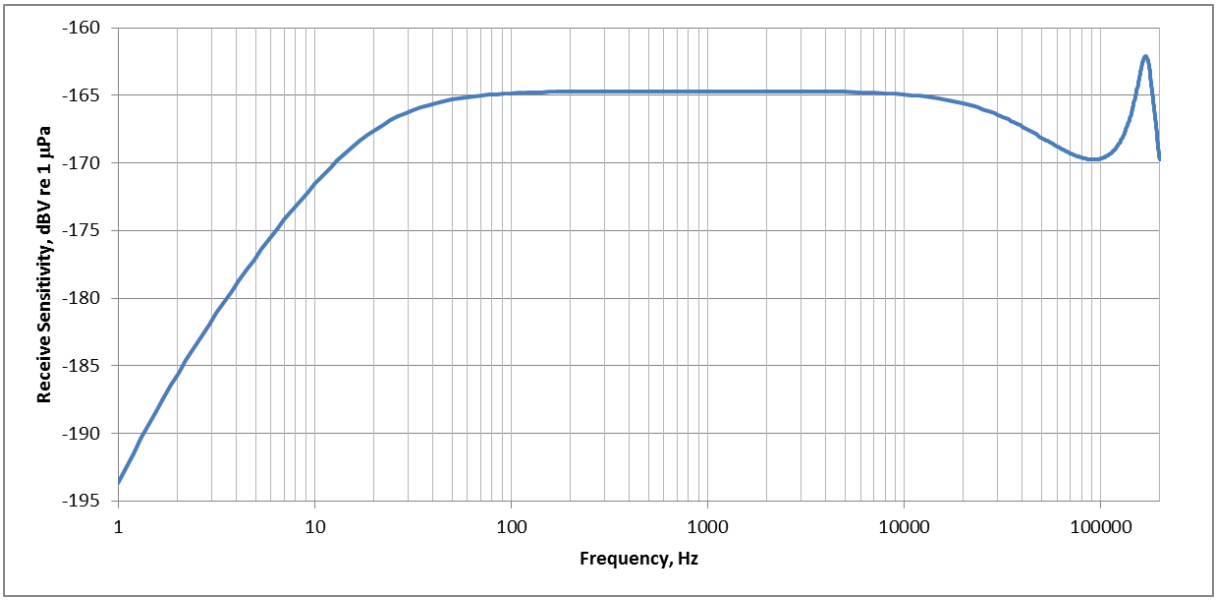

Figure E-1. Modeled frequency response of the M8E hydrophone.

E.2 HIGH-FREQUENCY CALIBRATION

The raw high frequency calibration performed by GeoSpectrum is shown in Figure E-2. This plot is not adjusted for the resonances in the test projector. The hydrophones were omnidirectional and had

a response of -175 dBV re 1 µPa +/- 2 dB from 210 to 250 kHz. The three calibration signals in Figure E-2 are 234, 235 and 237 Hz.

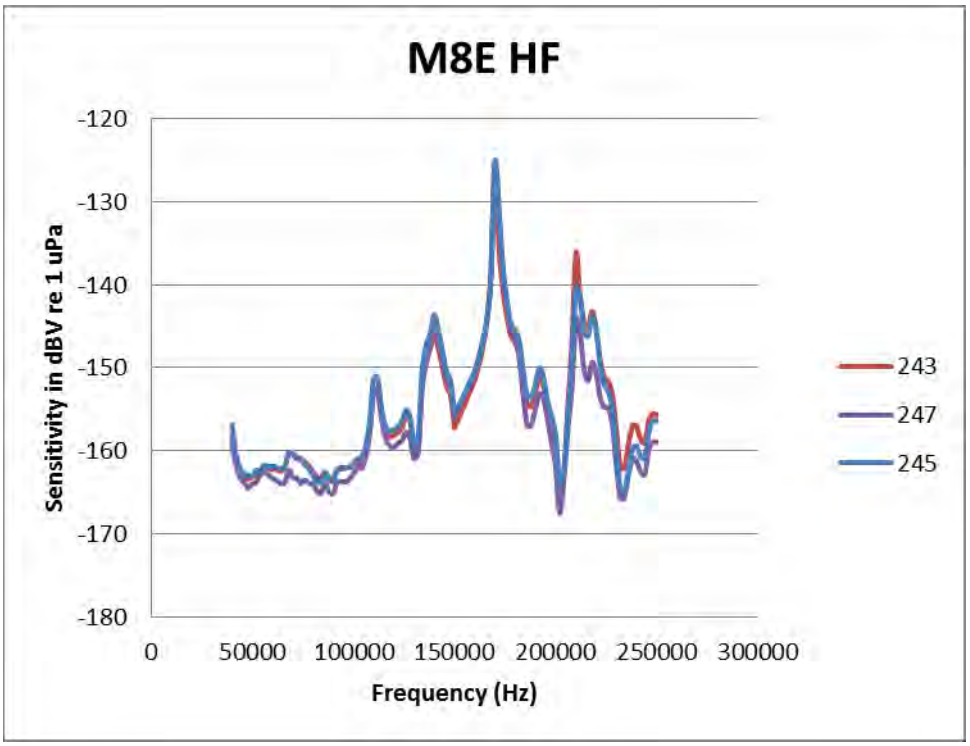

Figure E-2. High Frequency calibration of M8 Hydrophones. These are the raw results, which are not compensated for the resonances and response of the source. The adjusted response is -175 dBV re 1 µPa +/- 2 dB in the range of 210 to 250 kHz.

The Department of the Interior Mission

As the Nation's principal conservation agency, the Department of the Interior has responsibility for most of our nationally owned public lands and natural resources. This includes fostering the sound use of our land and water resources, protecting our fish, wildlife and biological diversity; preserving the environmental and cultural values of our national parks and historical places; and providing for the enjoyment of life through outdoor recreation. The Department assesses our energy and mineral resources and works to ensure that their development is in the best interests of all our people by encouraging stewardship and citizen participation in their care. The Department also has a major responsibility for American Indian reservation communities and for people who live in island communities.

The Bureau of Ocean Energy Management

The Bureau of Ocean Energy Management (BOEM) works to manage the exploration and development of the nation's offshore resources in a way that appropriately balances economic development, energy independence, and environmental protection through oil and gas leases, renewable energy development and environmental reviews and studies.

www.boem.gov